**Rui André
Simões Dias Maio**

**Mitigação do Risco Sísmico em Edifícios Urbanos
Antigos**

**Earthquake Risk Mitigation of Urban Cultural
Heritage Assets**

**Rui André
Simões Dias Maio**

Mitigação do Risco Sísmico em Edifícios Urbanos Antigos

Tese apresentada à Universidade de Aveiro para cumprimento dos requisitos necessários à obtenção do grau de Doutor em Engenharia Civil, realizada sob a orientação científica do Professor Doutor Romeu da Silva Vicente, Professor Associado do Departamento de Engenharia Civil da Universidade de Aveiro , e coorientação científica do Professor Doutor Sergio Lagomarsino, Professor Catedrático do Departamento de Engenharia Civil, Química e Ambiental da Universidade de Génova e do Doutor Tiago Miguel Ferreira, Investigador Doutorado do Departamento de Engenharia Civil da Universidade do Minho.

**Rui André
Simões Dias Maio**

**Earthquake Risk Mitigation of Urban Cultural
Heritage Assets**

Thesis submitted to the University of Aveiro to fulfil the requirements
for the degree of Doctor of Philosophy in Civil Engineering, under the
scientific supervision of Doctor Romeu da Silva Vicente, Associate Professor
at the Department of Civil Engineering of the University of Aveiro and co-
supervision of Doctor Sergio Lagomarsino, Full Professor at the Department
of Civil, Chemical and Environmental Engineering of the University of
Genoa and of Doctor Tiago Miguel Ferreira, Postdoctoral researcher at
the Department of Civil Engineering of the University of Minho.

Dedico este trabalho, aos meus pais, pelo apoio e amor incondicional, pela educação e valores transmitidos, ao meu irmão, por ocupar um lugar tão especial no meu coração, e à Marta, por ser a minha "estrela do mar".

the jury

president   **Prof. Doutor João Manuel Nunes Torrão**
Professor Catedrático da Universidade de Aveiro

Prof. Doutora Graça de Fátima Moreira de Vasconcelos
Professora Auxiliar da Universidade do Minho

Doutor Bartolomeu Pantò
Investigador do Imperial College of London

Prof. Doutora Rita Bento
Professora Associada com Agregação da Universidade de Lisboa

Prof. Doutor José António Raimundo Mendes da Silva
Professor Associado da Universidade de Coimbra

Prof. Doutor Romeu da Silva Vicente
Professor Associado da Universidade de Aveiro

agradecimentos

A presente tese marca o final de uma etapa importante da minha vida, pelo que devo agradecer primeiramente às pessoas que mais me motivaram para abraçar este desafio. Assim, ao Professor Romeu Vicente, que tem acompanhado de perto o meu trajecto enquanto investigador, o meu obrigado pelo apoio constante e incondicional, e sobretudo pela paciência demonstrada ao longo destes anos. O meu obrigado ao Doutor Tiago Miguel Ferreira pelo grande companheirismo, dedicação, conselhos e motivação. Foi de facto, um enorme privilégio para mim poder ter-te tido como braço direito ao longo deste percurso, dentro e fora de água. Não posso deixar de agradecer também ao Professor João Estêvão pelo seu contagiante entusiasmo e otimismo, por todas as frutíferas reuniões e intensa colaboração, durante praticamente todo o meu percurso como investigador.

A todos os meus colegas do Departamento de Engenharia Civil da Universidade de Aveiro, do Programa Doutoral Infrarisk, do Joint Research Centre, e ainda outros com quem tive oportunidade de me cruzar ao longo destes 4 anos, nomeadamente os colegas da Universidade de Génova e a equipa de investigadores do Gruppo Sismica. Aqui, gostaria de deixar um agradecimento especial ao Professor Sergio Lagomarsino e à Professora Serena Cattari, pela inspiração, simpatia e assertividade, e ainda ao Professor Ivo Caliò e ao Doutor Bartolomeo Pantò, pela colaboração e apoio prestado durante e após a minha estada em Catânia, que se revelou determinante para o desenvolvimento do projeto de tese.

Deixo uma palavra de agradecimento à Comissão Administrativa do Programa Doutoral Infrarisk-, em particular ao Professor Carlos Sousa Oliveira e à Professora Rita Bento, pela paciência, confiança e apoio demonstrado. Agradeço também ao Professor Aníbal Costa, pela disponibilização da base de dados relativa ao processo de reconstrução da ilha do Faial, a partir da qual foi selecionada a grande maioria dos casos de estudo analisados nesta tese. Não posso deixar de agradecer também à Fundação para a Ciência e Tecnologia (FCT), por ter financiado o meu projeto de doutoramento, através das bolsas PD/BI/113762/2015 e PD/BD/128100/2016.

Por último mas não menos importante, um agradecimento especial à minha família, à Marta, e a todos os meus amigos.

acknowledgements

As the present thesis marks the ending of an importante chapter in my life, I would like to express my gratitude first to those who motivated me to embrace this challenge. Hence, to Professor Romeu Vicente, who has been following closely my evolution as researcher, my heartfelt thanks for your constant and unconditional support, and above all for his patience demonstrated over the last few years. A warm thanks to Doctor Tiago Miguel Ferreira, for his companionship, commitment, dedication, guidance, and motivation. It was indeed, a lovely journey, both inside and outside the water. I extend my gratitude also to Professor João Estêvão for his contagious enthusiasm and optimism, for all the productive meetings, and for his close collaboration throughout my journey as researcher.

I would like to leave a thank-you note to all my colleagues and friends from the Department of Civil Engineering of the University of Aveiro, the Doctoral Programme Infrarisk-, and the Joint Research Centre, and several others with whom I had the opportunity to cross paths with over the past four years, namely to the colleagues at the University of Genoa and to the Gruppo Sismica research team, for their input and motivation. Here, I would like to thank to Professors Sergio Lagomarsino and Serena Cattari for the inspiration, know-how and assertiveness, and to Professor Ivo Caliò and Doctor Bartolomeo Pantò, for their collaboration, and support demonstrated during and after my stay in Catania, which has proved to be determinant for the development of the research project.

I would like to thanks the Board of Studies of the Doctoral Programme Infrarisk- "Analysis and Mitigation of risks in Infrastructures", in particular Professors Carlos Sousa Oliveira and Rita Bento, for their patience, trust and support demonstrated. I would also like to thank Professor Aníbal Costa, for having made available the database related to the reconstruction process of Faial island, from which the great majority of the case studies presented in this thesis were selected. I cannot but offer my thanks to the Portuguese Foundation for Science and Technology (FCT), for having funded my PhD project through the fellowships PD/BI/113762/2015 and PD/BD/128100/2016.

Last but not least, a special thanks to my family, to Marta, an to all my friends.

palavras-chave   Mitigação do risco sísmico; edifícios urbanos antigos; análises estáticas não lineares; modelação com macroelementos; funções de custo de reparação; análise custo-benefício.

resumo   A presente tese tem por objetivo contribuir para o estudo da avaliação da vulnerabilidade sísmica de edifícios urbanos antigos, e subsequentemente, para a mitigação do risco sísmico em centros históricos, através da investigação da eventual correlação entre métodos analíticos e semi-empíricos, que possa levar ao desenvolvimento de uma nova abordagem híbrida. Assim, no Capítulo 1, é feita uma breve contextualização do tópico principal da tese e dos respetivos objectivos e motivações, sendo ainda apresentada a estrutura e organização do documento, assim como a lista das publicações que suportam o trabalho aqui desenvolvido. O Capítulo 2 apresenta uma revisão exaustiva da literatura, de forma a que se possam identificar não só as atuais linhas de investigação neste tópico, mas também lacunas na investigação e eventuais janelas de oportunidade para melhorar o conhecimento científico nesta área específica. No Capítulo 3 são discutidos alguns dos principais desafios associados com as técnicas de inspecção e diagnóstico de edifícios urbanos antigos, com foco para as particularidades dos edifícios integrados em agregados urbanos. Numa segunda fase, são também discutidos os desafios associados à avaliação da resposta sísmica de edifícios urbanos antigos, nomeadamente no que diz respeito às vantagens e limitações da utilização de métodos analíticos baseados em abordagens por macrolementos. O Capítulo 4 apresenta a análise custo-benefício associada à adopção de soluções tradicionais de reforço sísmico na reabilitação de edifícios urbanos antigos. Se numa primeira fase, é analisada, de forma isolada, a viabilidade dessas soluções de reforço, num segundo momento, é aplicado um modelo de análise custo-benefício a quatro casos de estudo considerados representativos, quer do edificado rural quer do edificado urbano da ilha do Faial, nos Açores. O Capítulo 5 apresenta o estudo da correlação entre duas abordagens reconhecidas internacionalmente para a avaliação do risco sísmico de edifícios de alvenaria localizados em centros históricos: o método do "índice de vulnerabilidade" e a "curva de capacidade" resultante da utilização de um modelo numérico simplificado juntamente com uma abordagem estática não-linear. Finalmente, no Capítulo 6, são resumidas as principais conclusões de cada um dos capítulos anteriores, assim como as principais linhas orientadoras para novos desenvolvimentos e trabalhos futuros.

keywords

Earthquake risk mitigation; urban cultural heritage assets; nonlinear static analyses; macroelement approach; repair cost functions; cost-benefit analyses.

abstract

The present thesis aims at contributing for the study of the seismic vulnerability assessment of urban cultural heritage assets, and subsequently, for the earthquake risk mitigation in historic centres, through the investigation of the eventual correlation between analytical and semi-empirical methods, that could possibly lead to the development of a new hybrid approach. Hence, in Chapter 1, the framework of the main topic of the thesis, and the respective aims and motivations, are presented and briefly discussed, along with the outline and organisation of the document, as well as the list of publications that support the work carried out in this thesis. Chapter 2 provides a comprehensive literature review on disaster risk mitigation of UCH assets located in historic centres, by means of adopting a holistic framework about the features of such a complex system. This exercise is fundamental to understand the current streams of thought and to identify new gaps and opportunities that could eventually enhance the knowledge level on this particular field of research. Chapter 3 discusses some of the main challenges associated with survey and inspection techniques for input data acquisition of UCH assets, with particular focus to the investigation of assets located in historic centres, which are most likely enclosed in aggregate. In a second moment, the main challenges concerning the seismic response assessment of UCH assets are discussed, namely focusing on the pros and cons of macroelement approaches. Chapter 4 presents the main findings of a cost-benefit analysis model applied to investigate the integration of traditional seismic strengthening solutions in the rehabilitation of UCH assets. While in a first phase, only the economic viability of using such strengthening solutions was investigated, in a second phase, a cost-benefit model is applied to four different case studies considered representative of both rural and urban masonry building typologies of Faial island, in Azores. Chapter 5 presents the investigation of the correlation between two well-known approaches for the seismic risk assessment of UCH assets in historic centres: the "vulnerability index" method and the seismic "capacity curve" derived by using a simplified numerical model together with a nonlinear static procedure. Finally, Chapter 6 summarises the key conclusions that have been pointed out in the previous chapters of the thesis and outlines the grounds of future developments and research paths.

Research is what I'm doing when I don't know what I'm doing

by Wernher von Braun

Table of Contents

List of Figures

List of Tables

List of Acronyms

ASCE	American Society of Civil Engineers
BC	Building Contents
BCR	Benefit-Cost Ratio
BIM	Building Information Modelling
CBA	Cost-Benefit Analysis
CF	Confidence Factor
CPI	Consumer Price Index
DL	Damage Limitation (limit state)
DPM	Damage Probability Matrix
DT	Destructive Test
EFM	Equivalent Frame Model
EMS-98	European Macrosseismic Scale
FEMA	Federal Emergency Management Agency
GFA	Gross Floor Area
GIS	Geographic Information System
GNDT	*Gruppo Nazionale per la Difesa dai Terremoti*
HL	Human Loss
KL	Knowledge Level
LREC	Regional Laboratory of Civil Engineering of Azores
MDOF	Multi-Degree of Freedom System
MDT	Minor-Destructive Test
NC	Near Collapse (limit state)
NDT	Non-Destructive Test
NGO	Non-Governamental Organisation
NTC	*Norme Tecniche per le Costruzioni*
NZSEE	New Zealand Society of Earthquake Engineering
OPCM	*Ordinanza del Presidente del Consiglio dei Ministri*
PCTL	Percentile
RC	Reinforced Concrete
RD	Repair of seismic-induced damage
RSA	*Regulamento de Segurança e Acções para Estruturas de Edifícios e Pontes*
RSCCS	*Regulamento de Segurança das Construções Contra os Sismos*
RSEP	*Regulamento de Solicitações em Edifícios e Pontes*
SD	Significant Damage (limit state)
SDOF	Single-Degree of Freedom System
SPES	Portuguese Society for Seismic Engineering
SPRHI	Society of Promotion for Housing and Infrastructures Rehabilitation

SRHE	Regional Secretariat for Housing and Equipment of Faial Island
UCH	Urban Cultural Heritage
UN	United Nations
UNESCO	United Nations Educational, Scientific and Cultural Organization
URM	Unreinforced Masonry

List of Symbols

$A_{1,i}$	Exponential curve fitting parameter for a given i
a_g	Peak ground acceleration (PGA)
a_{gC}	Acceleration associated with the performance point, d^*_t
a_{gD}	Structure's demand acceleration
a_{gR}	Reference ground acceleration
$a_{g\,DL}$	Ratio a_{gC}/a_g associated with NC limit state
$a_{g\,NC}$	Ratio a_{gC}/a_g associated with NC limit state
$a_{g\,SD}$	Ratio a_{gC}/a_g associated with NC limit state
BCR_{CC}	Benefit-Cost Ratio obtained for current construction replacement cost
BCR_{CT}	Benefit-Cost Ratio obtained for traditional construction replacement cost
C_b	Shear coefficient
C_{BC}	Replacement cost of the building contents
C_{HL}	Costs associated with human loss
C_R	Replacement cost of the building
C_{RD}	Repair cost
$\overline{C_{RD}}$	Median repair costs
C_{RD_i}	Repair cost associated with a given i
C'_{RD_i}	Updated repair cost associated with a given i
$C_{R,CC}$	Replacement cost for current construction
$C_{R,CT}$	Replacement cost for traditional construction
C_{RS}	Specific cost of each retrofitting strategy
$\overline{C_{SS}}$	Median strengthening costs
C_{vi}	Vulnerability class
d_{cn}	Control node displacement
d_e	Economic damage index
ds	Damage state
d^*_{NC}	Displacement of the equivalent SDOF system associated with the NC limit state
d^*_t	Performance point or target displacement
d^*_u	Ultimate displacement of the equivalent SDOF system
d^*_y	Yielding displacement of the equivalent SDOF system
E	Young's modulus (general)
$E_{1,eq}$	Young's modulus parallel to the floor warping direction
$E_{2,eq}$	Young's modulus perpendicular to the floor warping direction
f	Natural frequency
f_c	Factor to update repair costs based on the annual average rates of change
f_k	Factor to weight replacement costs
$f_{k,BC}$	Normalised deviation between the median C_{BC} for a given damage state

$f_{k,HL}$	Factor associated with the severity level and a given damage state
$f_{k,RD}$	Normalised deviation between the median C_{RD} values and the probability of exceeding a given damage state, p_k
f_m	Mean compressive strength of masonry
f_s	Factor to take into account the variability between the costs of the construction sector in Faial Island and mainland Portugal
f_{tm}	Mean tensile strength of masonry
f_u	Factor to reflect the variability of the intervention cost in rural and urban building typologies
f_{wm}	Timber mean compressive strength
F^*	Base shear strength of the equivalent bilinear SDOF system
F^*_y	Yielding base shear strength of the equivalent SDoF system
F^*_y/m^*	Yielding acceleration of the equivalent SDoF system
G	Shear modulus
G_{eq}	Equivalent shear modulus of horizontal diaphragms
GFA_i	Gross Floor Area for a given i
G_k	Gravity loads
H_0	Average inter-story height
I	Macroseismic Intensity
i	Type of intervention and contract considered
I_{EMS-98}	European Macroseismic Intensity Scale
I_v	Normalised vulnerability index
I^*_v	Vulnerability index (non-normalised)
k	Number of a given damage state
k^*	Stiffness of the equivalent SDoF system
L	Maximum span between load-bearing walls
M_x	Mass participation ratio in the X direction
M_y	Mass participation ratio in the Y direction
m^*	Total mass of the equivalent SDOF system
p_i	Weight of parameter i
p_k	Occurrence probability of a given damage state
Q	Ductility factor
Q_k	Live loads
R^2	Coefficient of determination
r_k	Residuals of the exponential curve fitting
S	Soil factor
s	Average wall thickness
S_d	Spectral displacement
S_{d_u}	Ultimate spectral displacement
S_{d_y}	Yielding spectral displacement
$\overline{S}_{d,ds}$	Median value of the spectral displacement at which a building reaches the threshold of a given damage state
SS_{res}	Residual sum of squares
SS_{tot}	Total sum of squares
$t_{1,i}$	Exponential curve fitting parameter for a given i
T_B	Corner period in the elastic response spectrum
T_C	Corner period in the elastic response spectrum
T_D	Corner period in the elastic response spectrum
T_L	"Nominal life" return period

T^*	Period of the equivalent SDoF system
t_{eq}	Horizontal diaphragm's equivalent thickness
t_{ew}	External walls' thickness
V	Vulnerability factor
V_b	Base shear strength
W	Structure's seismic weight
w	Specific weight of masonry
$y_{0,i}$	Exponential curve fitting parameter for a given i
β_{ds}	Standard deviation of the natural logarithm of the spectral displacement for the damage state ds
Γ	Transformation factor
γ_I	Structure's importance factor
μ_D	Mean damage grade adopted by the EMS-98 scale
υ	Poisson's coefficient
ξ	Equivalent viscous damping
τ_0	Pure tangential shear strength of masonry
Φ	Standard normal cumulative distribution function

Chapter 1

Introduction

Abstract *This introductory chapter will focus on the presentation of the research project that lies behind the present thesis, and includes the discussion of the background and motivation, research aims, and finally, the outline and list of supportive publications.*

Chapter outline

1.1 Background and motivation

Over the past several years there have been numerous large-scale disasters that have caused enormous loss of life, property and widespread damage worldwide. Some of the most recent examples were the 2016 Amatrice earthquake [1] sequence, the armed conflict in Syria [2], or the series of hurricanes that in 2017 hit the island of Puerto Rico, Florida and Houston, in the United States of America. Historic records continue to place earthquakes as one of the most frightening, destructive and deadliest natural disaster ever known by human kind. An evidence of this relies, for example, in the April 2015 Nepal (also known by Gorkha earthquake), the August 2016 Central Italy or the September 2017 Central Mexico earthquakes. The damaged caused by these earthquakes, there is to say, the damaged caused by a poor performance of structures and infrastructures when under seismic loads, depends not only on the intensity, magnitude and epicentral distance of the earthquake, but also on their seismic response. The September 2017 Central Mexico earthquake is one of the most recent examples of how earthquake risk mitigation and preparedness is a worthwhile investment. When comparing the global indexes from the 1985 shock with the September 2017 earthquake, it was possible to observe that, the 32-year investment on a national early-warning system, earthquake drill program, and on enacting adequate seismic regulations to ensure that buildings were correctly designed, helped to reduce the death toll from 10,000 to about 333, and the number of collapsed buildings from 3,000 to 38.

In Europe, particularly in Mediterranean bordering countries, earthquakes have been triggering significant destruction and loss over the last decades. The causes and consequences associated to earthquake risk mitigation of existing structures have been acknowledged by the

European Union, which has expressed great concern about this issue, either by supporting the development and implementation of Eurocodes, promoting supplementary coordination with civil protection bodies, or even by funding numerous research programmes in this particular field. However, there is still much to be done as regards seismic risk assessment and mitigation of old masonry structures, often erected without anti-seismic provisions. The seismic response assessment of these structures brings additional challenges to engineers, as their complex nature in terms of cultural significance, boundary conditions and materials' heterogeneity, for example, hinders the acquisition of input data on the material properties and structural details, and consequently, the correct interpretation of output data. Moreover, while few of these structures retain their original morphology, the great majority have been subjected to many structural transformations in favour of economic interests, often non-engineered, which have been proven to exacerbate their seismic vulnerability. This reality is particularly truth in the case of historic centres. In fact, these are frequently the areas at highest risk, due to the combination of several factors such as: high concentration of old masonry structures and therefore, high seismic vulnerability; high exposure (as historic centres feature the majority of cultural heritage assets and represent a crucial part of our cultural identity), and high population and building density, for example. As the majority of Mediterranean bordering countries' economy is firmly reliant on tourism, the protection and safeguarding of historic centres has becoming one of the hotly debated topics in the political agenda of these countries' leaders.

In Portugal, a country that has experienced one of the most severe earthquakes ever recorded in Europe (the well known November 1755 Lisbon earthquake), great part of the building stock was constructed before the introduction of a more demanding seismic design code (RSA - Safety regulations for buildings and bridges) in 1983 [3]. Additionally, the living conditions offered by historic centres worsen significantly during the last decades, resulting in a massive exodus to peripheral areas, contributing therefore, to an accentuated degradation of disused buildings. To worsen this unfavourable atmosphere, the ageing population and low birth rate index, associated to the financial-economic crisis between 2010 and 2014, contributed, and somehow explain the balance of about 1 million unoccupied dwellings in this country.

Despite this negative framework, the Portuguese economy and in particular the construction sector, encouraged by a substantial increase in tourism in recent years, has begun to reverse this situation by carrying out a series of renovation works in historic centres nationwide. Nonetheless, there are reasons to believe that this wave of renovations is being pursued either on a too superficial (non-structural or minor structural interventions) or intrusive way, in which little respect has been shown by existent materials and construction techniques, usually implying the demolishing of the building apart from its façade (a practice also known as "façadism"). These type of practices are particularly alarming in seismic prone areas such as the metropolitan area of Lisbon or the Algarve region, for example, specially when the latest estimates indicate that within the next decades Portugal might be severely hit by a strong earthquake similar to the 1755 event. Hence, it is of upmost importance to assess the actual seismic response of historic centres, not only to understand to what extent renovation works are respecting existing materials and the good-practices of seismic design, but also to identify the most vulnerable structures, and in this way, minimise the consequences of an eventual earthquake. However, there is not yet a generally accepted methodology or tool that presents an attractive balance between accuracy and applicability at the scale of historic centres. Another challenge that lies behind developing such a methodology is the language

and the terminology used, which should be easily understandable by governing authorities, civil protection bodies, and ultimately, by the common citizen. Despite being often presented as a very interesting alternative, index-based methods (also referred in literature as "Italian approach") are frequently criticised, for example, for using the Macrosseismic Intensity scale to estimate damage in countries where observed damage data from real ground motions is limited [4], or by the ductility value used in the macroseismic approach proposed by Giovinazzi [5]. The latter aspect in particular, is poorly addressed in literature, being for this reason, an issue of great controversy. In addition to this, there is limited understanding about to what extent these index-based methods are sensitive to the structure's ductility, stiffness and base shear capacity.

Bearing in mind the above considerations and giving the wide variety of building typologies in Portuguese historic centres, it was necessary to establish a new taxonomy to better define the class of structures that will be object of study in the present thesis, hereinafter designated as urban cultural heritage (UCH) assets. To understand the concept of UCH assets one should recall the classification proposed by Abbas et al. [6] to architectonic assets, based on a strictly "mechanical" criteria that foreseen the identification of the most relevant macroelements in historic buildings and on the prevailing damage mechanisms which they may be subjected to. According to Abbas et al. [6], the need for this classification arose from the systematic observation of certain damage patterns in function of the assets' morphology (architectonic form, proportions) and technology (type of masonry, nature of horizontal diaphragms, effectiveness of wall-to-wall and floor-to-walls connections), as these behavioural dissimilarities call for different modelling approaches and different damage variables. Thus, UCH assets include existing structures that are theoretically subjected to prevailing in-plane damage, in particular stone masonry residential buildings, palaces and other collective buildings inserted in an urban environment, which yet corresponds to the great majority of the building stock in Portuguese historic centres, as demonstrated, for example, by Vicente [7], Maio et al. [8] or Ferreira et al. [9]. Despite the already mentioned structural transformations that UCH assets might have been subjected to ever since their construction, they usually present a relatively regular plan, both in plan and in height, which fits the intent of using software codes based on the macroelement approach. Finally, it is worth referring that most of the case studies that are going to be analysed in this thesis were selected from a wider database collected during the 10 years' reconstruction process of Faial Island that followed the 1998 Azores earthquake, which was kindly made available by professor Aníbal Costa in the framework of the URBSIS project PTDCECM-URB2564 [10].

1.2   Aims of the research project

Encouraged by the research carried out by Mota de Sá [4] or Ortega [11], this research project aims at investigating and bridging the existing methodological gap between simplified methods, used for the seismic vulnerability assessment at the urban scale, and analytical methods, whose computational efforts are not bearable in large-scale assessments, neither cost- nor time-wise. The ultimate goal of this research project is that of casting a new light on the seismic risk assessment of historic centres through simplified methods. To this end, some of the most important issues that govern the seismic response of UCH assets will have to be addressed before investigating how numerical models can be used to support the development and validation of simplified scoring methods.

From the cultural heritage viewpoint, this research project aims at promoting the preservation and conservation of traditional construction techniques, in order to avoid the loss of identity and the mischaracterisation of historic centres to the so-called new technologies. Moreover, in a time in which more and more economic interests seem to dominate the decision-making process in our society, it is indeed fundamental to emphasise other no less important arguments, associated with the patrimonial value or sustainability in construction. Following the explanation of the general aims of this research project, in the next paragraphs, the objectives outlined for each task are going to be presented in detail.

Task A

In this initial task, a literature review on how earthquake risk mitigation of UCH assets is being tackled worldwide will be presented, emphasising the Portuguese framework and identifying a series of barriers that are hampering progress in this field. Complementarily, this exercise is going to be extended to each particular topic of the research subject. The approach that is going to be used is that of discussing the most recent advances and relevant research projects developed around each particular topic, highlighting the main findings and research opportunities. This is seen as of fundamental relevance not only to identify the main challenges to be addressed but also to understand which and how these challenges might be tackled and investigated.

Task B

Amongst the elements usually present in the classical definition of earthquake risk, the seismic vulnerability is the one most likely to be engineered in order to reduce the seismic risk in a more sustainable and effective away. Therefore, with this Task B, and in line with the candidate's research background, some of the most challenging issues concerning the seismic vulnerability assessment of UCH assets are going to be addressed, in a first moment by identifying the survey and inspection techniques currently available for input data acquisition of UCH assets, and highlighting the particularities of investigating existing structures enclosed in "aggregate". In a second moment, the pros and cons of using different numerical models based on the macroelement approach, which are incorporated in some of the most widely used software codes for the numerical modelling of existing masonry structures, namely the 3Muri® [12] and 3D-Macro® [13], are going to be discussed.

Task C

The investigation of cost-benefit analysis for seismic strengthening is fundamental to investigate the binomial relationship between the investment (cost) associated to different strengthening or retrofitting interventions, and their efficiency on ensuring a certain seismic performance. The need for implementing strengthening interventions results from the main findings identified in the previous tasks, which alert for the following facts: the majority of UCH assets in Portugal were designed without anti-seismic provisions; lack of maintenance and a poor conservation state, constituting, therefore, a highly vulnerable class of structures.

The goal of Task C is that of raising the awareness of property owners and stakeholders not only to the actual cost or investment that seismic strengthening represents in the budget of the global project, but also to the benefits and consequences of preserving traditional construction techniques and materials. It is thus expected that the findings resulting from Task C might assist the prioritisation of intervention strategies and the decision-making process of all agents that are directly and indirectly associated to the renovation of historic centres.

Task D

The final task of this research project, and the most ambitious one, is that of investigating a possible correlation between two well-known measures of seismic vulnerability, widely applied to the assessment of urban UCH assets in seismic prone areas. These measures are the "vulnerability index", a method developed by Vicente et al. [14], and the seismic "capacity curve", obtained by applying, for example, the N2 Method proposed by Fajfar [15], after the computation of nonlinear static analyses.

The idea is to apply the know-how and the findings uncovered in the previous tasks to investigate this correlation. As mentioned above, this task also aims at overcoming some of the drawbacks usually pointed out to such vulnerability index methods (also referred in literature as the Italian approach), as for example by attempting to avoid using the macroseismic intensity scale. Additionally, the relationship between the vulnerability index and the results obtained through nonlinear static analyses [16], and how one can take advantage of numerical models to increase the reliability of such simplified methods, are other aspects that are expected to be investigated in this thesis.

1.3   Thesis outline

The following paragraphs are dedicated to the outline and organisation of the thesis. The correspondence between the chapters of the thesis, the tasks of the research project, described in the previous Section 1.2, and the list of supportive publications (presented in the following Section 1.4) is illustrated in Figure 1.1.

This introductory chapter presents the background and motivations behind the research project and points out the main issues and opportunities to be addressed.

Chapter 2 provides a comprehensive literature review on disaster risk mitigation of UCH assets located in historic centres, by means of adopting a holistic framework about the features of such complex systems. This exercise was fundamental to understand the current streams of thought and to identify new research gaps and opportunities that could eventually enhance the knowledge level on this particular field of research.

Chapter 3 discusses the main challenges associated with survey and inspection techniques for input data acquisition of UCH assets, with particular focus to the investigation of assets located in historic centres, which are most likely enclosed in aggregate. In a second moment, the main challenges concerning the seismic response assessment of UCH assets are going to be discussed, namely focusing on the pros and cons of different macroelement approaches.

Chapter 4 presents the main findings of a cost-benefit analysis (CBA) model applied to investigate the integration of traditional seismic strengthening solutions in the rehabilitation of UCH assets. While in a first phase, the economic viability of using such strengthening solutions was investigated, in a second phase, the mentioned CBA model was applied to four different case studies.

Chapter 5 investigates the correlation between two well-known approaches for the seismic risk assessment of UCH assets located in historic centres: the "vulnerability index" method and the seismic "capacity curve" derived from simplified numerical models.

Chapter 6 summarises the key conclusions by chapter and outlines the grounds of future developments and research paths.
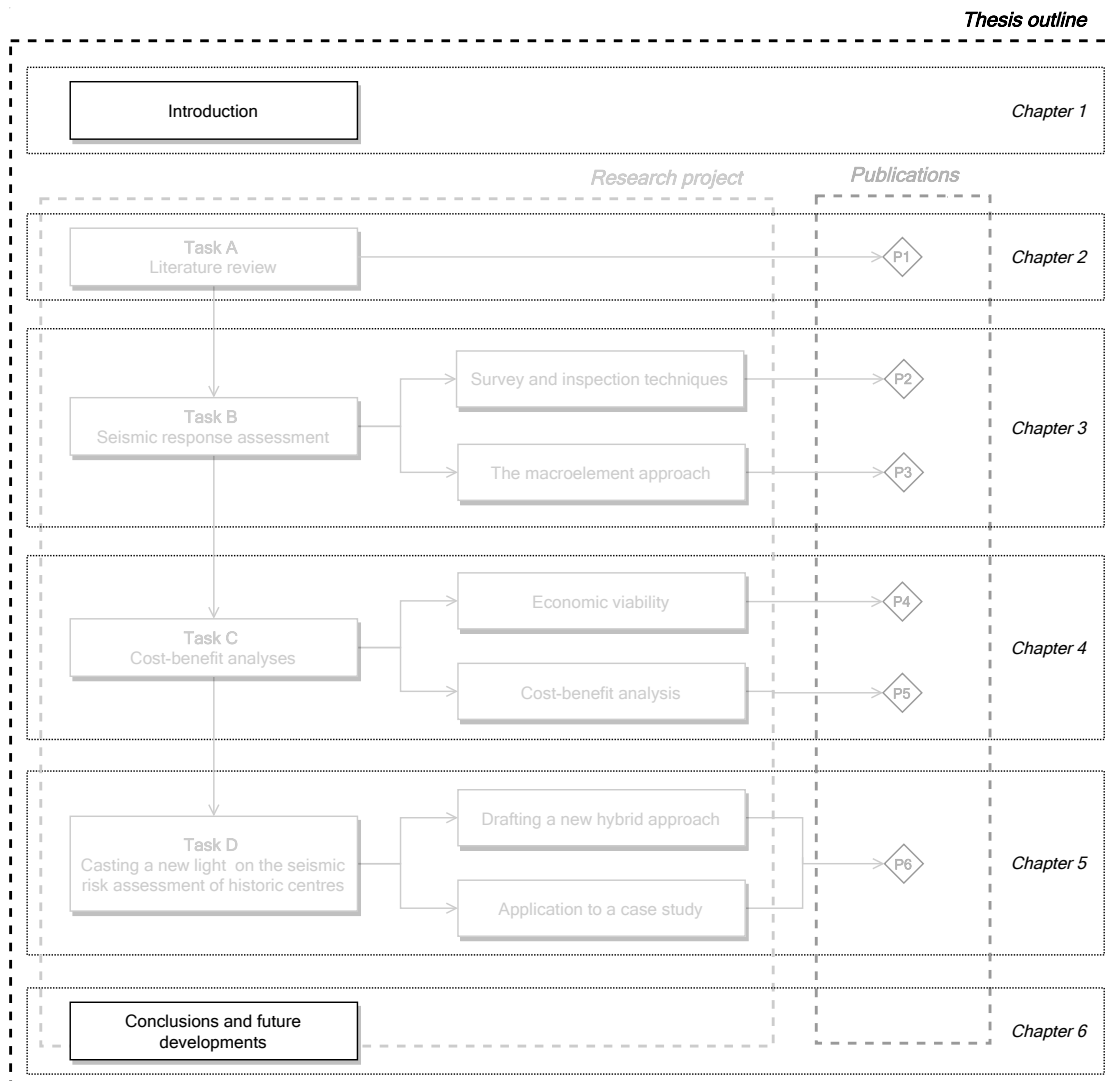
Figure 1.1: Outline of the thesis and the correspondence with the research project and list of supportive publications.

1.4 List of supportive publications

Below, the publications that support the present thesis are listed following the same nomenclature as in the previous Figure 1.1. More information about these publications is available at `www.ruiamaio.weebly.com`.

P1: **Maio, R.**, Ferreira, T.M. and Vicente, R. (2018). A critical discussion on the earthquake risk mitigation of urban cultural heritage assets. *International Journal of Disaster Risk Reduction*, 27(2018), 239–247. URL `http://dx.doi.org/10.1016/j.ijdrr.2017.10.010`.

P2: **Maio, R.**, Santos, C., Ferreira, T.M. and Vicente, R. (2018). Investigation techniques for the seismic response assessment of buildings located in historical centres. *International Journal of Architectural Heritage*, 12(7–8), 1245–1258. URL `https://doi.org/10.1080/15583058.2018.1503363`.

P3: **Maio, R.**, Ferreira, T.M., Estêvão, J.M.C., Pantò, B., Caliò, I. and Vicente, R. (2020). Seismic performance-based assessment of urban cultural heritage assets through different macroelement approaches. *Journal of Building Engineering*, 29(2020), URL `https://doi.org/10.1016/j.jobe.2019.101083`.

P4: **Maio, R.**, Ferreira, T.M., Vicente, R. and Costa, A. (2018). Is the use of traditional seismic strengthening strategies economically attractive in the rehabilitation of urban cultural heritage assets in Portugal? *Bulletin of Earthquake Engineering*, 17, 2307–2330. URL `https://doi.org/10.1007/s10518-018-00527-7`.

P5: **Maio, R.**, Estêvão, J.M.C., Ferreira, T.M. and Vicente, R. (2020). Cost-benefit analysis of rehabilitation interventions carried out in urban cultural heritage assets by integrating the use of traditional seismic strengthening strategies. *Engineering Structures*, 206.URL `https://doi.org/10.1016/j.engstruct.2019.110050`.

P6: **Maio, R.**, Estêvão, J.M.C., Ferreira, T.M. and Vicente, R. (2020). Casting a new light on the seismic risk assessment of historic centres. *Structures*, 25(2020), 578–592. URL `https://doi.org/10.1016/j.istruc.2020.03.008`.

Chapter 2

Literature review

Abstract *This chapter provides a comprehensive literature review on disaster risk mitigation of UCH assets located in historic centres, by means of adopting a holistic framework about the features of such a complex system. This exercise was fundamental to understand the current streams of thought and to identify new research gaps and opportunities that could eventually enhance the knowledge level on this particular field of research.*

2.1 Introduction

This first section aims at highlighting some of the most relevant phenomena and external pressures affecting UCH assets worldwide. In the past decades we have witnessed an increased political focus on cultural heritage, not only because of higher public interest in heritage-related issues but also because cultural heritage is often seen as a means to stimulate economic activity in countries with economic-downturn problems. In fact, cultural heritage is more and more perceived as "a powerful engine of economic development" [17], as it participates directly in the generation of economic value through, for example, tourism activities [18]. When addressing urban cultural heritage, one should adopt a holistic approach to take into account the multitude of intrinsic features of these complex systems, such as

social, cultural, historic, artistic and architectonic, economic, morphologic and sustainable aspects. The need for this holistic approach derives from the dynamic nature of cities, which are continually changing according to society's demands over time. Therefore, to pursue the sustainable preservation of urban cultural heritage, UNESCO suggested the need of building up strategic and dynamic alliances between the various actors in the urban scene, foremost between public authorities, developers and entrepreneurs that operate in there [19].

There are multiple causes that have been identified as responsible for transforming urban settlements and their historic areas in drivers of economic growth in many regions of the world, acquiring a new role in both cultural and social life, such as, for example, the sharp increase in the world's urban population, the scale and speed of development and the changing economy [20]. However, if this transformation and economic growth are not placed on a sustainable footing, it may foster the development of undesirable phenomena in UCH assets, such as urbanisation and globalisation, market over-exploitation and mass tourism, for example.

According to the UN [21], it was estimated that 54% of the world's population was living in urban areas by 2014. If in 1950 this percentage was estimated in 30%, by 2050 it is expected that 66% of the world's population will live in urban areas. This unprecedented and generalised urbanisation phenomenon observed in many urban areas might trigger, according to Agapiou et al. [20], the fragmentation and deterioration of heritage. However, in many other urban areas across the globe, the opposite scenario has been observed, where several factors have been contributing to this loss of centrality and the exodus of historic centres: poor conservation or comfort conditions of existing buildings; increased air pollution rates; increased criminality and insecurity rates, and poor accessibility [22, 23]. In order to aid reversing this phenomenon up to more balanced and sustainable terms, Laprise et al. [24] developed an innovative study about regeneration strategies for disused urban areas. In the same scope, Radoslav et al. [25] have done some very creditable research about revitalisation strategies suitable to historic centres.

2.2 Disaster risks to UCH assets

Given the current rate of urbanisation, and the inherent risks that are faced by densely populated urban areas, there is an increasing need for a specific approach to assess and manage disaster risk in such complex areas. As documented in [26], these disasters have been causing widespread damage to cultural heritage assets located in urban areas worldwide.

As one might be aware of, many UNESCO world heritage sites are exposed to several hazards and threats, which may endanger their integrity and compromise the values of the Convention, triggering irrevocable consequences to both local communities and cultural heritage assets itself, particularly in situations where local authorities and site managers are unprepared. UNESCO [27] understands that disaster risk to cultural heritage comes from both external and internal causes. While external causes are associated with the disturbance or damage to cultural heritage sites motivated by several hazards such as earthquakes, tsunamis, destructive sabotage, or military conflicts, internal causes are related to the intrinsic fragility of a determined cultural heritage asset and its sensitivity to the surrounding environment, which contributes to the asset vulnerability. Wang [28] however, proposed a different classification for disasters with the potential to harm cultural heritage, based on their predictable nature.

In this thesis, emphasis will be given to earthquakes, as they are still one of the most destructive hazards to urban cultural heritage not only in Portugal [29, 30], but also in most of the Mediterranean countries [31, 32, 33, 34]. Therefore, it is clear that proactive measures should be implemented to mitigate the earthquake risk of UCH assets and increase the awareness and preparedness of communities. These measures should be designed together by skilled professionals, administrators and policy makers, and must respect both the principles of risk management and the historic, aesthetic and other values of cultural heritage. Complementarily, it is important that these measures are implemented on the ground by building contractors, engineers, architects, and all the actors involved in the renovation and strengthening of UCH assets. To this end, it is fundamental to have transparent legislation and supervision monitoring all the stages of the design and building operations. Bearing in mind the above, and given the lack of international guidelines concerning disaster risk mitigation and structural assessment of UCH assets, the present literature review features a brief policy-driven framework covering some of the most relevant challenges and projects recently carried out on this subject.

2.3 Earthquake risk mitigation of UCH assets

Earthquake risk mitigation is today placed as a top priority in the political agenda of the governing authorities of most of the Mediterranean countries. Recent devastating earthquakes raised the awareness of scientists and national civil protection bodies, encouraging the development of proper risk mitigation strategies geared for earthquake risk in urban areas, which can be found for example in [26, 35, 36, 37, 38, 39, 40, 41]. These strategies, recently assembled by Maio et al. [42], are typically focused on identifying the most vulnerable zones within urban areas, which are often associated to historic centres, in order to enhance both the response and recovery capacity in the event of an earthquake. Neglecting the implementation of adequate risk mitigation measures naturally limits this response and recovery capacity. Hence, identifying and perceiving the potential hazards affecting urban cultural heritage is imperative to guarantee an effective post-event response [8]. Investing in prevention, is cost-wise, the most sustainable strategy to mitigate earthquake risk, being, therefore, one of the reasons this literature review is essentially focused on preventive strategies.

The following set of measures have been compiled, for example, in Maio et al. [42] for the improvement of preparedness and urban resilience of communities located in seismic-prone areas:

- Development of effective communication, warning and response systems, adequately integrated in the action plans;

- Development of emergency, escape, rescue and rehabilitation plans, which might be rapidly activated in the event of a seismic catastrophe;

- Development and implementation of awareness-raising campaigns targeted to citizens, with a strong educational component on basic information about earthquake risk and emergency procedures;

- Development and follow up of prevention and earthquake risk mitigation plans by governing authorities and civil protection bodies;

- Implementation of special life and damage insurance policies for earthquakes, in order to enhance the recovering capacity of the affected victims and enable international funding to support as many victims as possible;

- Early establishment of search and rescue teams, as well as volunteering groups;

- Preparation of financing mechanisms for rehabilitation and reconstruction programmes, ready to be activated at any time;

- Implementation of training programmes and emergency drills to identify and rectify eventual flaws in the action plans.

Earthquake risk mitigation of UCH assets should involve at least the evaluation of three fundamental elements, highlighted in the diagram of the following Figure 2.1: hazard, vulnerability and exposure. The data processing phase should culminate by evaluating the direct physical damage. Finally, as output data, direct and indirect economic losses should be evaluated as a function of direct physical damage.

The preservation of UCH assets must guarantee not only their capacity of lasting over time against natural decay without losing their authenticity and usability but also their capacity to withstand natural hazards and extreme events with a certain and expected structural performance. This means that the need of guaranteeing an "acceptable level" of structural safety for building's occupants should be always related to the principle of "minimum intervention" on the building itself. However, the definition of "acceptable" safety levels, as well as the concept of "safety", still represents an open issue, particularly in the case of monumental buildings [43]. Thus, the risk assessment of such buildings is a great challenge not only due to structural and architectural components but also to movable and unmovable artistic assets.
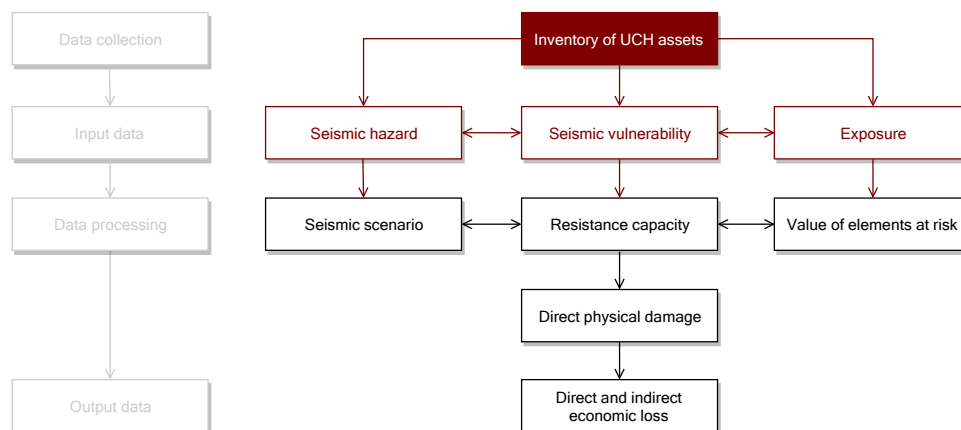
Figure 2.1: Flow diagram with the fundamental elements and steps for the evaluation of earthquake risk in UCH assets.

As already mentioned in Chapter 1, the causes and consequences associated with earthquake risk mitigation of existing structures have been acknowledged by the European Union, which has expressed great concern about this issue, either by supporting the development and implementation of Eurocodes, or by funding numerous research programs in this particular field, as the EU-CHIC [44], ONSITEFORMASONRY [45], PROHITECH [46], NIKER [47],

or the PERPETUATE [48, 49] research projects. The later, was recently funded by the European Community's Seventh Framework Programme, and aimed at developing not only a new methodology for the assessment of earthquake risk of cultural heritage assets in Mediterranean bordering countries, but also a new framework for the design of strengthening interventions. The strategy proposed within the PERPETUATE project [48], to tackle this very important and complex issue, is illustrated in the following Figure 2.2.
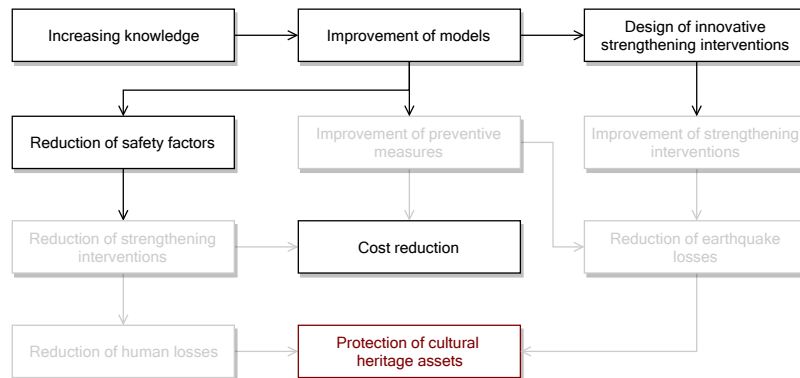
Figure 2.2: Flow diagram presenting the strategy proposed in the PERPETUATE project for the protection of cultural heritage assets. Adapted from Lagomarsino and Cattari [48].

Despite all these efforts, there is still much to be done in this regard, particularly in which concerns the oldest and most vulnerable buildings constructed without any anti-seismic provisions, often referred to as non-engineered structures. Furthermore, these assets underwent many transformations over centuries and often reveal a lack of efficient connections among structural elements, being therefore considered highly vulnerable to earthquakes.

Within the broad range of typological classes and building materials that might be included in the definition of UCH assets, masonry structures are one of the most common not only in Europe, but worldwide. Hence, in order to mitigate the earthquake risk of such structures, it is necessary not only to develop reliable models, and adequate performance-based assessment procedures, but also to account for uncertainties that should be interpreted and differentiated with regard to their type and source.

Coming back to the main topic, in the following sub-sections the discussing of earthquake risk mitigation of UCH assets will be undertaken at the three main phases: pre-event; emergency and response, and post-event.

2.3.1 Pre-event phase

The idea of "preventive conservation" is now the primary focus of cultural preservation worldwide [28]. The use of friendly-user multi-risk assessment tools, connected to a relational database within GIS (Geographical Information System) environments, data about the constructive characteristics, the conservation state or the seismic vulnerability, but also the development of integrated risk assessment analysis, loss scenarios, and cost-benefit analysis. Therefore, these tools became essential for the prediction of vulnerability and fragilities on UCH assets, proving a global and easy-to-read view of the area under assessment.

In this sense, on the one hand, acknowledging both the general poor conservation state and the high vulnerability, normally associated with UCH assets, it is crucial to implement

adequate structural strengthening interventions for mitigating this vulnerability and therefore, its associated risk.

On the other hand, forces should be also concentrated on raising communities' preparedness, awareness, and perception on earthquake risk and the value of cultural heritage. This is only possible through the implementation of proper education and communication initiatives. The factors that affect how risks are perceived determine a person's emotional response to risk information [50]. Levels of fear, worry, anxiety, anger, and outrage tend to be lower when a risk is perceived to be well understood and relatively well known by scientific community [51]. One of the most common ways to increase risk awareness and assess the risk perception of communities is the creation and dissemination of both information and communication initiatives, such as the organisation of risk awareness campaigns. Finally, volunteering and aiding mechanisms should be established in order to build capacity for the emergency and response phase.

2.3.2 Emergency and response phase

In this phase, the key priority is the safeguarding of human life by implementing rescue action plans. Thus, the promptness of the support provided by volunteers, NGOs, neighbouring countries and external partners will define the preparedness level of a determined urban area. The involvement of these actors is particularly important in terms of social support. The second priority is usually the preparation of temporary settlement camps and infrastructures to host homeless and injured people. In addition to this, medical aid and psychological support should also be rapidly made available. Moreover, it is in the emergency and response phase that the first in-field technical surveys are carried out to assess the level of damage inflicted on infrastructures. These surveying activities are usually conducted on the basis of a strong cooperation between the scientific community and civil protection bodies. Some insightful considerations regarding the general framework for emergency planning in Portugal and worldwide, are presented in [42].

2.3.3 Post-event phase

Even though the damage assessment of buildings and infrastructures is initiated quite soon in the emergency and response phase, these activities are very likely to continue several months following the event, being, therefore, a very demanding and complex task since it involves in-field cooperation of different actors. Given their particular structural complexity and economic value, UCH assets require very good surveying and judgement skills, and for this reason, trained professionals. The following priority measures are usually taken into consideration in the post-event phase: temporary sheltering; recovery of local public system as a whole; revitalisation of local economy and transport networks; structural retrofitting and strengthening interventions of industrial infrastructures and of other assets and facilities. In addition, containment works should be promptly carried out to avoid further degradation of UCH assets. Usually, these containment works are implemented by means of provisional tie-rods, steel strapping or wooden containment structures, as outlined for example in [52, 53].

2.4   The context of historic centres in Portugal

In Europe, particularly in Mediterranean bordering countries, earthquakes have been triggering significant destruction and loss over the last decades. The causes and consequences associated to earthquake risk mitigation of existing structures have been acknowledged by the European Union, which has expressed great concern about this issue, either by supporting the development and implementation of Eurocodes, promoting supplementary coordination with civil protection bodies, or even by funding numerous research programmes in this particular field. However, there is still much to be done as regards seismic risk assessment and mitigation of old masonry structures, since they are often erected without anti-seismic provisions.

The seismic response assessment of masonry structures brings additional challenges to engineers, as their complex nature in terms of cultural significance, boundary conditions and materials' heterogeneity, for example, hinders the acquisition of input data about the material properties and structural details, and consequently, the correct interpretation of output data. Moreover, while few of these structures retain their original morphology, the great majority have been subjected to many, often non-engineered, structural transformations in favour of economic interests, which have been proven to exacerbate their seismic vulnerability. This reality is particularly truth in the case of historic centres. In fact, these are frequently the areas at highest risk, due to the combination of several factors such as: high concentration of old masonry structures and therefore, high seismic vulnerability; high exposure, as historic centres feature the majority of cultural heritage assets and represent a crucial part of our cultural identity, high population, and building density, for example. As the majority of Mediterranean bordering countries's economy is firmly reliant on tourism, the protection and safeguarding of historic centres has becoming one of the hotly debated topics in the political agenda of these countries' leaders.

Portugal, in particular, has experienced both the most devastating and the most severe earthquake ever recorded in Europe, in terms of magnitude, respectively the well known November 1755 Lisbon earthquake and the 1969 earthquake that struck western Portugal and Morocco [54]. In addition to this, great part of the building stock in Portugal was constructed before the introduction of a more demanding seismic design code (RSA - Safety regulations for buildings and bridges) in 1983 [3]. Additionally, the living conditions offered by historic centres worsen significantly during the last decades, resulting in a massive exodus to peripheral areas, contributing therefore, to an accentuated degradation of disused buildings. To worsen this unfavourable atmosphere, the ageing population, low birth rate index, and the financial-economic crisis that overtook the country between 2010 and 2014, contributed, and somehow explain, the balance of about 1 million unoccupied dwellings. For these reasons, the last decade has been marked by an unceasing dialogue between, the Portuguese scientific community alongside SPES, and the public authorities and governments' leaders, regarding the urgent need to promote active actions for the earthquake risk mitigation in Portugal.

Given the substantial growth in tourism observed in the past few years in Portugal, the economy, and the construction sector in particular, has been recovering from a severe economic crisis, and many interventions have been carried out ever since nationwide. The revitalisation of urban renovation was assumed as one of the top priorities of the XVII Constitutional Government of Portugal, as at the time, the renovation of the existing building stock only represented about 6.5% of the construction sector, far below the 37% of the European average [55]. This led the Government to issue the Decree Law 307/2009 of

October 23, 2009 [56]. where the legal framework for urban renovation was designed.

The Government that followed made the first amendments to the Decree Law 307/2009, by issuing the Decree Law 32/2012 of August 14, 2012 [55], designed to provide specific framework for the protection and renovation of existing structures exclusively located in classified urban areas. The Decree Law that followed, the 53/2014 of April 8, 2014 [57], allowed the non-observance of legal framework supervening the original construction period, if, and only if, these interventions would not cause or exacerbate the non-compliance with the current legislation in force, or improve the safety and salubrity conditions of the building, and if the respective constructive provisions would be adequate for the structural and seismic safety of the building. Despite its exceptional character, the Decree Law 53/2014 has been a subject of great controversy, as it is known, for example, that at the time of the Building Census Survey of 2011, 25% of the Portuguese building stock was designed with no explicit seismic provisions (i.e., constructed before 1958). Moreover, 37% of the building stock was constructed while the first seismic design codes (RSCCS, RSEP), which might not guarantee adequate seismic performance, were in force [3]. In any case, and disregarding the eventual lack of assertiveness and clarity of the Decree Law 53/2014, the non-observance of current legal framework must be identified and justified by the civil engineer responsible for the renovation design project through a declaration of responsibility.

Despite this encouraging atmosphere, which could have constituted an excellent opportunity to conciliate the implementation of adequate seismic strengthening with the renovation of UCH assets, there are reasons to believe that the upsurge of interventions to UCH assets has been pursued either on a too superficial or intrusive way. While in the first case, non-structural or minor structural interventions have been carried out without any anti-seismic provisions, in the second case, little respect has been shown to traditional construction techniques and materials, usually involving the demolition of the whole building except for its façade (a common reconstitution practice also known as "façadism"). If the carrying out of these practices is undeniably wrong from the conservation viewpoint, their legitimacy from the structural viewpoint raises many questions, particularly in seismic prone areas such as the metropolitan area of Lisbon or the Algarve region, as latest estimates foresee that within the next decades Portugal may be severely hit by a strong earthquake similar to the historic 1755 event.

Fortunately, a new arrangement applicable to the renovation of existing buildings and building units, within or outside classified urban areas, was recently issued in Portugal [58]. This new arrangement takes precedent over the previous legislation, and includes the compliance not only with the structural Eurocodes, but also with a new Ordinance 302/2019 [59] specifically designed to better address the always controversial "seismic vulnerability" issue. In short, the Ordinance 302/2019 defines not only the terms on which the seismic vulnerability of existing buildings must be or not evaluated and subsequently reported, but also the terms on which seismic retrofitting or strengthening is required. This new arrangement naturally brings a new opportunity for doing things right, or at least better.

2.5 Seismic vulnerability and risk assessment

Risk assessment analysis encompasses a broad set of necessary instruments, such as multi-criteria decision analysis, probability analysis, Bayesian networks, event and fault trees, Monte Carlo simulation, which are far from being accessible by non-academic audiences. If not

carefully used, they may lead to erroneous conclusions and decisions supported by "recognised scientific knowledge", with undesirable and serious impact in several domains [4]. According to Mota de Sá [4], even if an adequate method for measuring the impact of earthquakes on multiple criteria would be developed, aggregating the results at a convenient scale remains a huge challenge. The process of ranking solutions with respect to risk, a common goal of complex approaches, is usually hindered by a broad degree of inconsistency [60]. Moreover, the aggregation of multiple criteria in a unique final number to classify risks, can result in an aleatory combination of contents [61]. Despite the merit and contributions of these approaches as a result of their complexity, the number of variables involved, their degrees of uncertainty, and the ways in which they are combined, render these models too hard to understand by non-academic audiences and so, mostly useless to citizens and stakeholders [4]. Furthermore, given the existing conflicting interests and lack of understanding of scientific findings, final decisions are often based on political and economical interests rather than on the technical ones, as argued by Hunter and Fewtrell [62].

The seismic vulnerability can be understood as the intrinsic predisposition of an element to suffer damage from a seismic event of a given intensity, and is considered by many authors, as the most eager element to be mitigated [63]. This section will be exclusively dedicated to the literature review of seismic vulnerability assessment methodologies suitable to UCH assets.

This field of research has been developed according to different streams of thought over the years, hindering the possibility of achieving a unique and consensual categorisation of all the existing methodologies. One of the first proposals for such a classification was given by Corsanego and Petrini [64], in which seismic vulnerability assessment methodologies were categorised in four main groups, as a function of the potential of their output: direct; indirect; conventional, and hybrid methodologies.

Calvi et al. [65] instead, classified these methodologies into the following categories: empirical; analytical, and hybrid. The stream of thought implicit in empirical methods usually fall upon damage probability matrices (firstly proposed by Whitman et al. [66]), vulnerability index methods (firstly developed by Benedetti and Petrini [67] and further adapted to the Portuguese building stock by Vicente et al. [14]), continuous vulnerability curves, or screening methods, for example. Analytical (or mechanical) methods tend to feature slightly more detailed and transparent vulnerability assessment algorithms with direct physical meaning, that not only allow detailed sensitivity studies to be undertaken, but also the straightforward calibration of various characteristics of the building stock and hazard sources [65]. Finally, hybrid methods have demonstrated their usefulness particularly when there is a lack of damage data at certain intensity levels for the geographical area under consideration. Hybrid methods can also be used to calibrate analytical models [65]. These methods combine post-earthquake damage statistics with analytical damage statistics from a mathematical model for a given building typology, as demonstrated, for example, in the research developed by Giovinazzi [5].

In 2012, Chever [68] proposed a classification defined in function of the scale and purpose of each methodology, which is indirectly associated with the resources and time available for carrying out the required assessment. This will in turn dictate the type of approach or methodology to be used, and subsequently, the level of accuracy and type of output. In Chever's proposal, these methodologies can essentially operate at the following assessment scales: that of thousands of buildings, as for example by Silva et al. [69]; few hundreds to few dozens as in [14] or [70], and of individual buildings, as for example in [71] or [72].

2.6   Criteria for the classification of methodologies

Even though there are several other proposals for the classification of seismic vulnerability and risk assessment methodologies for masonry buildings in the current literature [5, 73, 74, 75, 76, 77], there is still a clear lack of consistency in the terminology used in these studies. For the sake of simplicity, and given the vast number of reviews focusing on the discussion of some the most widely used methodologies, this section aims at providing a consistent and consensual criteria for the classification of such methodologies, that can directly or indirectly address the most distinct aspects underscored by the above-mentioned authors. Thus, instead of developing a new criteria with an entirely new technical terminology, the aim of this section is that of promoting a shared understanding among the global scientific community, concerning the taxonomy used for classifying existing methodologies. The criteria given in the following Figure 2.3 was adopted from Boschi [73], and it is one of the most complete and comprehensive classification proposals, consisting on the categorisation of three fundamental aspects: the detail level, type of output, and quality of data and assessment tools.
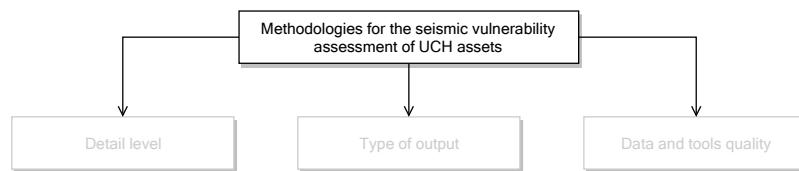
Figure 2.3: Criteria for the classification of existing methodologies for the seismic vulnerability and risk assessment of existing masonry buildings, adapted from Boschi [73].

2.6.1   Detail level

This first aspect concerns to the "level of detail" of the elements under study and it is highly reliant on the detail of the input data available and on the purpose of the assessment. This aspect is addressed in [68, 73], however by means of a different terminology. As shown in the flow diagram of Figure 2.4, there are three different approaches, of increasing level of detail, to evaluate seismic vulnerability: first; second, and third level approaches.
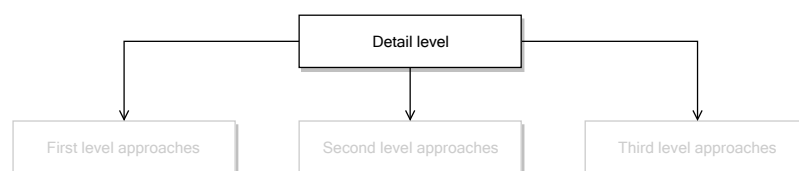
Figure 2.4: Detail level of existing methodologies for the seismic vulnerability and risk assessment of existing masonry buildings.

First level approaches are suitable to large-scale assessments (e.g. urban areas or historic centres) and include methodologies that resort to large amount of simple and mainly qualitative data. According to Boschi [73], the level of detail of the input data is not sophisticated, and it is usually provided either by census data, municipalities' archives, or through "in

situ" survey and inspections. Examples of this type of approach can be found, for instance, in [14, 69].

Second level approaches are based on mechanical models that rely on a higher quality of both geometrical and structural information of a given building typology, as the case of the studies carried out by D'Ayala and Speranza [70] or by Restrepo-Vélez and Magenes [78], for example.

Finally, third level approaches involve the use of numerical models that require a complete and rigorous survey of individual buildings and a throughout knowledge of geometry and materials' properties of all structural elements, as the case of the 3Muri® [79] and 3D-Macro [13] programs based on the macrolement approach, or the DIANA FEA software [80], for example. It is worth noting that when moving from first to third level approaches one should be aware of the following consequences:

- Increased computational effort resulting from shifting from rapid or simplified to detailed and more complex structural analyses;

- The need of more specialised and skilled workforce;

- Shifting from large-scale assessments to individual buildings' scale.

2.6.2   Type of output

The second criterion refers to the type of output or "intended results" of these methodologies (in Figure 2.5), an aspect that was first addressed in [64] and that has been adopted by many scientists ever since, as in Calvi et al. [65] or Vicente et al. [14]. In 2016, Boschi [73] adapted this criterion that distinguishes the existing methodologies in three main groups: direct; indirect, and hybrid techniques. These techniques differ on the number of steps involved in the definition of the risk assessment.

Direct techniques use only a one-step process to estimate the damage caused to a structure by an earthquake, and usually employ two different types of methodologies: typological and mechanical. Typological methodologies assign typological classes to each structure located within the building stock, accounting for different aspects that influence the seismic response of each class, as in the case of methods based on Damage Probability Matrices (DPM) [81, 82]. The damage probability of a determined building class is then determined through post-event damage observation data. On the other hand, mechanical methodologies represent structures either through simplified [70, 83] or more detailed models [13, 79, 80].

Indirect techniques, instead, require a two-step process to estimate damage. Vulnerability index-based methodologies (also known as "scoring methods") are one the best examples of indirect techniques, and can be found for example in [8, 67, 84]. In this type of methodologies, seismic vulnerability in the form of an index is estimated in a first phase either through available information (census data or municipalities' archives, for example) or "in-situ" survey and inspection campaigns. In a second phase, the damage associated with each structure is estimated by using existing statistically-based correlations derived from post-event damage observation data.

Finally, hybrid techniques combine the features of both direct and indirect techniques. An example of such techniques is the macrosseismic method developed by Lagomarsino and Giovinazzi [85], which combines the characteristics of typological methodologies (direct) and indirect techniques, by considering the vulnerability classes defined in the EMS-98 scale [86] and a vulnerability index, respectively.
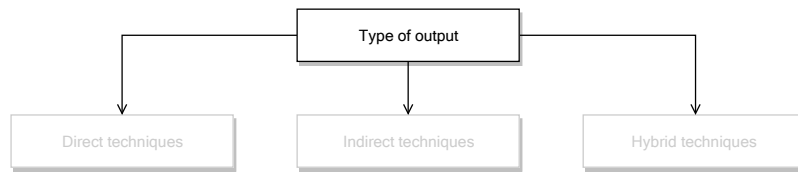
Figure 2.5: Type of output of existing methodologies for the seismic vulnerability and risk assessment of existing masonry buildings.

2.6.3 Data and tools quality

The third and final criterion, shown in the following Figure 2.6, concerns to the quality of the input data and the tools (or methods) intended to be used in the assessment. This criterion covers the same three categories as in the classification proposed by Calvi et al. [65]: empirical; analytical, and hybrid methodologies. In the following paragraph, each category will be explained in detail.

Empirical methods are either based on expert's judgement opinions or on post-event damage observation data. The results of empirical methodologies are usually presented by means of damage-motion relationships such as DPM, as in [81, 82], and fragility curves, as for example in [87]. As these methodologies are used for large-scale assessments (first level approach) they usually require the qualitative evaluation of few parameters, which is often carried out through "in situ" inspections. The outputs of empirical methodologies are usually qualitative and representative of a building class or typology with similar structural characteristics.

Analytical methods use mechanical or numerical procedures to evaluate the seismic vulnerability of structures, and can be distinguished between methods that use simplified approaches, to which a low computational effort is associated, and more complex methods that resort to modern and refined analyses, being therefore, more demanding in terms of computational effort. These methodologies require a large amount of information and a throughout knowledge of all structural components under study. For this reason, the adoption of analytical methods is naturally associated with small samples of buildings [73].

Finally, hybrid methods combine the two above-mentioned categories and are generally used at the urban scale, as in [88, 89, 90].
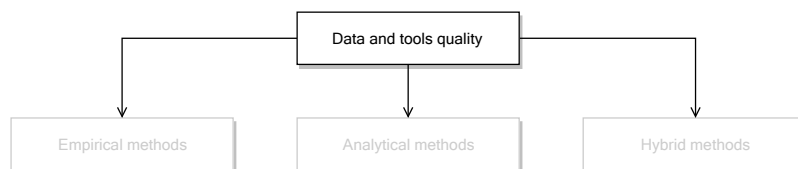
Figure 2.6: Data and tools' quality of existing methodologies for the seismic vulnerability and risk assessment of existing masonry buildings.

2.7 Intervening in UCH assets

It is known that, urban cultural heritage brings significant challenges either in phases such as diagnosis, monitoring, conservation, maintenance, strengthening or retrofitting. This inher-

ent complexity naturally limits the application of modern legal codes and building standards. Therefore, specific recommendations are desirable and necessary to both ensure rational methods of analysis and repair methods appropriate to the cultural context.

Asteris and Giannopoulos [91] addressed some of these issues by presenting a strategy for the vulnerability and structural assessment of masonry structures, whose flow diagram is illustrated in Figure 2.7.
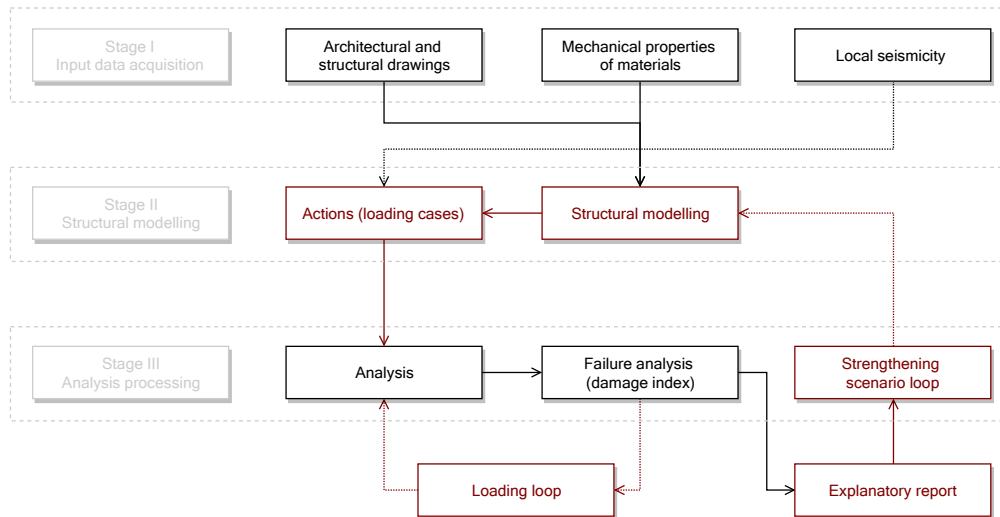
Figure 2.7: Flow diagram with the methodology proposed by Asteris and Giannopoulos [91] for the vulnerability and structural assessment of masonry structures.

According to these authors, the seismic vulnerability assessment of masonry structures should include three different stages: input data acquisition; structural modelling, and analysis processing. According to Spyrakos [92], by considering the seismic response of both structural and non-structural elements and artistic assets, performance levels may be defined in relation to different performance targets, associated with the functionality and the cultural features of structures. Modern seismic design codes, applicable both for the design of new buildings and for the assessment and rehabilitation of existing ones, are based on these performance-based assessment approaches. The EN 1998-3 [93], recently in force in Portugal [58], specifies as T_L equal to 50 years, the "nominal life" period of a structure. Additionally, it defines three building performance levels (limit states) considered appropriate for the seismic protection of ordinary new buildings: near collapse (NC); significant damage (SD), and damage limitation (DL). The methodology proposed by Spyrakos [92] introduced the term "nominal life of an intervention", which defines the time for which the intervention ensures a given performance level. Furthermore, as historic buildings may be considered to belong to importance class III or IV, requiring higher standards and actions characterised by high return periods, their preservation is likely to require more intrusive interventions in order to meet the safety standards for new constructions [92]. However, according to the principles for interventions in historic buildings and monuments, less intrusive strategies should be imposed. In general, interventions in UCH assets should satisfy the following three principles: reversibility, durability in time, and feasibility of the proposed strategy.

The principles for the selection of a determined seismic vulnerability methodology should be based on the above-mentioned criteria that cover the classification of such methodolo-

gies: the "scale" of the assessment (or detail level), the type of output, and the type of data and tools used. The insightful discussion about the advantages and drawbacks of each methodology, carried out in [4, 65, 73], allows one to better understand the most significant differences between some of the most widely used methodologies, and therefore to make a more sustained decision. Naturally that the likelihood of deciding for third level approaches increases when the level of detail concerning the geometrical and structural properties of our sample of buildings is high. Ideally, and according to Calvi et al. [65], an optimal methodology should: incorporate the most recent developments in the field of seismic hazard; explicitly account for all sources of uncertainty; be transversal to different construction practices and building typologies; allow for the inclusion of retrofitting measures, and find a balance between the computational effort and the amount of detailed input data that is required and the consequent degree of confidence in the results. However, it is very unlikely that a single methodology can eventually fulfil all of these requirements simultaneously. Thus, it appears that the ideal approach needs to incorporate the positive aspects of different vulnerability assessment methodologies, the so-called hybrid approaches.

Independently from the nature of the approach, it is important that the outputs resulting from such methodologies are clearly oriented to end-users, meaning that they should be user-friendly and have an easily understandable language, so that they might be properly interpreted by civil protection bodies and decision-makers in general.

2.8   Final remarks

The present chapter aimed at addressing the most important aspects concerning the earthquake risk mitigation of UCH assets. Due to the acknowledged relevance of seismic vulnerability in this complex equation, particular attention was given to existing vulnerability methodologies for the assessment of masonry buildings located in historic centres, and to their respective conceptual differences. In this regard, a criteria for the classification of such methodologies, which included the most important aspects frequently covered in the literature, was presented and discussed. Finally, the major challenges regarding the protection of masonry UCH assets were highlighted.

From the policy-driven and decision-making viewpoints, the protection of UCH assets should be based on a comprehensive knowledge of earthquake risk in order to define more proficient mitigation strategies and outline strengthening interventions that can possibly contribute to the reduction of their specific vulnerability and, consequently, for the increase of the overall resilience of historic centres. Moreover, the need for a common approach and adequate recommendations for the structural assessment of UCH assets should be further considered a must-need priority. From the risk modelling and analysis viewpoint, if on the one hand it is fundamental to address uncertainties and inconsistencies often concealed in estimations, avoiding this way the dissemination of erroneous conclusions and biased results, on the other hand, it is not less important that risk intensity measures and indicators can be easily understood and interpreted not only by governing and civil protection authorities, but also by stakeholders and citizens.

Chapter 3

Seismic response assessment

Abstract *This chapter discusses, in a first moment, the main challenges associated with survey and inspection techniques for input data acquisition of UCH assets. In a second moment, the main challenges concerning the seismic response assessment of UCH assets through different macroelement approaches is going to be discussed.*

3.1 Survey and inspection techniques

The preparation of an adequate investigation plan and the extent of data to be collected is highly reliant on many aspects, such as the category of the architectonic asset, the importance of the built environment and of the site morphology, or the resources available, for example.

In what regards the seismic response assessment of UCH assets, the amount and detail of data also depends on the scale of assessment, and current state of occupation and conservation. Within this framework, this section provides an overview of the investigation techniques currently used in survey operations for improving the knowledge level of UCH assets within historic centres. These survey and inspection techniques can play a crucial role on supporting the seismic response assessment of UCH assets, not only for a preliminary acquisition of input data, but also in a latter stage, where initial estimations might need to be updated or revised. Finally, and despite the investigation of the "aggregate effect" is outside the scope of this thesis, in this Section, the main particularities associated with the survey and inspection of UCH assets enclosed in aggregate, are going to be addressed.

3.1.1 Introduction

The reliability of seismic response assessment and earthquake risk mitigation of UCH assets is strongly influenced by the completeness and the accuracy of the outlined investigation plan. Cultural heritage assets located within historic centres naturally require a closer attention given the inherent complexity usually associated with these ancient constructions. On one hand, these assets would ideally require both an intensive and extensive investigation of all structural and non-structural elements, as they are often subjected to many transformations over the centuries, hindering the extrapolation of the data acquired for a single element representative of diagnosis of the global structure. However, this is not always conceivable in large-scale assessment practice, due to both economic and human resources constraints. On the other hand, it is known that the accuracy and usefulness of a given diagnostic testing technique is highly dependent on the intrusiveness level of the test. Nevertheless, the range of diagnosis techniques and number of tests allowed over UCH assets is, in most of cases, quite limited due to internal and external constraints related to the cultural integrity and conservation of these assets, such as the current state of occupation, the value and dimension of the asset, and the patrimonial value of the respective urban environment, among others. Therefore, deciding for an adequate investigation plan for UCH assets involves seeking for the optimal balance between the above-mentioned aspects.

It is no novelty that the more the knowledge path associated to a determined structure is complete, the more accurate a numerical model will result, and subsequently more reliable will be the evaluation of the seismic response. To this aim, an interdisciplinary approach that goes beyond simple technical considerations is needed, for designing adequate investigation plans that might involve the cooperation between professionals of different fields of expertise, such as architects, structural engineers, geotechnical and geological engineers, archaeologists, historians, conservators, urban planners and other specialists. Usually, investigation plans for UCH assets are carried out either for maintenance or preventive management activities. While the first, the most frequent one, includes monitoring, renovation, seismic retrofitting or strengthening works, the second focuses on documenting and cataloguing the cultural value of the asset.

Because investigations can be carried out with distinct levels of detail, it is fundamental to establish a cost-benefit plan proportional to the asset's complexity and architectonic value [94]. However, current standards, such as the EN 1998-1 [95], foresees the use of different importance factors to account for the variation in terms of both human and economic losses in existing structures. These factors are multiplied by the reference peak ground acceleration of type A, a_{gR}, to obtain the design ground acceleration value. However, in this

approach no reference is made to the economic and cultural consequences associated with the loss of integrity and damage of architectonic and artistic assets. Even though public safety should be always ranked as a top priority in earthquake risk mitigation, the protection and preservation of both tangible and intangible heritage should be also considered to be at stake.

The need to extend the rehabilitation requirements that are usually adopted for ordinary buildings, concerning the state of occupation and safety of citizens, to conservation requirements related to architectonic and artistic cultural outstanding value, has led to the development of target performance levels defined with reference to three groups of safety and conservation requirements, namely: use condition and human life, building conservation, and artistic assets [48]. These performance levels were specifically designed to be implemented in probabilistic-based assessment procedures to evaluate the seismic response of cultural heritage assets, such as that developed within the framework of the PERPETUATE project [48], considered as one of the first attempts to establish a direct correlation between damage and performance levels. In this procedure, target return periods for each performance level are obtained from the return period by applying an importance factor that considers the conditions of use (public, strategic) and the architectonic and artistic value of the examined building. However, the values of these importance factors corresponding to each of these safety and conservation requirements, are not yet fully detailed.

International standards provide general recommendations about the type of investigation tests and number of specimens to be analysed, independently from the specific particularities of each structural typology. The current approach proposed in these standards to face the intrinsic incomplete knowledge of investigation plans, included both in the Italian Building Code NTC [96], the OPCM [97] and the EN 1998-3 [93], is based on the definition of a discrete number of Knowledge Level (KL), defined as a function of the amount of information gathered to overcome the incomplete knowledge (mainly related to geometry, construction details and material properties of the structure), and on the "a priori" application of a Confidence Factor (CF) to a specific parameter set, which is selected to be representative of the most worst-case scenario [98]. Some critical issues concerning the application of such procedure to ancient masonry structures, such as the case of UCH assets, have been recently discussed for example by Franchin et al. [99] or Tondelli et al. [100], and motivated the development of alternative procedures [101, 102, 103], in which a preliminary analysis during the investigation process is recommended to the identify critical areas and structural components. According to Haddad et al. [103], this preliminary analysis, when combined with sensitivity analysis (performed to identify the parameters mostly affecting the response), allows the design of specific investigation plans. This approach was also adopted in the framework of the PERPETUATE project [48], in which the introduction of sensitivity analysis was found essential for a reliable assessment of existing structures, allowing to explicitly include the evaluation of the effect of uncertainties and to identify the parameter(s) that most affect the structural response, which in turn would support the optimisation of the investigation plan. Finally, uncertainties may be included in the analyses according to different approaches: probabilistic uncertainties propagation, in which uncertain parameters are defined as random variables; logic tree approach, where plausible intervals and a set of deterministic case analyses assuming proper weights are considered, and deterministic approach, in which confidence factors are used as suggested in current seismic codes.

Many authors have been supporting the idea that an investigation plan suitable to UCH assets should encompass ideally the following steps: the definition, description and under-

standing of the asset's historic and cultural significance; historic research covering the entire life of the asset and its transformations over time; the description of the geometry and construction of the asset; the description of the original building materials and construction techniques; the description of the asset in its present state including damage identification, decay and the eventual progressive phenomena, by using appropriate testing techniques; the description of the actions involved, structural behaviour and materials, and the survey of the site, soil conditions and the respective surroundings [94, 104]. The latter aspect brings us to the specific particularities of assets enclosed in aggregate. The lack of accuracy when evaluating the seismic response of an asset enclosed in aggregate as an isolated structure, due to unavoidable interactions with adjacent buildings when under seismic loads, has retained more and more attention to this matter in the last decade. Hence, one of the main focus of this subsection rests precisely on identifying the particularities inherent to UCH assets enclosed in aggregate and how to properly investigate these sources of uncertainties so that they can be considered in the evaluation of the seismic response. It is known, for example, that the seismic response of old masonry UCH assets, is highly dependent on the variety and quality of materials and execution techniques, the state of preservation, the in-height and in-plan regularity, the quality of connections between walls and horizontal elements and between orthogonal walls, the misalignment of openings, and the foundation's quality, for example. Figure 3.1 illustrates the idea that a UCH asset enclosed in aggregate encompasses the investigation of several aspects apart from those usually considered when assessing an isolated building (i.e. not enclosed in aggregate).
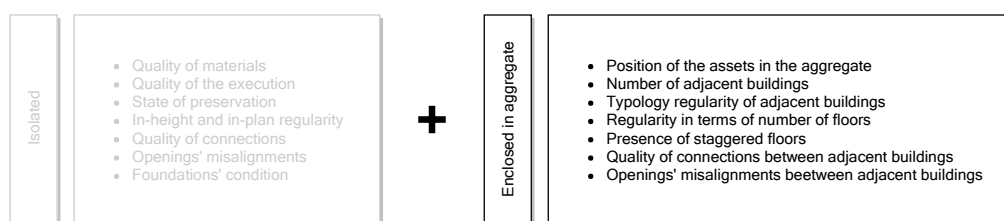
Figure 3.1: Fundamental aspects responsible for influencing the seismic response of UCH assets in function of their neighbouring conditions (isolated or enclosed in aggregate).

Usually, isolated buildings are more likely to be found in rural areas [72], whereas buildings enclosed in aggregate are more frequent in historic centres. Therefore, and contrarily to old masonry buildings located in rural areas, the fact that UCH assets are frequently enclosed in aggregate elevates the complexity level of the problem in hands, as they interact with adjacent structural units when under seismic loads. For this reason, the position of the asset within the aggregate, the number of structural units and adjacent buildings, the structural typology regularity, the regularity in terms of number of storeys, the presence of staggered floors or thrusting roofs, the quality of the connections between the asset and the adjacent structural units, and the eventual misalignment of façade walls and respective openings, should be added up to the basic aspects associated with the investigation of isolated structures [23, 31, 105, 106]. Most of these aspects are also included in the methodology proposed by the Italian "Guidelines on Cultural Heritage" [97]. In what concerns the knowledge path associated to the investigation plan of UCH assets, this guideline emphasises the following aspects: identification of the asset and its position in relation to the aggregate by means of preliminary visual inspection; complete geometric survey of the asset and adjacent structures in its

current condition including eventual cracking and deformation phenomena; identification of the evolution of the diachronic construction process of the aggregate; identification and characterisation of structural elements in terms of construction techniques and constituting materials (state of decay and mechanical properties), as well as their connections, and the investigation of foundation elements.

3.1.2 Investigation techniques

Investigation techniques for the structural evaluation of UCH assets can be divided in two main groups of tests: "in-situ" and laboratory tests. For the sake of simplicity, and even though material samples can be tested in the laboratory, these testing techniques were not included in the present subsection. Hence, investigations of UCH assets should understand the preparation of the investigation plan (preliminary visual inspection), the implementation of the investigation plan ("in-situ investigation" and office work), and the writing of the final report, as illustrated in the flow diagram of Figure 3.2 [107].

A preliminary visual inspection of the asset is an essential step that precedes the investigation plan. Usually carried out by a qualified team, this visual inspection is important to have an initial understanding of the structure and also provide an appropriate direction to the investigation plan, supporting the identification of the testing techniques needed, and that are more adequate to the asset in hands. Even though this preliminary visual inspection and basic "in-situ" measurements are capable, in most of the cases, to provide a reliable answer to these above-mentioned aspects, there might be cases where some of these aspects might not be easily investigated, depending on the cultural relevance and state of conservation of the asset. Hence, every time the knowledge on a particular feature of the building under investigation is limited, the uncertainty associated to this lack of knowledge should be accounted for in the subsequent analyses. It is worth referring that the biggest difficulties usually arise during the "in-situ" investigation phase, either due to time constraints, the occurrence of unexpected technical problems or even accessibility or financial limitations. Once the interpretation and analysis of the data collected from the "in-situ" investigation is complete, and just before the final report is written, it might be necessary to repeat or conduct additional or more intensive investigations. The present subsection will focus on the preliminary visual inspection and "in-situ" investigation phases, which are highlighted in Figure 3.2 (in red).

In the Italian "Guidelines on Cultural Heritage" [97] the seismic safety assessment of UCH isolated assets can be verified at three different detail levels: LV1 - used to assess the seismic safety of protected heritage at large scale; LV2 - used for evaluating local interventions (first mode mechanisms) on building components or limited parts, and LV3 - used either to design strengthening or retrofitting interventions influencing the whole structural behaviour or to perform an accurate building seismic safety evaluation. Naturally, the input data that needs to be collected during the investigation phase for each one of these levels varies considerably. Therefore, the set-up of the investigation plan is highly reliant on the scope of the assessment (information being sought) and the resources available. Similarly to other fields of expertise, investigation plans can be extensive or intensive. Extensive investigation plans are more appropriate in the case of large-scale assessments, which usually involve more qualitative information, while intensive investigation plans are associated to a single-asset scale and to both quantitative and qualitative information. However, in the particular case of UCH assets enclosed in aggregate, both intensive and extensive investigations can be intended, depending

not only on the value and dimension of the asset and the respective urban environment, but also on its current condition and integrity, from the cultural heritage conservation viewpoint. The latter aspect plays a crucial role on setting up the investigation plan and deciding which investigation techniques are more appropriate for a given UCH asset, since these techniques must not compromise the value, uniqueness and authenticity of the asset.
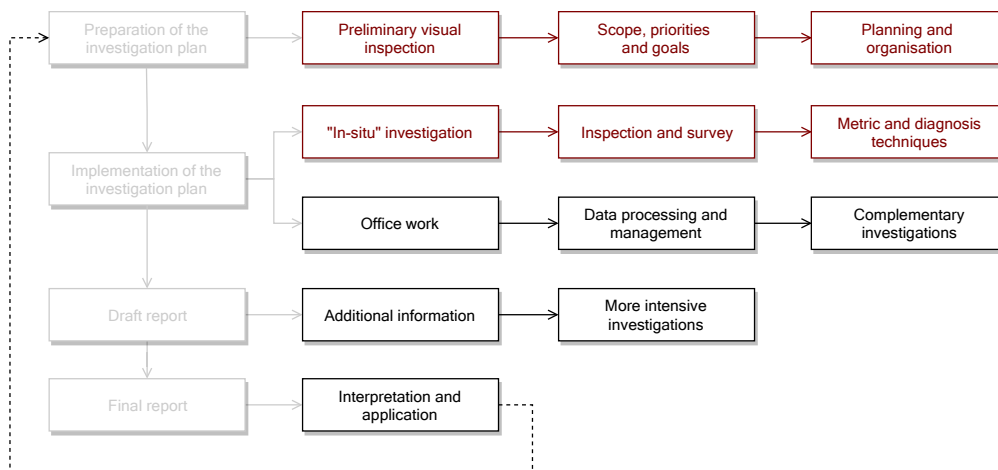
Figure 3.2: Flow diagram for the design of investigation plans for UCH assets, adapted from Vicente et al. [107], from where the preliminary visual inspection and "in-situ" investigation phases are highlighted (in red).

The importance of investigations for structural diagnosis (including historic, material, and structural aspects) was emphasised in the Venice Charter in 1964. This document also stressed out that conservation should be based on the knowledge of the structure's response and on the real causes of structural changes and damages. According to Cattari et al. [101], setting up of an effective knowledge and assessment procedure in the particular case of masonry cultural heritage assets, is related not only to the cost-benefit optimisation with respect to the reliability of the outcome, but also to the minimisation of the intrusiveness nature of that procedure. Moreover, according to Watt [108], a thorough investigation to evaluate the condition of an asset is essential if sound judgements are to be made about issues such as the design of policies for repair, strengthening and retrofitting. This is especially so in the case of UCH assets, which have suffered long exposure to different agents of deterioration and natural ageing, but may also have been subjected to unsuitable uses, ill-considered structural interventions and negligent maintenance and repair.

Before going into detail on the techniques currently available for the investigation of UCH assets, it is important to highlight the role of the surveyor in this process. Independently from the strategy adopted for the investigation plan (intensive or extensive), the quality of an investigation is largely affected by the surveyor's expertise and judgement ability. Hence, it is essential that surveyors or technicians responsible for performing the "in-situ" investigations, are able to fully understand how a given asset was constructed and how it has evolved over the years.

At the current state of the art, there are several documents and guidelines in literature that summarise and describe the vast number of investigation techniques suitable for intervening in existing buildings, as the case of Binda et al. [109], Silva and Lourenço [110], Cóias

[111], or the numerous research projects funded by the European Commission, such as the ONSITEFORMASONRY [45], NIKER [105], or the PERPETUATE [94] projects, for example. In this study, the approach proposed by Bosiljkov et al. [94] was adopted, which considers that in conservation actions, there are two distinct groups of investigation techniques with a degree of overlap between them, metric and diagnosis techniques.

Metric surveying and recording techniques, summarised in Table 3.1, are used to establish the quantifiable physical disposition of form and space, also known as "base recording", a term that is often used for the gathering of measurements and data to be compiled in a preliminary report together with complementary drawings and photographs, which in turn will guide and support the decision-making process on designing an investigation plan suitable to the conservation purpose.

Diagnosis surveying and recording techniques, summarised in Table 3.2, are used instead to locate, isolate, evaluate or monitor physical phenomena affecting the UCH asset [94], as for example the constructive details of the asset, estimation of mechanical properties of materials, to control the effectiveness of a determined intervention or even for structural health monitoring purposes.

Table 3.1: Metric surveying and recording techniques.

Investigation tests, devices and techniques	Geometrical survey	Mechanical properties	Model validation	Monitoring	Contact to surface	Intrusiveness level	Average cost	Reliability of data
Computer-aided design, drafting and computer modelling	✓	✗	✗	✗	✗	NDT	L	M
Hand survey and sketch diagram	✓	✗	✓	✗	✗	NDT	L	M
Global position system	✓	✗	✗	✗	✗	NDT	L	H
Laser scanning	✓	✗	✗	✗	✗	NDT	L	H
Total station theodolite (topography)	✓	✗	✓	✗	✗	NDT	L	H
Rectified photography	✓	✗	✗	✗	✗	NDT	M	M
Pictorial imagery	✓	✗	✗	✗	✗	NDT	M	H
Photogrammetry	✓	✗	✗	✗	✗	NDT	M	H
Inclinometer	✓	✗	✗	✓	✓	MDT	L	M

The information given in Table 3.1 and Table 3.2 was collected from the above-mentioned sources [45, 94, 109, 110, 111] and it includes the purpose of each surveying and recording technique (geometrical survey, mechanical properties, model validation and monitoring), the contact to surface requirement and respective level of intrusiveness (Non-Destructive, NDT, Minor-Destructive, MDT, and Destructive, DT), and the rating concerning the average cost and reliability of data acquired. The estimation of an average cost associated with each investigation technique is a very complex task, as it should not only include time-based professional fees and expenses related to subsistence, travel, equipment costs and charges (which vary significantly from country to country), but also include repayment rates and the time spent on data acquisition and analysis, which in turn is highly reliant on the expertise of the user, the size of the asset, number of tests required and nature of the information require. Moreover, such estimation would also depend if one is interested in service rendering or purchasing the necessary equipment, adding further complexity to this task. Therefore,

in this subsection, only a simplistic rating of the average cost is provided, low (L), medium (M), and high (H), based on expert judgement and on the information specified in [94].

Table 3.1 and Table 3.2 aim at providing a clear overview on the applicability and intrusiveness level of each technique. Additionally, they provide a qualitative rating of these techniques in function of the average cost and reliability of the output data. It is important to stress that for an in-depth explanation and comparison between these techniques, the above-mentioned studies must be consulted. Nevertheless, it is possible to confirm the previously mentioned theory concerning the high dependency between the reliability and usefulness of investigation techniques, and their intrusiveness level.

Table 3.2: Diagnosis surveying and recording techniques.

Investigation tests, devices and techniques	Geometrical survey	Mechanical properties	Model validation	Monitoring	Contact to surface	Intrusiveness level	Average cost	Reliability of data
Dynamic vibration test	✗	✓	✓	✗	✓	NDT	M	H
Geo-electrical tomographies	✓	✗	✓	✓	✓	NDT	H	M
Hardness test	✗	✓	✓	✗	✓	NDT	L	L
Impact-echo	✗	✗	✓	✗	✓	NDT	H	L
IR thermometer	✓	✗	✓	✗	✗	NDT	L	M
Pachometer	✓	✗	✗	✗	✓	NDT	L	M
Pulse sonic test	✓	✓	✓	✗	✓	NDT	M	M
Radar (echo method)	✓	✗	✗	✗	✓	NDT	M	M
Standard penetration test	✗	✓	✗	✗	✓	NDT	M	M
Thermography	✓	✗	✓	✗	✗	NDT	M	M
Hole drilling method	✗	✓	✓	✗	✓	MDT	L	L
Telecoordinometer	✗	✗	✓	✓	✓	MDT	L	L
Tell-tale crack monitor	✗	✗	✗	✓	✓	MDT	L	L
Colouring and sampling	✗	✓	✓	✗	✓	MDT	L	H
Optical and digital endoscopy or boroscopy	✓	✗	✗	✗	✓	MDT	L	H
Transducer movement sensing	✓	✗	✓	✓	✓	MDT	L	H
Ultrasonics	✓	✓	✗	✗	✓	MDT	M	L
Percussion penetration test	✗	✓	✗	✗	✓	MDT	M	M
Resistography	✗	✓	✗	✗	✓	MDT	M	M
Flat-jack test (single and double)	✗	✓	✓	✗	✓	MDT	M	H
PNT-G penetrometric method	✗	✓	✓	✗	✓	MDT	H	M
"In-situ" testing (e.g. compressive test)	✗	✓	✓	✗	✓	DT	H	H

3.1.3 The historic centre of Faro as case study

In this subsection, both extensive and intensive investigation plans are going to be presented together with illustrative examples collected from a surveying campaign carried out in the historic centre of Faro, in Portugal. The idea here is to underline the most relevant aspects that one should take into consideration when designing an investigation plan for UCH assets enclosed in aggregate, by providing illustrative examples on how to collect input data needed for setting up extensive and intensive investigation plans.

3.1.3.1 Extensive investigation plan

Extensive investigation plans are more appropriate for large-scale assessments, such as those recently carried out by Maio et al. [8], Ferreira et al. [9], or Formisano et al. [112], for example. Usually, methodologies that require extensive investigation plans take advantage of the use of open-source GIS tools, since it allows the spatial representation of the seismic response within the historic centre and eases the identification of the most vulnerable UCH assets, being therefore, of great utility for both urban planning and management purposes [113].

In the methodology applied in Maio et al. [8] and Ferreira et al. [9], for example, the seismic vulnerability of the masonry building stock at the historic centre level is evaluated by assigning a vulnerability index value to each masonry building within a given delimited urban area. This methodology, also known as the vulnerability index method, understands the investigation of the building characteristics in two different levels of detail. In a first phase, the evaluation of the vulnerability index is carried out for the buildings to which detailed information is available, namely architectural drawings and basic measurements, hand-drawn surveys and sketch diagrams, and detailed visual inspection (supported by photographs) of both the asset's environment, envelope, interiors, and detail of structural elements. The information is usually compiled in a set of survey and inspection forms from F1 to F11 [107]. The layout of forms F1 and F2, for example, are illustrated in Figure 3.3 (left), and were designed to collect general information on the building (structural typology, general conservation state, location and foundations, soil type and slope, state of occupation, or record of past interventions, for example) and the main characteristics of façade walls (geometry, materials, claddings, damage and pathological condition, attached non-structural elements), respectively. The information gathered in these forms is then used to evaluate a set of 14 parameters that address the most important aspects that rule the seismic vulnerability of masonry structures located in historic centres [14]. The effect in aggregate is evaluated in a simplified way by means of a parameter that considers four different classes of increasing vulnerability for the position and interaction of the building under investigation with the adjacent buildings.

Since the access to part of these buildings is often limited (either due to safety or simply logistic issues), in the second phase, a more expeditious investigation is performed by assuming the mean values estimated in the first phase of assessment to all parameters that are not possible to evaluate with an exterior visual inspection. By doing so, it is assumed that the building characteristics and typology is somehow homogeneous within the area under study. The example presented in Figure 3.3 (right), highlights not only the most vulnerable assets in the Ribeirinha area of the historic centre of Faro (in light red), but also identifies the assets that were investigated in the first (Detailed) and second (Non-detailed) assessment phases.

Similar vulnerability index methodologies were developed by Ferreira et al. [114] and Formisano et al. [115], for example, for the rapid assessment of buildings enclosed in aggregate. In both methodologies, parameters such as the quality of the masonry fabric, misalignment of openings, irregularities in height and in plan, and the location and soil conditions, are evaluated by means of a rapid visual inspection or available drawings. While in the methodology developed by Ferreira et al. [114] these parameters are used separately, in Formisano et al. [115], they are added up to the respective original formulation conceived for the rapid vulnerability assessment of isolated buildings, presented for example in Formisano et al. [112].
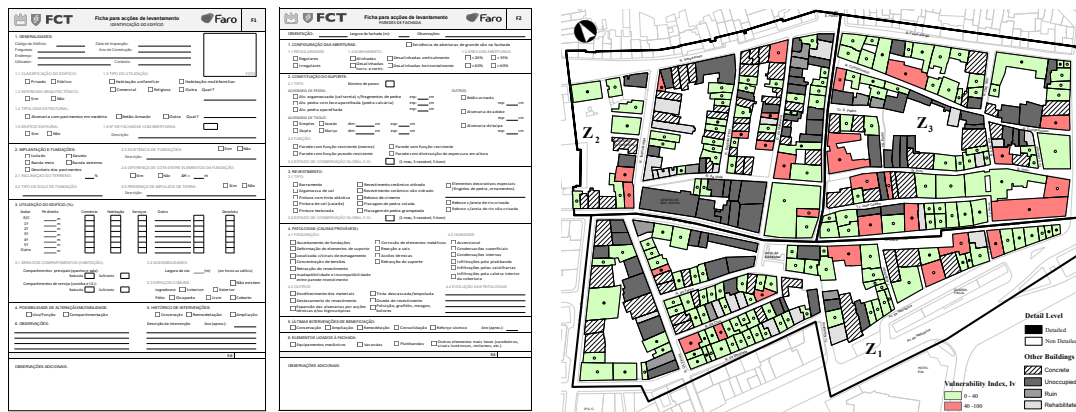
Figure 3.3: Layout example of survey and inspection forms (left) for the asset identification (F1) and façade wall characteristics (F2), respectively from left to right, and a typical output of the vulnerability index method estimated for the Ribeirinha area of Faro (right).

3.1.3.2 Intensive investigation plan

Intensive investigation plans are associated to a single-asset scale assessment and to both quantitative and qualitative information. Here, all sources of information and data collection are important to fully understand the asset in hands and achieve a thorough knowledge about the architectonic and structural features. The morphological and constructive characterisation of the area under investigation, for example, is not only fundamental to understand the evolution of the historic centre itself, which might drop a hint about the evolution of a particular building aggregate, but it may also support municipal authorities and civil protection bodies on the design of mitigation strategies for reducing the seismic vulnerability and risk of historic centres, promoting this way, the cultural valorisation of such areas [23, 116]. However, depending on the scope of the assessment (e.g. conservation or renovation interventions) the detail level of the gathered data might vary. Intensive investigations are preferentially carried out by means of comprehensive field ("in-situ") surveys, to which information taken from archive and documentary sources might be added. The descriptive document that follows the blueprint plan presented in Figure 3.4, dates back from 1930 and it describes the main characteristics of the building, including, among other, general information about the typology of masonry walls and of the horizontal structure. The cross-checking between the data collected from different sources is recommended by current seismic codes to minimise uncertainty sources [93].

Given the notable variety of materials and construction techniques existing in UCH assets, both on a geometric and historic level, it is useful to define local rules of thumb for the proper judgement of architectural and structural elements. The recording of a scheme of structural functionality of the asset requires the knowledge of constructive details and the quality of the connections between the various elements: typology of walls; quality of connections between load-bearing walls; quality of lateral joints and walls; elements of discontinuity (chimneys); typology of horizontal structures; typology and effectiveness of architraves; the presence of structurally efficient elements chosen to balance any eventual thrust, and the presence of highly vulnerable non-structural elements.

The integration of information collected through intensive investigation plans in BIM tools is becoming more and more popular. Even if originally intended for new structures,
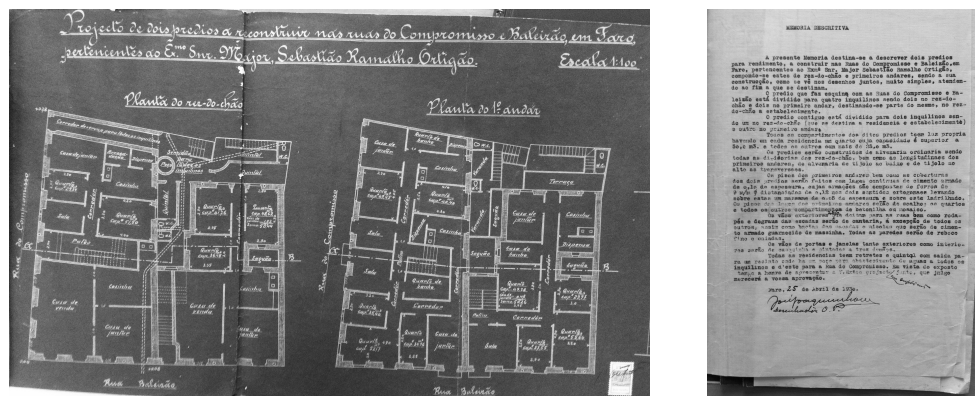
Figure 3.4: Example of a blueprint plan (left) and respective description report (right) of a design project for a building located within the Ribeirinha area, from circa 1930.

BIM has been successfully adapted to existing structures, inclusively in the field of cultural heritage documentation and preservation [117, 118].

As mentioned before, several other aspects should be taken into consideration when investigating UCH assets enclosed in aggregate, namely the number of structural units or adjacent buildings, the differences in terms of structural typology, the number of storeys, the presence of staggered floors or thrusting roofs, façade walls and openings misalignments, and the quality of the connections between the asset and the adjacent structural units. The optimal evaluation of the seismic response of buildings enclosed in aggregate remains a challenging topic in this field, that has therefore merited the attention of several authors throughout the years, such as Senaldi [119], Ferrari [120], Maio et al. [121], Boschi [73], Fagundes et al. [122], or Formisano [31], just to cite a few. However, and contrarily to the above-referred studies, this subsection does not aims at assessing the seismic response of UCH assets enclosed in aggregate, but rather highlight some of the aspects that are believed to be determinant to the optimal modelling and subsequent estimation of the seismic response of such assets. Hence, the following paragraphs are dedicated to the discussion of these aspects, which are, whenever possible, illustrated with a few practical examples collected in the Ribeirinha area of the historic centre of Faro, in Portugal.

When assessing UCH assets enclosed in aggregate, the identification of the structural system or typology should not only concern to the asset under investigation, but also to all the structural units that might have influence on the seismic response of the asset (as illustrated in Figure 3.5). It is known that the response to earthquakes of non-engineered structures and their ancient technologies (e.g. rammed-earth or stone masonry) is quite different in the case of "new" building technologies (e.g. reinforced-concrete frame structures), due for example to the inherent resistant properties of the materials. In fact, even structures apparently executed using the same building technology can have a very distinct response under seismic actions, due to several external factors, such as the quality of the execution, the quality of the materials used or even the geometrical properties of the building. Nevertheless, larger deviations in terms of stiffness (or rigidity) and ductility are expected when in the presence of buildings constructed with different building technologies. The coexistence of assets constructed with different building technologies is particularly relevant in the case of historic centres, when these assets often interact among each other when subjected to seismic actions. Motivated by this disparity in terms of stiffness and strength, during an earthquake, this

interaction may trigger unexpected stresses in boundary walls with potential to activate local damage mechanisms, both in-plane and out-of-plane, as highlighted by Ferreira et al. [123]. Therefore, when assessing buildings enclosed in aggregate, it is important to investigate the structural typology of adjacent buildings.

Figure 3.5: Identification of the UCH asset (in red) and of the structural units composing the aggregate: similar to the case study asset (in light grey) and distinct structural typologies (in dark grey). The pictures correspond to the structural units in dark grey.

This exercise, can be carried out through a direct visual inspection complemented, whenever possible, by small local sampling (as illustrated in Figure 3.6), i.e., eliminating the renders and plasters of small portions or removing stones/bricks and mortar joints in order to investigate the section's morphology, allowing the examination of the masonry fabric quality on the surface and inside the wall section, and the connections between walls, the constraints between floors and walls, and between roofs and walls. The same sampling points can be later on used to perform sonic and flat-jack tests, or even endoscopic observations. When necessary, more refined non-destructive techniques can be applied to observe the heterogeneity of walls on larger portions (as thermography or geo-radar, for example).
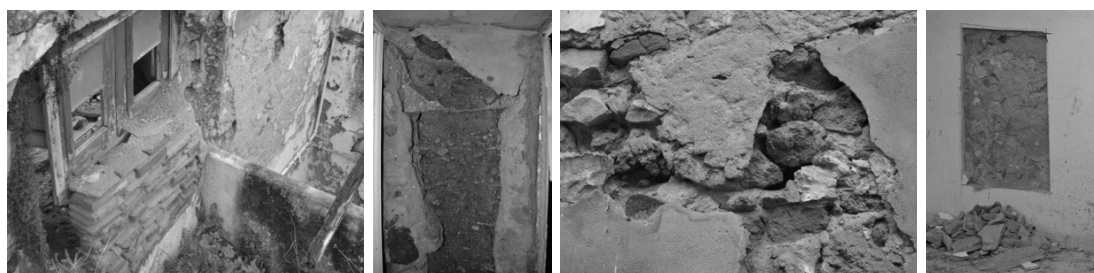
Figure 3.6: Examination and appraisal of load-bearing walls' typology and respective fabric quality through direct visual inspections and local sampling.

Apart from the structural heterogeneity between the UCH asset under investigation and adjacent structural units, and the position of this asset within the aggregate, the number of adjacent units is also a crucial aspect to take into consideration in the evaluation of the seismic response. However, in cases where the aggregate is composed of numerous structural units (as illustrated in Figure 3.7), the investigation of each single unit can be a very time-consuming task and for this reason, unmanageable in most of cases. There is, however, scarce recommendations or guidelines in literature regarding this aspect, particularly to the minimum intervention units that one should take into consideration in the analyses [73, 124].

As illustrated in Figure 3.8, the accuracy on the estimation of the seismic response of an UCH asset enclosed in aggregate varies in function of the number of structural units

Figure 3.7: Example of the different possible configurations of assets enclosed in aggregate, observed in the historic centre of Faro (in Portugal): mid-row, end-row and corner-end (respectively from left to right).

Accuracy, modelling complexity, global to local response
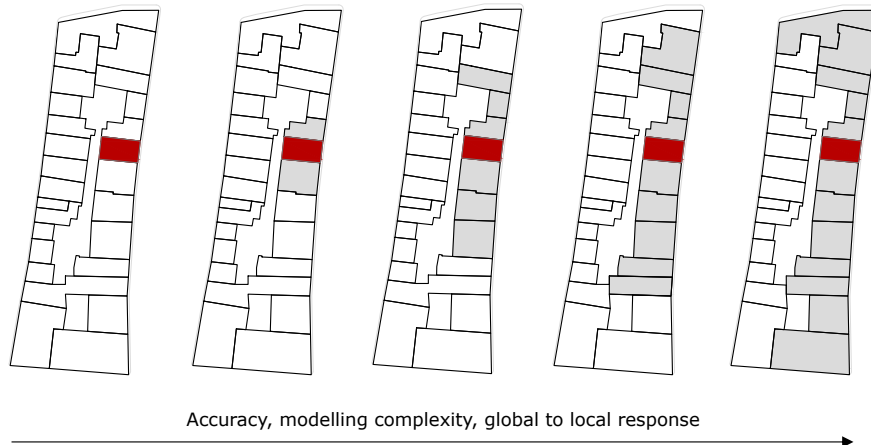
Figure 3.8: Different modelling options to simulate the aggregate effect of a given UCH asset (in red), that will determine the extent of the investigation plan, from the "isolated" condition (left) to the discrete consideration of the whole building aggregate (right).

considered in the model. Another issue that might arise is that the global response might not be any more representative of the asset under investigation, but of the whole aggregate, being therefore, necessary to perform complementary local analyses at the wall level, for example.

The difference between adjacent structural units in terms of number of storeys, and total and inter-storey height, is also acknowledged in literature as one the most critical factors, responsible for causing local thrusting forces that can trigger the so-called pounding effect [121, 122, 125]. The presence of staggered floors is frequently observed in historic centres, particularly when structural units composing the aggregate were not built in the same

period, as well as when the aggregate lays on a sloped ground, as in the case illustrated in Figure 3.9. Hence, it is of utmost importance to examine these aspects during the investigation phase, in order to take them into account in the subsequent analyses. Horizontal and vertical misalignments of openings between the asset under investigation and adjacent buildings, also depicted in Figure 3.9, are responsible for worsening the in-plane seismic capacity of masonry load-bearing walls, and subsequently the seismic response of a given wall in the event of an earthquake. Therefore, and once more, it is important to detect these irregularities during the investigation phase.
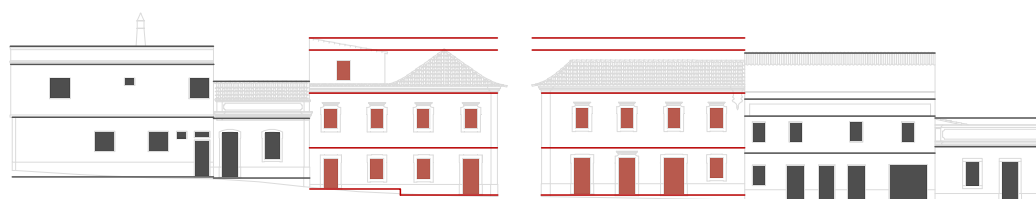
Figure 3.9: Example of the main elevation drawing of the asset enclosed in aggregate (in red), from which is it possible to observe the differences in terms of number of storeys, inter-storey and total height, as well as the presence of staggered floors and the misalignment of openings.

The investigation of the quality of the connections between walls, the constraints between floors and walls, and between roofs and walls should be carefully addressed. Even though the visual inspection of the connections between mid-walls of adjacent buildings is often impracticable, as demonstrated in Figure 3.10, two configurations are usually observed: a separate and shared configuration. According to the common diachronic evolution process in historic centres, the new building to be constructed in a mid-row situation (in black) can transmit vertical loads either to its own side walls (separated configuration), or to the existent buildings' side walls (shared configuration). These configurations are respectively illustrated in the upper and bottom row of Figure 3.10. This uncertainty can potentially introduce significant bias on the seismic response assessment of the given asset.

Figure 3.10: Illustration of the two possible configurations of buildings erected in different time periods: pre-existent (in grey) and a new building (in black).

Finally, in Figure 3.11, an example of the connection between horizontal and vertical structural elements is given. While the pictures on the left-hand side of Figure 3.11 illustrate the connection of timber joists to stone masonry load-bearing walls, the picture on the right-hand side shows how the roof structure is typically connected in the case of the UCH assets

located in the historic centre of Faro. However, when assessing well-maintained UCH assets, the visual inspection of these connections is often quite limited.

Figure 3.11: Examination of timber joists support on load-bearing walls (left) and the connection between the roof structure and perimetral walls (right), through direct visual inspections and local sampling.

3.1.4   Final remarks

Acknowledging the difficulty of assessing an asset as an independent structure in historic city centres, resulting from unavoidable interactions between adjacent buildings when under seismic loads, this subsection focused on the identification of the key features that should be taken into account when investigating UCH assets enclosed in aggregate, and on how to design adequate investigation plans in accordance to the their location in the urban context. Moreover, this study aimed at defining a set of survey operations that can be repeatable for other UCH assets despite their dimension, heterogeneity and importance level.

In the context of historic centres, survey operations are particularly difficult to handle due to several inherent uncertainties and therefore the need for a specific investigation plan is of great importance for the effectiveness of conservation interventions in terms of structural and seismic safety. Therefore, the most widely used investigation techniques for the conservation and structural safety assessment of UCH assets were herein compiled and ranked in terms of intrusiveness level, average cost, and reliability of data. This subsection ultimately aimed at encouraging surveyors and technicians to incorporate the aggregate effect when investigating UCH located in historic centres, by conducting adequate investigation plans and techniques, suitable not only to the scope and scale of the assessment, but also to the resources and techniques available. By doing so, one is not only contributing for a more reliable and accurate assessment of the seismic response of assets located in historic centres, but also supporting the documentation and recording of UCH assets, whose building techniques and materials are an inexorably part of our tangible and intangible cultural heritage.

3.2   The comparison of different macroelement approaches

Over the past several years numerous earthquakes around the world have caused significant loss of life, property and widespread damage to UCH assets, and Europe was no exception. As explained in [126], this category comprehends masonry architectonic assets that are expected to be subjected to prevailing in-plane damage, such as palaces, religious buildings

and corporate or residential assets of accredited heritage value. In this thesis particular focus is given to residential masonry buildings, since they represent the majority of the building stock in many historic centres in Portugal [127].

For a long time, research on earthquake engineering has been mainly focused on reinforced concrete structures, as an attempt to improve the design of new structures rather than analysing the existing ones [128]. However, in many seismic prone areas worldwide, unreinforced masonry structures (URM) still constitute a significant part of the building stock. Therefore, the study of such structures has been a research topic of increasing relevance, particularly if considering the crucial role it plays on the protection and preservation of cultural heritage assets. In the European context, some of the most relevant studies regarding this research field were developed by Lagomarsino et al. [49], Penna [129, 130], D'Ayala [131], or Asteris et al. [132], just to name a few.

In this study attention will be given to the seismic vulnerability component of the holistic definition of earthquake risk, which is more likely to be controlled in engineering terms. The latter gains particular relevance in countries such as Portugal, where a set of socio-economic factors, recently identified by Maio et al. [72] and summarised in Section 2.4, are exacerbating the response of the building stock, and subsequently, the risk of experiencing severe loss and damage in the event of an earthquake.

In light of the above, and encouraged by previous benchmark studies carried out by Marques and Lourenço [71], Marques and Lourenço [133] or Pantò et al. [134], this section aims at comparing the seismic performance of a UCH case study, by using three different models based on the macroelement approach. These models are commercially available in two of the most widely used software codes for the numerical modelling of URM structures, in which the category of UCH assets is included. Moreover, in this section, the main advantages and drawbacks of each model and the respective software code are going to be thoroughly discussed from the user viewpoint, hoping that it might be useful to both researchers and engineering offices.

3.2.1 The macroelement approach

The development of reliable and accurate models to predict the seismic performance of existing structures is seen as one of the most challenging issues to address in this particular research field. The study of complex structures such as UCH assets brings additional difficulties related to computational effort, access to reliable input data (geometry, mechanical properties of the materials), limitations inherent to the nonlinear constitutive laws currently available for masonry or even related to the interactions these assets often share with adjacent buildings (the so-called "aggregate effect").

From the wide range of methods available for assessing the seismic performance of URM structures, thoroughly reviewed for example by Magenes et al. [135], Marques and Lourenço [133], Calvi et al. [65], Casapulla et al. [136], or Caddemi et al. [137], this study focuses on the comparison of two of the most widely known software codes based on macroelements.

According to Marques and Lourenço [138], macroelement models were initially based on two-dimensional macroelements, aiming at performing planar wall analysis by assuming a "no-tension" hypothesis. However, as stated by the same authors, the necessity of considering the global response of buildings led many researchers to idealise one-dimensional macroelements to simulate a similar behaviour to that of framed structures, incorporating then conventional methods of structural mechanics [138]. It is within this framework that SAM II [139] and

TreMuri [140] software codes appeared. The use of these software codes by engineers was also motivated by the introduction of the then new Italian Building Code OPCM 3274/2003 [141] and its subsequent revision, OPCM 3431/2005 [142], which explicitly recommended the use of nonlinear analyses for assessing the seismic performance of existing structures.

Within the frame modelling approach, the user-friendly computer code TreMuri, which was continually upgraded to its current commercial version, 3Muri® [12], is one of the software codes considered in this study. The graphic representation of the macroelement model available in 3Muri® is illustrated in Figure 3.12 (left).

However, due to the limitations in the use of beam-type macroelements, namely associated with the inaccurate simulation of the interaction between macroelements and the weak modelling of the cracked condition of panels [138], different two-dimensional discrete macroelement approaches emerged. These approaches were endowed with strut and tie elements [143] or plane elements with discrete interfaces and nonlinear springs [144, 145]. The latter approach, shown in Figure 3.12 (middle), was incorporated into the software code 3D-Macro® [13], and it was also considered in this comparative study.

More recently, Pantò et al. [146] identified the assumptions "box-like behaviour" and "in-plane damage as the primary source of damage", as important drawbacks of simplified numerical strategies for the seismic performance assessment of URM structures, particularly in the case when structures have flexible and poorly anchored floors. To overcome these limitations, Pantò et al. [146] developed an innovative three-dimensional macroelement model able to simulate the combined in-plane and out-of-plane response of URM walls. This model, depicted in Figure 3.12 (right), and recently incorporated into the software code 3D-Macro®, was also considered in this study.
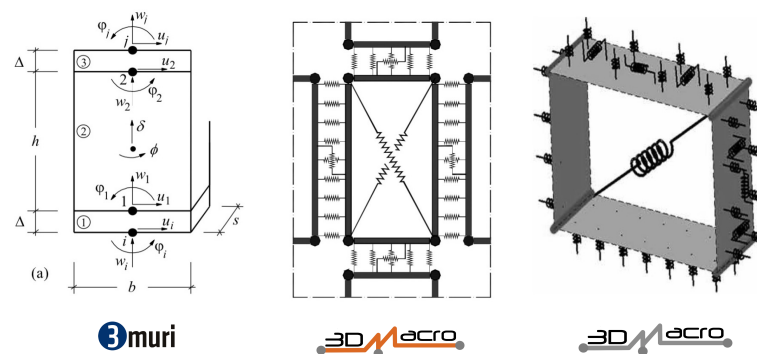
Figure 3.12: Graphic representation of the macroelements considered in this study: one-dimensional macroelement model incorporated in 3Muri® [12] (left); two-dimensional macroelement model of 3D-Macro® [13] (middle) and the three-dimensional macroelement model, developed by Pantò et al. [146] (right), and recently incorporated in 3D-Macro® [13].

3.2.1.1 3Muri® software code

This software code is based on the equivalent frame model (EFM) approach, following the assumption that the in-plane response of masonry walls with openings can be discretised by a set of one-dimensional macroelements (piers and spandrels) [147, 148]. In the EFM approach, piers are vertical elements that support both dead and live loads. Spandrels

instead, are horizontal elements placed in between two vertically aligned openings, which couple piers when seismic loads are activated. Both piers and spandrels are modelled as nonlinear beams [147] with the following features:

- Initial stiffness calibrated according to the masonry elastic properties;

- Bilinear constitutive inelastic behaviour with maximum values corresponding to the shear and bending moment associated with the ultimate limit states for in-plane failure mechanisms;

- Redistribution of the internal forces according to the element equilibrium;

- Detection of damage limit states considering global and local damage parameters [149];

- Stiffness degradation in the plastic range;

- Ductility control by means of defining in-plane drift limits;

- Element expiration at ultimate drift without interruption of the global analysis.

Rigid nodes represent the connections between piers and spandrels and are representative of those masonry portions for which an undamaged condition is assumed.

The wall-assemblage process is carried out by assuming the full coupling among the connected walls, and by condensing the degrees of freedom of two two-dimensional nodes incident and introducing floor elements modelled as orthotropic membrane finite elements [147].

The shear response is governed by the diagonal cracking failure criteria, initially developed by Turnšek and Sheppard [150] and adapted for existing masonry buildings in the Italian Building Code, NTC [96]. The flexural response, combining compressive and bending failure is evaluated neglecting the tensile strength of the material and assuming a rectangular normal stress distribution at the compressed toe [151].

The modelling accuracy of different EFM approaches for regular URM walls in the nonlinear field, was recently investigated by Siano et al. [152]. The conclusions of this study highlighted the need for a cautious use of EFM to existing URM structures, in particular to historic buildings. Quagliarini et al. [153] and Marino et al. [154] underlined some of the shortcomings of EFM approaches, which are usually associated with:

- Geometric inconsistency due to the idealisation of URM walls as "equivalent frames";

- The assumption of "box-like behaviour" and the overlooking of the out-of-plane response;

- Difficulties to identify an equivalent frame for irregular distribution of openings;

- Difficulties associated with modelling the masonry-beam interaction for confined or infilled frame structures.

3.2.1.2   3D-Macro® software code

The two-dimensional macroelement model, depicted in the previous Figure 3.12 (middle), consists of a pinned quadrilateral shape with four rigid edges, in which two diagonal springs are connected to the corners to simulate the shear response. A discrete distribution of springs normal to the sides simulates the flexural interaction between macroelements. A single spring parallel to the side is also included to simulate the sliding mechanism [13, 145]. In the case of the two-dimensional model of 3D-Macro®, the structural global response is governed by the in-plane behaviour of the masonry panels, being the out-of-plane behaviour avoided by the presence of wall-to-wall and wall-to-diaphragms connections.

The three-dimensional discrete macroelement model, represented in Figure 3.12 (right), was originally proposed in [155] and recently polished by Pantò et al. [146]. It represents the spatial extension of the planar (two-dimensional) macroelement model described above, aiming at simulating the nonlinear behaviour of masonry structures by taking into account the combined in-plane and out-of-plane response. This three-dimensional model of 3D-Macro® was herein used to evaluate the contribution of the out-of-plane wall stiffness to the building dynamics (periods and modes of vibrations) and the characteristics of the capacity curve: initial lateral stiffness, ultimate strength and ductility capacity.

According to Pantò et al. [146], this new approach is based on the concept of macroelement discretisation [156] and has been conceived with the aim of capturing the nonlinear behaviour of an entire building through the assemblage of several discrete macroelements. These macroelements are characterised by different levels of complexity according to the role played by the element in the global model [146]. Three additional degrees of freedom were added to the original two-dimensional macroelement model to describe the out-of-plane kinematics. Thus, each three-dimensional macroelement is governed by a total of seven degrees of freedom. Moreover, further nonlinear links have been introduced to account for the three-dimensional mechanical behaviour of these elements according to a simplified discrete fibre discretisation strategy [146]. More information about the theoretical basis of the considered models and the main differences between these and both similar and more advanced approaches for the numerical strategies for modelling masonry structures, can be found in [137, 157, 158], for example.

3.2.2   Seismic response assessment

3.2.2.1   Nonlinear static analysis

Nonlinear static procedures directly incorporate the nonlinear force-deformation constitutive laws of the elements, which are representative of the inelastic behaviour of the material. The result of the analysis is summarised by a nonlinear force-displacement relationship (pushover curve) usually represented in terms of global base shear and top displacement of the structure. This relationship is obtained by monotonically increasing a constant spatial distribution of horizontal forces until the structure reaches a given failure condition.

In this study, the seismic performance was evaluated by comparing the displacement capacity of an idealised single degree of freedom system (SDOF), defined from the pushover curve, with the demand inelastic response spectra corresponding to a given seismic action. In the case of regular structures, pushover analyses can be performed considering simple loading distributions proportional to the fundamental vibration mode in the considered direction. However, in the case of tall or irregular buildings, more complex multi-modal or adaptive

pushover procedures should be considered, as higher and torsional modes of vibration generally play a more important role [128].

Despite the use of nonlinear static procedures through simplified analytical models is trusted to find a good compromise between computational effort and the number of input parameters [159], its applicability to URM structures with flexible diaphragms has been recently discussed by Betti et al. [160] and Nakamura et al. [161]. When adopting EFM approaches, for example, nonlinear static procedures should include specific requirements for different structural elements, which should be, in turn, consistent with appropriate definitions of force (strength criteria) and displacement capacity [162]. According to Lu et al. [162], further indications for modelling horizontal diaphragms (in-plane and out-of-plane stiffness) should be also addressed, as well as issues related to the definition of minimum modelling requirements for dynamic analysis, the definition of limit states compatible with existing stone masonry typologies, convergence of nonlinear analyses, and the use of sensitivity studies, for example.

According to the Italian and European codes [93, 96], the software codes adopted in this study allow nonlinear static analyses to be performed with bi-directional loading patterns along the two main planar directions of the building: 100% and $+/- 30\%$ of lateral loads can be simultaneously applied along the building main directions. Accidental (positive and negative) eccentricity, automatically set equal to 5% of the maximum length of the building, can be considered or not in the analyses. Additionally, two different patterns for the horizontal load distribution should be considered: uniform mass-proportional load pattern (from now on referred to as "uniform"), and pseudo-triangular load pattern, proportional to the product between the mass of the control node and its height with respect to the base, as an approximation to the first mode of vibration. The complete set of analyses, automatically generated by these two software codes, allows 72 analysis to be performed. This number decreases to 24 if only uni-directional loading patterns are considered.

In addition to the previous default set of analyses, the current releases of 3Muri® and 3D-Macro® software codes allow for the computation of angular scanning analyses, in which the loading direction ranges along any possible direction by means of the definition of a given incremental angular step. These analyses allow the determination of the most vulnerable directions of the building [163].

In this comparative study, both global and local displacement capacities were defined according to the EN 1998-3 [93]. The global displacement for the Near Collapse (NC) was defined by the magnitude of the roof displacement at the point corresponding to a 20% decay of the maximum base shear strength. The global displacement capacity for the Significant Damage (SD) limit state was defined as 75% of the NC value. Finally, in the case of the Damage Limitation (DL) limit state, the displacement capacity was defined at the yield point of the idealised elasto-plastic pushover curve. In what concerns the local displacement capacity, the drift limits proposed in the Annex C of the EN 1998-3 [93] were adopted.

3.2.2.2 Seismic performance-based assessment

The seismic performance of the case study was evaluated according to the N2 Method [164], following the recommendations of EN 1998-1 [95], and by considering the above mentioned limit states recommended in the EN 1998-3 [93]. Despite its inherent simplicity, the use of the N2 Method provides a very interesting compromise between computational effort and precision in the estimation of the seismic performance of existing structures. More complex

approaches such as nonlinear incremental dynamic analyses are more time consuming, and for that reason, less adopted in the current engineering practice. Moreover, the use of such approaches is more adequate when using more detailed and complex models.

The N2 Method is commonly used to determine the structure's performance point, d^*_t, which is in turn computed from the intersection between the capacity curve of the structure (drawn in terms of displacement-acceleration spectral coordinates) and the inelastic response spectrum associated with a given seismic demand, following the iterative procedure recommended in the NP EN 1998-1 [165].

The capacity curve is obtained by applying a transformation factor [95, 164] that allows converting the pushover curve (associated to the Multi Degree of Freedom system, MDOF) into an equivalent bilinear Single Degree of Freedom (SDOF) system, assuming an elasto-perfectly plastic force-displacement relationship.

The seismic demand for the Azores region, where the present case study is located, corresponds to a zone 2.1 with a horizontal elastic response spectrum of type 2, according to the recommendations of the NP EN 1998-1 [165]. Moreover, a reference ground acceleration, a_{gR}, equal to 2.50 m s^{-2}, is recommended to this region [165]. The structure's demand acceleration, a_{gD}, compatible with the fulfilment of each limit state, was then obtained multiplying the peak ground acceleration, a_g, by the coefficients proposed in [166], equal to 0.55, 0.89, and 1.22, respectively for the DL, SD and NC limit states. The peak ground acceleration, a_g, was obtained by multiplying a_{gR} by the importance factor, γ_I, herein considered equal to 1.00 (assuming an importance class II). The horizontal elastic response spectrum was defined by considering: $T_B = 0.10$ s; $T_C = 0.25$ s; $T_D = 2.0$ s; a soil factor, S, equal to 1.30, and an equivalent viscous damping, ξ, equal to 5%. These values are recommended in [165] for structures with a foundation soil type C.

In this study, the seismic performance was evaluated by computing the parameter %a_g, given by the ratio a_{gC} / a_g, being a_{gC} the acceleration associated to the performance point, whose displacement corresponds to the value imposed for each limit state.

3.2.3   The case study in Horta

The case study building adopted in this comparative study, depicted in Figure 3.13, has been featured in previous works, such as in Costa and Arêde [167], and more recently in Diz et al. [168]. This UCH asset is a three-storey row-end stone masonry building located in the historic centre of Horta (Faial island, Azores archipelago, Portugal). This case study, of both commercial (first storey) and residential use (upper storeys), has a total height of 14.5 m, presents a square-shaped plan of about 10.0 x 12.0 m, and bonds its posterior wall with another building of identical typology, however of inferior architectural value.

Unlike rural building typologies of Faial island, the quality of constituent materials, masonry fabric and execution works is generally improved in urban areas [168, 169]. Stones, for example, have more straight edges and sides, being, therefore, better arranged. For this reason, the connections between orthogonal walls are expected to be more efficient in this case. Additionally, as depicted in Figure 3.13, the building is ornamented with some architectonic details and embellishments, which highlight its significance from the cultural heritage viewpoint.

External masonry walls are about 0.7 m thick and made of basalt stone masonry, while internal walls have two different typologies: basalt stone masonry approximately 0.2 m thick and timber panelling with an interior timber structure (the so-called "tabique"), which pro-

Figure 3.13: Overview of the case study building: façade walls W1, W2, and W3 (respectively from left to right in the upper row), and some architectonic details such as gable dormers, balconies and rounded openings and timber staircase (form left to right in the bottom row).

vides additional support to the floors' timber joists [168, 170]. "Tabique" walls however, were not considered in the modelling phase, as the presence of such low-stiffness elements has a negligible impact over the global seismic performance of the building [171]. The vertical and horizontal structure is repeated in height, being the latter composed of timber planks 2.5 cm thick supported by 9.0 x 14.0 cm primary timber joists spaced in 0.6 m, which are in turn supported on the façade walls and on two 7.0 x 19.0 cm cross timber joists that ensure further support to the primary joists.

The roof structure ("francesa" style) consists of a traditional kingpost hip roof truss of three hip rafters, forming an additional storey by taking advantage of the attic of a total of seven gable dormers, giving the building an additional architectural value. The roof structure is composed of 7.0 x 19.0 cm ceiling joists supported on external walls, which in turn provide support to the gable dormers timber frame. Finally, 3.0 x 12.0 cm purlins are spaced in 0.4 m. Even though no information was available about the foundations of this building, these are typically executed in the same type of masonry but slightly wider than external walls and with a depth of at least 1.0 m, depending on the total height of the building [123].

3.2.4 Preliminary analyses

Sensitivity analyses were performed, in a first phase, to grasp the influence of a few modelling aspects over the global seismic performance of the case study building. In a second phase, and based on the results of the sensitivity analysis, a reference model was defined for the purpose of the comparative analysis.

3.2.4.1   Sensitivity analysis

In this subsection some of the most important issues related to the construction of the respective numerical models using both 3Muri® and 3D-Macro® software codes, are going to be addressed. Furthermore, all simplifications and assumptions considered in this modelling phase are going to be explicitly declared. For the sake of simplicity, these aspects will only be discussed for the one-dimensional macroelement model of 3Muri® and the two-dimensional macroelement model of 3D-Macro®. Although these models differ substantially in their formulation (as mentioned in the Section 3.2.1), where possible, the same values were assigned to both geometrical and mechanical properties.

One of these prime issues has to do with the selection of the control point. Unlike 3D-Macro®, and even if pushover curves are computed for the average displacement at the upper storey level, 3Muri® does not allows the consideration of the barycentre of the structure as a control point, a criterion suggested by the EN 1998-1 [95] in the case of rigid diaphragms. Instead, 3Muri® requires the selection of a single node. However, since the case study has flexible diaphragms, the criterion suggested by Simões et al. [172] for the selection of the control point, was adopted. This criterion recommends the control point to be located in the wall that first fails [172]. According to these authors, the displacement of the control point during the analysis has a little increase, while the displacements of nodes located in other walls decrease [172]. Hence, nodes N8 and N12, located at the upper storey and highlighted in Figure 3.14, were selected as control points, respectively for the X and Y directions.
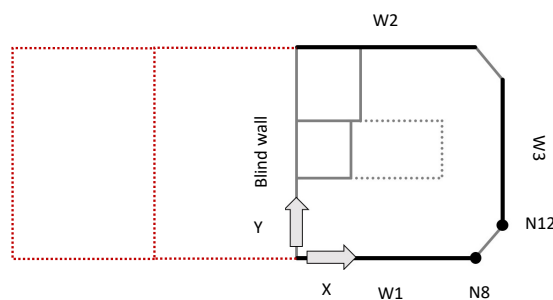
Figure 3.14: Scheme of the structural plan of the first storey, with the identification of the two main directions X and Y, façade walls W1 to W3, the blind wall, and control nodes N8 and N12. "Tabique" walls, which were not considered in the modelling, are here denoted in grey dots. As demonstrated in this scheme, the blind wall is actually the physical boundary that separates the case study building from the adjacent one (represented in red dots).

In what regards the characterisation of the vertical structure, masonry walls were modelled by assuming a constant thickness in height and by disregarding the heterogeneity associated with the masonry material. Both software codes require only a few parameters to define the masonry walls. The values of these mechanical parameters, described in the following paragraph, were adopted from the Italian Building Code, NTC [96] for a stone masonry typology with square blocks, considering the cracked condition for the masonry panels, as recommended in the EN 1998-1 [95], and a knowledge level KL1, to which corresponds a confidence factor, CF, equal to 1.35.

The elastic properties of masonry, E (Young's modulus) and G (shear modulus), were assumed equal to 615 MPa and 205 MPa, respectively, values that are in line with those adopted by Diz et al. [168] for the same case study building. The specific weight of masonry,

w, was assigned equal to 20 kN m^{-3}. In terms of masonry strength properties, the compressive strength, f_m, and pure tangential shear strength, τ_0, were assigned equal to 1.48 MPa and 0.026 MPa, respectively.

Unlike 3Muri$^{\circledR}$, that assumes a "no-tension" hypothesis, 3D-Macro$^{\circledR}$ requires the attribution of a non-zero tensile strength value for masonry panels, f_{tm}. Therefore, to allow the comparison between both software codes, the f_{tm} value in 3D-Macro$^{\circledR}$ was assigned equal to 0.001 MPa (practically zero), limiting the tensile ductility to 3.0. Moreover, the tensile strength, f_{tm}, assigned by default by 3D-Macro$^{\circledR}$ as equal to 1/20 of the compressive strength, f_m, was also considered in the sensitivity analysis. Figure 3.4 compares not only the global sensitivity of the two-dimensional model of 3D-Macro$^{\circledR}$ to the different tensile strength values considered, f_{tm}, but also the deviations between the former and the no-tension approach implemented in 3Muri$^{\circledR}$.
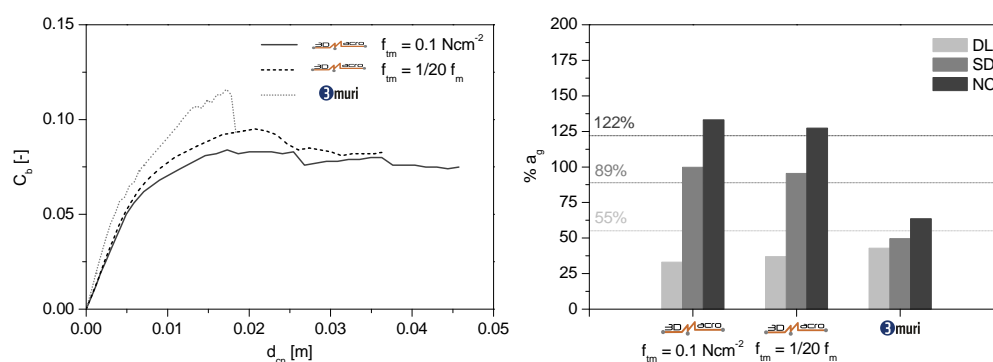
Figure 3.15: Global sensitivity to masonry tensile strength, f_{tm}. Pushover curves (left) were computed along the +X direction, for a uniform load pattern distribution and by disregarding accidental eccentricity. The respective %a_g values (right) were obtained for limit states DL, SD and NC.

The pushover analyses in Figure 3.15 (left) represent the nonlinear relationship between the shear coefficient, C_b, and the displacement of the control node, d_{cn}. The shear coefficient was obtained by diving the base shear strength, V_b, by the total seismic weight of the building, W equal to 5893 kN and 5888 kN, respectively in the case of 3Muri$^{\circledR}$ and 3D-Macro$^{\circledR}$. From Figure 3.15 (left), and regardless from the f_{tm} value considered in the two-dimensional model of 3D-Macro$^{\circledR}$, it is possible to observe that the pushover curves obtained by both software codes vary significantly. Such discrepancy suggests that the model of 3Muri$^{\circledR}$ tends to overestimate the base shear capacity. The difference observed in terms of seismic performance, illustrated in Figure 3.15 (right), can be explained by a significantly lower ductility capacity of the 3Muri$^{\circledR}$ model with respect to the 3D-Macro$^{\circledR}$ one.

Horizontal diaphragms (floors and roofs) were modelled as polygonal diaphragms elastically deformable considering orthotropic slab elements characterised by an equivalent thickness, t_{eq}, equal to 0.025 m. Young's moduli $E_{1,eq}$ and $E_{2,eq}$, were considered equal to 5.96 GPa and 3.91 GPa, respectively in the parallel and perpendicular direction of the floor warping. These values were adopted from the technical specifications available for the Cryptomeria of Azores. An equivalent shear modulus, G_{eq}, equal to 8.60 GPa, was assigned according to the guidelines NZSEE [173], after [174], considering a straight single sheathing timber floor typology in a fair rating condition.

In Figure 3.16, the sensitivity to different G_{eq} values is investigated. The reference value of 8.60 MPa, for example, is compared to the values proposed in the NZSEE [173] guide-

lines for the same floor typology but considering a poor (6.80 MPa) and good (10.60 MPa) rating condition. In 3Muri®, the minimum G_{eq} value suggested for a single sheathing timber floor typology with an equivalent thickness of 0.04 m is 10 MPa. Additionally, G_{eq} values of 50 MPa, 150 MPa and 300 MPa, representing a double straight sheathing timber floor typology, were also compared. The last of these values corresponds, in fact, to the minimum value recommended by 3Muri® for this floor typology. 3D-Macro® instead, suggests a G_{eq} value equal to 1628 MPa as a function of the geometrical and elastic properties of timber floors with good diaphragm behaviour. However, the maximum value recommended in NZSEE [173] for a similar typology is 52.50 MPa, demonstrating a great inconsistency between the G_{eq} values suggested in both software codes and those proposed in the NZSEE guidelines [173]. When examining the results in Figure 3.16, it is possible to observe that this inconsistency affects significantly the ductility capacity, and subsequently the seismic performance of these models. Moreover, it is also clear that, in the case of 3D-Macro®, the increasing of G_{eq} values provides a gradual increase of the respective %a_g values.
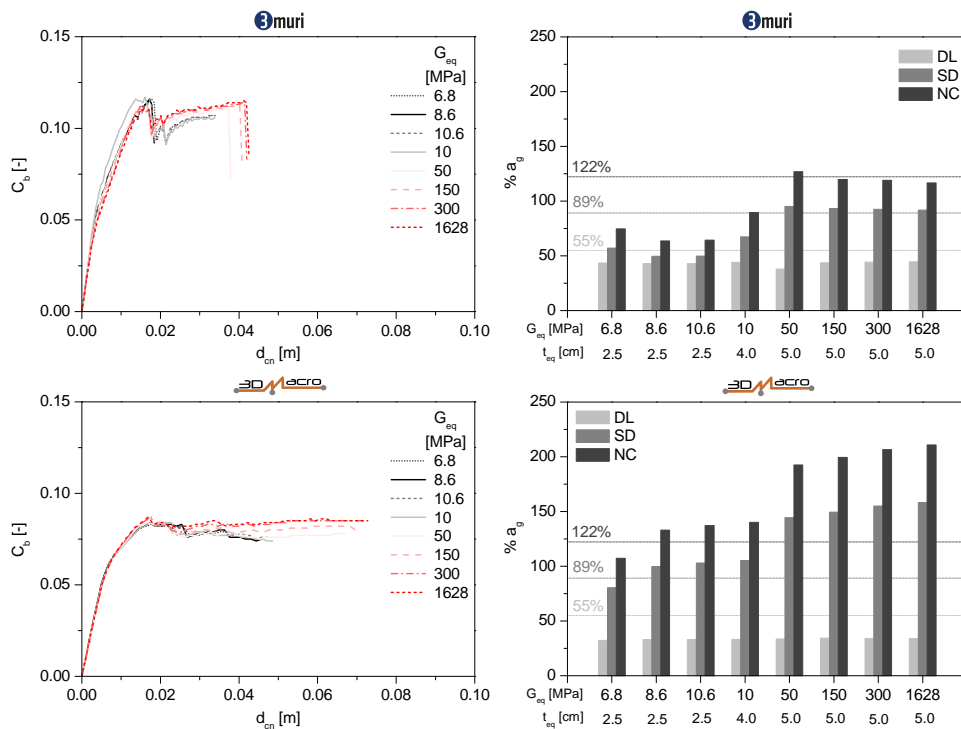
Figure 3.16: Global sensitivity to the equivalent stiffness of horizontal diaphragms, G_{eq}: pushover curves for the +X direction without accidental eccentricity (left column), and the respective %a_g values for the limit states DL, SD and NC (right column).

Another important aspect that might be determinant when assessing the seismic response of unreinforced masonry buildings is associated with the effective thickness of masonry walls. The visual inspection of this aspect might be extremely limited when dealing with architectonic assets of relevant cultural value. Thus, in Figure 3.17, the sensitivity to the variation of external walls' thickness, t_{ew}, is going to be investigated by considering a thickness variation of 10% of the value suggested in the technical drawings (0.70 m). For the sake of simplicity, the analyses presented in Figure 3.17 were again performed only for the +X direction.

If focusing on Figure 3.17 (left), the variability in terms of shear coefficient, C_b, was more

significant in the case of 3D-Macro®. However, while the increase of external walls thickness in 3D-Macro® led to a decrease in terms of ductility capacity, in the case of 3Muri®, pushover curves showed practically the same ultimate displacement. Figure 3.17 (right) demonstrates that the seismic performance assessment through the application of the N2 Method, herein represented by the $\%a_g$ values for each limit state, is highly sensitive to the ductility capacity. Contrarily, the variation of the shear coefficient, C_b has demonstrated little influence over the $\%a_g$ values.
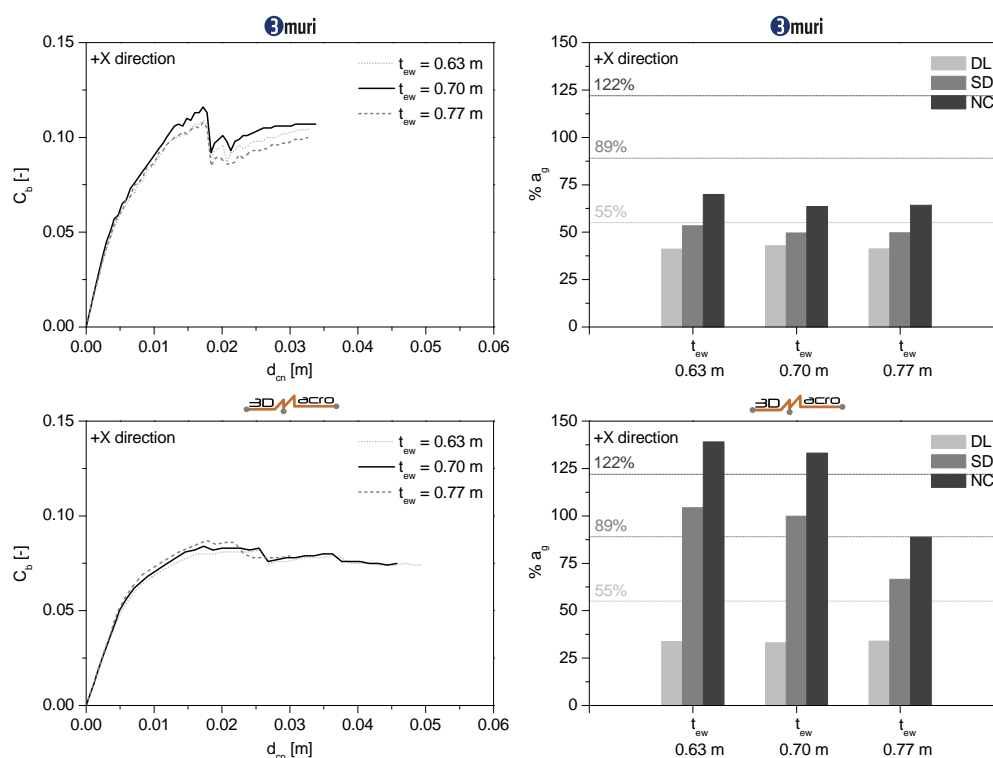
Figure 3.17: Global sensitivity to the thickness of load-bearing walls, t_{ew}: pushover curves for the +X direction without accidental eccentricity (left column), and the respective $\%a_g$ values for the limit states DL, SD and NC (right column).

3.2.4.2 Reference model

The 3D-view of the reference model designed by using the previously mentioned software codes, are illustrated in Figure 3.18. This reference model was built by taking into consideration the following aspects:

- Despite the aggregate effect is an important issue when assessing the seismic performance of UCH assets, as demonstrated for example in Bernardini et al. [175], Pantò et al. [146], Formisano et al. [112], given the comparative nature of this study, its effect was disregarded;

- Nodes N8 and N12, located at the upper storey and highlighted in Figure 3.14, were considered as control points for the X and Y directions, respectively;

- Masonry was assumed as a homogeneous material. A constant thickness in height equal to 0.70 m, the cracked condition recommended in the EN 1998-1 [95], and a knowledge level KL1, were considered for masonry panels. The Young's modulus, E, and shear modulus, G, were assumed equal to 615 MPa and 205 MPa, respectively. The specific weight of masonry, w, was assigned equal to 20 $kN\,m^{-3}$. In terms of masonry strength properties, the compressive strength, f_m, and pure tangential shear strength, τ_0, were assigned equal to 1.48 MPa and 0.026 MPa, respectively. The tensile strength of masonry panels, f_{tm}, was assigned with limited tensile ductility of 3.0 and equal to 0.001 MPa in both 3D-Macro® models. The contribution of "tabique" walls was disregarded;

- A straight single sheathing timber floor typology in a fair rating condition was adopted to horizontal diaphragms, with t_{eq} equal 0.04 m and G_{eq} equal to 5.38 MPa, following the recommendations of the NZSEE guidelines [173];

- Gravity (G_k) and live (Q_k) loads equal to 1.00 $kN\,m^{-2}$ and 2.00 $kN\,m^{-2}$ were assigned to all horizontal diaphragms. The timber structure of the internal staircase, being an element of low stiffness, was not considered in the models, as its contribution over the global seismic response of the structure was assumed negligible;

- The presence of gable dormers was simulated by introducing the respective vertical loads, adopted by Diz et al. [168], as linear loads over the respective walls at the upper storey level. This procedure is recommended in [12] when in the presence of complex roof structures;

- A linear elastic constitutive model was considered to simulate the deformability of timber elements in the numerical analyses;

- Arched windows were considered rectangular, assuming, therefore, a more conservative approach. Architrave elements were modelled as timber beams with a C18 resistance class and mean compressive strength, f_{wm}, equal to 26.0 MPa. The values of w (2.70 $kN\,m^{-3}$) and of the Young's modulus E (3.91 GPa), were assumed in accordance to [168] and to the previously mentioned specifications for the Cryptomeria of Azores. The same mechanical properties were assigned to other timber elements, such as rafters and joists;

- The underlying soil (foundations) was modelled as rigid;

- For the sake of simplicity and given the focus of this study, only the global response of the structure was considered. However, for a more comprehensive seismic assessment, the investigation of local out-of-plane mechanisms and the use of a more detailed mesh should be deemed.

3.2.5   Comparative analyses

The comparison of the three different macroelement models was carried out firstly in the linear field by performing modal analysis, and secondly in the nonlinear field by performing pushover analyses and examining the respective damage pattern distribution. Finally, the seismic performance of these models was evaluated and compared by applying the N2 Method. For
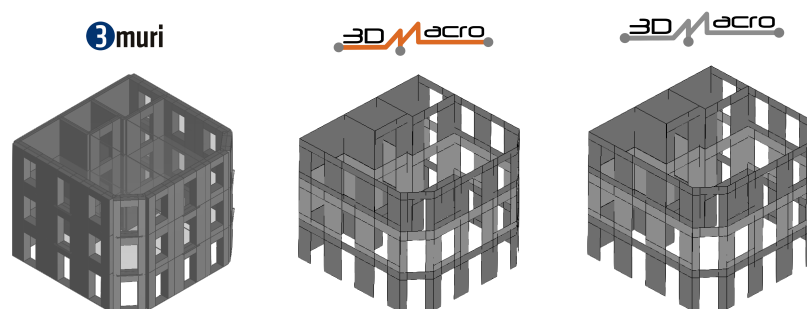
Figure 3.18: 3D-view of the reference model built by using the three different macroelement models: 3Muri® (left), two-dimensional (middle) and three-dimensional model incorporated in 3D-Macro® (right). To ease the viewing, horizontal diaphragms are not displayed.

the sake of simplicity, only the uniform mass-proportional load pattern was considered, since it is believed to be sufficiently representative of the inertia actions acting on medium-low height UCH assets [176]. Moreover, unidirectional load patterns with and without additional eccentricities were considered. Thus, for each model, 12 analyses were performed: 6 analyses along the X direction and 6 analyses along the Y direction.

3.2.5.1 Modal analysis

The main outputs obtained from the modal analysis performed by using each one of these macroelement models are summarised in Figure 3.19, namely the natural frequencies, f, mass participation ratios, M_x and M_y (along the X and Y directions), and the first three vibration modes. It is worth noting that the plan modal shape configurations reported in Figure 3.19 refer to the deformed shape of the top storey level. At first glance, and when compared to the results obtained for the two- and three-dimensional model of 3D-Macro®, it seems that the first two vibration modes of 3Muri® are swapped. It is also possible to observe that the fundamental mode of vibration in the one-dimensional macroelement model of 3Muri® corresponds to the translation in the Y direction, where masonry walls appear to move in phase. Conversely, in case of the two- and -three dimensional macroelement models of 3D-Macro®, the fundamental mode corresponds to the translation in the X direction, together with a slight rotation. The second and third vibration modes are characterised by the combined effect of the previous two (translation and rotation). Moreover, it is worth to highlight that the natural frequencies, f, obtained with the 3D-Macro® models are lower than those of 3Muri® model. This suggests that the model of 3Muri® is more rigid and less ductile than those of 3D-Macro®, a statement that will be confirmed further on by the results of pushover analyses.

The three-dimensional model of 3D-Macro®, however, shows a good agreement with the model of 3Muri® in terms of natural frequencies, as the average deviation between these two models when considering the three first vibration modes, is about 10%.

The two-dimensional model of 3D-Macro® provides lower natural frequencies associated with the first and second modes (translation modes) when compared to the remaining models. This suggests that the out-of-plane stiffness contribution of the walls plays, in this case, a non-negligible role over the global lateral stiffness of the building. When comparing the two- and three-dimensional models of 3D-Macro®, the average difference in terms of natural

frequencies is about 17%. These results can be justified because the investigated building is characterised by thick walls with in-plane slim panels.
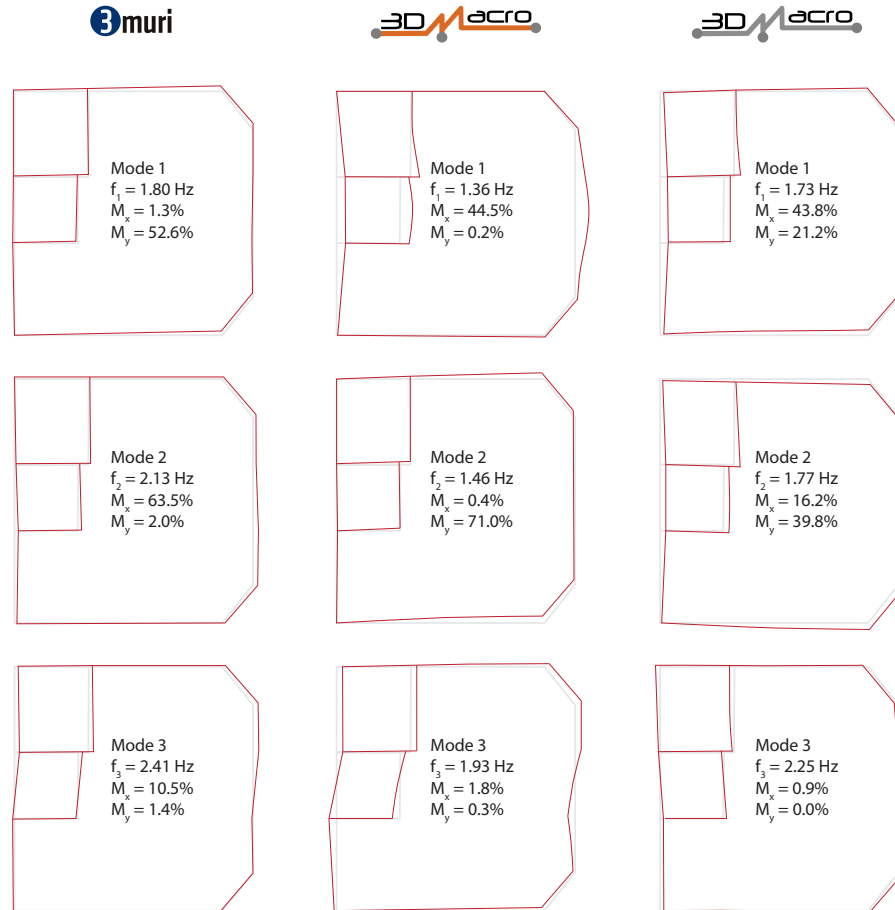
Figure 3.19: Deformed shape of the first three modes (from M1 to M3) obtained for each macroelement model at the upper storey level and by considering a deformation scale equal to 50: one-dimensional macroelement model of 3Muri® (left column); two- (middle column) and three- (right column) dimensional macroelement models of 3D-Macro®.

3.2.5.2 Pushover analysis

The comparison in terms of pushover curves is presented in Figure 3.20. The curves in light grey correspond to the analyses performed by considering accidental eccentricity (positive and negative), according to the recommendations of EN-1998:3 [93]. From these results, it is clear that the one-dimensional model of 3Muri® is more sensitive to accidental eccentricity. Even though there is no information available that could possibly sustain any conclusions about which model predicts with more precision the real behaviour of the case study, more conservative results are always preferable from the seismic safety viewpoint, since in theory, to fulfil the safety requirements, the demand in terms of strengthening will be naturally higher. However, if results are too conservative, we might be oversizing the structure, which is not sustainable from the economic viewpoint.
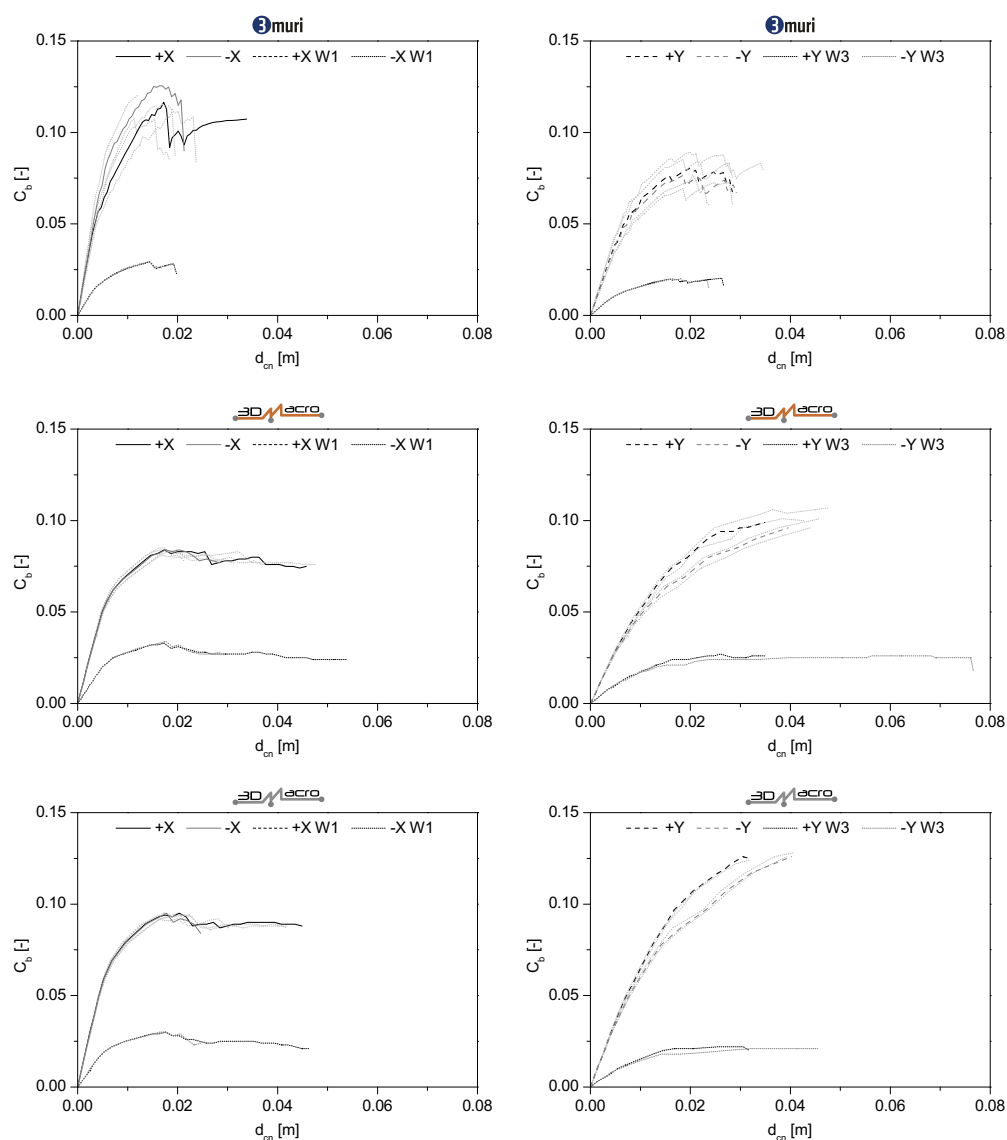
Figure 3.20: Pushover curves of the reference model for the X (left column) and Y (right column) directions, computed for each macroelement model: one-dimensional macroelement model of 3Muri® (upper row); two- (middle row) and three- (bottom row) dimensional macroelement models of 3D-Macro®.

When comparing the pushover curves computed in both directions, it is possible to observe that those along the X direction present in general a higher initial stiffness, while the Y direction is characterised by a higher ductility. This evidence is transversal to all the considered models. However, these curves exhibit significant deviations in terms of shear coefficient, C_b. The shear coefficient peak values in the case of the 3Muri® model range from 0.107 and 0.125 in the X direction, and from 0.070 and 0.089 in the Y direction. In the case of the two-dimensional macroelement model of 3D-Macro®, C_b peak values vary from 0.083 to 0.085 in the X direction, and from 0.096 and 0.107 in the Y direction. Finally, in the case of the three-dimensional macroelement model of 3D-Macro®, C_b peak values range

from 0.093 and 0.095 in the X direction, and from 0.113 and 0.128 in the Y direction.

When comparing the two models incorporated in 3D-Macro®, it is possible to observe that the two-dimensional model underestimates the base shear strength, with respect to the three-dimensional one, in about 10% and 15%, respectively in the X and Y directions. However, from Figure 3.20, it can be observed that the contribution of the out-of-plane response of the walls does not have a significant impact over the post-peak behaviour and displacement capacity of these models. These results appear to be consistent with the geometrical configuration of the case study and the thickness of the respective masonry walls. Furthermore, it has to be considered that, in the actual nonlinear response of masonry buildings, the connections between orthogonal walls are weak or often ineffective, leading to a global behaviour in which the out-of-plane stiffness contribution of these walls tends to be negligible.

The results of the pushover analyses demonstrate that the model of 3Muri® provides a higher lateral peak-strength when compared to the 3D-Macro® models. A discrepancy of about 25% was observed when comparing the model of 3Muri® with the three-dimensional model of 3D-Macro®. At the same time, the model of 3Muri® provides a lower ultimate displacement capacity. These differences can be partially justified by the different modelling strategies adopted in the simulation of flexural mechanisms. In the case of 3D-Macro®, the flexural mechanism is governed by a progressive distribution of damage in the adopted fiber discretization (distributed plasticity), while in the case of 3Muri®, this mechanism is ruled by plastic hinges in the frame model (concentrated plasticity). These results are in line with the trend previously observed in the modal analysis (in Section 3.2.5.1), where the values of natural frequencies in the model of 3Muri® are higher than those of 3D-Macro® models. Although significant deviations were found between these macroelement models, it is indeed necessary to extent the analysis in terms of seismic performance before drawing further conclusions, a matter that is going to be tackled further on in this study.

In addition to the global pushovers, the pushovers of façade walls W1 and W3 are also plotted in Figure 3.20. In this case, the base shear coefficient C_b, was obtained by dividing the wall base shear strength by the global weight of the building, W. When comparing these two walls, it is possible to observe a good agreement between the three models in terms of base shear capacity. However, the ductility capacity of these walls diverges substantially from model to model. In the following subsection, façade walls W1 and W3, will be used as reference walls in the comparison of the expected damage pattern distribution by each one of these macroelement models.

3.2.5.3 Damage distribution pattern analysis

The analysis of the damage distribution pattern is of great usefulness for a correct interpretation of the results obtained from the pushover analysis. Furthermore, this type of analysis is also of great utility to better locate and prioritise eventual strengthening or retrofitting measures [72]. The verification of the distribution damage pattern of UCH assets in the context of seismic performance assessment should also include the displacement corresponding to the damage limitation (DL) limit state.

For the sake of simplicity, Figure 3.21 and Figure 3.22 present the damage distribution pattern of façade walls W1 and W3, that correspond to the pushover analyses performed along the +X and +Y directions, respectively (accidental eccentricity was disregarded). The damage pattern predicted by the three different macroelement models is illustrated for the

step that activated the displacement corresponding to the achievement of each limit state (DL, SD, and NC). To better scrutinise the behaviour of the masonry panels, beam elements were not displayed.
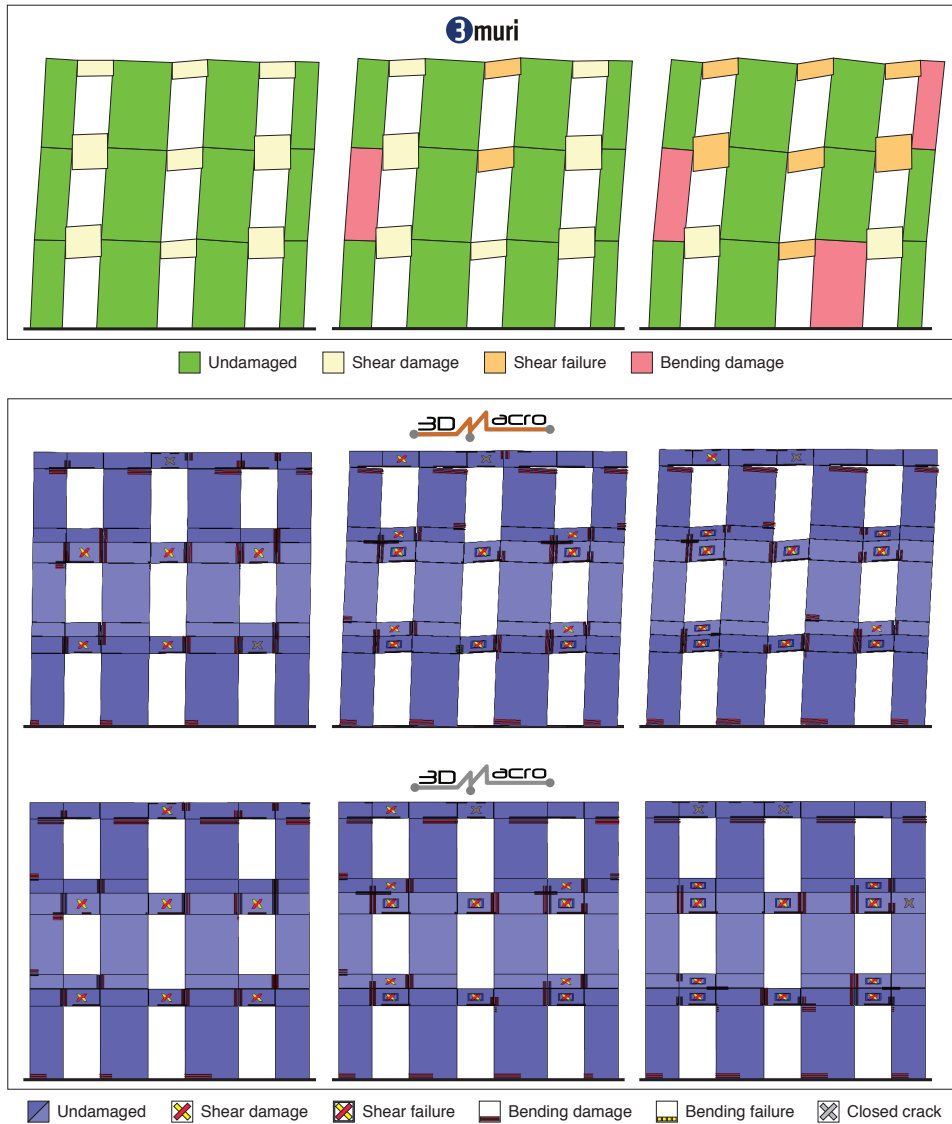
Figure 3.21: Comparison of the damage distribution pattern in façade wall W1 (in the +X direction and without accidental eccentricity) at the displacements corresponding to DL, SD, and NC limit states (from left to right, respectively).

If looking at Figure 3.21, it is possible to observe that the damage in wall W1 is concentrated in spandrels and caused by the diagonal shear failure mechanism. The shear damage or failure conditions can be distinguished by means of the graphical icons available in the user graphical interfaces of the two software codes. This mechanism, which is associated with the loss of shear capacity of each panel, is particularly relevant not only for the seismic safety assessment of structures but also for the design of strengthening interventions. While in the 3Muri® model most of the masonry piers remain undamaged even at the NC limit state, in the models of 3D-Macro®, bending damage in piers prevails. In fact, bending damage
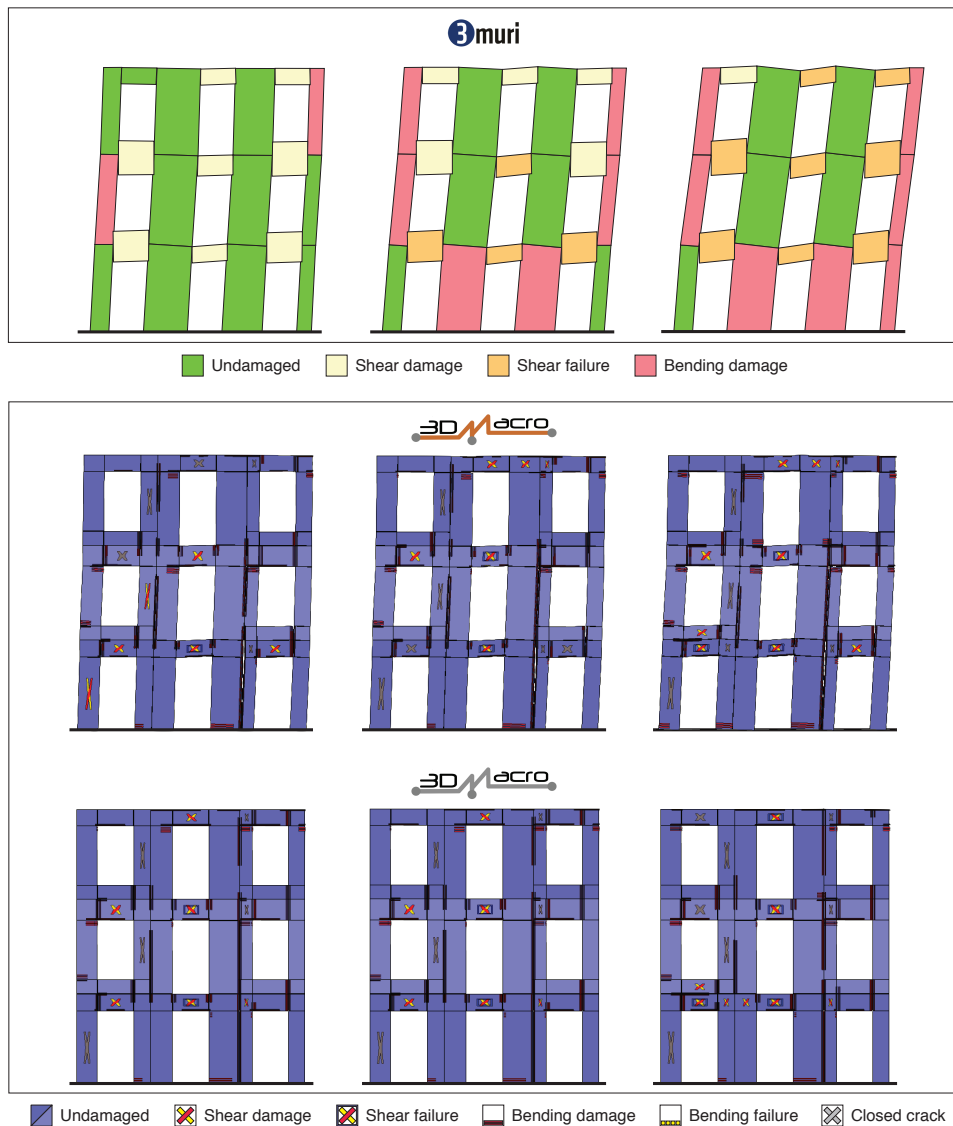
Figure 3.22: Comparison of the damage distribution pattern in façade wall W3 (in the +Y direction and without accidental eccentricity) at the displacements corresponding to DL, SD, and NC limit states (from left to right, respectively).

in 3D-Macro® models is mostly concentrated in the base sections of the piers at the first storey and in the top sections of the upper storey. It is worth noting that, unlike the 3Muri® software code, where joint sections are considered rigid by default, in 3D-Macro® these sections are expected to undergo plastic damage. When examining the behaviour of spandrels in wall W1, it is observed that shear damage is the prevailing mechanism, progressing from a situation of widespread damage (at the DL limit state), up to a situation where practically all spandrel elements reached failure (at the NC limit state). In line with the previous results, the two-dimensional macroelement of 3D-Macro® appears to provide a more conservative estimation, as the extent of damage is significantly higher than in the remaining models. At the other extreme, the model of 3Muri® provides a less conservative damage estimation, particularly in the case of piers. In fact, the greatest deviation between the model of 3Muri®

and those of 3D-Macro® resides on the percentage of undamaged piers, which is significantly higher in the first case. Moreover, the damage expected for the spandrel elements located at the roof level constitutes another significant difference between both software codes. While in the case of the 3D-Macro® models, spandrels appear to remain practically undamaged, in the case of the 3Muri®, shear failure is reached, particularly at the NC limit state. Still referring to Figure 3.21, it is possible to observe that, occasionally, in 3D-Macro® models, few macroelements are expected to undergo an unloading phenomenon from plastic to elastic phase, meaning that at the current step of the analysis these elements were in elastic phase, but some plastic damage, had been however, accumulated.

When observing the damage distribution pattern of wall W3, illustrated in Figure 3.22, it is possible to observe again that, in the case of the 3Muri® model, widespread shear failure is expected to occur in spandrels. Bending, however, appears to be the predominant damage mechanism in piers, particularly in those located at the first storey or at the intersection between adjacent walls. In the case of 3D-Macro® models, the percentage of spandrel elements damaged by bending and shear mechanisms is way more balanced. Bending damage is more widespread in piers, even if a combined shear-bending failure occurs in some piers. Most of the above-mentioned differences between these three models, in terms of plastic damage distribution and failure mechanisms, can be justified by the fact that the nonlinear flexural behaviour of masonry panels in 3D-Macro® is simulated by means of a fibre discretisation approach, which allows to predict combined failure mechanisms. Thanks to the planar scheme of the macroelement incorporated in 3D-Macro®, a more realistic interaction mechanism between spandrels and horizontal diaphragms (and floor-beams) can be simulated.

3.2.5.4 Seismic performance-based assessment

Table 3.3 summarises the main outputs from the seismic performance-based assessment, namely the total mass of the equivalent Single-Degree-of-Freedom (SDOF) system, m^*, the transformation factor, Γ, and the $\%a_g$ values, obtained for each limit state and macroelement model (for the sake of simplicity, the results referring to the analyses considering accidental eccentricity were not presented).

The deviations between the considered models in terms of the total mass of the equivalent Single-Degree-of-Freedom (SDOF) system, m^*, represent about 13% and 73% of the m^* value estimated by 3Muri®, respectively for the X and Y directions. When looking at the transformation factor, Γ, it is possible to observe a good agreement between these models in the X direction. In the Y direction, however, the Γ factor estimated by 3Muri® is 38% higher than that of 3D-Macro® models. When comparing the total weight of each model, W, presented in the previous Section 3.2.4, deviations lower than 0.1% were found between the considered models.

The results presented in Table 3.3 highlighted that the Y direction is, to the exception of limit state DL, the most vulnerable direction. When comparing the two- and three-dimensional models of 3D-Macro®, and average increase of 10% and 7% was found in terms of $\%a_g$ values for the DL and NC limit states. This outcome appears to be consistent with the observed in terms of initial stiffness and ultimate strength (see Figure 3.20). With respect to the X direction, the average $\%a_g$ value considering all the models investigated and both positive and negative loading directions, resulted 32%, 62% and 82% respectively for limit states DL, SD and NC. In the Y direction instead, average $\%a_g$ values of 40%, 49% and 63% were estimated for the same limit states.

Table 3.3: Input parameters for the application of the N2 Method and the %a_g values for each limit state and macroelement model.

	Direction	m^* $[\mathrm{kN\,s^2\,cm^{-1}}]$	Γ [-]	%a_g DL	%a_g SD	%a_g NC
❸muri	+X	3.95	1.09	43.2	49.6	63.5
	-X			42.1	60.5	80.6
	+Y	2.33	1.66	31.8	49.9	66.6
	-Y			30.4	51.0	68.0
3D/\acro.	+X	4.64	1.07	33.1	99.8	133.1
	-X			33.4	61.6	82.2
	+Y	4.03	1.20	48.4	55.6	72.3
	-Y			52.8	59.5	75.2
3D/\acro.	+X	4.64	1.07	35.3	104.0	138.7
	-X			35.3	57.0	76.0
	+Y	4.03	1.20	54.3	58.0	74.7
	-Y			61.4	66.9	85.4

The results in Figure 3.23 compare the %a_g values obtained for the positive and negative directions of X and Y, respectively. In general, and contrarily to the results of 3D-Macro® models in which only a few limit states verified the safety requirements in terms of a_g, in the case of the 3Muri® model, none of the limit states were verified. Deviations are more significant when comparing the 3Muri® model with the three-dimensional model of 3D-Macro®, varying in average, between -119% and 18%, respectively in the positive and negative direction of X. In the case of the Y direction, these deviations varied, in average, between -12% and -102%.

3.2.6 Discussion

The main features the investigated software codes have in common, as well as the key aspects where they most diverge, are summarised in Table 3.4, and discussed in the following paragraphs. Furthermore, some of the most important advantages and drawbacks of each software code and the respective macroelement model are going to be scrutinised from the end-user viewpoint.

Both software codes have in common the type of failure mechanisms of masonry panels (diagonal and sliding shear failure and bending failure mechanisms). As for the range of analyses available, both software codes are pretty much alike. In fact, the most recent versions of both 3Muri® and 3D-Macro®, allow performing a multi-directional seismic assessment of a structure, by defining a set of nonlinear static analyses with a constant step of loading direction, usually referred to as "angular scanning" analyses.

Moreover, both software codes allow the computation of pushover analyses at the wall level, a very handy feature, particularly when modelling masonry structures with flexible floors, where the global response of the structure is largely conditioned by the seismic capacity of its weakest wall. Additionally, it is worth referring that both 3Muri® and 3D-Macro® have a quite intuitive interface, facilitating the visualisation and operation during the modelling phase. Another differentiating aspect these software codes have in common, and perhaps one the most attractive, is the relatively low computational effort.

Since the default models incorporated in 3Muri® and 3D-Macro® were developed to ex-
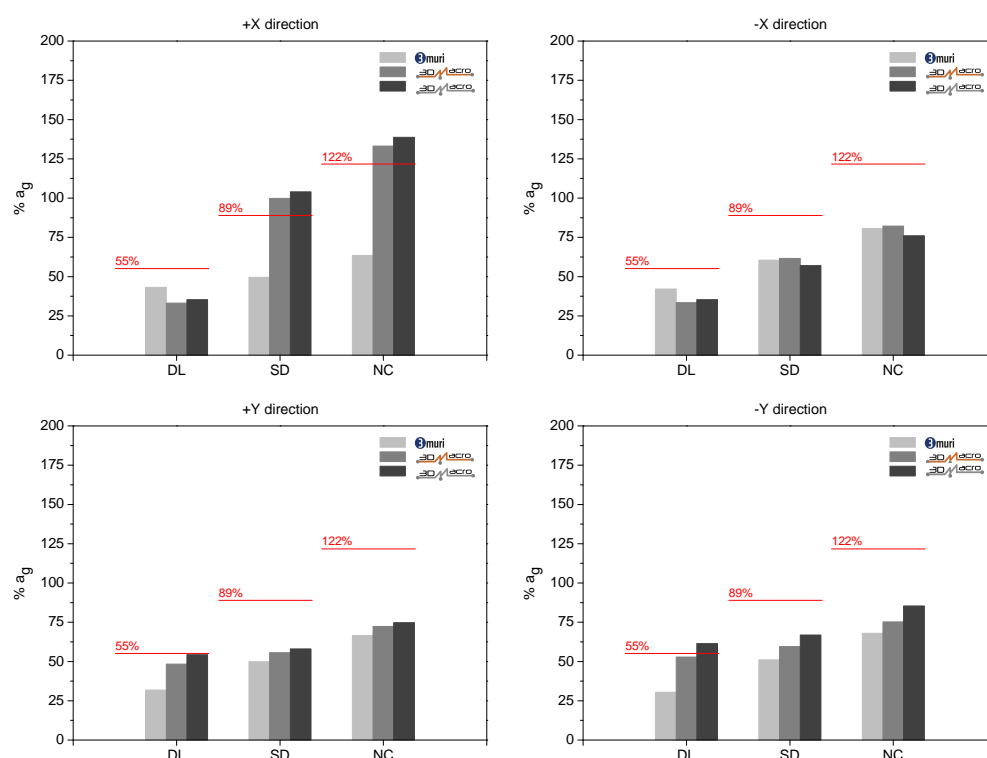
Figure 3.23: Comparison of the %a_g values for each limit state obtained for the positive (left) and negative (right) direction of X (upper row) and Y (bottom row).

clusively assess the in-plane global response of unreinforced masonry buildings, these software codes have an embedded module for the evaluation of local mechanisms. Without entering in big details, as the assessment of local mechanisms is out of the scope of the present study, 3Muri® allows for the evaluation of both simple and complex overturning, while in the case of 3D-Macro®, only the first is available.

A major difference between these software codes concerns to the very conceptual definition of each macroelement. While 3D-Macro® resorts to two- and three-dimensional macroelements, in the case of 3Muri®, where the equivalent frame model approach is adopted, the final 3D model is required to be closed, inhibiting modelling a wall without being connected in a "box-like" shape. Moreover, whenever an opening is inserted in a 3Muri® model, the ultimate drift is evaluated in function only of the deformable portion of piers, which is naturally smaller than the actual height of the wall due to the presence of a rigid node. This fact is believed to contribute to a less conservative estimation of the actual response of piers, as their geometrical configuration is slightly improved by inducing this "flattening" effect. In the case of 3D-Macro® instead, the resistant area of a given wall in the model is closer to the actual area of the wall.

As discussed earlier in this study, the consideration of the tensile strength is indeed another distinctive aspect between these software codes. While 3Muri® assumes a "no-tension" hypothesis for the flexural failure mechanism, the tensile strength has to be defined in 3D-Macro®. However, the sensitivity analysis carried out in Section 3.2.4, has demonstrated that, contrarily to what was expected, the consideration of a f_{tm} close to zero (0.001 MPa) in the two-dimensional model of 3D-Macro® aggravates the discrepancy between this and

the 3Muri® model, in which a "no-tension" hypothesis is assumed.

Some of the main advantages of 3Muri® with respect to 3D-Macro®, consist on a few add-on modules offered in the latest version of this software code, namely concerning the selection of the calculation method, the possibility of using multiple processors, of performing sensitivity analyses, and also the possibility of using a wide number of seismic codes. Performing the calculation by using the FEM method (Finite Element Method), 3Muri® allows the selection of the calculation method, either by using dense or sparse matrices [12]. Performing operations using dense matrix algorithms can take, in some cases, a long time and a large amount of memory. In this case, the use of sparse matrices can reduce the computational effort, both in terms of memory usage, and time spent in the operation. Moreover, this new module of 3Muri® allows the possibility of performing simultaneously different calculations on multiple processors. However, while the incorporation of different seismic codes is fully established in 3Muri®, in the case of 3D-Macro® minor upgrades regarding the editing of the seismic demand parameters according to the National Annex of the EN 1998-1 [95] of each country, are still needed, to extend its commercial use across borders.

One of the main advantages of 3D-Macro® with respect to 3Muri® consists on the possibility of using the new three-dimensional macroelement model, which, as already explained in this thesis, accounts for the combined in-plane and out-of-plane response. In this way, two of the main criticisms commonly addressed to this type of software, related to the assumption of the so-called "box-behaviour" and that "in-plane damage is the primary source of damage", are overcome. Indeed, this assumption is particularly questionable in the case of structures with flexible floors. In what regards the vertical load re-distribution, Bessi et al. [177] have reported that 3Muri® appears to exacerbate the loads transferred from horizontal diaphragms to walls along walls' axial stiffness, independently from the direction of the floors' warping, as a result of the EFM approach. Another substantial difference identified by Marques and Lourenço [138], is that the methods implemented in 3Muri® for simulating the interaction between macroelements through rigid nodes, as well as for modelling the cracked condition of panels (lumped at middle/end parts of the element), are improved when considering the two-dimensional model implemented in 3D-Macro®.

3.2.7   Final remarks

The comparison of different macroelement approaches has confirmed that the selection of a numerical tool for the seismic response assessment of unreinforced masonry structures is indeed a very complex and often non-consensual task that should be supported by weighing several aspects, namely the compatibility between the analysis tool and the study object, the type and the amount of input data, as well as the financial resources available and eventual time constraints. Associated with these aspects, a deep knowledge of the main features and drawbacks of each model, as well as the end-user ability to critically analyse the quality of both input and output data, is also highly recommendable to guarantee the efficiency of the analysis and the reliability of the results.

Good-judgement capacity and utmost care on interpreting the results provided by analytical methods should be key skills for the new generation of structural engineers. This is of paramount importance given the new arrangement applicable to the renovation of existing buildings and building units [58], namely after the approval of the Ordinance no. 302/2019 [59]. that defines, not only the terms in which the seismic response of existing buildings must be or not evaluated and reported, but also the terms where seismic retrofitting

Table 3.4: Comparison of the main features of 3Muri® and 3D-Macro® software codes.

Set of features	Feature	❸muri	3D Macro
In-plane failure mechanisms	Flexural (rocking)	✓	✓
	Shear (diagonal cracking)	✓	✓
	Shear (sliding)	✓	✓
Type of analyses	Modal analysis	✓	✓
	Static linear	✓	✓
	Static nonlinear	✓	✓
	Angular scanning	✓	✓
	Dynamic nonlinear	–	–
	First mode mechanisms	✓	✓
Modelling and calculation	User friendly interface	✓	✓
	Closed geometry	✓	–
	Tensile strength	–	✓
	Multiple processors	✓	–
	Sensitivity analysis	✓	–
	Combined in- and out-of-plane response	–	✓
Local collapse mechanisms	Overturning (simple)	✓	✓
	Overturning (mixed)	✓	✓
	Vertical bending	✓	✓
Building codes	EN 1998 (Eurocode 8)	✓	✓
	NTC (Italian Building Code)	✓	✓
	SIA (Swiss code)	✓	–
Section of verification	Middle of the panel	✓	✓(shear)
	Base of the panel	–	✓(flexural)
Distribution of vertical loads	Along axial stiffness	✓	✓
	Along floors' warping direction	–	✓

or strengthening is required. Therefore, critically analysing and double-checking outputs by considering different modelling assumptions or even different analytical methods, and not just simply accept them blindly or as an absolute truth, is now more important than never.

In addition to the results provided by these simplified models, and from the seismic safety viewpoint, it is essential to extend the assessment with complementary approaches at the local level, particularly when dealing with UCH assets with flexible diaphragms and of complex geometry. In this sense, understanding the potential and limitations of different models and software codes currently available for the seismic response assessment of UCH assets is fundamental to promote a more conscious decision not only on the type of software that could possibly serve the best interest of end-users and stakeholders, but also represent in a more accurate way, the actual response and the particularities of each case study in hands.

In short, the natural frequencies obtained in the modal analysis showed a good agreement between the one-dimensional model of 3Muri® and the three-dimensional model of 3D-Macro®, with average deviations of about 10%. When compared to the remaining models, the two-dimensional model of 3D-Macro® underestimates the natural frequencies associated to the first and second modes (translation modes).

With respect to the nonlinear static analysis, the pushover curves of the two- and three-dimensional models of 3D-Macro® demonstrated a very similar behaviour, being the shear

coefficient, C_b, slightly lower in the first case. When compared to the models of 3D-Macro®, the one-dimensional model of 3Muri® tends to underestimate the ultimate displacement capacity.

From the damage pattern analysis, it is worth highlighting that the planar scheme of the macroelement incorporated in 3D-Macro®, enables a more realistic interaction mechanism between spandrels and horizontal diaphragms (and floor-beams).

The results in terms of seismic performance-based assessment are consistent with the discrepancies observed between the two- and three-dimensional models of 3D-Macro®, in terms of initial stiffness and ultimate strength.

As a final comment, it is important to stress out that the use of models based on macroelements, despite the limitations and assumptions herein identified and discussed, still offers a very interesting compromise between computational effort and accuracy on the estimation of the nonlinear response of existing masonry buildings, being recommendable, with due diligence, also in the case of UCH assets.

Chapter 4

Cost-benefit analyses

Abstract *This chapter presents the main findings of a cost-benefit analysis (CBA) model applied to investigate the integration of traditional seismic strengthening solutions in the rehabilitation of UCH assets. While in a first phase, the economic viability of using such strengthening solutions was investigated, in a second phase, the mentioned CBA model was applied to four different case studies.*

Supportive publications
P4: Maio, R., Ferreira, T.M., Vicente, R. and Costa, A. (2018). Is the use of traditional seismic strengthening strategies economically attractive in the rehabilitation of urban cultural heritage assets in Portugal? *Bulletin of Earthquake Engineering*, 17, 2307–2330. URL `https://doi.org/10.1007/s10518-018-00527-7`.

P5: Maio, R., Estêvão, J.M.C., Ferreira, T.M., Vicente, R. (2020). Cost-benefit analysis of rehabilitation interventions carried out in urban cultural heritage assets by integrating the use of traditional seismic strengthening strategies. *Engineering Structures*, 206.URL `https://doi.org/10.1016/j.engstruct.2019.110050`.

4.1 Economic viability

This section aims not only at raising awareness for the preservation of traditional construction techniques and materials when intervening in UCH assets, but also at demystifying whether or not the integration of traditional seismic strengthening strategies in the renovation process of such assets is economically viable. In Portugal, over the last decades, countless UCH assets have been massively demolished and replaced by modern construction solutions. As this phenomenon is contributing both to the mischaracterisation of the existing building stock within the majority of historic centres, and to the gradual loss of knowledge on these construction techniques, it is fundamental to tackle this issue from its very foundations, i.e., by raising the awareness and consciousness of all the involved stakeholders to the need of preserving such techniques and materials as part of the patrimonial value of UCH assets. Hence, in order to investigate the above-mentioned issues, the database created in the framework of the 1998 Azores earthquake by the Regional Secretariat for Housing and Equipment (SRHE) of Faial Island, was herein revisited. By critically handling and analysing this database, it was possible not only to investigate the economic prospects of UCHs assets' renovation in Portugal, but also to derive new repair cost functions suitable to the Azorean traditional stone masonry building stock, that might be used to support post-disaster emergency plans and the design of earthquake risk mitigation strategies.

Cultural heritage is generally described as a wide set of cultural aspects, engineering and architectonic features, from physical artefacts and social customs, to traditions and practices, which are inherited from past generations [178]. Safeguarding cultural heritage is therefore essential to preserve the identity of communities and cultural diversity worldwide. The values of cultural built heritage are commonly divided into two different categories: economic (which may be expressed in monetary terms) and sociocultural (non-monetary) values. Several studies have been developed addressing the evaluation of these categories by means of both qualitative and quantitative approaches [18, 178, 179, 180, 181]. Despite the integration of economic values in the valorisation of built heritage is accredited to be a strong force shaping heritage conservation, it is often left out of the traditional purview of conservation professionals. Rather than tap into the evaluation of utterly sociocultural values, which require a completely distinct approach, the present study aims at investigating the economic impact resulting from preserving traditional construction techniques and materials in the renovation of UCH assets, as an integral part of the engineering and architectonic features included in the definition of urban cultural heritage. By doing so, it is expected that one of the most-frequently preconceived ideas usually attributed to such traditional construction techniques and materials, that they are economically unattractive or unreliable when compared to modern construction solutions (e.g. steel or reinforced-concrete structures), can be demystified.

Despite the wide spectrum of traditional construction techniques and materials used in UCH assets in Portugal, as demonstrated for example in [23], its use has been declining abruptly. Several aspects have been appointed to this gloomy reality, such as the lack of awareness and sensitivity of all the involved stakeholders for the cultural relevance and benefits from preserving these traditional solutions, and for the long-term consequences that the loss of such heritage would represent to each stakeholder and ultimately, to the nation's patrimonial welfare. This has also contributed to the continuous decline of the number of skilled professionals (from masons and technicians to engineers and architects) with expertise on these techniques and materials, leading to a natural increase of the labour

cost associated with such specific works. Hence, this study aims not only at investigating the economic prospects of UCHs assets' renovation in Portugal, but also to develop new functions for the estimation of repair costs of seismic damage derived from the database provided by the SRHE of Faial Island, which refers to the 1998 Azores earthquake.

4.1.1 The 1998 Azores earthquake

The Azores archipelago, located at the triple junction of the Eurasian, North American and Nubian plates, is considered the most important seismogenic region in Portugal, both in terms of magnitude and frequency [29]. On July 9th, 1998, the central group of the archipelago, and in particular the Faial Island, was severely hit by an earthquake of magnitude 6.2, which has been extensively documented in literature [29, 182, 183, 184]. This event, also felt on the islands of Faial, Pico and S. Jorge, left behind a massive trail of destruction, as about 70% of the building stock was damaged (see Figure 4.1), and has directly affected the life of over 5000 people, from which 150 injured, 1500 homeless and 8 fatalities were reported [29].

The 1998 earthquake, considered as one of the worse natural disasters in the living memory of archipelago, and the reconstruction process that has followed on from it, allowed for the collection of an unprecedented amount of data that has been encouraging the development of many studies ever since, as for example those carried out by [72, 167, 185, 186]. The data collected during the 10 years-long reconstruction process of Faial Island, that was conducted by the Society of Promotion for Housing and Infrastructures Rehabilitation (SPRHI), was compiled in 2007 by the SRHE of Faial Island and included in the commemorative publication of the 10 years after the event entitled "Sismo 1998 Açores - uma década depois" [29].

Figure 4.1: Illustration of the damage observed in the sequence of the 1998 Azores earthquake in some of the most affected parishes of Faial Island: Castelo Branco, Flamengos and Pedro Miguel (respectively from left to right). Source: Faial database.

4.1.2 The Faial database

As mentioned above, the hereinafter designated Faial database resulted from the data collected during the 10 years-long reconstruction process of Faial Island that followed the 1998 Azores earthquake. Over the last years, this database has supported the development of a wide range of studies in numerous research fields, covering, among other issues, the general characterisation of the earthquake, considering its historic context and both geological and geophysical aspects [182, 183, 184], the typological characterisation of the building stock of Faial Island and of observed damage [185, 187], as well as many other experimental (on-site) and analytical studies that aimed not only at characterising the mechanical properties and the seismic response of traditional stone masonry structures [169, 185, 186, 188], but also on investigating the effectiveness of traditional seismic strengthening measures [72, 167, 168, 187].

However, given its unique character, there is room to further exploit the referred database, particularly in what regards the costs of renovation works and seismic strengthening strategies that were implemented at the time. This information is considered of great interest all the more when considering the current paradigm of renovation and rehabilitation of existing buildings in Portugal, described in Chapter 2. Hence, the research opportunity to address this issue emerged not only by realising the great potential and uniqueness of the collected data, but also by combining both the necessity of demystifying the preconceived idea that the renovation of UCH assets is invariably, economically unattractive and disadvantageous, with the need for the protection of traditional construction techniques and materials, particularly in historic centres, which are a fundamental part of our cultural identity.

Before introducing the economic aspects behind the reconstruction process of Faial Island, it is important to stress out that the sample of buildings herein analysed was extracted from the original Faial database according to the aims of the present study, i.e., disregarding for example deficient and unreliable data, or even data related to reinforced concrete structures (RC). Thus, the distribution and full description of the sample herein considered is going to be presented and analysed. It comprises a total of 1395 stone masonry buildings that were subjected to different types of interventions. The stone masonry building stock of Faial Island features a wide variety of typologies resulting from the intrinsic properties of the buildings and its surrounding, and the emergence of new technologies and materials (such as steel or concrete), which have been re-shaping the traditional Azorean stone masonry construction over the years.

Firstly, it is fundamental to highlight the differences between rural and urban typologies, an issue that was firstly addressed by Costa [169]. As illustrated in Figure 4.2, while in rural areas one- up to two-storey buildings are typically found, generally isolated and with very modest architectonic details, in urban areas of Faial Island the same buildings can vary in between two- and four-storeys and are invariably enclosed in aggregate. Another substantial difference between such typologies is that the basalt stone masonry of buildings located in urban areas is generally more regular, well-cut, shaped and arranged, in contrast to that of buildings located in rural areas, in which masonry is predominantly irregular and disorganised. According to Costa [169], this fact is generally true, even though the quality of the stone masonry is invariably reliant on the economic resources of property owners and on the expertise and care of the building contractor at the time of construction. The urban typology of Faial Island's stone masonry buildings falls within the category of UCH assets described in Chapter 1. In this study, only the data corresponding to the parish of Matriz (located within the historic centre of Horta), was considered as representative of the UCH category.

Figure 4.2: Illustration of three stone masonry buildings representative of the rural (left) and urban (centre and right) typologies of Faial Island building stock. Source: Faial database.

There were, however, a few sub-categories identified during the on-site survey and investigation works carried out in the sequence of the 1998 earthquake that are common to both rural and urban typologies [29, 189]. As mentioned above, these are associated with the advent of new technology and materials, namely the introduction of RC elements. These typologies are classified and described in the following Table 4.1 as SM1 to SM5, respectively from a more traditional Azorean stone masonry typology to its most "intrusive" variant. It is worth noting that despite the same nomenclature is used to classify the horizontal structure of SM2 and SM4 typologies, according to Oliveira et al. [29, 189], while in the first case the presence of timber floors prevails over RC slabs, which are usually limited to kitchen and bathrooms, in the case of SM4 typologies, the use of RC slabs is more generalised.

An overview of the distribution of the sample among the above-mentioned typologies is given Figure 4.3, from which it is worth highlighting that the original Azorean stone masonry typology (SM1) stills represented, at the time, the majority of the building stock of Faial Island (about 55% of the sample) for both rural and urban typologies, disregarding RC and other current building typologies. In fact, the distribution given in [29, 189], which accounted for all type of existent building typologies in the Islands of Faial and Pico (a sample of 3210 buildings), confirmed SM1 as the prevailing building typology, representing about 60.3% of these Islands' building stock. Coming back to this study's sample, it can be observed from Figure 4.3 that that SM4 is the second most common building typology of Faial Island, an observation that is again in line with the results presented by Oliveira et al. [29, 189]. In the following Section 4.1.4, this sample is going to be analysed in terms of observed damage.

Table 4.1: Material's description of the different variants of the traditional Azorean stone masonry typology, according to [29, 189].

Typology	Vertical Structure	Horizontal Structure	Roof Structure
SM1	Stone masonry	Timber	Timber truss
SM2	Stone masonry	Mixed	Timber truss
SM3	Stone masonry	RC slabs	Timber truss
SM4	Stone masonry with RC columns and beams	Mixed	Timber truss
SM5	Stone masonry with RC columns and beams	RC slabs	Timber truss or RC slabs

4.1.3 Damage assessment and classification

It is known that earthquakes have the potential to cause both an immediate- and long-term impact on communities, which might be classified in different categories, from physical, social, economic to environmental impact. In this study however, only the physical impact over residential buildings is going to be addressed. Moreover, given the current policies in Europe concerning energy efficiency, the so-called green retrofitting, is becoming more and more an integral aspect in the renovation process of traditional buildings. Even though several studies have been recently developed to understand how energy demand in traditional buildings can be reduced, as in the case of studies carried out by Filippi [190], Mazzarella [191], or Webb [192], this issue was not addressed in the present study as it refers exclusively to seismic strengthening strategies, as further explained in Section 4.1.7.
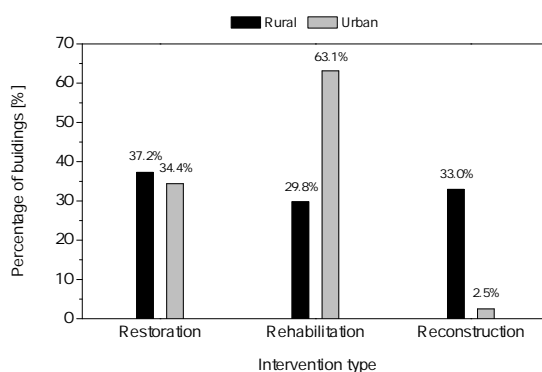
Figure 4.3: Relative percentages in terms of building typology of rural and urban buildings for the considered sample of 1395 buildings of the Faial Island.

In this subsection, the damage assessment and classification of the traditional masonry building stock of Faial Island will be briefly discussed by recapping and treating the information gathered in the Faial database, which was featured in the past by Neves et al. [185, 193]. The damage assessment herein presented concerns to the damage mechanisms observed in the sample of 1395 buildings of the Faial Island.

Hence, based on the classification proposed by Neves et al. [185], the exterior damage is herein classified into the following six damage states, from ds_0 to ds_5: No damage (ds_0) - Buildings that do not present any sign of damage; Slight cracking (ds_1) - Widespread cracking around openings and hair line cracks (cracks less than 1 mm wide); Moderate cracking (ds_2) - Typical shear cracking (involving the relative displacement between stones and the detachment of the wall rendering) without out-of-plane displacements; Extensive cracking (ds_3) - Typical shear cracking (involving the relative displacement between stones and the detachment of the wall rendering) with out-of-plane displacements; Partial collapse (ds_4) - Partial collapse of structural elements, and Ruin (ds_5) - Majority of the structural elements totally collapse. An example of each damage state is given in Figure 4.4 to clarify the classification herein considered.

Figure 4.4: Example of observed damage states ds_1 to ds_5 based on the classification proposed by Neves et al. [185], from left to right, which correspond to slight cracking, moderate cracking, extensive cracking, partial collapse and ruin, respectively. Source: Faial database.

The above-mentioned damage classification can be directly correlated to that defined in the European Macroseismic Scale [86], allowing for its use in earthquake risk and loss assessment applications. Moreover, from the damage data provided in the Faial database it is possible to establish a correlation between repair costs and damage states, allowing ultimately for the development of economic damage indexes and repair cost functions that might be applied to the Portuguese stone masonry building stock, as it will be discussed further on in Section 4.1.6.2.

Each category was subdivided into a set of subcategories, according to the area or element where the damage was observed, such as façade (F) or gable-end (G) walls or both (GF), roofs (R) or corner angles (C). Damage state ds_5, includes partial (P) and total (T) ruin or collapse of the structure. Moreover, acknowledging that different types of damage often coexist in earthquake-damaged structures, the final damage classification refers to the highest degree of damage observed, as suggested by Neves et al. [185]. Hence, in Figure 4.5 (left), the number of buildings for each damage state is presented together with the respective distribution for each subcategory, considering the sample of 1395 buildings. It is observed that only 2.1% of the sample was classified with damage state ds_0. At the other extreme, 30.2% of the buildings were classified with ds_3. Moreover, 56.9% suffered out-of-plane damage (ds_3, ds_4 and ds_5), highlighting the importance of accounting for out-of-plane mechanisms in the seismic response assessment of these building typologies.
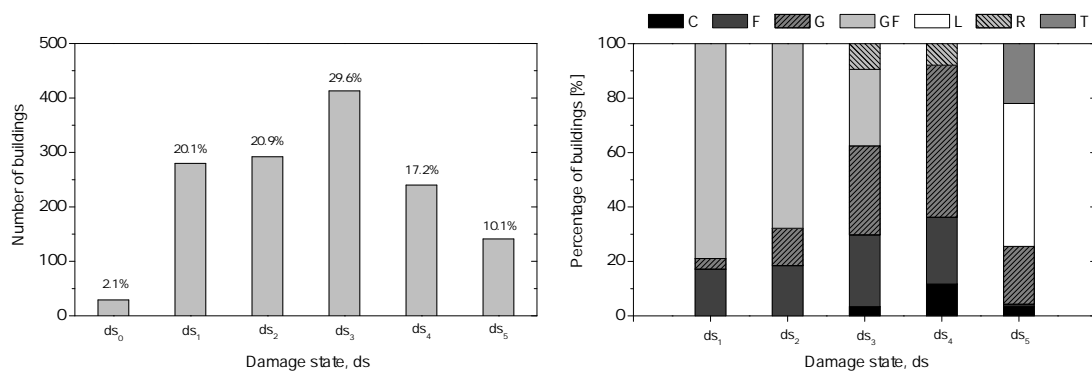
Figure 4.5: Observed damage distribution based on the classification proposed by Neves et al. [185], from ds_0 to ds_5 (no damage, slight cracking, moderate cracking, extensive cracking, partial collapse and ruin), and the corresponding subcategories depending on the extent and location of the damage, considering a sample of 1395 buildings.

If looking at the percentage distribution of each subcategory by damage state, given in Figure 4.5 (right), it can be observed that in the case of damage states ds_1 and ds_2, the vast majority of the buildings presented cracking damage at gable-end and façade walls simultaneously. Furthermore, with the exception of damage state ds_3, it is possible to observe that the damage was more concentrated in gable-end walls than in façade walls, a fact that might be explained either due to the poor quality of the connection between the façade and gable-end walls, or to the lack or poor quality of the connection between the horizontal structures (floors and roof) and gable-end walls, or even to the general low quality of the masonry fabric used to construct gable-end walls (when compared to façade walls). Another cause for this might be related to the fact that most of these buildings are "isolated", meaning that they do not share mid-walls with adjacent structures and therefore, gable-end walls are less constrained than in situations where buildings are enclosed in "aggregate". From Figure 4.5 (right), it is also possible to conclude that corner angle damage (C) was observed to damage states ds_3 to ds_5, as a result of the combined extensive cracking in both gable-end and façade walls and of eventual torsional effects. Finally, it is possible to observe that about 50% of the buildings classified with damage state ds_5 (74 out of 141) were totally collapsed after the 1998 Azores earthquake.

4.1.4   The reconstruction process of Faial Island

The preservation of traditional construction techniques and materials was one of the main premises for the reconstruction process of Faial Island that followed the 1998 earthquake [189]. These interventions were executed based on two types of contract: Direct Administration contracts, in which the financial support and the full responsibility was transferred to the claimant, and Fixed Price contracts. In the first case, the Reconstruction Promotion Centre (CPR), established by the Regional Legislative Decree Law 15-A/98/A of September 25, 1998, was appointed as the supervisory authority to assign the instalments in function of the overall progress of the work [189]. Fixed Price contracts, instead, were legislated by means of the Decree Law 300/98 of October 7, 1998, which entitled these contracts to five companies without the need of public tender [189]. From analysing the sample of 1395 buildings considered in this study, it was possible to observe that about 58% of these buildings underwent Fixed Price contracts, against 42% of Direct Administration contracts.

The reconstruction of the Faial's building stock was thus carried out at three different levels of intervention, herein referred as: restoration, rehabilitation, and reconstruction. These interventions were distinguished on the basis of the on-site evaluation of an global sensitivity parameter, ranging from 0% to 100%. This parameter was evaluated in function of the extent of damage observed during the post-event on-site investigations, to which 0% corresponded to a no-damage condition and 100% to total collapse. Naturally, this evaluation was highly reliant on the personal analysis and sensitivity of experts. The three previously mentioned levels of intervention were thus defined as a function of the global sensitivity parameter, according to the following thresholds [189]. A global sensitivity varying between 0% to 20% meant that the structure would be subjected to a minor intervention, generally associated with the repairing of plasters and painting of walls (restoration). Rehabilitations were assigned for a global sensitivity from 20% up to 50% and required interventions at the structural level, most of the times including the seismic strengthening of structural elements. Finally, a global sensitivity parameter higher than 50% was associated with structures severely damaged or collapsed and therefore in need of reconstruction. In the latter case, a substantial effort was made to preserve the original architectural layout and by using the same construction techniques and materials of the traditional Azorean building typology [189]. Cases where reconstructions were carried out by adopting new layouts and materials, were not included in the sample herein analysed. However, the reassessment after the on-site appraisal was carried out to validate the assigned type of intervention. As it can be observed from Figure 4.6, the percentage of rural buildings subjected to the different intervention types is quite well distributed. In the case of urban buildings, which represent 11% of the total sample of 1395 buildings, only 4 buildings were subjected to reconstruction, explaining therefore the extremely low percentage of severe damage observed in urban typologies (about 2.5%).

Figure 4.7 instead, shows the global sensitivity distribution in terms of percentage of buildings and type of intervention carried out. From the analysis of Figure 4.7 (left), it is possible to observe a relatively high and well distributed percentage of buildings assessed with a global sensitivity range between 0% and 30%. However, the percentage of buildings that fall within the global sensitivity range from 30% to 95% is quite low. This might be explained due to the ranges previously defined to establish the type of intervention to be conducted in a determined building, meaning that for the decision-making purpose the outcome of assigning a global sensitivity of 55% or 100%, for example, was exactly the same, as in both cases buildings would be subjected to a reconstruction intervention. If looking at Figure 4.7 (right),

it is possible to observe that in the parishes of Angústias, Capelo and Praia do Norte, most of the buildings were subjected to a restoration intervention. Following the same reasoning, it is possible to conclude that a higher relative percentage of rehabilitation and reconstruction interventions were conducted in the parishes of Matriz and Ribeirinha, respectively.
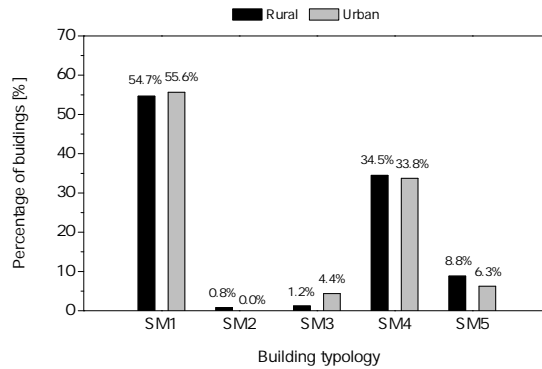
Figure 4.6: Relative percentages in terms of intervention type of rural and urban buildings for the considered sample of 1395 buildings of the Faial Island.
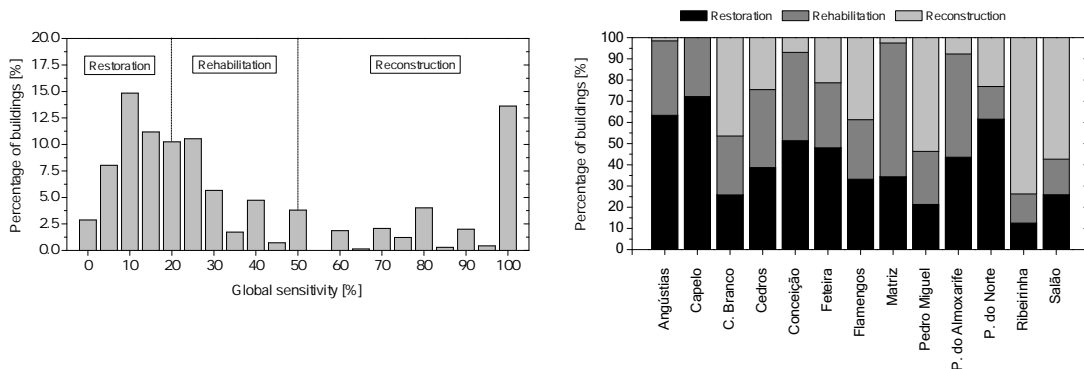
Figure 4.7: Global sensitivity parameter distribution in terms of percentage of buildings and type of intervention for the considered sample of 1395 buildings of the Faial Island: overall distribution (left) and distribution by parish (right).

4.1.5 Analysis of repair costs

Even though some authors suggest that intervention costs following an earthquake event can be affected by the cost increase of materials, equipment and workmanship as a result of the rise in demand [194], there are no evidences that such fluctuation could've been possibly present in the particular case of the reconstruction process of Faial Island. Moreover, although interventions inevitably involve some loss of value to the UCH asset, they are fundamental to preserve these assets for future generations. There are several intervention strategies that might be directed to UCH assets in function of their state of conservation, performance demands, or of the purpose of such intervention, for example. In this study however, focus will be given to the same three intervention types described in the previous Section 4.1.4, as there was made a clear effort to respect and ensure the longevity of the Azorean traditional

building typology, preventing it from falling into disuse, which could have ultimately led to its inexorable loss.

According to Oliveira et al. [189], the Regional Legislative Decree 15-A/98/A of 25 September 1998 has defined the cost for new construction at 400 €m^{-2}, which was updated in 2000 to 450 €m^{-2}. The later value was then adopted to define unitary prices for the budget of each project. It is important to highlight that whenever the total budget of a restoration transcended the limit of 15000€, the process was directly transferred to the rehabilitation intervention type [189]. It should be also noted that all the cost data herein presented refers to the repair costs, C_{RD}, in €m^{-2}. These are associated with the interventions carried out in the Faial Island between 1998 and 2001, which naturally include the cost of all the repairing works that were found necessary to ensure each building an adequate seismic performance. Such interventions were designed to comply with the seismic actions defined both in the Regulation of Safety and Actions for Buildings and Bridges Structures (RSA), which was in force at the time, and in the General Guidelines for Rehabilitation and Reconstruction, recommended by the Regional Laboratory of Civil Engineering (LREC). Even though the efficiency of such interventions is beyond the aim of the present study, the costs associated with the implementation of a few traditional seismic strengthening strategies are going to be brought into discussion in Section 4.1.7, so that they can be compared to the total repair costs.

In the following paragraphs, an overview of the observed repair costs is going to be presented and discussed to understand their variability by type of intervention, contract and building typology. Such repair costs ($\overline{C_{RD}}$) are analysed by assuming the median values as the central tendency measure and the respective 16th and 84th percentiles (PCTLs), as suggested when in the presence of non-uniform distributions. In addition to this, repair cost are going to be analysed in two different lines of reasoning based on the nature of their potential applications in future studies. While in the first, repair costs are going to be discretised in function of the gross floor area (GFA), in the second line of reasoning, repair costs are analysed in function of the damage state classification described in Section 4.1.3. These two lines of reasoning are going to be used in Section 4.1.6 as the grounds to develop new repair cost functions for the Azorean traditional stone masonry typology.

Hence, the statistics of repair costs, C_{RD}, referring to the sample of 1395 buildings are presented below in Table 4.2 as a function of both intervention and contract types (numbered from 1 to 6). The total number of buildings analysed for each type of intervention and contract is also given in Table 4.2.

Table 4.2: Statistics of repair costs (in €m^{-2}), C_{RD}, estimated from the sample of 1395 buildings of Faial Island and discretised for each intervention and contract type.

Intervention Type	i	Contract Type	Total Number of Buildings	16th PCTL [€m^{-2}]	Median [€m^{-2}]	84th PCTL [€m^{-2}]
Restoration	1	Direct Administration	285	61	139	325
	2	Fixed Price	230	263	545	1102
Rehabilitation	3	Direct Administration	204	96	224	438
	4	Fixed Price	265	344	609	1072
Reconstruction	5	Direct Administration	103	175	315	599
	6	Fixed Price	308	434	718	1229

From the analysis of these results, it is possible to observe not only a general increase when moving from less to more intrusive interventions (i.e., from restoration to reconstruction), but also a quite substantial difference in the $\overline{C_{RD}}$ values for each type of contract. In fact, it can be observed that the repair costs of interventions carried out by means of Fixed Price contracts were roughly 2, 3 and 4 times more expensive that those resorting to Direct Administration contracts, respectively in the case of reconstruction, rehabilitation and restoration interventions. If disregarding the intervention type, it is possible to conclude that the repair cost, $\overline{C_{RD}}$, of the contracts celebrated through Direct Administration resulted about 31% of the Fixed Price contracts.

In what concerns rural and urban typologies, and given the quite low number of urban buildings present in the sample (160 out of 1395), an equivalent sample of 160 buildings for the rural typology was selected to estimate the median repair cost, $\overline{C_{RD}}$, of both typologies. The selection of these 160 rural buildings was carried out by respecting the following criteria: the number of buildings per type of intervention and contract was considered equal to the urban sample, buildings were equally distributed by parish and selected in function of the closeness of their repair cost in relation to the median repair cost observed in each parish. Based on these criteria and disregarding the discretisation in terms of intervention and type of contract signed, the median repair cost, $\overline{C_{RD}}$, for rural and urban typologies was estimated in 420 and 652 €m^{-2}, respectively. The fact that the average repair cost in urban typologies is higher than in rural typologies might be explained by the fact of a higher structural complexity and architectonic richness being usually associated with urban typologies.

If assuming instead the different variants of the traditional Azorean stone masonry typology, which were previously described in Table 4.1, it is possible to compare $\overline{C_{RD}}$ in function of the global sensitivity parameter. Hence, from Figure 4.8 (left) it can be observed that higher C_{RD} values were obtained for building typologies SM1 and SM4. If looking at the median values of the global sensitivity parameter, it is clear that the SM1 was the most vulnerable typology in the 1998 Azores earthquake.
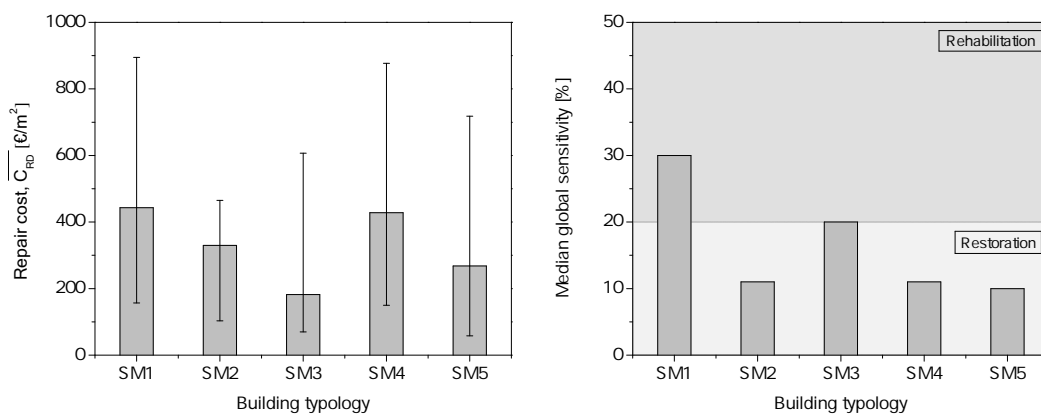
Figure 4.8: Plot of the median repair costs, $\overline{C_{RD}}$, and respective 16th and 84th PCTL values (left), and median global sensitivity (right) associated with building typologies SM1 to SM5.

This evidence has aroused the need for adequate design of seismic strengthening strategies for this particular typology, without compromising its cultural integrity. For this reason, the strengthening strategies adopted in the Faial Island as a result of the 1998 Azores earthquake, and their respective cost, are going to be subject of analysis in Section 4.1.7.

4.1.5.1 Analysis of the relationship between repair costs and gross floor area

As already mentioned, over and above analysing the sample by using central tendency measures, it is fundamental to understand its distribution in absolute terms. Thus, Figure 4.9 presents the relationship between the repair cost, C_{RD}, and the Gross Floor Area, GFA, for the sample of 1395 buildings, and considering each type of intervention and contract (numbered from 1 to 6).
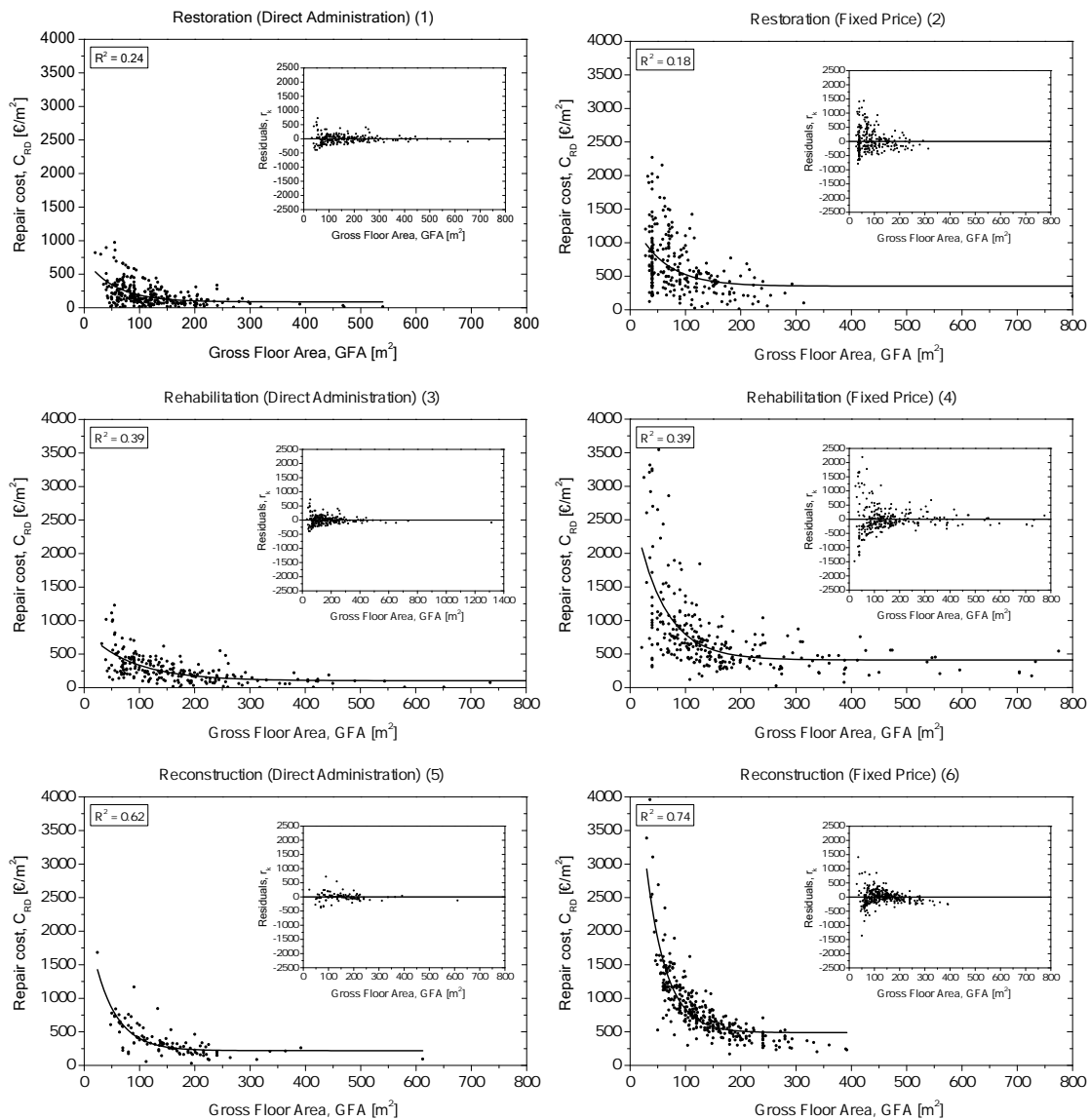
Figure 4.9: Observed data points and respective curve fitting of the repair cost, C_{RD}, versus the GFA for each building of the considered sample of 1395 buildings: Direct Administration (left) and Fixed Price (right) contracts. The residuals, r_k, obtained from applying the least square fitting method to compute the curves that best fit the observed data, are also provided.

From Figure 4.9 it is clear that the data related to Fixed Price contracts presents a higher variability in terms of C_{RD}. In line with the main outcomes of Table 4.2, the distribu-

tion of the data points reveals indeed a gradual increase in the values from Restoration to Reconstruction, as the scatter of both contract types move slightly upwards.

Moreover, in order to allow for the estimation of the repair cost, C_{RD}, for a given building of Faial Island as a function of its GFA, and in view of its application on the estimation of current costs, the data presented in Figure 4.9 was approximated to an exponential curve. This curve, represents the best fit for each set of observed data points (plotted in the same figure) whose explicit function is given by the Equation (4.1), where $y_{0,i}$, $A_{1,i}$ and $t_{1,i}$, are the respective curve fitting parameters, and i, stands for the different types of intervention and contract considered. The least square fitting method was used to find the best-fitting curve for each set of observed data points by minimising the sum of the squares of the residuals, r_k (also given in Figure 4.9), of these data points, from the curve.

The analysis of the goodness of fit was evaluated by calculating the respective coefficients of determination, R^2, computed according to Equation (4.2) and by considering C_{RD} as the only independent variable. SS_{res} and SS_{tot} represent the residual and total sum of squares, respectively. For the sake of simplicity, the results of the trial-error process that sustained the selection of the exponential curve among other functions, are not herein presented.

$$C_{RD_i} = y_{0,i} + A_{1,i} \times e^{(-GFA_i / t_{1,i})} \tag{4.1}$$

$$R^2 = 1 - \frac{SS_{res}}{SS_{tot}} \tag{4.2}$$

The parameters obtained for each curve and the respective R^2 coefficients are summarised in Table 4.3, from where it is possible to observe a gradual increase of the R^2 value from restoration to reconstruction interventions. In general terms, it is reasonable to admit that the computed curves fit quite well each set of data points. In fact, the curve-fitting in the case of reconstruction interventions is particularly interesting, as R^2 values of 0.68 and 0.74 were obtained.

Table 4.3: Exponential curve fitting parameters and respective R^2 coefficients obtained for each dataset of the sample of 1395 buildings of Faial Island. The respective standard error values associated with the curves' parameters are given in brackets.

Intervention Type	i	Contract Type	Number of Points	$y_{0,i}$	$A_{1,i}$	$t_{1,i}$	R^2
Restoration	1	Direct Administration	304	87.6 (24.6)	652.6 (125.7)	53.3 (12.6)	0.24
	2	Fixed Price	248	352.0 (89.1)	1046.8 (234.0)	55.6 (23.3)	0.18
Rehabilitation	3	Direct Administration	221	102.9 (31.1)	759.6 (100.7)	84.3 (18.0)	0.39
	4	Fixed Price	278	411.5 (57.7)	2466.5 (323.8)	53.7 (8.7)	0.39
Reconstruction	5	Direct Administration	107	219.7 (25.2)	2193.1 (355.4)	40.2 (5.2)	0.62
	6	Fixed Price	327	488.0 (26.2)	5586.0 (507.7)	36.2 (2.3)	0.74

Moreover, while it is observed a substantial increase in the R^2 values for each type of intervention, with exception for the case of reconstruction, no significant deviations were found

in terms contract type. The parameters of the computed curves will be used in Section 4.1.6 to construct new expressions that will ultimately allow the prediction of updated costs for the same interventions and building typologies in other seismic prone areas in Portugal, as a function of the GFA value of each building.

4.1.5.2 Analysis of the relationship between repair costs and damage limit states

The analysis of repair costs in terms of observed damage states is seen in this study as an extremely valuable exercise that might support the formulation of new repair cost functions for the Azorean traditional stone masonry building stock. Hence, and before introducing the investigation of a new repair cost function, which will be addressed in Section 4.1.6, it is important to discuss the median repair costs in function of the observed damage states, ds, presented in Figure 4.10 for both types of contract but, independently in this case, from the type of intervention. It is worth noting that the number of buildings that underwent damage state ds_0 to ds_5 were accounted respectively in 14, 136, 136, 188, 88, and 30, for the case of Direct Administration contracts. In the case of Fixed Price contracts instead, these values were estimated in 15, 144, 156, 225, 152, and 111. According to Figure 4.10, it can be observed that, in the case of Fixed Price contracts, $\overline{C_{RD}}$ gradually increases as the damage state increases (from ds_0 to ds_5). However, in the case of Direct Administration contracts this increase is not so evident. Finally, the difference between damage states ds_0 to ds_5, in terms of $\overline{C_{RD}}$, was estimated in 134 and 305 €m^{-2}, respectively for Direct Administration and Fixed Price contracts.
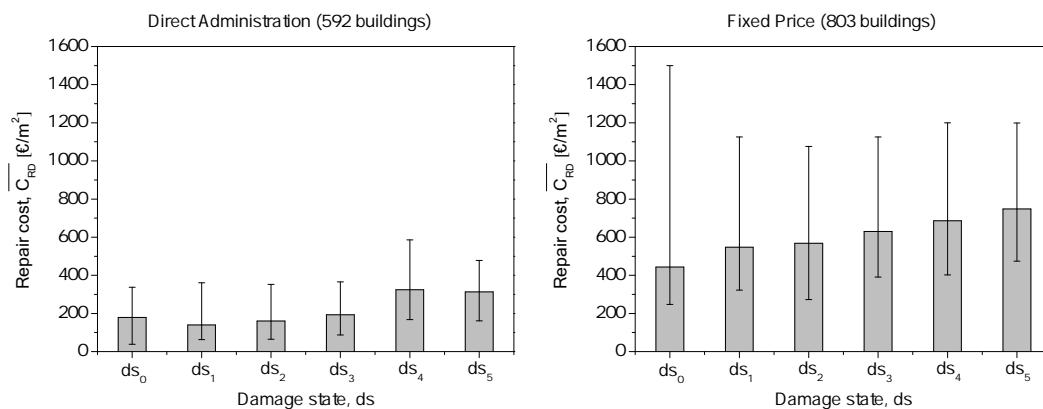
Figure 4.10: Overview of the median repair costs, $\overline{C_{RD}}$, and respective 16th and 84th PCTL values, by damage state, ds, for both Direct Administration (left) and Fixed Price (right) contracts.

4.1.6 Derivation of repair cost functions

In countries where post-earthquake damage data is scarce, such the case of Portugal, it is common practice to accept well-known repair cost functions to have a rough estimation of the repair costs associated with a determined earthquake scenario. Despite only a few proposals of repair cost functions for existing masonry structures are available in literature [195, 196, 197, 198], their applicability to different case studies is always quite questionable. Hence, acknowledging the crucial role that loss estimation plays in the planning and implementation of earthquake risk mitigation strategies, and the potential of the damage data collected in

the framework of the 1998 Azores earthquake, this exercise presents a great opportunity to investigate the possibility of developing repair cost functions for the Azorean traditional building stock, which might be eventually applicable with due consideration to similar building typologies in different regions of Portugal. Similarly, two different approaches for deriving repair cost functions were herein considered. As previously mentioned, while the first is more suitable to loss estimation in large-scale assessments (e.g. macroseismic applications), the second is based on damage limit states, and could be used either to support post-disaster emergency plans or to design risk mitigation strategies.

4.1.6.1 Updated repair costs as a function of the gross floor area

This first approach consists on updating the observed repair cost functions, C_{RD_i}, derived in Section 4.1.5, so that they might be compared and calibrated to other functions used in large-scale loss assessment studies in Portugal. These observed repair costs were updated, C'_{RD_i}, by means of the annual average rates of change in the Consumer Price Index (CPI) in Portugal, herein represented by the factor f_c, assuming that all works carried out during the reconstruction process of Faial Island were completed by 2001. This factor can be obtained through the tool made available by the Statistics Portugal Institute (INE). If updating the 2001 costs to 2017, for example, a f_c value of 1.329 should be used. Moreover, in order to reflect the variability between the costs of the construction sector in Faial Island and mainland Portugal, the factor f_s was defined. Thus, and according to expert judgement of the main actors involved in the reconstruction process of Faial Island [29, 189], the values of 1.00 and 0.70 shall be used for buildings located on the Islands and on mainland Portugal, respectively, as it is suggested that in mainland Portugal, these costs are approximately 30% lower than in the Azores archipelago. Finally, based on the $\overline{C_{RD}}$ values reported in Section 4.1.5, for both rural and urban typologies, a third factor, f_u, was defined to reflect the variability of the intervention cost in function of these typologies. In this study and given the lack of information available in this regard, the median repair cost values $\overline{C_{RD}}$, obtained for the equivalent sample of 160 buildings that were presented in Section 4.1.5, were considered as representative of the deviation between the repair cost associated with rural and urban typologies. Considering the equivalent sample, the repair cost for urban typologies resulted about 1.55 times higher than the rural ones, being therefore, this the f_u value suggested for urban typologies. For rural typologies instead, a f_u factor equal to 1.00 shall be used.

Bearing in mind the above, the updated repair cost, C'_{RD_i}, for the respective i combination, can be represented by Equation (4.3), in which the functions resulting from the curve-fitting process are multiplied by the above-described corrective factors.

$$C'_{RD_i} = C_{RD_i} \times (f_c \times f_s \times f_u) \tag{4.3}$$

Hence, in Figure 4.11, repair cost curves updated for 2017 are plotted for four different scenario combinations: Islands and Rural (I+R); Islands and Urban (I+U); Mainland and Rural (M+R); and Mainland and Urban (M+U). Similarly to Figure 4.9, the curves in Figure 4.11 are presented for each type of intervention and contract type. Since C'_{RD_i} values increase substantially for GFA values lower than 100 m^2 and are practically constant for GFA values larger than 300 m^2, a higher focus was given to the range between 100 and 300 m^2. Another fact that supports the investigation of a narrower range of GFA values is related to the median GFA values observed for all apartment types (from T1 to T6) in Faial Island,

which were estimated to vary in between 100 and 125 m^2, falling therefore, within the range of values considered.
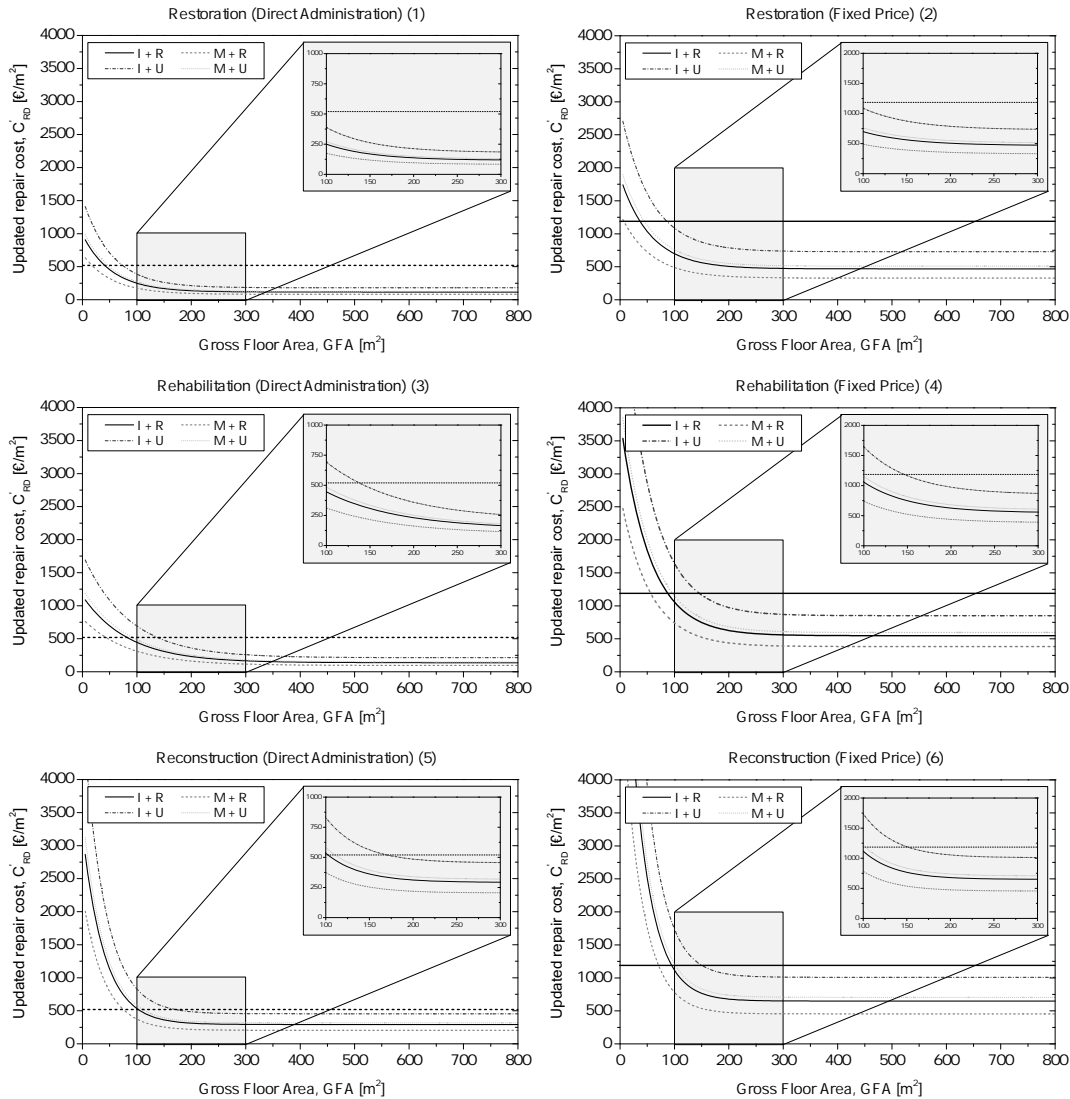
Figure 4.11: Updated repair costs, C'$_{RD_i}$, versus the GFA for each type of intervention, type of contract, and for the following scenarios: I+R (Islands + Rural); I+U (Islands + Urban); M+R (Mainland + Rural) and M+U (Mainland + Urban). These plots are zoomed in the top-right corner in order to better understand the position of the proposed curves in relation to the replacement costs of 520 and 1185 €m^{-2} in the case of Direct Administration and Fixed Price contracts.

To understand whether these combinations and respective idealised scenarios are economically attractive, it is indispensable to compare the resulting repair costs to a determined replacement cost, C$_{R,CC}$. In this study, the replacement cost was defined as the monetary value associated with reconstitution interventions that are often observed in historic centres, which normally entail the demolition and the subsequent construction of a new building following the same geometrical characteristics but resorting to modern construction solutions and according to current costs. Hence, the replacement cost, C$_{R,CC}$, was herein estimated by

summing up the cost of demolition works to the current average cost of a new construction in Portugal (resorting to modern construction solutions), which was kept in 2017 at 482.4 €m^{-2} in mainland Portugal according to the Decree Law 379/2017 of December 19 [199]. Thus, and after checking standard costs for demolition works in Portugal, it seems reasonable to assume an average replacement cost of 520 €m^{-2}. As in the case of the reconstruction process of Faial Island, the disparity observed in the repair cost between the two contract types was quite significant, this average replacement cost was broke into two values, suitable to each type of contract. Thus, assuming that the value of 520 €m^{-2} should be adopted in the case of Direct Administration contracts and considering the median values from the 1998 Azores earthquake database for each type of contract of reconstruction interventions (293 and 669 €m^{-2}, respectively to Direct Administration and Fixed Price contracts), the replacement cost for Fixed Price contracts was estimated in 1185 €m^{-2} by applying a simple linear correlation.

Therefore, when comparing the results of Figure 4.11 for the case of Direct Administration contracts, it is possible to observe that the great majority of combinations are below the respective replacement cost set in this case equal to 520 €m^{-2}, exception made for rehabilitation and reconstruction interventions of urban typologies located in the Islands (I+U combination). When analysing the curves referring to Fixed Price contracts, it can be observed that apart from the combination I+U (urban typologies located in the Islands) for rehabilitation and reconstruction interventions, the repair costs of all the remaining combinations are lower than the respective replacement cost (1185 €m^{-2}).

Globally these results show that, apart from the exceptions identified in the previous paragraph, carrying out adequate and respectful interventions is actually more attractive from the economic viewpoint than replacing existing structures for new ones (resorting to modern construction solutions), where the cultural value of the assets is entirely lost. The validity of this conclusion appears to cut across different types of interventions and contracts, independently from the location (islands or mainland) and typology (rural or urban) of UCH assets.

4.1.6.2 New repair cost function derived from observed damage limit states

The study of repair cost of seismic-induced damage brings the opportunity to estimate the direct economic losses associated with damages to structural and non-structural elements. One of the most common approaches in this regard was developed in FEMA-NIBS (1999) and embodied in the HAZUS methodology [197], which uses a loss ratio of the building replacement cost in function of the damage limit states derived from the occurrence probability of a damage state obtained from the fragility curves in correspondence to a given Engineering Demand Parameter (EDP), for the most unfavourable seismic action and building direction.

The prediction of repair costs due to seismic damage based on damage states is typically represented by a mathematical expression similar to Equation (4.4), where the economic damage index, d_e, is given by Equation (4.5). Factors f_k, are used to weigh the replacement cost of a given building, $C_{R,CC}$, as a function of the occurrence probability of each damage state, p_k. In this study, these f_k values represent the normalised deviations between the median repair cost, $\overline{C_{RD}}$, estimated in Section 4.1.5.2 to each damage state. Usually, the following physical meaning is associated to damage states ds_0 to ds_5: no damage; slight damage; moderate damage; heavy damage; very heavy, and collapse. This is the case of the damage classification presented in Section 4.1.3, which can be directly correlated to the

mean damage grade, μ_D, adopted by the EMS-98 scale [86].

In the case of analytical approaches, these damage states obtained from macroseismic post-earthquake assessment, are used to support the definition of performance levels, which are in turn correlated to the seismic response of the structure. Despite the new multi-linear constitutive laws recently developed within the framework of the PERPETUATE project [48], which are based on a phenomenological approach that allows to describe the nonlinear response of masonry panels until very severe damage levels (from ds_1 to ds_5), the majority of analytical models for masonry structures considers only four damage levels, given the difficulty in differing between damage states ds_4 and ds_5 (very heavy or near collapse and collapse) in the capacity curve.

$$C'_{RD} = C_{R,CC} \times d_e \qquad (4.4)$$

$$d_e = \Sigma_{n=0}^{k}(f_k \times p_k) \qquad (4.5)$$

Therefore, so that the economic damage indexes might be used in a wider range of methodologies and applications, two different sets of f_k values are herein proposed: the first with $k = 4$ (Proposal 1) is applicable in cases where ds_4 and ds_5 are aggregated, and a second one with $k = 5$ (Proposal 2), in which damage states vary from ds_4 to ds_5. The comparison between these f_k values, derived from the sample of 1395 buildings of Faial Island, and those found in literature, for each damage state, ds, are presented in Table 4.4 and in Figure 4.12 (left). From these results, it is possible to observe that the proposed values are, in general, slightly lower than those found in literature.

Table 4.4: Comparison between the f_k values herein obtained from the sample of 1395 buildings of Faial Island ((Proposal 1 and Proposal 2) and some reference values found in literature, for each damage state, ds.

Author	None (ds_0)	Slight (ds_1)	Moderate (ds_2)	Heavy (ds_3)	Very heavy (ds_4)	Collapse (ds_5)
Proposal 1 ($k = 4$)	**0.000**	**0.031**	**0.059**	**0.338**	**1.000**	**1.000**
Proposal 2 ($k = 5$)	**0.000**	**0.025**	**0.048**	**0.272**	**0.697**	**1.000**
ATC-13 [195]	0.000	0.050	0.200	0.550	0.900	1.000
Bramerini et al. [196]	0.000	0.010	0.100	0.350	0.750	1.000
FEMA-NIBS [197]	0.000	0.020	0.100	0.500	1.000	1.000
Dolce et al. [198]	0.000	0.035	0.145	0.305	0.800	1.000

The economic damage index, d_e, is commonly correlated with a mean damage grade value, μ_D, given by the EMS-98 scale [86] that represents the mean value of the damage grade used to define a discrete damage distribution, D_k, given by Equation (4.6), where p_k is the occurrence probability of each for each set of damage states ($k = 4$ and $k = 5$), and μ_D the "barycentric value" of the discrete damage distribution. The correlations between the economic damage index, d_e, and the mean damage grade, μ_D, are usually established by means of a damage probability matrix (DPM), which is defined by a discrete "beta" distribution, discretised into 6 damage grades and considering parameter t equal to 8, as recommended by Vicente [7]. In Figure 4.12 (right), the discrete beta distributions obtained

for Proposal 1 (k = 4) and Proposal 2 (k = 5) are compared to envelope curves of those found in literature (area coloured in gray).

$$\mu_D = \Sigma_{n=0}^{k}(p_k \times Dk) \tag{4.6}$$
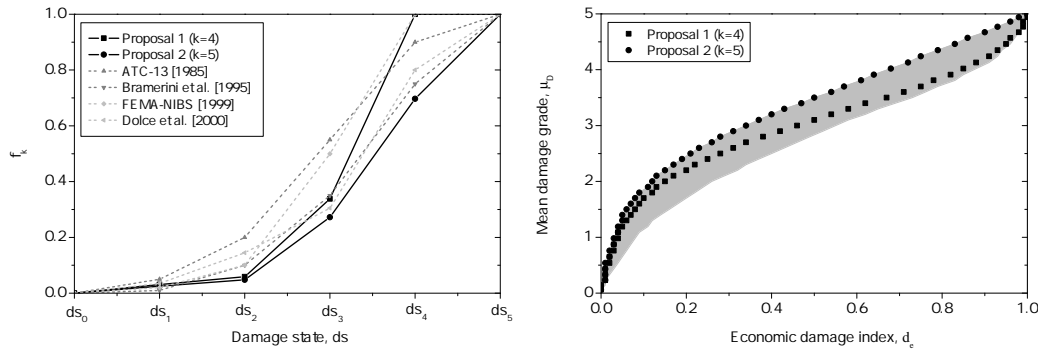
Figure 4.12: Discrete correlation between f_k values and each damage state ds (left), and the corresponding beta distribution in function of the economic damage index, d_e (right), estimated for the sample of 1395 buildings of Faial Island, based on the respective median repair costs, C'_{RD}.

4.1.7 Seismic strengthening costs

The negotiations with the respective claimants took place right after the on-site architectural survey operations in order to establish the grounds of the execution project and necessary provisions, which had to look upon some legislative issues, namely its adequacy to the family household, the necessity of improving salubrity conditions, and last but not least, the necessity of endowing the structure with an adequate seismic performance.

For the sake of simplicity and consistency, attention will be exclusively given to a set of widely known traditional strengthening strategies that have been employed in the reconstruction process of Faial Island [200], and whose effectiveness is strongly sustained in literature, as for example in [72, 168, 200]. This set of strategies, which is illustrated in Figure 4.13 and fully described in the referred literature, can be distinguished into three main solutions: consolidation of the vertical (1) and horizontal (2) structures, and the shear strengthening and confinement of the vertical structure through the use of steel tie-rods (3).

The costs associated with each strengthening solution were derived from the careful examination of both inspection reports and full renovation projects, specifically designed to 16 randomly selected case studies of the overall sample of 1395 buildings of Faial Island [168, 200]. The validation of the values herein presented is a very complex task, not only due to the general lack of data regarding the costs of strengthening strategies in literature, but also because, even when such data is available, it is extremely difficult to establish any sort of comparison or validation, as it usually aggregates different strengthening techniques and is a very country-specific issue. In addition to this, in countries where strong earthquakes are not frequently experienced, such as Portugal, the lack of such data is even more accentuated.

In order to understand the representativeness of these 16 randomly selected case studies in the overall sample of 1395 buildings, the deviations between the median repair costs for each strengthening solution, from (1) to (3), were compared to the $\overline{C_{RD}}$ value corresponding to the total number of buildings subjected to rehabilitation interventions from the overall

sample (469 out of 1395). It is worth referring that each strengthening solutions (1) to (3) were respectively applied to 11, 8, and 6 buildings of these 16 cases (in Table 4.5). The following $\overline{C_{RD}}$ values of 76964 €, 90916 €, and 70369 €, were found in the case of strengthening solutions (1) to (3), respectively. The $\overline{C_{RD}}$ value referring to rehabilitation interventions was evaluated in 68559 €. Hence, deviations of 12%, 18% and 3%, in relation to the $\overline{C_{RD}}$ value of rehabilitation interventions, were found for strengthening strategies from (1) to (3), respectively. These deviations can be considered relatively low when compared to the variability observed in the repair costs of rehabilitation interventions (given in the previous Figure 4.9), minimising therefore, the drawback of using such a small sample.

Thus, and even though the sample used to estimate median strengthening costs, $\overline{C_{SS}}$, for the mentioned strategies is quite small when compared to the overall sample of 1395 buildings, the values presented in Table 4.5, are believed to constitute a unique source for both scientific and policy-driven research nationwide. The economic impact of each solution was evaluated by means of the Cost Ratio, which represents, the ratio between the median repair cost, $\overline{C_{RD}}$, and the seismic strengthening cost, $\overline{C_{SS}}$, of rehabilitation interventions associated with the respective cases showed in Table 4.5. Hence, and apart from the consolidation of the vertical structure, which is by far the most intrusive and expensive solution, it was found that reducing the seismic vulnerability of such building typologies actually entails a quite low financial effort, particularly if these strategies are thought to be integrated with the other specialties of the design project.

Table 4.5: Median strengthening costs, $\overline{C_{SS}}$, (in €m^{-2}) and respective Cost Ratio for traditional strengthening strategies applied to the Faial Island's building stock in the sequence of the 1998 Azores earthquake. The number of buildings that contributed to the median estimate of each solution is placed in brackets following the respective $\overline{C_{SS}}$ value.

Strengthening Strategy	Strengthening Cost, $\overline{C_{SS}}$	Cost Ratio $\overline{C_{SS}}$ / $\overline{C_{RD}}$
(1) Consolidation of the vertical structure	117 €m^{-2} (11)	17%
(2) Consolidation of the horizontal structure	22 €m^{-2} (8)	3%
(3) Steel tie-rods	16 €m^{-2} (6)	3%

4.1.8   Final remarks

The preconceived idea that investing in strengthening strategies to reduce the seismic vulnerability of UCH assets is extremely costly was demystified in this section. In fact, the results obtained proved not only that this investment is easily dissolved in the total renovation costs, but also the implementation of such strategies have a major impact on the reduction of damage and losses in the event of an earthquake. The repair costs associated with interventions strategies implemented by preserving traditional construction techniques and materials, resulted, in the majority of the scenarios considered, quite attractive from the economic viewpoint. According to these results, it is more likely that the costs associated with seismic strengthening may become even more dissolved when operating in UCH assets.

It is believed that the functions herein proposed can be used to derive rough estimates of repair costs for similar building typologies and different scenarios in Azores. However, it is important to stress these results require further validation with current intervention costs practiced in different regions in Portugal. Moreover, the repair cost functions derived from
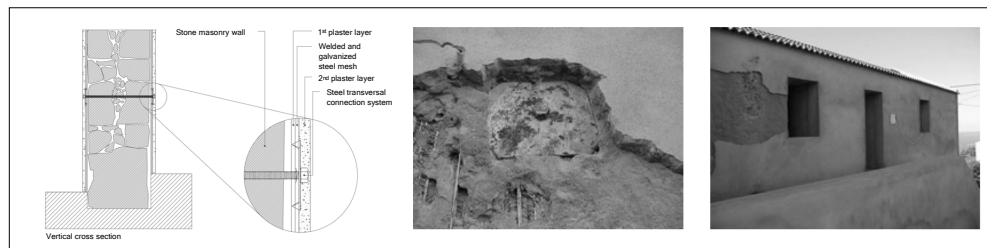
(1) Consolidation of the vertical structure
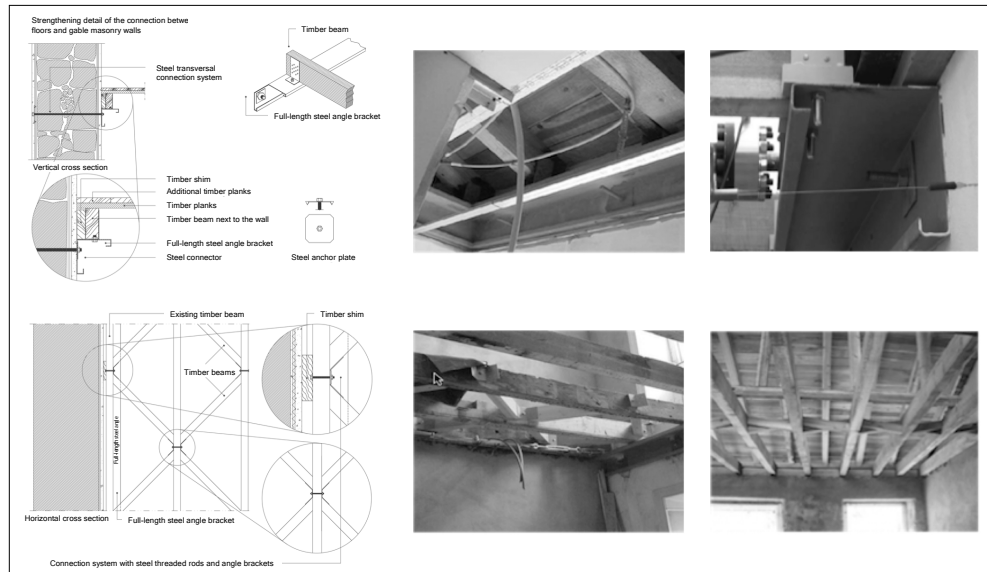
(2) Consolidation of the horizontal structure

(3) Steel tie-rods

Figure 4.13: Technical drawings and execution details of some of the most common strengthening strategies adopted in the reconstruction process of Faial Island, which are recalled in the present study.

the Faial database might be extremely useful for academic purposes and studies to come, as well as to raise the awareness of all stakeholders involved in the renovation process of our building stock (from property owners to policy makers) to the importance of integrating seismic strengthening design into the structural project, and the consequences of not doing so.

Despite the definition and valuation of built heritage is always arguable since it is ultimately shaped by both individual perception and social interaction, which is constantly evolving over time, it is up to conservators and heritage professionals to raise their voices for

the protection of traditional construction techniques and materials in UCH assets, as part of the cultural identity of our historic centres. It is therefore necessary not only to conduct nation-wide operations on documenting and cataloguing these techniques and materials, but also to raise the society's awareness and consciousness for the value of cultural heritage and to the consequences of its loss.

The consideration of uncertainties, particularly those associated with the quantification of the strengthening costs herein presented, which, to a large extent, results from the small number of case studies examined, is one of the issues to be addressed in future developments. Additionally, it would be interesting to bring the costs associated to the patrimonial value of UCH assets into discussion, which alone would practically require an independent investigation, and that are believed to strengthen the benefits from integrating traditional seismic strengthening design into thoughtful renovation interventions. This issue, often disregarded or lightly addressed in literature, is indeed of great relevance for a more accurate evaluation of economic losses caused by both natural or man-made disasters.

4.2 Cost-benefit analysis

This section discusses the cost-benefit analysis resulting from the application of traditional seismic retrofitting strategies on four case studies considered representative of both the rural and urban stone masonry building typologies of Faial Island, in Azores (Portugal). The seismic performance-based assessment was carried out by applying the N2 Method procedure, and the global seismic capacity of each case study estimated by using the three-dimensional model based on the macroelement approach presented in Section 3.2, which combines both the in-plane and out-of-plane response of masonry buildings, to perform nonlinear static analyses. Fragility and loss estimation was evaluated according to the HAZUS methodology.

One of the preferred arguments used to underpin the phenomenon of both architectonic and constructive mischaracterisation in Portugal is that, allegedly, structural renovation works compliant with existing materials and traditional building techniques are not viable from the economic viewpoint. Another often cited argument is that such traditional materials and building techniques do not comply with the regulatory requirements in force in terms of seismic performance.

As a follow-up of the research published by Maio et al. [201], the current study aims not only at investigating the authenticity of the arguments mentioned above but also to demystify the generalised idea that traditional strategies for the seismic retrofitting of UCH assets have a significant impact over the total renovation cost. In literature, the term "traditional techniques" usually refers to enhancing measures of the buildings' structural integrity by using compatible and local materials such as earth and wood, and solutions as ring beams, wooden ties interconnecting parallel walls, corner keys, or the addition of buttresses, for example. However, "traditional" has been given in this thesis an additional meaning, in the sense that these strategies are quite common and have been widely applied in the framework of the reconstruction process of Faial island (in Azores, Portugal), after the 1998 Azores earthquake [29]. The validation of the former hypotheses is going to be investigated by assessing the Cost-Benefit Analysis (CBA) of two of these strategies.

One of the first cost-benefit models for the seismic retrofitting of buildings was issued

by the Federal Emergency Management Agency in 1994 [202, 203], which encouraged the development of several studies in this topic ever since [204, 205]. In the past few years, several compelling studies within this particular research field have been published, focusing either on residential [206, 207] or public-school buildings [208, 209]. It is worth noting that despite being widely acknowledged worldwide as a significant decision-supporting tool commonly used for evaluating the efficiency of projects, CBA does not provide an absolute answer about whether or not to undertake the seismic retrofitting of a given asset. This because the decision-making process usually depends on many factors beyond the boundaries of benefit-cost analysis, such as the definition of life safety and post-earthquake performance levels [202]. Notwithstanding these limitations, this study aims at investigating the referred hypotheses associated with the mischaracterisation phenomenon witnessed in many historic centres in Portugal, which causes and consequences, have been identified and discussed in [201].

Even though numerous techniques are available in literature for the seismic retrofitting of traditional stone masonry structures, as demonstrated by Bento et al. [210], Costa and Arêde [167], Branco and Guerreiro [211], or Scotta et al. [212], in this study, focus will be given to traditional retrofitting techniques, which has been addressed for example in Diz et al. [168], Moreira [213], Maio et al. [72], or Ortega [11]. From these, only the two most widely applied retrofitting solutions that were adopted by the Regional Government of Azores in the framework of the reconstruction process of Faial Island, were considered: the consolidation of the vertical and horizontal structures (full description follows in Section 2.2). The mean costs associated with these seismic retrofitting techniques were presented in [201], after a careful examination of the renovation cost records available in the database generated at the time of the referred reconstruction process of Faial Island.

As previously mentioned, in this Section, a CBA model is going to be applied to a total of four case studies, taken, after Costa [169] and Maio et al. [201], as representative of both rural and urban traditional stone masonry typologies of Faial Island. The information available of these case studies included technical drawings, detailed documentation and photographic survey not only of the main structural features but also of the extent of damage observed in the aftermath of the 1998 Azores earthquake [29]. It also included both renovation and seismic retrofitting design projects, which supported the formulation of the retrofitting strategies herein adopted.

4.2.1 Geometry and building typology

As demonstrated in Figure 4.14, these case studies (from A to D) present a plan which is kept regular in height, with gross floor area (GFA) of 73, 129, 256 and 714 m^2, respectively.

When comparing the main elevations of rural (A and B) and urban (C and D) typologies, in Figure 4.14, it is evident that urban typologies are adorned with several architectonic features that highlight the grandness of these assets, such as the presence of ashlar stone masonry quoins, balconies, parapets, gable fronted dormers, among other decorative features.

If exclusively focusing on the characteristics of the elements of the vertical structural, these typologies fundamentally differ on the type and quality of the masonry fabric used for load-bearing walls, which was highly reliant on the wealth of their original owners and the location of the building [169]. According to Costa [169], the most common stones used in the construction of Faial Island masonry building stock were basalt, cinerite, andesite, trachyte and volcanic tuff. The two rural typologies herein considered were built with double-leaf

Figure 4.14: Overview of the geometry and building typology of each case study (from A to D): ground floor plans and the respective main façade elevations. Please note that traditional stone masonry elements are coloured in grey, while masonry brick blocks are coloured in light grey. Moreover, the reference axes (X and Y) considered throughout this subsection to each model are identified in the respective ground floor plans.

masonry walls resorting to stones slightly larger than half the wall width, being the gap between rocks filled with rubble, mud and lime mortar. The rendering of the external walls is variable, being the mixture of clay and lime, wherein 2.0 cm thick, over which a fine lime and sand mortar is applied. Urban typologies, instead, are built with regular-sized stones or "blocks". As demonstrated in Figure 4.14, there are also a few walls made of concrete blocks (highlighted in light grey), such as those associated with the extension of building A, for example. The foundations are believed to be made of the same stone of masonry used for external walls but slightly wider and with a depth of at least 1.0 m, depending on the number of storeys of the building [169].

In what concerns to the horizontal structure, while the ground floor has a screed finishing, upper floors are composed of timber planks supported by timber joists, which are in turn supported on load-bearing walls. The roof structure is made of traditional timber trusses of two hip rafters, forming in the particular case of building D an additional storey by taking advantage of the attic and four gable dormers. Even though gable dormers are a prominent feature of the Azorean architecture, these elements were disregarded in the numerical models considering the modelling limitations of the software code used in the case of very complex roof systems. Timber staircases provide access between storeys. Again, given the modelling

constraints of the software code used, and also the insignificant influence of such lightweight and low stiffness elements over the global response of the building, timber staircases were not considered in the numerical models.

4.2.2 Numerical models

In this study, a three-dimensional macroelement model developed by Pantò et al. [146] and compatible with the software code 3D-Macro® [13] was used. It includes both rocking and diagonal shear cracking mechanisms in the combined response (in-plane and out-of-plane) of masonry structures. The resulting numerical models are illustrated in Figure 4.15. It is worth referring that a more refined mesh was used to better approximate the response of these models to the real behaviour of the respective case studies. However, as this operation involves a substantial increase in the number of the degrees of freedom, the search for a plausible compromise between computation time and reliability of results is inevitable. Hence, the maximum dimension of masonry panels was set equal to $1.0\,\mathrm{m}$.

In the software code 3D-Macro® [13], masonry panels are defined by the following mechanical properties: Young's modulus (E); shear modulus (G); specific weight (w), compressive strength (f_m), shear strength (τ_0), and tensile strength (f_{tm}). The values of these properties, which were adopted for similar masonry typologies from the Italian Building Code, NTC [96], are going to be presented in the next subsections for each retrofitting condition considered. Horizontal diaphragms (floor and roof elements) were modelled as rectangular diaphragms elastically deformable considering orthotropic slab elements, which are characterised by an equivalent thickness, s, Young's moduli, $E_{1,eq}$ and $E_{2,eq}$, adopted respectively in the orthogonal and perpendicular direction of the floor warping, and an equivalent shear modulus, G_{eq}. The values of the Young's moduli $E_{1,eq}$ and $E_{2,eq}$, were determined as a function of the geometry of the cross-section and the elasticity of timber planks and beams. Architrave elements (or lintels) were modelled as timber beams with a linear-elastic response, considering a Poisson's coefficient (υ) equal to 0.2. In this study, all timber elements were defined for the Azorean cryptomeria class, considering a mean elasticity modulus equal to 3.9 GPa and a specific weight of 2.6 $\mathrm{kN\,m^{-3}}$. Gravity loads (G_k) equal to 1.0 $\mathrm{kN\,m^{-2}}$ were assumed to all horizontal diaphragms, while live loads (Q_k) were taken equal to 2.0 and 0.5 $\mathrm{kN\,m^{-2}}$, respectively in the case of floor and roof elements. Finally, the interaction between the foundations and the underlying soil was disregarded in this study.
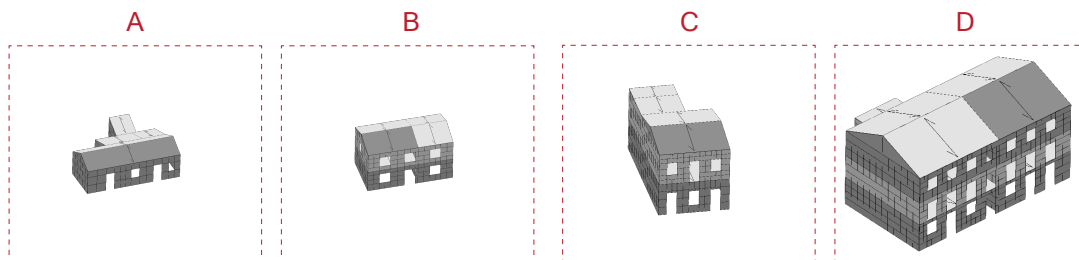
Figure 4.15: Overview of the three-dimensional model of each model (A to D), developed by using the 3D-Macro® software code. Please note that the control node considered for each model was assigned at the centre of rigidity of the floor elements, highlighted in dark grey. The geometry of macroelements was limited to a maximum dimension of 1.0 m to have a more refined mesh and subsequently, a less conservative model.

4.2.2.1 Unreinforced model (0)

The values assigned to mechanical properties of masonry panels presented in Table 4.6, were adopted from NTC [96] for "masonry in disorganised stones" and "dressed rectangular stone masonry" masonry classes, respectively in the case of rural (buildings A and B) and urban (buildings C and D) building typologies. However, and despite the values of elastic properties are in line with the upper limit values proposed by Costa [169], for example, a knowledge level KL1 was considered [166]. The equivalent shear modulus of horizontal diaphragms, G_{eq}, was assigned equal to 6.8 MPa, according to the guidelines published by the NZSEE guidelines [173], after ASCE [174], considering a straight single sheathing timber floor typology in a poor rating condition. The equivalent thickness of horizontal diaphragms, s, was considered equal to 2.5 cm. The tensile strength of the masonry panels, f_{tm}, was assumed equal to 5% of the compressive strength value, f_m.

Table 4.6: Mechanical properties of masonry walls assumed for the unreinforced condition. [*1]Please note that a cracked stiffness condition for masonry panels was considered, and for this reason, the elastic properties' values given below are halved, according to the recommendation of the EN 1998-1 [95]. [*2]These values are divided by a confidence factor, CF, equal to 1.35, which corresponds to a knowledge level, KL1 [166], adopted from Table C8A.2.1 of [96].

Masonry type	Building typology	E[*1] [MPa]	G[*1] [MPa]	w [kNm^{-3}]	f_m[*2] [Ncm^{-2}]	f_{tm}[*2] [Ncm^{-2}]	τ_0[*2] [Ncm^{-2}]
Stone	Rural	435	145	19	74.1	3.7	1.5
	Urban	615	205	20	148.1	7.4	2.6
Concrete blocks	Rural/Urban	700	175	12	111.1	5.6	7.0

4.2.2.2 Consolidation of the vertical structure (1)

The first retrofitting strategy considered is the consolidation of the vertical structure, ensured by the application of the reinforced render system specified by Costa [169], on both sides of the external stone masonry walls, as illustrated in Figure 4.16. The application of this reinforced render system is divided into three phases. A first layer of filling mortar in the proportion of 1:3 (local sand extracted from Fajã Beach: Portland cement: water) is applied for voids and surface regularisation. Then, a 0.5 mm thick welded and galvanised steel net made of S275 steel and 10.0 mm spaced steel rebars are installed and fixed on both sides of the masonry wall through a system composed of M20 galvanised screws, Φ20 galvanised steel threaded rods, and 4.0 mm thick anchor plates (20.0 x 20.0 mm wide and spaced each 1.5 m). Finally, a 3.0 cm thick second layer of fine sand-blasted finishing mortar is applied [169].

The consolidation of the vertical structure was simulated in 3D-Macro® by improving the mechanical properties of the masonry according to a set of corrective coefficients suggested by the NTC [96], which are given in Table 4.7. These coefficients were multiplied by the values assigned to the unreinforced condition (0), presented in the previous Table 4.6. In this case, it was considered a stiffness reduction of 25% of the initial (uncracked) value. As for the tensile strength provided by the reinforced render system applied to external stone masonry walls, f_{tm}, a value of 126.6 N cm^{-2}, proposed by Braga and Estêvão [214] for a similar cement-based render, was considered. This value was then divided by a confidence
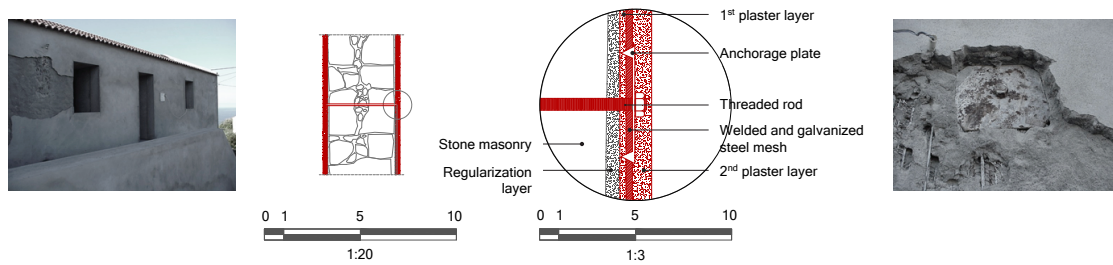
Figure 4.16: Consolidation of the vertical structure (1) with a traditional reinforced render system.

factor, CF, equal to 1.35, which corresponds to a knowledge level KL1, again following the recommendations of the NP EN 1998-3 [166]. In the case of concrete blocks, the f_{tm} value was also assumed equal to 5% of the compressive strength value, f_m.

Table 4.7: Masonry corrective coefficients considered for the consolidation of the vertical structure (1), assigned according to the recommendations of the NTC [96].

Corrective coefficient	E	G	f_m	τ_0
Transversal connectors	1.00	1.00	1.50	1.50
Mortar injections	2.00	2.00	2.00	2.00

4.2.2.3   Consolidation of the horizontal structure (2)

The second retrofitting strategy consisted on the consolidation of the horizontal structure (improving the so-called box-behaviour), which comprised not only the improvement of the connections between the horizontal and the vertical structure, but also the in-plane stiffness of the original diaphragms. As demonstrated in Figure 4.17, this was made possible by installing a full-length angle bracket system connecting timber beams to external walls and by adding a new layer of timber sheathing, laid perpendicular and adequately nailed to the original timber sheathing.

Additionally, 7.5 cm thick diagonal timber braces between timber beams at both floor and roof levels were installed and anchored through a system composed of Φ10 galvanised steel threaded rods and 3.0 mm thick galvanised steel angle brackets. Furthermore, an effort was made to keep and restore the original timber elements as much as possible, rather than replacing the whole timber structure by a new one.

This upgrading was simulated by increasing the equivalent thickness of the membrane, s, to 5.0 cm, and the equivalent stiffness, G_{eq}, to 30.6 MPa, as recommended by the NZSEE guidelines.

4.2.2.4   Consolidation of both vertical and horizontal structure (3)

Finally, a third strategy was considered, which consisted of the application of retrofitting strategies 1 and 2 simultaneously.
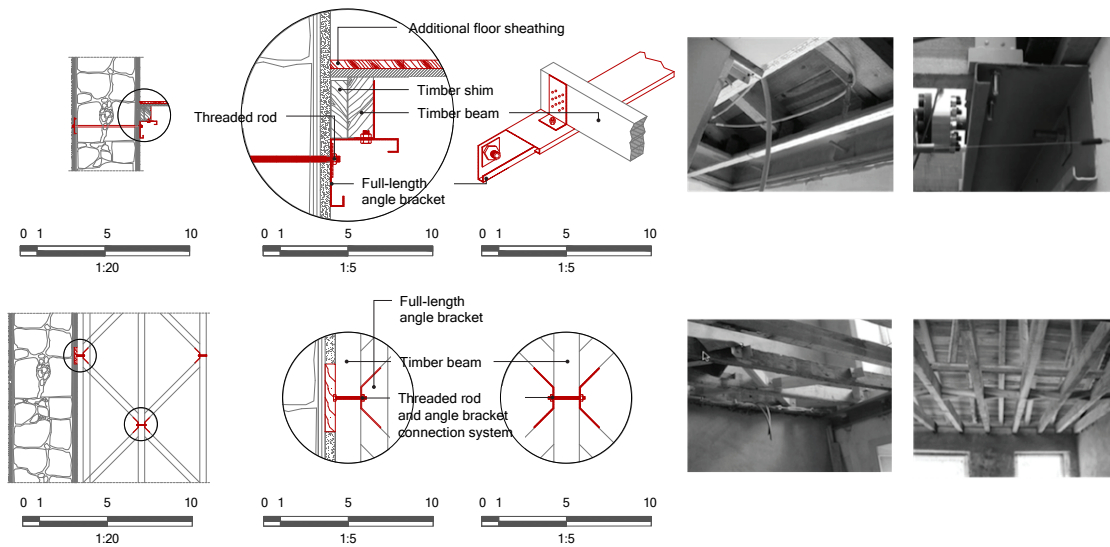
Figure 4.17: Consolidation of the horizontal structure (2) by improving the connections between the horizontal and the vertical structure and the in-plane stiffness of the original diaphragms.

4.2.3 Global seismic performance-based assessment

The seismic performance of the models described in Section 4.2.3, was evaluated according to the nonlinear static analysis procedure [164] recommended by the EN 1998-1 [95]. This procedure is commonly used to determine the structure's performance point, d^*_t, which is in turn computed from the intersection between the capacity spectrum of the structure (derived from the capacity curve) and the inelastic response spectrum associated with the demand in terms of seismic action, following the iterative procedure recommended in the NP EN 1998-1 [165]. Even though more sophisticated procedures are available, such as nonlinear dynamic incremental analysis for example, the N2 Method presents a good balance between precision and computational effort. Moreover, such procedure is well suited to the simplicity of the numerical model herein used, which is based on the macroelement approach.

In this study, and for each model, a set of 40 pushover analyses was performed, 24 of which along different planar directions considering an incremental angular step of 30° and two different load pattern distributions (uniform, proportional to mass, and pseudo-triangular, proportional to the product between mass and height). The remaining 16 analyses were performed along the two main planar directions (X and Y) and by considering the accidental eccentricity as recommended by the NP EN 1998-1 [165]. This set of pushover curves, obtained for each model and retrofitting condition, represent the nonlinear relationship between the shear coefficient, C_b, and the displacement of the control node, d_{cn}. The shear coefficient C_b is obtained diving the base shear strength, V_b, by the total weight of each model, W. The following W values were obtained for each model from A to D: 1189.5 kN; 2108.3 kN; 3874.7 kN, and 11899.0 kN.

For the sake of an example, only the results referring to model C are going to be discussed in detail in this subsection. Hence, while the pushover curves in Figure 4.18 (left) correspond to the unreinforced condition (0), the curves in Figure 4.18 (right), correspond to the consolidation of both vertical and horizontal structures (3) of model C. Each set of curves is grouped in function of the type of load pattern distribution (uniform and pseudo-

triangular), from were it is possible to observe that the uniform load pattern distribution reaches, in general, higher C_b values. From Figure 4.18, it is also possible to observe a significant increase both in terms of base shear coefficient and initial stiffness with the application of retrofitting strategy 3. To the contrary, the ductility capacity of the retrofitting strategy 3 has decreased in comparison to the unreinforced condition (0). The pushover curves obtained for the remaining models are given in Appendix A.
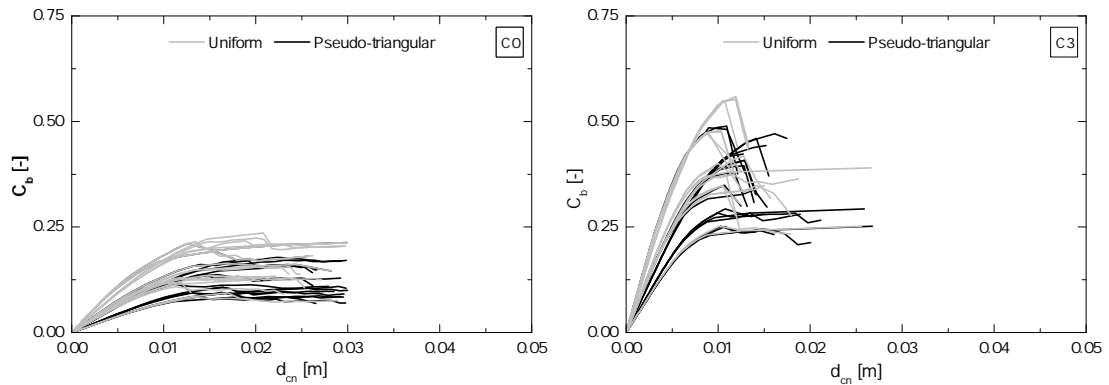
Figure 4.18: Example of the pushover curves obtained for model C, grouped by horizontal load pattern distribution (uniform and pseudo-triangular), associated with the unreinforced condition (left) and the consolidation of both vertical and horizontal structures (right).

The global displacement capacity of each model was evaluated by considering the damage limit state thresholds proposed by Barbat et al. [215], which are directly dependent on the values of the yielding and ultimate spectral displacement, S_{d_y} and S_{d_u}, respectively. The limit states from Equation (4.7) to Equation (4.10), refer to the slight damage, moderate damage, severe damage and collapse damage limit states.

$$S_{d_1} = 0.7 \times S_{d_y} \tag{4.7}$$

$$S_{d_2} = DL = S_{d_y} \tag{4.8}$$

$$S_{d_3} = S_{d_2} + 0.25 \times (S_{d_u} - S_{d_y}) \tag{4.9}$$

$$S_{d_4} = NC = S_{d_u} \tag{4.10}$$

As demonstrated in Equation (4.7) to Equation (4.10), limit states S_{d_2} and S_{d_4}, are, in fact, directly correlated to the DL and NC limit states, which are recommended by the NP EN 1998-3 [166]. Hence, the global displacement capacity for the NC limit state was defined by the magnitude of the roof displacement at the point corresponding to a 20% decay of the maximum base shear strength [166]. In the case of the DL limit state, the displacement capacity was defined at the yielding point of the idealised elasto-plastic pushover curve. The control point for each model was selected at the rigidity centre of the horizontal diaphragms highlighted in Figure 4.15 (at the roof level).

The capacity curves presented in Figure 4.19, were obtained by applying a transformation coefficient [95, 164] that allows converting the pushover curves (associated to the Multi-Degree-of-Freedom system, MDOF) into an equivalent bilinear Single-Degree-of-Freedom (SDOF) system, assuming an elasto-perfectly plastic force-displacement relationship. Figure 4.19, also presents the capacity curves corresponding to the median, 16th and 84th PCTLs of the set of the 40 analyses performed. These central tendency measures are going to be considered for the computation of fragility curves and subsequently on the cost-benefit analysis, as explained in Section 4.2.4 and Section 4.2.5, respectively.

Again, for the sake of an example, the capacity curves in Figure 4.19, were derived from the pushover curves presented in the previous Figure 4.18, being, for this reason, associated with the unreinforced condition (left) and consolidation of both vertical and horizontal structures (right) of model C. If focusing on the base shear strength of the equivalent bilinear SDOF system, F^*, in Figure 4.19 (left), the average values of 500 kN and 406 kN, were obtained for the analyses associated with the uniform and pseudo-triangular lateral load pattern distribution, respectively. On the contrary, in the case of Figure 4.19 (right), which presents the capacity curves associated with the retrofitting strategy 3, the average F^* values of 1301 kN and 1119 kN were estimated, respectively to the uniform and pseudo-triangular lateral load pattern distribution. The capacity curves obtained for the remaining models are provided in Appendix A.
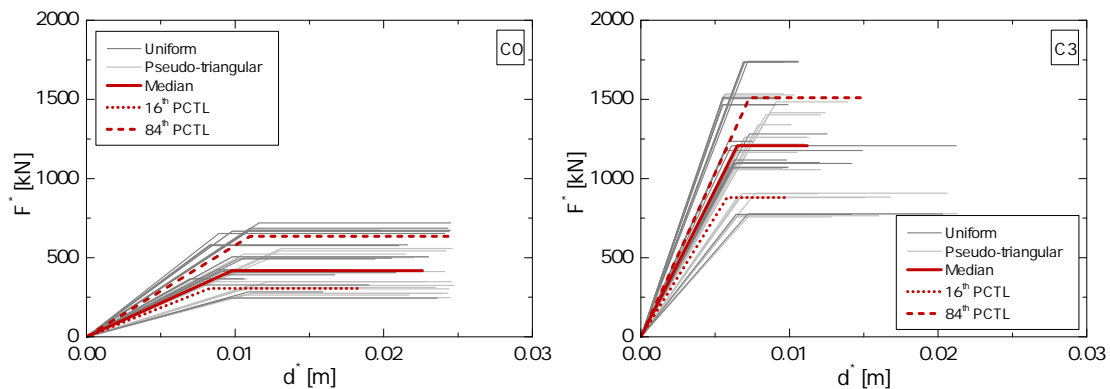
Figure 4.19: Capacity curves obtained for model C, grouped by horizontal load pattern distribution (uniform and pseudo-triangular), associated with the unreinforced condition (left) and the consolidation of both vertical and horizontal structures (right).

Finally, the global seismic performance of these models and the respective retrofitting conditions, were evaluated by calculating the parameter $\%a_g$, defined as in Section 3.2.2.2. The seismic demand for the Azores region (zone 2.1 and horizontal elastic response spectrum of type 2) was defined for a reference ground acceleration, a_{gR}, equal to 2.50 m s^{-2}, as recommended by the National Annex of the NP EN 1998-1 [165]. These values are recommended for structures with an importance class II, to which corresponds an importance factor, γ_I, equal to 1.00. In addition to the reference ground acceleration, the horizontal elastic response spectrum is fully characterised after the definition of the following parameters: $T_B = 0.10$ s; $T_C = 0.25$ s; $T_D = 2.0$ s; soil factor, S, equal to 1.30; equivalent viscous damping, ξ, equal to 5%, and foundation soil type C [165].

In this study three levels of the seismic action, associated to three different return periods, were considered, in accordance to the Portuguese National Annex of the EN 1998-3 [166]:
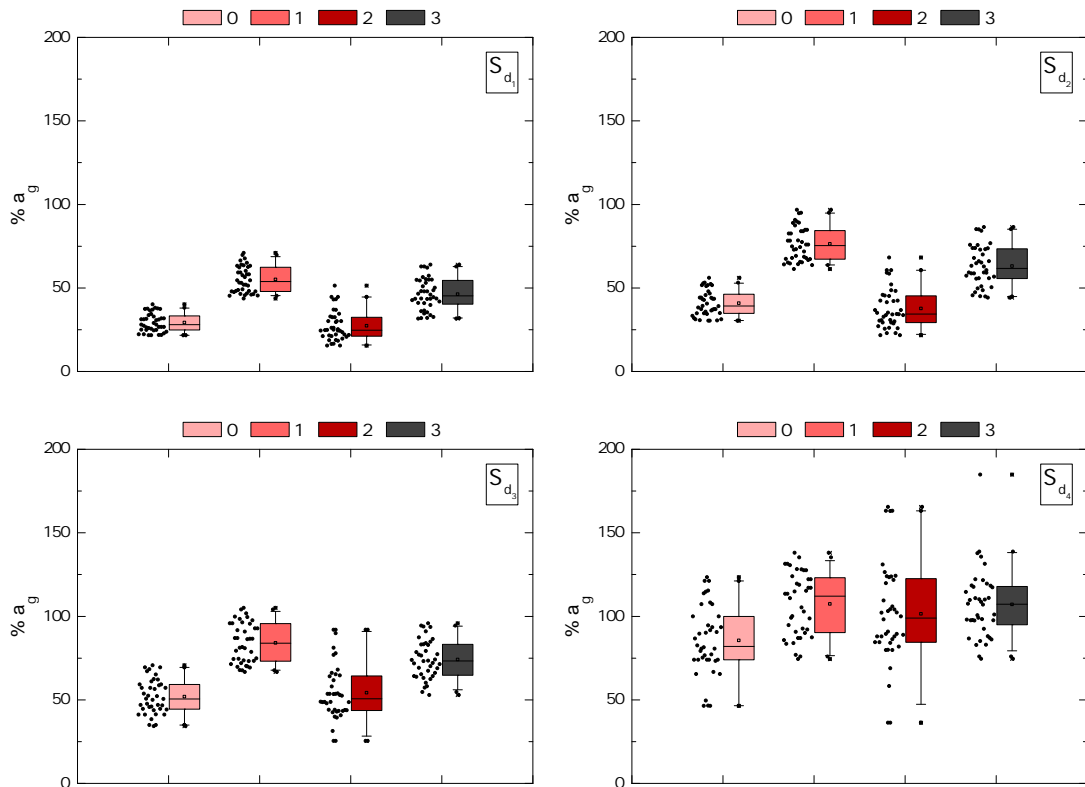
Figure 4.20: Box-plot diagrams in terms of %a_g for the set of 40 pushover analyses performed for model C, grouped by limit state (from S_{d_1} to S_{d_4} and retrofitting condition (from 0 to 3).

975 years for NC limit state; 308 years for the SD limit state, and 73 years for the DL limit state. This is the approach that it is currently in force in Portugal for strengthening and retrofitting purposes.

The box-plot diagrams in terms of the %a_g values, obtained for model C, are presented in Figure 4.20 for each limit state (from S_{d_1} to S_{d_4}) and retrofitting condition (from 0 to 3). It is possible to observe a greater dispersion on the results as one moves from limit state S_{d_1} to S_{d_4}. Another interesting observation, in the particular case of model C, is that the consolidation of the vertical structure (1) appears to substantially improve the median %a_g values for all the considered limit states, when compared to the unreinforced condition (0). To the contrary, the efficiency of the consolidation of the horizontal structure (2) is only observed in the case of limit state S_{d_4}. Moreover, from comparing the results in Figure 4.21 it is possible to observe that retrofitting strategy 3 is far from representing a summation of the response obtained with retrofitting strategies 1 and 2 in terms of %a_g. Instead, if considering the median %a_g values, retrofitting strategy 3 is placed in an intermediate position between these two retrofitting strategies. This fact is observed for all limit states and for the great majority of the models herein considered, as demonstrated in Appendix A.

4.2.4 Fragility and loss assessment

In this study, the loss assessment was carried out by following the HAZUS methodology [216] for the computation of fragility curves, which represent the relationship between seismic intensity, herein expressed in terms of spectral displacement, and damage in terms of the conditional cumulative probability of reaching or exceeding a given damage state, ds. Hence, and according to [216], the following damage states should be considered: no damage (ds_0), slight damage (ds_1), moderate damage (ds_2), severe damage (ds_3), and complete damage or collapse (ds_4). The probability density function was assumed to follow a lognormal distribution [216]. Thus, the probability of a reaching or exceeding a given damage state, ds, is defined by Equation (4.11), as a function of the spectral displacement, S_d:

$$P\left[ds \mid S_d\right] = \Phi\left[\frac{1}{\beta_{ds}} \times \ln\left(\frac{S_d}{\overline{S}_{d,ds}}\right)\right] \tag{4.11}$$

where Φ is the standard normal cumulative distribution function, β_{ds} is the standard deviation of the natural logarithm of the spectral displacement for the damage state ds, and $\overline{S}_{d,ds}$, is the median value of the spectral displacement at which a building reaches the threshold of damage state ds [216]. The standard deviation β_{ds}, which accounts for the variability and uncertainty associated with the numerical model, capacity curve, seismic demand, and the definition of each damage states threshold, was computed according to the formulation proposed in the framework of the European project Risk-UE [38], given in Equation (4.12) to Equation (4.15). According to this formulation, the values of β_{ds} are closely related to the ultimate ductility of the structure, μ_u, defined as the ratio between d_u and d_y. Finally, the median values of the spectral displacement associated to each damage limit state, $\overline{S}_{d,ds}$, were adopted from Barbat et al. [215], according to the previous Equation (4.7) to Equation (4.10).

$$\beta_{ds_1} = 0.25 + 0.07 \times \ln\left(\mu_u\right) \tag{4.12}$$

$$\beta_{ds_2} = 0.20 + 0.18 \times \ln\left(\mu_u\right) \tag{4.13}$$

$$\beta_{ds_3} = 0.10 + 0.40 \times \ln\left(\mu_u\right) \tag{4.14}$$

$$\beta_{ds_4} = 0.15 + 0.50 \times \ln\left(\mu_u\right) \tag{4.15}$$

Following the same reasoning as hitherto, and again for the sake of an example, the fragility curves in Figure 4.21 are associated with the median capacity curves of each retrofitting condition of model C only.

From observing these results, it is possible to conclude that the consolidation of the vertical structure (1) is indeed the most effective retrofitting strategy in this particular case, reducing the probability of reaching or exceeding the limit state S_{d_4} from 59% to 28%. In line with the results presented in Figure 4.21, when comparing the consolidation of both vertical and horizontal structures simultaneously (3) with retrofitting strategies 1 and 2 individually, the probabilities of reaching or exceeding a given damage state (ds) are clearly exacerbated. In fact, in this particular case, the probabilities of exceeding each damage state for retrofitting strategy 3 are practically identical to the unreinforced condition (0). However, and as demonstrated in Appendix A, this abnormal outcome, which is highly influenced by
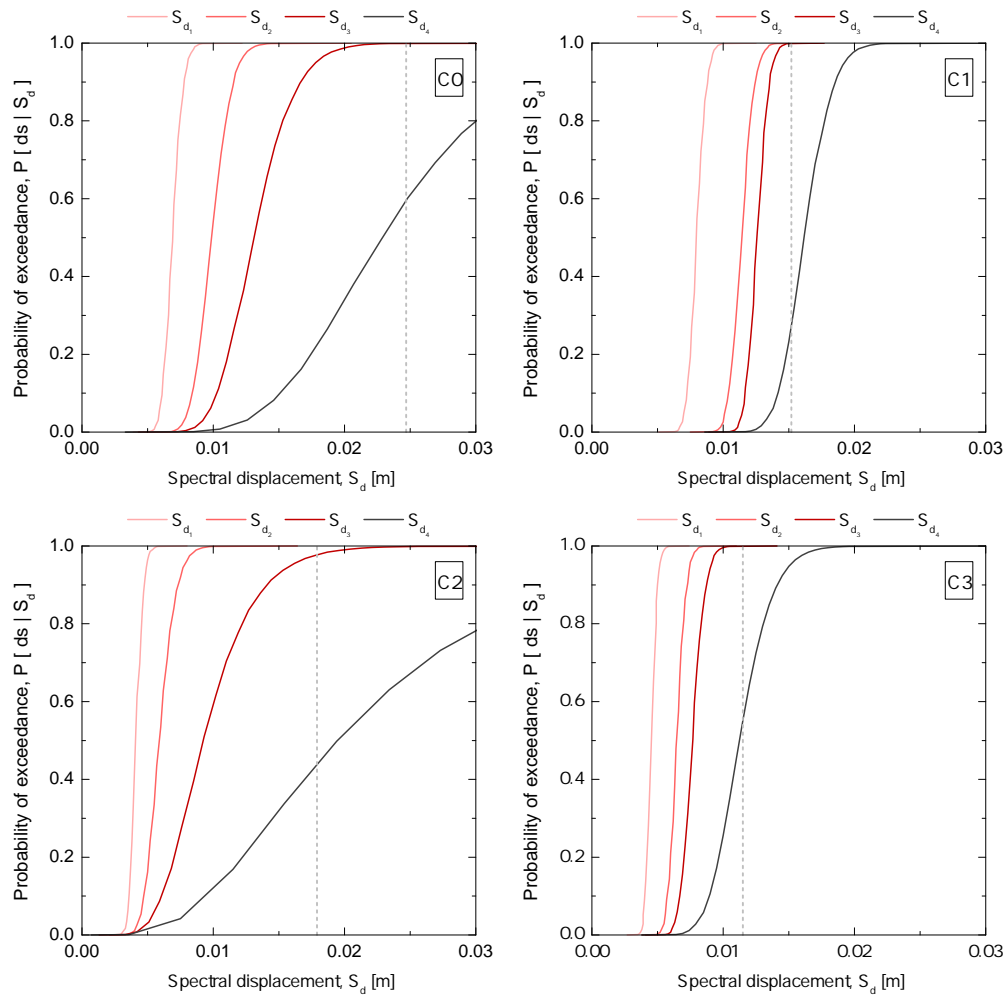
Figure 4.21: Fragility curves associated with the median values of the capacity curves of model C, for each limit state (from S_{d_1} to S_{d_4}) and retrofitting condition (from 0 to 3). Please note that the performance point of the equivalent bilinear SDOF system, d^*_t, is represented for each case by the vertical dashed line in light grey.

the low displacement ductility capacity of model C when subject to retrofitting strategy 3, was not observed in the remaining models.

The computation of fragility curves is a necessary step to determine the probabilities p_k, of exceeding each damage state ds, and subsequently, apply the HAZUS loss assessment methodology [216]. These probabilities are summarised in Table 4.8 for each model, central tendency measure and retrofitting condition. It is worth referring that the loss assessment in this study included the estimation of economic losses resulting from the need of repairing seismic-induced damage (RD), the damage caused to building contents (BC), and also from human casualties (HL), as detailed in the following subsections.

4.2.4.1 Repair damage (RD)

One of the most widely used approaches for the estimation of direct economic loss associated with a given damage level was included in the HAZUS methodology [216], through the seismic

Table 4.8: Probabilities of exceeding each damage state (from ds_0 to ds_4), for each model and retrofitting condition, here only for median values. The probabilities associated with the 16th and 84th PCTLs are summarised in Table A.1 of Appendix A.

Model	Retrofitting condition	ds_0 No damage	ds_1 Slight damage	ds_2 Moderate damage	ds_3 Severe damage	ds_4 Collapse
A	0	0%	0%	0%	60%	40%
	1	80%	20%	0%	0%	0%
	2	0%	0%	0%	54%	46%
	3	93%	7%	0%	0%	0%
B	0	0%	0%	0%	35%	65%
	1	0%	12%	65%	22%	2%
	2	0%	0%	0%	34%	66%
	3	0%	20%	63%	16%	1%
C	0	0%	0%	0%	41%	59%
	1	0%	0%	0%	72%	28%
	2	0%	0%	2%	54%	44%
	3	0%	0%	0%	44%	56%
D	0	0%	0%	0%	6%	94%
	1	0%	0%	1%	70%	29%
	2	0%	0%	0%	42%	58%
	3	0%	0%	2%	68%	30%

damage repair cost, C_{RD}, defined in Equation (4.16):

$$C_{RD} = C_R \times \Sigma_{n=0}^{k} \left(f_{k,RD} \times p_k \right) \tag{4.16}$$

where C_R represents the replacement cost of the building, $f_{k,RD}$ the normalised deviation between the median C_{RD} values for each damage state (determined for the building stock of Faial Island by Maio et al. [201]), and p_k, the probability of exceeding each one of these damage states (given in the previous Table 4.7). The $f_{k,RD}$ values of 0.000, 0.031, 0.059, 0.338, and 1.000 (respectively for damage states ds_0 to ds_4) were also adopted from Maio et al. [201].

It is worth noting that the two values presented in the previous Section 4.1.7, for the building replacement cost, C_R, were herein considered. The first value, referring to the current construction replacement cost, $C_{R,CC}$, was assumed equal to 530 € m^{-2}. The second value instead, refers to a traditional construction replacement cost, $C_{R,CT}$. The $C_{R,CT}$ values were derived in Section 4.1.7, as a function of the GFA value, and represent about 137%, 101%, 89% and 89% of the $C_{R,CC}$ value, respectively for model A to D. Hence, the resulting C_{RD} values are summarised further on, in Table 4.8 (Section 4.2.5).

4.2.4.2 Building contents (BC)

By building contents, one refers to the set of all movable assets present in a given building, from furniture and household appliances to increased value objects. These assets are particularly vulnerable to accelerations. For this reason, it's fundamental to consider damage to building contents in loss assessment procedures, even for low seismic intensity levels. The HAZUS methodology recommends that the losses associated with the replacement of build-

ing contents are determined as a function of the damage limit states of each building [216]. The reason why the recommendations of FEMA & NIBS [216] for the estimation of building contents loss were considered, had to due with the context where this study is inserted (more focused on urban-scale assessment) and to the fact that very little literature is available on this topic worldwide.

Since the value of buildings' contents is unknown, the replacement cost of the building contents, C_{BC}, equal to 50% of the repair cost C_R, was considered. The replacement cost of the building contents, C_{BC}, are determined by means of Equation (4.17). The $f_{k,BC}$ factors, which represent the normalised deviation between the median C_{BC} values for each damage limit state (from ds_0 to ds_4), were assigned equal to 0.000, 0.010, 0.050, 0.250, and 0.500, according to [216]. The resulting C_{BC} values are summarised further on, in Table 4.8 (Section 4.2.5).

$$C_{BC} = 0.5 \times C_R \times \Sigma_{n=0}^{k} \left(f_{k,BC} \times p_k \right) \tag{4.17}$$

4.2.4.3 Human loss (HL)

Human losses were also estimated according to the HAZUS methodology [216], again as a function of the damage limit states. According to this procedure, four severity levels are considered: injuries requiring basic medical aid, but without hospitalisation; injuries requiring medical attention and hospitalisation, but not considered to be life-threatening; casualties that include entrapment and require expeditious rescue and medical treatment to avoid death, and immediate deaths. The $f_{k,HL}$ factors associated with each severity level and damage limit state were adopted from FEMA & NIBS [216], considering the unreinforced masonry bearing walls typology (URM) and a scenario where the earthquake would occur at 2 a.m., i.e., residents were assumed to be inside their households.

The number of residents according to the information available in the inspection surveys carried out after the 1998 Azores earthquake was 1, 4, 3 and 4, respectively for building A to D. The percentage of injured residents was determined according to the values proposed in FEMA & NIBS [216] for residential buildings. The monetary values associated with each severity level were adopted from Lamego [217], which were derived in turn from the cost data analysis of the 1994 Northridge earthquake. The final costs associated with human loss, C_{HL}, are given in Table 4.8 (Section 4.2.5).

4.2.5 CBA model application

The global outputs of the cost-benefit analysis carried out in this study, are summarised in the following Table 4.9, for each building and retrofitting strategy, considering only the median values and the $C_{R,CT}$ replacement cost. Economic losses are broken down in terms of repair damage (C_{RD}), building contents (C_{BC}), and human casualties (C_{HL}). The indicator BCR, represents the ratio between the gains obtained by preventing seismic-induced damage (Benefit), and the specific cost of each retrofitting strategy, C_{RS}. The cost of each retrofitting strategy, C_{RS}, was obtained by multiplying the average values proposed in the previous Table 4.5 in Section 4.1.8 (equal to 117 €m^{-2}, 22 €m^{-2}, and 139 €m^{-2}, respectively to retrofitting strategies 1 to 3), by the GFA of each case study building. When comparing the C_{RS} values with the $C_{R,CT}$ of each building, it is possible to observe that the cost of retrofitting strategies 1, 2, and 3, represent about 16%, 3%, and 19% of the $C_{R,CT}$ for model

A, and 22%, 4%, and 26% for model B. For the urban typologies, the cost of retrofitting strategies 1, 2, and 3, represent about 25%, 5%, and 30% of $C_{R,CT}$ (practically the same for models C and D). If instead the $C_{R,CC}$ is to be compared with C_{RS}, one can conclude that retrofitting strategies 1, 2, and 3, represent 22%, 4%, and 26% of $C_{R,CC}$, independently from the building in question.

From analysing the final costs estimated by following the HAZUS methodology and assuming the traditional construction replacement cost, $C_{R,CT}$ (in Table 4.9), the costs associated with human losses, C_{HL}, clearly stand out among the remaining ones (C_{RD} and C_{BC}). In fact, the relatively low values obtained for C_{HL} are closely related to the extremely low number of residents considered for each building.

Table 4.9: Global results of the cost-benefit analysis for each model and retrofitting condition (from 0 to 3), considering the median values and the traditional construction replacement cost, $C_{R,CT}$. The results associated with the 16th and 84th PCTLs are summarised in Table A.2 of Appendix A.

Model	Retrofitting condition	C_{RD} €	C_{BC} €	C_{HL} €	Total losses €	Benefit €	BCR_{CT} [–]
A	0	53010	15894	1029	69932	–	–
	1	338	169	0	507	69425	8.11
	2	28861	17034	1187	47082	22850	14.20
	3	277	156	8	442	69491	6.83
B	0	69392	20286	6549	96227	–	–
	1	4094	3487	360	7941	88286	5.84
	2	50832	20473	6653	77958	18269	6.42
	3	3872	2862	299	7032	89195	4.96
C	0	127119	19358	4526	151002	–	–
	1	18378	13846	2233	34457	116546	3.70
	2	27599	16502	3405	47507	103496	17.49
	3	33868	18704	4253	56825	94177	2.52
D	0	246394	25443	9411	281248	–	–
	1	24826	13949	3074	41849	51069	3.38
	2	46099	19163	5933	71196	51837	18.22
	3	25633	14062	3177	42871	238377	3.27

When analysing the benefit column in Table 4.9, which represents the gains obtained by preventing seismic-induced damage with the application of each retrofitting strategies, it is possible to observe that, in the case of rural typologies (models A and B), greater economic gains are associated with retrofitting strategies 1 and 3. In the case of urban typologies (models C and D), retrofitting strategies 1 and 2 appear to have a more similar impact in terms of economic gains. However, if looking at the BCR_{CT} indicator separately, the consolidation of the horizontal structure (2) presents the highest benefit-cost ratios for the majority of the cases, due to the fact its application cost is significantly lower than the remaining strategies. Despite the BCR_{CT} indicator suggests the consolidation of the horizontal structure (2) as the most viable retrofitting strategy, this strategy appears to be, in fact, the less efficient in terms of seismic damage prevention, as previously suggested by the results presented in Table 4.8. This fact might be related to the compatibility issues between the definition of horizontal diaphragms within the software code used and the recommendations of the NZSEE guidelines [173].

In the following Figure 4.22, the benefit-cost ratios obtained for both traditional and

current construction replacement costs (BCR_{CT} and BCR_{CC}, respectively) are opposed for each building and retrofitting strategy. For the sake of simplicity, only the median values are presented in Figure 4.22. It is possible to conclude that the benefit-cost ratios obtained by implementing traditional seismic retrofitting strategies when adopting replacement costs associated with a reconstruction process that makes use of the traditional construction techniques and materials, BCR_{CT}, are in fact higher than those associated with current construction replacement costs, BCR_{CC}, exception made to model C. In the case of model D, since the replacement costs $C_{R,CT}$ and $C_{R,CC}$ are practically the same, the resulting BCR_{CT} and BCR_{CC} ratios are also identical.
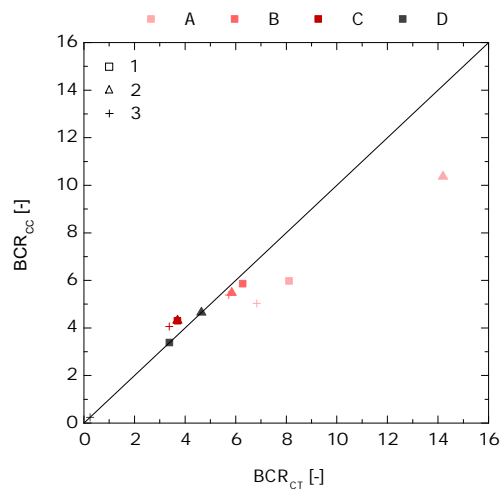
Figure 4.22: Comparison between the median BCR_{CT} and BCR_{CC} ratios obtained for each model and retrofitting condition (from 1 to 3).

4.2.6 Final remarks

This study aimed at outlining and testing a CBA model for evaluating the cost-benefit from integrating traditional seismic retrofitting strategies on the renovation of both rural and urban typologies of the vernacular architecture of Faial Island, in Azores (Portugal).

One of the first conclusions of this study is that, in general, the use of the seismic retrofitting strategies herein considered allows indeed, the improvement of the seismic performance of such building typologies. Furthermore, this study demonstrated that the cost of application of traditional retrofitting strategies does not embody a significant value over the total replacement cost, that could possibly turn the use of these strategies economically unviable. Another interesting conclusion has to do with the large dispersion of the results, as a consequence of considering in the analyses, aspects such as the type of lateral load pattern distribution (uniform and pseudo-triangular), accidental eccentricity, or loading direction, for example.

For the great majority of the cases analysed, the use of traditional seismic retrofitting strategies show a quite satisfactory benefit-cost ratio, being for this reason recommendable for both rural and urban building stock of Faial Island. In particular, the consolidation of the horizontal structure has proved to be the most attractive strategy for all the case studies if exclusively focusing on the benefit-to-cost ratio. However, and unexpectedly, this

attractiveness was not echoed in terms of seismic performance upgrading. This fact broaches the subject of how the formulation of horizontal diaphragms in this type of software codes should be revised or adapted in order to enhance the compatibility between numerical models and the values recommended by the NZSEE guidelines for flexible diaphragms. In this regard, and as further developments, the improvement of the connections between horizontal diaphragms and load-bearing walls should be numerically investigated in detail so that the seismic performance upgrading in the numerical models can be more approximated to the expected contribution of such retrofitting strategies.

Finally, it is worth referring that, since the replacement costs associated with the use of traditional materials and building techniques were in general lower than those associated with current construction, higher benefit-cost ratios were obtained. This finding constitutes, therefore, a great incentive for promoting the proper renovation of UCH assets particularly for the building stock of Faial Island.

Chapter 5

Casting a new light on the seismic risk assessment of historic centres

Abstract *This chapter investigates the correlation between two well-known approaches for the seismic risk assessment of UCH assets located in historic centres: the "vulnerability index" method and the seismic "capacity curve" derived by using a simplified numerical model together with a nonlinear static procedure.*

5.1   Introduction

Common seismic risk analyses encompass a broad set of necessary instruments that are far from being accessible by non-academic audiences. Moreover, aggregating the results of such detailed and complex analyses at a convenient scale is a huge challenge. This hinders their application to historic centres given the large amount of data and resources required. Furthermore, given the existing conflicting interests and lack of understanding of scientific findings, final decisions turn out to be often based on politic and economic interests rather than on the technical ones, as argued by Hunter and Fewtrell [62]. These are the grounds that served as motivation for the research carried out in this study, which fundamentally aims at casting a new light for the seismic risk assessment of stone masonry buildings located within historic centres. To better understand the scientific relevance of this research it is fundamental to start by understanding its framework. For this reason, the following section is dedicated to a pragmatic reflection about an eventual window of opportunity to investigate the development of a new hybrid methodology that could possibly help bridging the gap between empirical and analytical methods for the seismic risk assessment of historic centres.

5.2   Bridging the gap between empirical and analytical methods

The "assessment scale spectrum" in Figure 5.1 refers to the different methodologies or approaches available for the seismic vulnerability assessment of unreinforced masonry structures. This spectrum is often divided into first-, second- and third-level approaches, as described in [126, 218]. Without getting into much detail (more information is available in Section 2.6.1), first-level approaches are more suitable for large-scale assessments and include methodologies that resort to a large amount of data (usually of qualitative nature and provided either by the census, municipalities' archives, or "in-situ" survey and inspections). Second level approaches are based on mechanical models that rely on a higher quality of data (including geometrical and structural features). Finally, third level approaches involve the use of numerical models more or less sophisticated that require a complete survey of individual buildings and a thorough knowledge of both geometry and materials' properties.

1st level   2nd level   3rd level
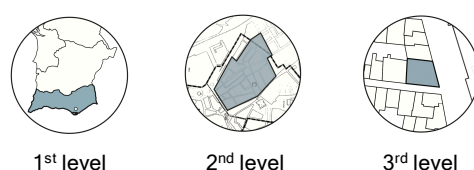
Figure 5.1: Illustration of the idealised "assessment scale spectrum", which can be subdivided into first-, second- and third-level approaches.

In recent years, significant efforts were put into the development of innovative hybrid methodologies as a mean of bridging the methodological gap that exists between empirical and analytical methods, whose computational efforts are not bearable with large-scale assessments neither cost- nor time-wise. This gap might be possibly explained due to the complexity and non-linearity of the phenomenon under study, the uncertainties associated to the methodologies behind these two measures of seismic vulnerability, or even due to the

general lack of interest of the scientific community on this topic, motivated by an eventual disbelief on the potential of combining the use of such measures and methodologies.

However, the research carried out for example, by Barbat et al. [219], Basaglia et al. [220], Ródenas et al. [221], Chieffo et al. [222], Liu et al. [223], Kassem et al. [224], brought a new hope for this type of approaches. In Portugal, the investigation of type of approaches has gained more and more attention by the scientific community, as demonstrated by the recently developed studies of Mota de Sá [4], Ortega [11], or Ortega et al. [225].

The ξ_m^3 method proposed by Mota de Sá [4], for example, is based on the assumption that the response of an existing structure to ground shaking, can be interpreted as a function of three main characteristics: stiffness, strength and ductility. The SAVVAS method developed by Ortega [11] instead, makes use of a set of parameters related to geometrical, structural, constructive and material characteristics of vernacular structures. However, the maximum seismic capacity of buildings in the SAVVAS method is evaluated in quantitative terms, as a result of an extensive (numerical parametric) analysis carried out to evaluate and quantify the influence of these parameters on the seismic capacity of such buildings.

Inspired by the previous studies, this chapter aims at investigating a new light for the seismic risk assessment of historic centres by using the simplified scoring method developed by Vicente [7], also known as vulnerability index method. This macroseismic approach adapted the use of the vulnerability index method developed by Benedetti and Petrini [67] and of the second-level vulnerability spreadsheet of the GNDT [226], also known as the Italian approach, to the Portuguese masonry building stock. This method has been applied to several historic centres in Portugal ever since [8, 14, 227], and was recently calibrated in [127], by using post-earthquake damage data derived from the 1998 earthquake of Azores, in Portugal.

At the current state-of-art, a common way to correlate hazard with the mean damage grade when considering the macroseismic approach is to use the analytical expression proposed by Bernardini et al. [82], and adapted by Vicente [7]. The macroseismic approach understands the definition of building typologies belonging to different vulnerability classes, and the classification of damage and intensity levels according to the European Macroseismic Scale, EMS-98 [86]. Hence, the average mean damage grade, μ_D, of a given damage distribution is given by Equation (5.1), where I is the seismic hazard described in terms of macroseismic intensity, V is the vulnerability index, and Q is a ductility factor that describes the ductility of a determined building typology (ranging from 1 to 4) [7]. While the vulnerability factor, V, controls the position of the curve, the ductility factor, Q, controls the slope of the vulnerability function. Equation (5.2) was proposed by Vicente [7] to correlate the vulnerability factor, V, to the vulnerability index, I_v. This correlation enables the estimation of the mean damage grade, μ_D, and subsequently, to perform loss assessment.

$$\mu_D = 2.5 \times \left[1 + \tanh\left(\frac{I + 6.25 \times V - 13.1}{Q} \right) \right] \qquad (5.1)$$

$$V = 0.592 + 0.0057 \times I_v \qquad (5.2)$$

However, the use of macroseismic intensities in countries with a limited observed damage data from real ground motions, as in the case of Portugal, restricts the applicability of such a ground motion measure to estimate damage [4]. Moreover, apart from only a few studies, as that of Sandi and Floricel [228], the value adopted for the ductility factor, Q, is often poorly addressed in the literature, being, for this reason, an issue of great controversy among

the scientific community. In addition to this, there is also limited understanding about to what extent the vulnerability index method developed in [7] is sensitive to the structure's yielding frequency, ductility, stiffness and base shear capacity. Hence, this exercise examines the potential of the vulnerability index method to identify and prioritise the most vulnerable buildings within a specific building typology.

To this aim, the correlation between the vulnerability index method developed by Vicente [7] and the seismic capacity curve derived from simplified numerical models, and further applied in the scope of the N2 Method [15, 164], as demonstrated for instance in [72], will be herein evaluated. Similarly to Section 3.2 and Section 4.2, the seismic capacity curve was derived by using the three-dimensional macroelement model recently developed by Pantò et al. [146]. Having this been said, the main research questions are:

- How could we possibly revert the use of the vulnerability index method by avoiding the use of the European Macroseismic Intensity Scale, I_{EMS-98}?

- How can we take advantage of the potential of simplified numerical models to this aim?

- Is there a correlation between the vulnerability index method and the main properties of the numerical capacity curves?

Finally, it is equally important to be aware of the possible limitations of the exercise that is intended to be investigated in this study. Firstly, the bounding of the available literature is naturally responsible for introducing some theoretical limitations on the investigation carried out. The incomplete knowledge of the state of the art is mainly related to subscription and content protection policies from publishers. However, even if one would have open access to all the literature relevant to our research, achieving a thorough knowledge would not be feasible time-wise. Therefore, the literature review consulted for this study is considered to be just a sample of all the current streams of thought.

When using models to simulate the real behaviour of a natural phenomenon, in this particular case, the effect of earthquakes on buildings and other infrastructures, one should recall that all models are wrong. From this fact, scientists have been developing methods to approximate their models to the real phenomena, but again, they are always a mere approximation. Bearing in mind the above, it is worth noting that the research herein developed has naturally some methodological limitations resulting from the fact that it utilises different methods for the seismic vulnerability assessment of existing masonry structures.

The empirical limitations of this research include the selection of the previously-mentioned methods for the vulnerability assessment of the buildings, the selection of the buildings as fully representative of the building typologies under study, the sample size, the assumption that these structures might be grouped in function of the number of storeys or period range, and finally, that the complexity of such a nonlinear problem can be reduced or simplified to a correlation between three fundamental parameters.

5.3   The vulnerability index method

As mentioned above, the vulnerability index method herein considered was developed by Vicente [7], and has been applied to several historic centres in Portugal [8, 14, 227]. As previously mentioned, this method was recently calibrated by Ferreira et al. [127], by using

post-earthquake damage data derived from the 1998 earthquake of Azores [29]. As demonstrated in Table 5.1, a vulnerability index is obtained by the calculation of a score for each building, as the weighted sum of 14 parameters.

Table 5.1: Vulnerability index method, developed by Vicente [7]. While the parameters coloured in "light grey" represent the parameters considered as independent, those in "red" were disregarded in this study. Finally, the remaining parameters P1, P3, P12 and P13 were considered as dependent.

Parameter		Class, C_{vi}				Weight, p_i	
		A	B	C	D	Original [7]	Calibrated [9]
1. Structural building system							
P1	Type of resisting system	0	5	20	50	0.75	2.50
P2	Quality of resisting system	0	5	20	50	1.00	2.50
P3	Conventional strength	0	5	20	50	1.50	1.00
P4	Maximum distance between walls	0	5	20	50	0.50	0.50
P5	Number of floors	0	5	20	50	1.50	0.50
P6	Location and soil condition	0	5	20	50	0.75	0.50
2. Irregularities and interactions							
P7	Aggregate position and interaction	0	5	20	50	1.50	1.50
P8	Irregularity in plan	0	5	20	50	0.75	0.50
P9	Irregularity in height	0	5	20	50	0.75	0.50
3. Floor slabs and roofs							
P10	Alignment of openings	0	5	20	50	0.50	0.50
P11	Horizontal diaphragms	0	5	20	50	1.00	0.75
P12	Roof system	0	5	20	50	1.00	2.00
4. Conservation status and other elements							
P13	Fragilities and conservation status	0	5	20	50	1.00	1.00
P14	Non-structural elements	0	5	20	50	0.50	0.75

Each parameter covers one aspect related to the building's seismic response and it is distributed into 4 vulnerability classes (C_{vi}) of growing vulnerability: A, B, C and D. Weights, p_i, range from 0.50, for the less important parameters (in terms of structural vulnerability), to 2.5, for the most important ones. In Table 5.1 two sets of weights are presented: those originally proposed by Vicente [7], and the set of weights recently calibrated by Ferreira et al. [127].

To have better control over this complex problem, it was necessary to establish dependency relationships between some of these parameters. These relationships are highlighted both in Table 5.1 and in Figure 5.2, where parameters coloured in "light grey" were considered as independent parameters. Parameters P7, P9 and P14 ("dark red") were disregarded from this study either due to the increased complexity or difficulty on representing such features numerically. Finally, P1, P3, P12 and P13 were taken as dependent. These dependencies were established according to the very same formulation of the vulnerability index method, fully described in [7].
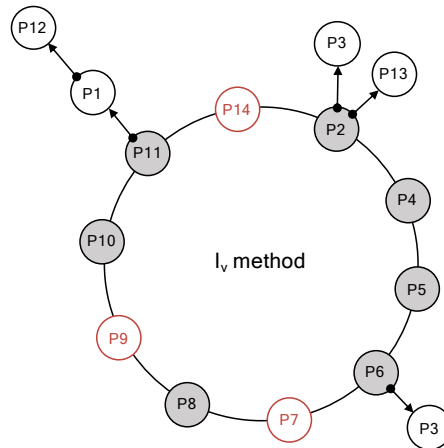
Figure 5.2: Dependency relationships assumed between the parameters of the vulnerability index method proposed by Vicente [7].

5.4 From I_v to numerical models

After establishing the dependency relationships between parameters, it is necessary to understand how each class of these parameters can be reflected in the numerical models. Thus, the explanation of how independent parameters were defined for the generation of the numerical models is given in this section. It is yet opportune to clarify that this investigation was applied, similarly to what has been done in the previous Chapter 4, to the vernacular stone masonry building stock of Faial island. Several studies have been carried out concerning the seismic vulnerability assessment and the typological classification of the vernacular architecture in Faial island ever since the 1998 earthquake of Azores [122, 127, 185, 187, 201].

5.4.1 Quality of resisting system (P2)

For the quality of the resisting system, the values of two different typologies were adopted from the last update of the Italian Building Code, NTC [229], by considering the minimum and maximum values of classes I and VI. These values, given in Table 5.2, match those usually associated to both rural and urban stone masonry typologies of Faial island [169], illustrated in Figure 5.3.

Table 5.2: Mechanical properties of both rural and urban stone masonry typologies of Faial island, adopted from the last update of the Italian Building Code, NTC [229].

Class C_{vi}	Masonry typology	w [kN m^{-3}]	f_m [N cm^{-2}]	τ_0 [N cm^{-2}]	f_{tm} [N cm^{-2}]	E [N mm^{-2}]	G [N mm^{-2}]	Cracked stiffness
A	VI max	22	607.4	8.9	30.4	3300	1100	1.00
B	VI min	22	429.6	6.7	21.5	2000	667	0.83
C	I max	19	148.1	2.4	7.4	700	233	0.67
D	I min	19	74.1	1.3	3.7	345	115	0.50

As demonstrated in Table 5.2, the value of the tensile strength of masonry, f_{tm}, was assumed equal to 5% of the compressive strength, f_t. While the resistance values given in Table 5.2 are divided by a confidence factor, CF, equal to 1.35, the values of the elastic properties instead, are multiplied by the corresponding cracked stiffness factor [165].

Figure 5.3: Example of the variability between rural (left) and urban (right) stone masonry typologies in Faial island.

5.4.2   Maximum distance between walls (P4)

According to Vicente [7], the estimation of the vulnerability class for parameter P4 essentially depends on the ratios L/s and H_0/s. While L/s represents the ratio between the maximum span between load-bearing walls, L, and the average wall thickness, s. H_0/s represents the ratio between the average inter-storey height, H_0, and the average wall thickness, s. After the careful and extensive examination of technical drawings and inspection reports of several stone masonry buildings located in the island of Faial, which were gathered in the framework of the reconstruction process of Faial in the aftermath of the 1998 Azores earthquake [29], the maximum distance between walls (L) and the inter-storey height, H_0, were assumed constant and equal to 10.0m and 2.5m, respectively. Additionally, average wall thicknesses of 0.70m, 0.60m, 0.50m, 0.40m were assigned to each vulnerability class, from A to D, respectively.

5.4.3   Number of floors (P5)

Once again, when examining the database collected during the reconstruction process of Faial island, one can observe that the number of floors of stone masonry buildings generally vary between 1 and 4. While in rural areas, buildings with 1 and 2 storeys are more frequent, in the case of urban areas, stone masonry buildings generally have 3 or 4 storeys. The vulnerability classes for parameter P5 were defined directly as a function of the number of storeys, being the vulnerability class A associated with 1-storey buildings, and the vulnerability class D with 4-storey buildings.

5.4.4   Location and soil condition (P6)

The vulnerability classes for parameter P6 were assigned as a function of the respective soil type, based on the definition given in the EN 1998-1 [95]. There are, however, a few aggravating factors, such as the slope of the soil where the building is located or the difference in the height of the foundations, which were disregarded in this study, given the inability of the software 3D-Macro® [13] to model the interaction between the foundation soil and the structure in such a detailed way. For this reason, the underlying soil (foundations) were modelled as rigid.

5.4.5 Irregularity in plan (P8)

As for the parameter P8, four different configurations were assumed as representative of the majority of both urban and rural typologies of Faial island's stone masonry architecture: square-shape; rectangular-shape; L-shape, and L-square shape. These configurations are illustrated in Figure 5.4. The association between each configuration and vulnerability class was established by considering the criteria described in [7].
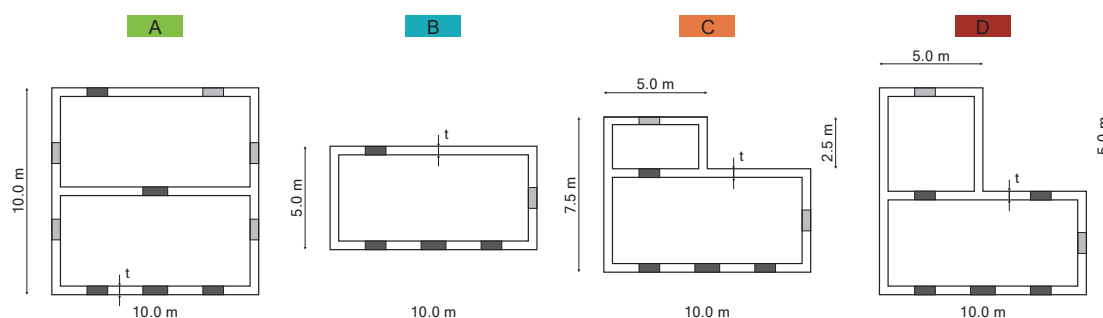
Figure 5.4: Vulnerability classes for the irregularity in plan parameter (P8). Openings in dark grey represent door elements while those in light grey represent windows.

5.4.6 Alignment of openings (P10)

This parameter classifies the irregularity of openings in height, again following the original formulation of the vulnerability index method proposed in [7]. As demonstrated in Figure 5.5, vulnerability class A corresponds to a configuration where openings are regular and aligned, vulnerability class B to a horizontal misalignment, and vulnerability class C to both horizontal and vertical misalignments. Finally, vulnerability class D corresponds to a situation where openings are both horizontally and vertically misaligned (vulnerability class C), aggravated by the presence of a large opening at the ground floor level, a common but erroneous practice observed in many buildings located in Portuguese historic centres.
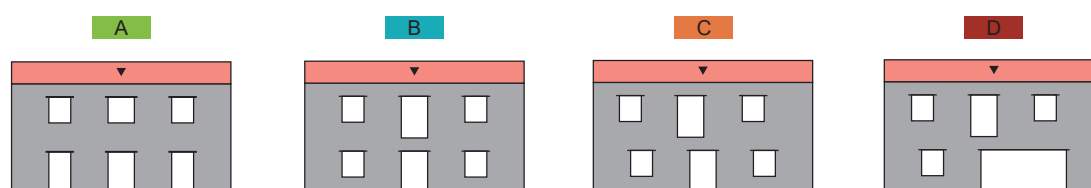
Figure 5.5: Vulnerability classes for the alignment of openings parameter (P10), herein exemplified for a 2-storey building.

5.4.7 Horizontal diaphragms (P11)

The Elastic modulus of horizontal diaphragms were calculated by 3D-Macro® [13] according to the geometrical properties of the floor typology. The equivalent thickness, t_{eq}, and equivalent stiffness, G_{eq}, were defined according to the NZSEE guidelines [173], as demonstrated in Table 5.3. Both gravity (G_k) and live (Q_k) loads, are also given in Table 5.3. There are a

few questionable aspects concerning the definition herein assumed for horizontal diaphragms. As an example, in the case of poorly connected diaphragms, it is not clear whether or not a flexible typology is actually more vulnerable than a rigid one. Moreover, the quality of the connections between horizontal diaphragms and the vertical structure was not modelled "numerically".

Table 5.3: Values adopted for equivalent thickness, t_{eq}, and equivalent stiffness, G_{eq}, for each floor typology considered, according to the NZSEE guidelines [173]. Gravity (G_k) and live (Q_k) loads are also shown for floor (left value) and roof (right value) elements.

Class C_{vi}	Floor typology	t_{eq} [m]	G_{eq} [MPa]	G_k [–]	Q_k [–]
A	Rigid and well connected	0.050	11920	3.00/3.00	2.00/0.40
B	Flexible and well connected	0.050	5.3	1.50/2.00	2.00/0.40
C	Rigid and poorly connected	0.025	11920	3.00/3.00	2.00/0.40
D	Flexible and poorly connected	0.025	6.8	1.00/1.50	2.00/0.40

5.5 Sample generation

In this study, a sample of 112 prototypes was considered as representative of Faial island's stone masonry building stock. To each vulnerability class of each parameter, 4 different models were built, being the classes of the remaining parameters randomly assigned.

From the histogram in Figure 5.6 (left) compares the I^*_v obtained for the sample of 112 prototype buildings by using both the original weights proposed by Vicente [7] and those recently calibrated by Ferreira et al. [9].

From Figure 5.6 (left), it is possible to observe that the histogram obtained by using the calibrated weights, which were derived from post-earthquake damage data from the 1998 Azores earthquake, is significantly shifted to the right, covering this way a broader range of I^*_v.

Figure 5.6 (right) instead, demonstrates the deviation, in terms of cumulative percentage, between the sample of 112 prototype buildings (or models) and 5 randomly selected samples of 1000 models. The I^*_v values in Figure 5.6 (right) correspond, exclusively, to the weighted sum of independent parameters P2, P4, P5, P6, P8, P10, and P11, by using the original weights [7].

5.6 Other considerations of the numerical models

A few other considerations and assumptions were assumed during the numerical modelling phase. The three-dimensional model developed by Pantò et al. [146] and incorporated in software 3D-Macro® [13], was used to perform a set of nonlinear analysis considering the positive and negative directions of the main planar directions X and Y for the uniform load pattern distribution and considering both positive and negative accidental eccentricity (in a total of 12 analyses for each model). The control point was fixed for each architectural layout at the same roof slab element. Moreover, macroelements were modelled with a maximum dimension of 1.50 m. One-storey buildings were modelled with a flexible pitched roof 1.50

m tall (assuming a non-accessible roof), even in the cases in which rigid diaphragms were to be assigned. Timber lintels were inserted over openings with the following properties (E = 3.907 GPa, w = 2.6 kN m^{-3}, b = depth of the wall, h = b/2).

As the use of the Eurocodes for structural design was recently approved by the new Ordinance no. 302/2019 [59], the global displacement capacity was defined according to EN 1998-3 [93]. Hence, the global displacement for the NC limit state was defined by the magnitude of the roof displacement at the point when the lateral capacity has reduced to 80% of its previous maximum value. The global displacement capacity for the Significant Damage (SD) limit state instead, was defined as 75% of the NC value. Finally, the displacement capacity for the Damage Limitation (DL) limit state, was defined as the displacement corresponding to the yield point of the idealised elasto-plastic pushover curve.

As mentioned previously, in this study, the capacity curves were derived by applying the N2 Method proposed by [15, 164], and illustrated in Figure 5.7, which is incorporated in the NP EN 1998-1 [165], and combines the use of nonlinear pushover analyses with the response spectrum method. Despite a non-iterative procedure is also recommended in the NP EN 1998-1 [165], in this study, the iterative procedure for the application of the N2 Method, described in detail by Estêvão [230], for example, was considered.
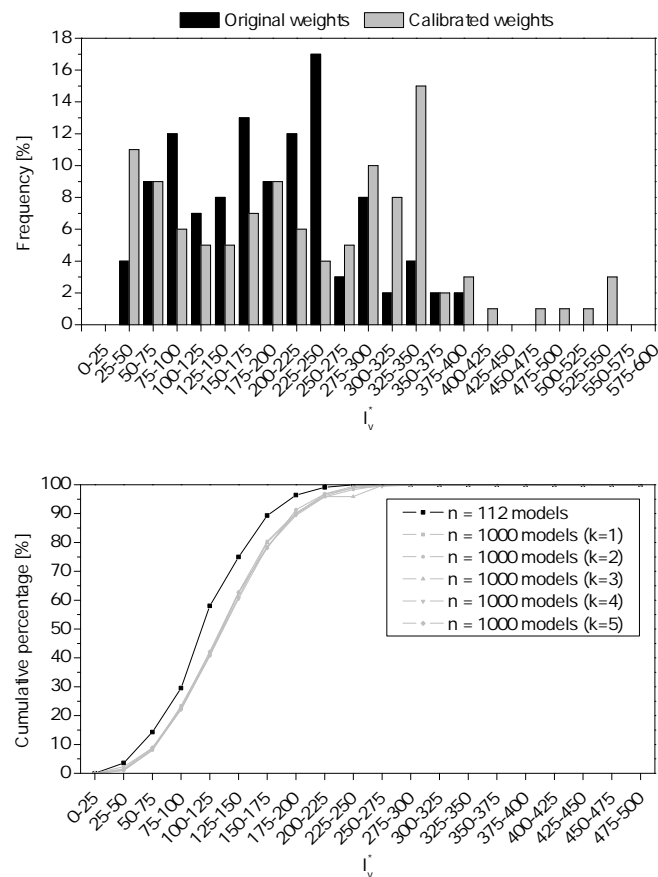
Figure 5.6: Histograms obtained for both original [7] and calibrated [127] weights of I$^{*}_{v}$ (left), and the deviations in terms of cumulative percentage between the sample of 112 models and 5 randomly selected samples of 1000 models (right).
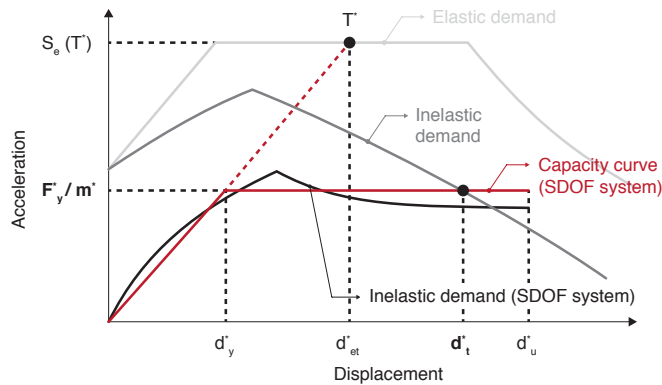
Figure 5.7: Generic graphical representation of the N2 Method proposed by [15, 164], with the determination of the target displacement of the SDOF system, d^*_t.

For the sake of simplicity, the ratio F^*_y/m^* in Figure 5.7, which represents the yielding spectral acceleration of the SDOF system, is going to be one of the two selected parameters for the comparison and discussion of the results, in the following Section 5.7. The other parameter, $\%a_g$, is given by the ratio a_{gC}/a_g, being a_{gC} the acceleration associated to the performance point, whose displacement corresponds to the value imposed for each limit state, and a_g, the peak ground acceleration. The latter value is obtained by multiplying the reference ground acceleration, a_{gR}, by the importance factor, γ_I, herein considered equal to 1.00 (assuming an importance class II) [93]. Please note that the structure's demand acceleration, a_{gD}, compatible with the fulfilment of each limit state, was then obtained multiplying the peak ground acceleration, a_g, by the coefficients proposed in the NP EN 1998-3 [166], equal to 0.55, 0.89, and 1.22, respectively for the DL, SD and NC limit states.

5.7 Discussion of the results

Given the multitude of outputs that can be possibly derived from the sample of 112 pro- totypes, this section was structured as follows: in a first moment a few scatter plots are going to be presented to illustrate different ways of examining the results and search for eventual data clusters or tendencies; in a second moment, the results obtained are going to be analysed in statistical terms, and finally, in a third phase, focus will be given to the goodness-of-fit itself, through the evaluation and comparison of the obtained adjusted-R^2 values. This indicator is often used to compare the goodness-of-fit for regression models that contain different numbers of independent variables.

On the one hand, the I^*_v value of each model can be compared, for example, to the following numerical outputs:

- Both yielding and ultimate displacements (associated with the DL and NC limit states) of the equivalent SDOF system, d^*_y and d^*_u, respectively;

- The yielding base shear strength of the equivalent SDOF system, F^*_y;

- The stiffness of the equivalent SDOF system, k^*;

- The ratio F^*_y/m^*;

- The parameter $\%a_g$.

On the other hand, these outputs can be disaggregated in multiple ways, as for example: for both original and calibrated weights; for each main direction X and Y; in function of the number of storeys or the equivalent period, T^*; in function of the horizontal diaphragm typology, or even soil type. The strategy herein adopted was that of starting examining the sample from a more global perspective and then, investigating the possibility of disaggregating the sample.

5.7.1 Scatter plots

As mentioned above, there is a multitude of output combinations that could be possibly generated in the study. However, for the sake of simplicity, only a few of these outputs are going to presented and discussed. Starting from a more global perspective, Figure 5.8 presents the scatter plot for the variables F^*_y/m^* and $\%a_{gNC}$ obtained for each model along the two main directions X and Y, considering a random distribution for the soil type, and both original [7], and calibrated [127] weights.
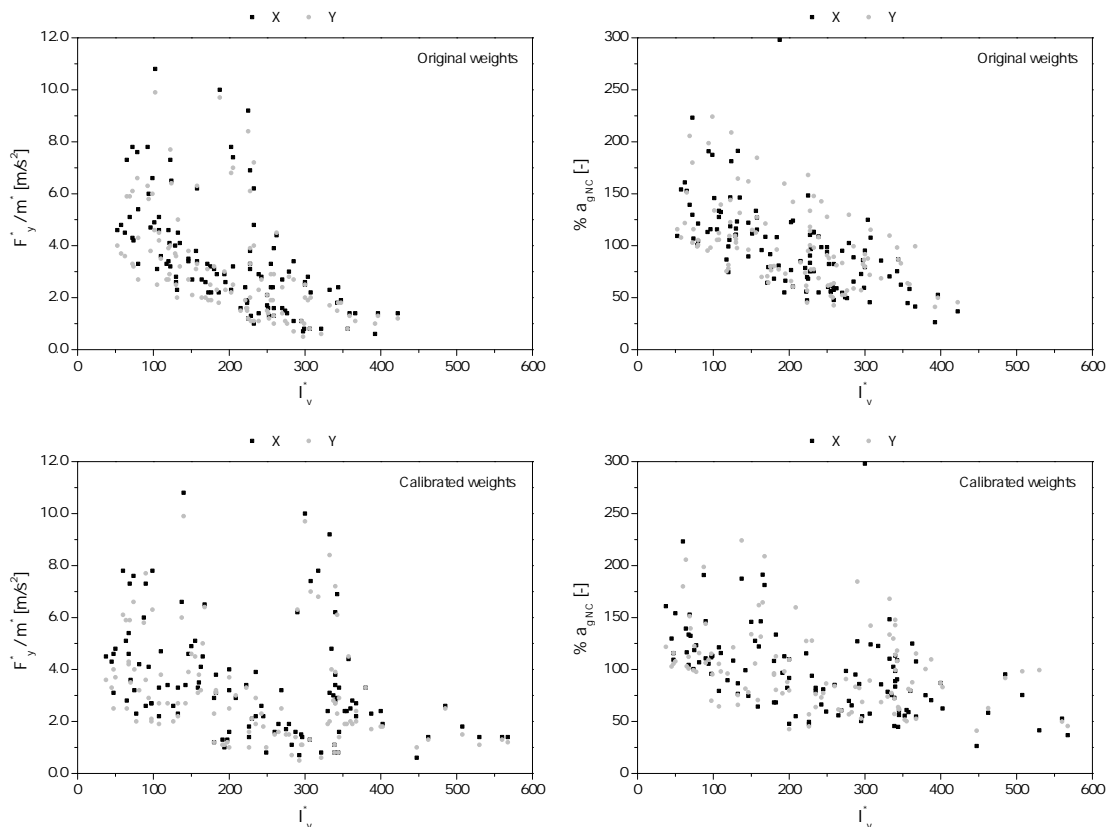
Figure 5.8: Scatter plot of the F^*_y/m^* and $\%a_{gNC}$ average values disaggregated for the X and Y direction, considering a random distribution for the soil type and both original [7] and calibrated [127] weights.

From observing Figure 5.8, it is possible to conclude that on the one hand, the acceleration at the yielding point, F^*_y/m^*, is slightly higher along the X direction, being the average deviation between the X and Y direction of about 11%. On the other hand, the acceleration ratio, $\%a_{gNC}$, is, on average, higher along the Y direction, with an average deviation between X and Y directions' average values of about 5%. If considering all the variables analysed, the yielding capacity, F^*_y, and the displacement at the NC limit state, d^*_{NC}, are those that show more significant deviations between the X and Y directions, 11% and 10%, respectively. The average deviations of the remaining variables are equal or lower than 5%.

Figure 5.9 presents the correlation between the same variables, this time disaggregating the sample by the number of storeys. As the vulnerability index, I^*_v, is not sensitive to the direction of the seismic action, in Figure 5.9, the average values between the X and Y direction are given. From Figure 5.9 it is possible to note that a higher dispersion in terms of both F^*_y/m^* and $\%a_{gNC}$ values, is generally observed in the case of 1- and 2-storey prototypes.
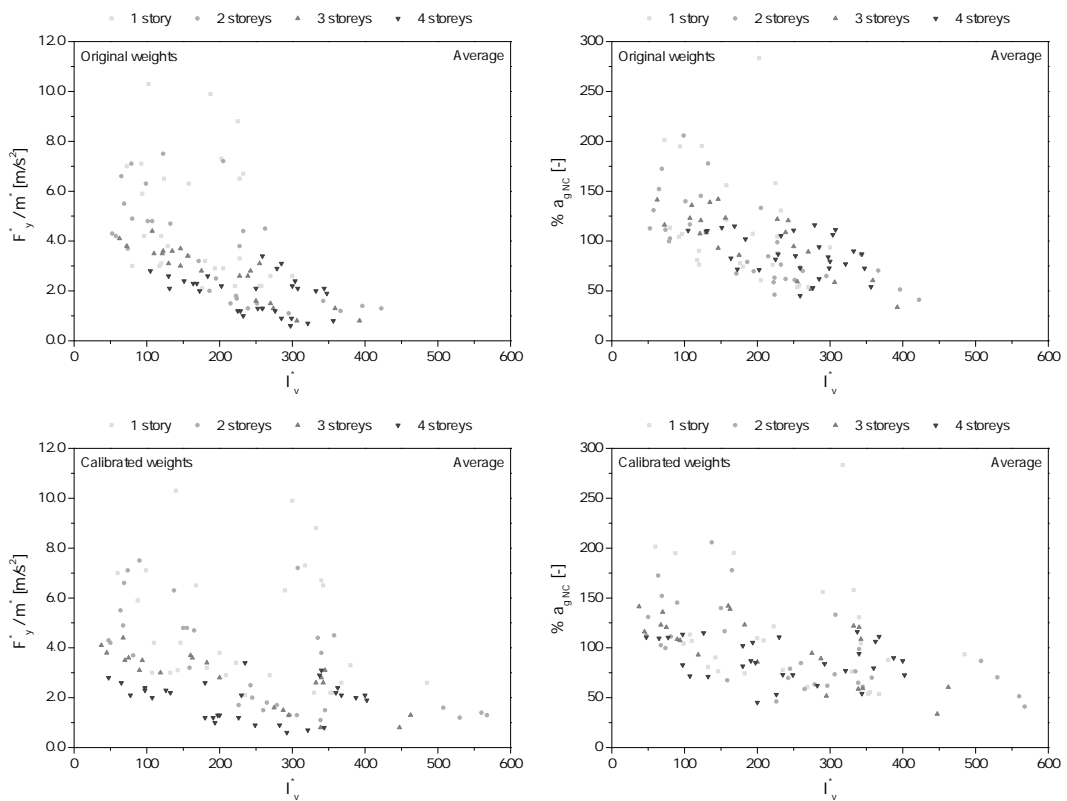
Figure 5.9: Scatter plot of the F^*_y/m^* (left) and $\%a_{gNC}$ (right) average values, considering a random distribution for the soil type, disaggregated in terms of number of storeys. While the upper row refers to the I^*_v values obtained by using the original weights [7], the lower row refers to those derived from the calibrated ones [9].

Figure 5.10 shows another possible disaggregation of the results, this time in function of the floor typologies considered. Similarly to the previous case, Figure 5.10 compares the results obtained by considering the original [7] and calibrated [127] weights, for the average values of the two main planar directions (X and Y) and a random distribution for the soil type. The scatter plots in Figure 5.10 clearly identify the different clusters of data as a function of

the floor typology. However, in global terms, the results derived from the numerical analyses are not in agreement with the respective vulnerability class definition (parameter P11). Even though this statement might need to be double-checked in future developments, the reason for this mismatch might be related to a inaccurate definition of the vulnerability class of parameter P11 in the first place, or to the lack of accuracy of the software on modelling not only the particularities of each floor typology, but also the interaction between horizontal and vertical elements, as initially suggested in Section 5.4.2.
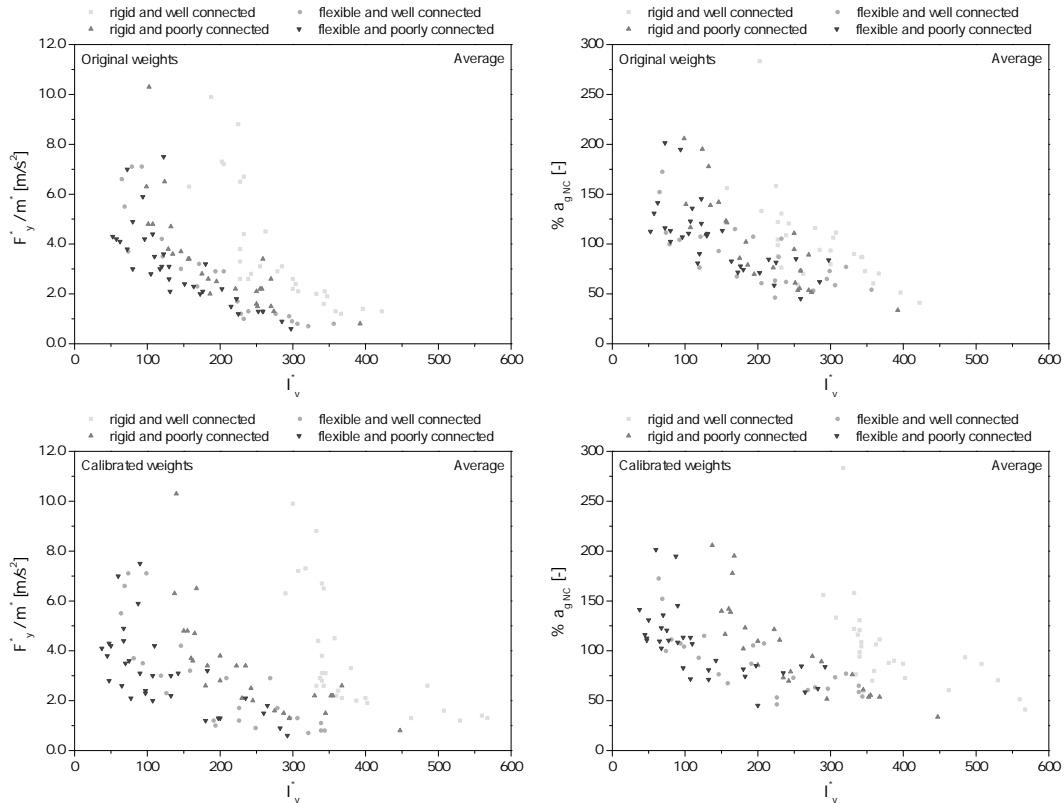
Figure 5.10: Scatter plot of the F^*_y/m^* (left) and $\%a_{gNC}$ (right) average values, considering a random distribution for the soil type and a disaggregation in terms of floor typology. While the upper row refers to the I^*_v values obtained by using the original weights [7], the lower row refers to those derived from the calibrated weights [9].

Figure 5.11 shows the scatter plots of the $\%a_{gNC}$ average values, considering the original weights [7] and different distributions for the soil type, disaggregated in terms of the number of storeys. Contrarily to prototypes with 1 and 2 storeys, the dispersion in terms of $\%a_{gNC}$ values in the case of 3 and 4 storeys is considerably smaller.

Finally, in Figure 5.12, the scatter plots for the average values of the same variables, F^*_y/m^* (left) and $\%a_{gNC}$ (right), are presented, considering the original weights [7] and a random distribution for the soil type. These results are disaggregated in terms of the number of storeys and type of curve fitting (linear, exponential and polynomial). Even though the goodness-of-fit of each regression curve is going to be discussed in the following Section 5.7.2, it is already possible to conclude that the polynomial fit is not indeed a reliable solution to describe the problem in hands, as in the initial branch of the curve (even if only for 1 storey buildings), $\%a_{gNC}$ increases proportionally to the increase of the I^*_v index.
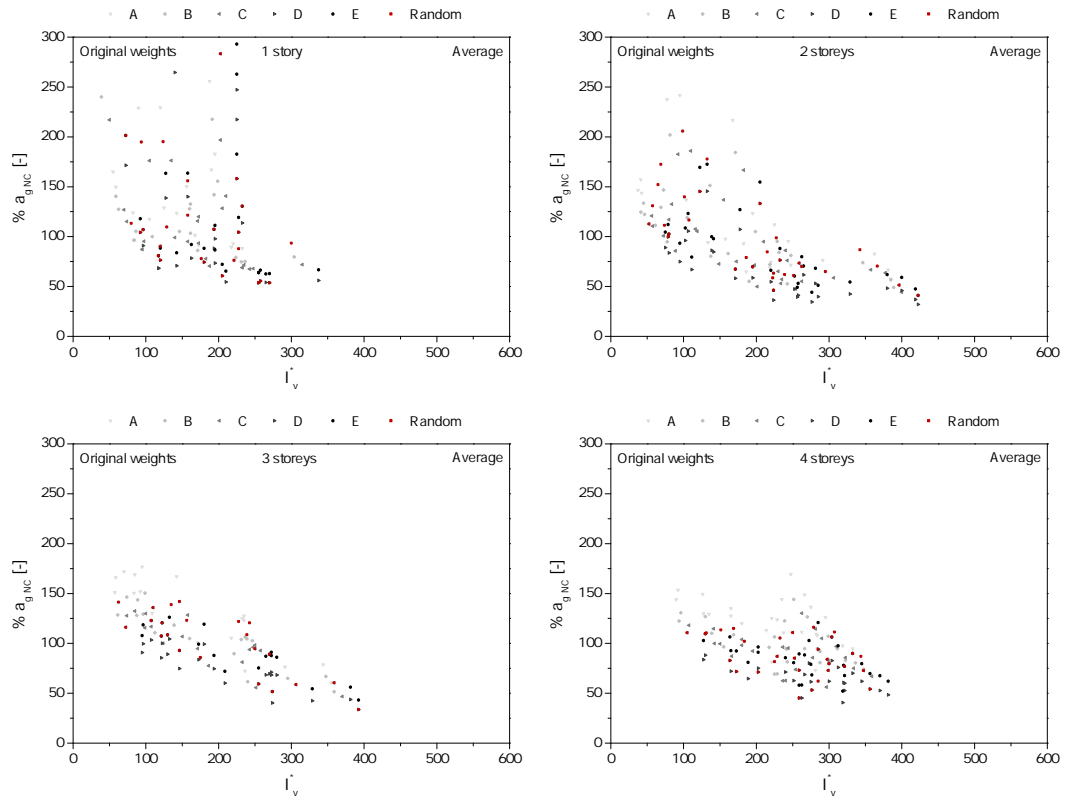
Figure 5.11: Scatter plot of the %a$_{gNC}$ average values, considering the original weights [7] and different distributions for the soil type, disaggregated in terms of number of storeys.

5.7.2 Statistical analysis

The following Table 5.4 summarises the average values of several numerical outputs, which resulted from the run of a set of 6 nonlinear static analysis in each direction and the subsequent application of the iterative procedure of the N2 Method, for each single model of the considered sample of 112 prototypes. These outputs, which are aggregated in terms of direction of the analysis and number of storeys, should be analysed with due care, because the features and properties defined in Section 5.4 and randomly assigned to each prototype, may vary significantly, even for the same loading direction and number of storeys. However, from analysing the results in Table 5.4, a few interesting remarks can be made. Firstly, it is possible to observe that in average, and as expected, the displacement capacity increases as we move from 1 to 4 storeys, regardless from the loading direction considered. To the contrary, the equivalent stiffness of the SDOF system, k*, as well as the yielding spectral acceleration of the SDOF system, F*$_y$/m*, decrease in height. If one compares the %a$_g$ with the structure's demand acceleration, a$_{gD}$, for each limit state, it is possible to observe that, in average, the majority of the prototypes verify the safety requirements imposed in the NP EN 1998-3 [166] in terms of acceleration (0.55, 0.89, and 1.22, respectively for the DL, SD and NC limit states). As highlighted in Table 5.4, the only exceptions are the prototypes with 3 and 4 storeys, which do not verify the SD limit state (in red).
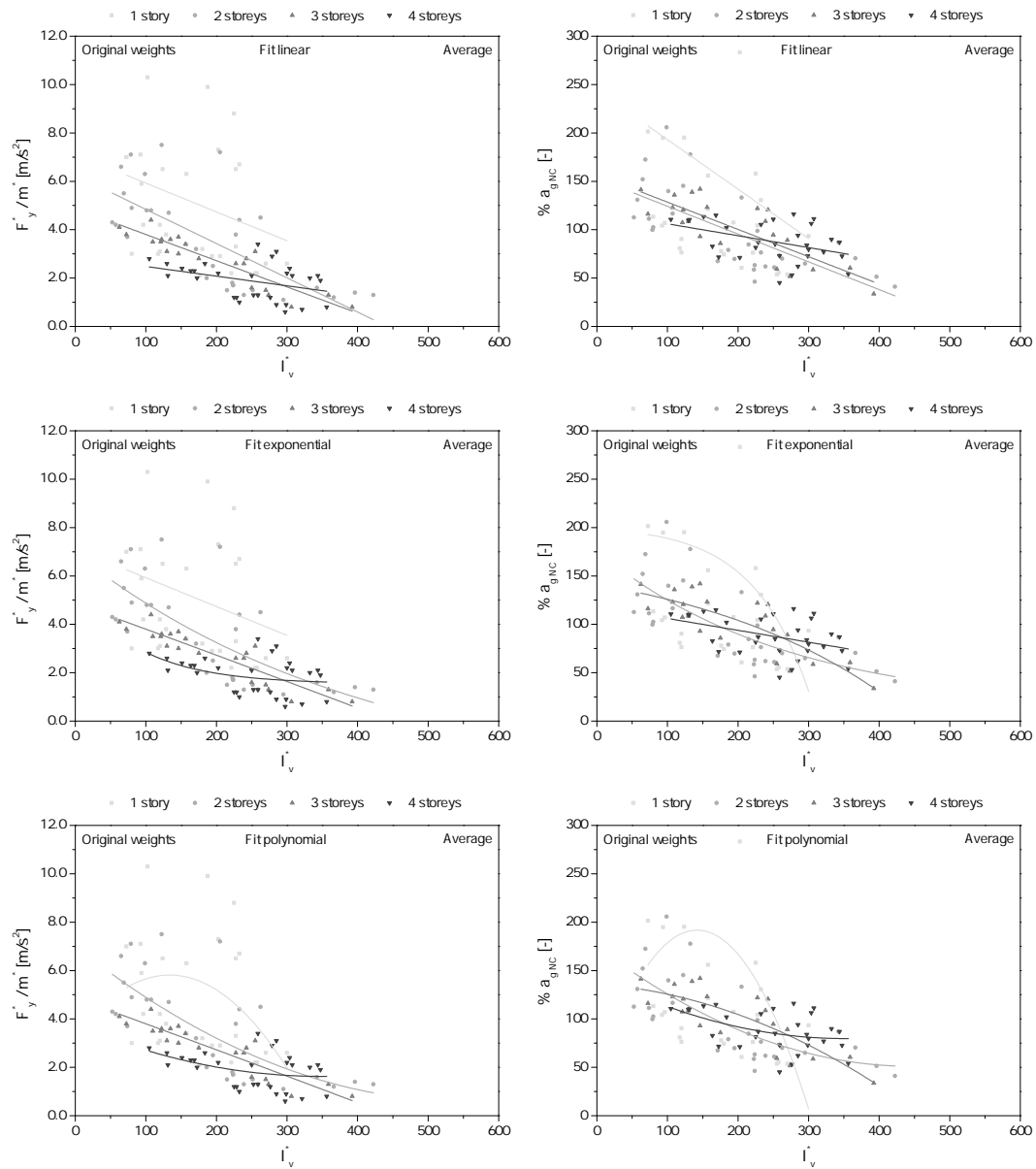
Figure 5.12: Scatter plot of the F^*_y/m^* (left) and $\%a_{gNC}$ (right) average values, considering the original weights [7] and a random distribution for the soil type. These results are disaggregated in terms of number of storeys and for different types of curve fitting.

Table 5.4: Average values obtained for each variable aggregated by direction of the analysis and number of storeys. Please note that the values coloured in green verify the respective limit state in terms of acceleration, while those in red don't.

Direction	Number of storeys	d^*_y [m]	F^*_y [kN]	d^*_{NC} [m]	k^* [kN m^{-1}]	F^*_y/m^* [m s^{-2}]	$\%a_{g\,DL}$ [–]	$\%a_{g\,SD}$ [–]	$\%a_{g\,NC}$ [–]
X	1	0.004	784.9	0.008	396511	5.53	102.4	121.9	171.5
	2	0.006	870.4	0.011	218780	4.07	77.7	89.7	124.6
	3	0.005	872.5	0.012	224936	3.21	64.1	80.4	129.1
	4	0.007	812.4	0.019	133414	2.26	56.1	72.6	122.9
	Av.	**0.006**	**833.2**	**0.013**	**243143**	**3.80**	**75.7**	**91.6**	**137.2**
Y	1	0.002	722.8	0.007	525772	5.08	103.1	132.3	210.1
	2	0.005	802.6	0.012	230942	3.73	73.9	89.2	133.7
	3	0.007	800.0	0.016	186731	2.88	65.0	83.6	137.8
	4	0.010	688.4	0.023	97728	1.88	57.4	73.2	122.4
	Av.	**0.006**	**750.9**	**0.015**	**262915**	**3.42**	**75.3**	**94.9**	**151.3**
Av.	1	0.003	753.9	0.008	461141	5.31	102.8	127.1	190.8
	2	0.006	836.5	0.011	224861	3.90	75.8	89.4	129.2
	3	0.006	836.3	0.014	205833	3.05	64.6	82.0	133.4
	4	0.009	750.4	0.021	115571	2.07	56.7	72.9	122.7
	Av.	**0.006**	**792.0**	**0.014**	**253029**	**3.61**	**75.5**	**93.3**	**144.2**

5.7.3 Curve fitting

In this subsection the goodness-of-fit is going to be evaluated and compared through the adjusted-R^2 values obtained for different curve-fitting models, disaggregating the data in function of the number of storeys and considering different distributions for the soil type. The use of the adjusted-R^2 is recommended when evaluating model fit and comparing alternative models. The main difference to the coefficient of determination, R^2, is that the adjusted-R^2 can evaluate the percentage of variation explained by only the independent variables that actually affect the dependent one.

The adjusted-R^2 values presented in the following Table 5.5 were computed for a set of 8 variables considering the original weights and a random distribution of the soil type. To have a better picture of which model provides the best fitting, the global average values (Av.), which were computed by aggregating the adjusted-R^2 values in function of each variable and number of storeys, are also given in Table 5.5 (in bold). If focusing on these values, it is possible to observe that the same trend was obtained in terms of number of storeys, regardless from the type of the curve fitting model considered (where the lower and higher adjusted-R^2 values are associated to buildings with 1 and 3 storeys, respectively). In general, the results obtained with the exponential curve fitting model presented the lowest average adjusted-R^2 values, and for this reason, the poorest fitting to the data. Even though this is, theoretically, a problem highly nonlinear, the average adjusted-R^2 values obtained for the linear curve fitting model are quite close to those obtained by the polynomial curve fitting model. In average, the lowest adjusted-R^2 values are associated with the displacement parameters, d^*_y and d^*_{NC}. Conversely, a better fit was observed for parameters associated with the stiffness and strength variables, such as F^*_y, m^*, and F^*_y/m^*.

In Figure 5.13, the average adjusted-R^2 values are plotted not only for each curve fitting model and soil type distribution but also for both original (left) and calibrated (right) weights. From Figure 5.13 (left), one can observe that the deviations between adjusted-R^2 values are

Table 5.5: Example of the obtained adjusted-R^2 values for a random distribution of the soil type and considering the original weights [7].

Curve fitting model	Number of storeys	d^*_y	F^*_y	d^*_{NC}	k^*	F^*_y/m^*	$\%a_{gDL}$	$\%a_{gSD}$	$\%a_{gNC}$	**Av.**
Linear	1	0.091	0.070	-0.023	0.210	0.031	0.053	0.044	0.015	**0.061**
	2	-0.009	0.388	0.032	0.229	0.485	0.546	0.547	0.482	**0.337**
	3	0.370	0.618	0.194	0.574	0.824	0.499	0.587	0.640	**0.538**
	4	0.249	0.279	0.085	0.388	0.107	-0.024	0.025	0.155	**0.158**
	Av.	**0.175**	**0.339**	**0.072**	**0.350**	**0.362**	**0.268**	**0.301**	**0.323**	0.274
Exponential	1	0.152	0.038	0.061	0.224	0.027	0.038	0.035	0.017	**0.074**
	2	-0.003	0.385	0.018	0.205	0.481	0.600	0.587	0.495	**0.346**
	3	0.340	0.603	0.185	0.602	0.815	0.502	0.594	0.644	**0.536**
	4	0.229	0.296	0.058	0.421	0.086	-0.042	0.005	0.139	**0.149**
	Av.	**0.158**	**0.338**	**0.021**	**0.366**	**0.344**	**0.257**	**0.292**	**0.313**	0.261
Polynomial	1	0.115	0.035	-0.072	0.223	-0.007	0.017	0.008	-0.002	**0.040**
	2	-0.049	0.381	-0.071	0.203	0.478	0.594	0.580	0.489	**0.326**
	3	0.339	0.602	0.172	0.592	0.815	0.492	0.591	0.642	**0.531**
	4	0.229	0.333	0.057	0.447	0.090	-0.075	-0.011	0.124	**0.149**
	Av.	**0.180**	**0.331**	**0.080**	**0.363**	**0.352**	**0.274**	**0.305**	**0.324**	**0.276**

lower when assuming a random distribution of soil type (presented in the previous Table 5.4). Moreover, the results in Figure 5.13 (left) also show that the exponential curve provides the worst fit, regardless of the soil type distribution considered. When looking at the results obtained in the case of the calibrated weights, in Figure 5.13 (right), the variation of the average adjusted-R^2 values according to each soil type distribution, is higher. It is interesting to observe that, on average, the highest values of adjusted-R^2 were obtained for a soil type C, which represents the average soil type for the island of Faial. Another interesting observation is that, contrarily to what was found in the case of Figure 5.13 (left), when using calibrated weights, the trend in terms of goodness-of-fit of the different curve-fitting models is no longer straightforward.
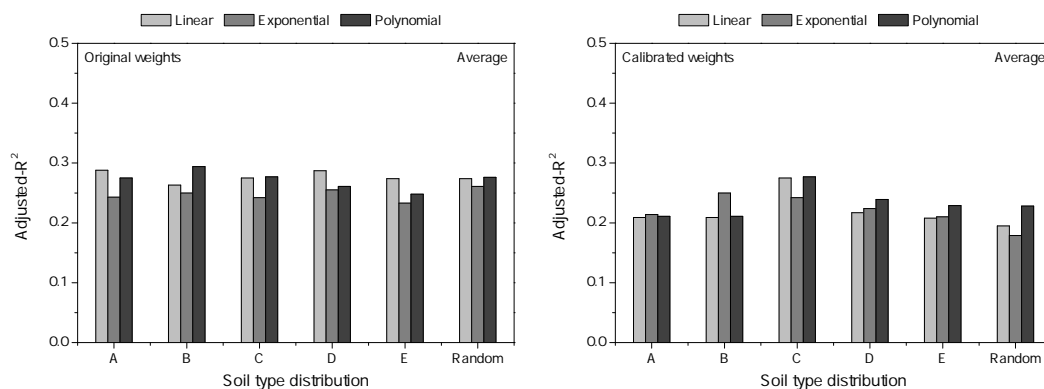
Figure 5.13: Comparison of the average adjusted-R^2 values obtained for each curve fitting model and soil type distribution, considering both original [7] (left) and calibrated weights [127] (right).

5.8 Application example

In this subsection, the full potential of the idealised approach is going to be demonstrated and applied to the same case studies analysed in Section 4.2, and illustrated in Figure 5.14. Since the volume of case study D exceeds by a large margin the average volume of the prototypes idealised in the sample of 112 models, a fifth case study, E, was considered as the result of the disaggregation of case study D into two separate structures.
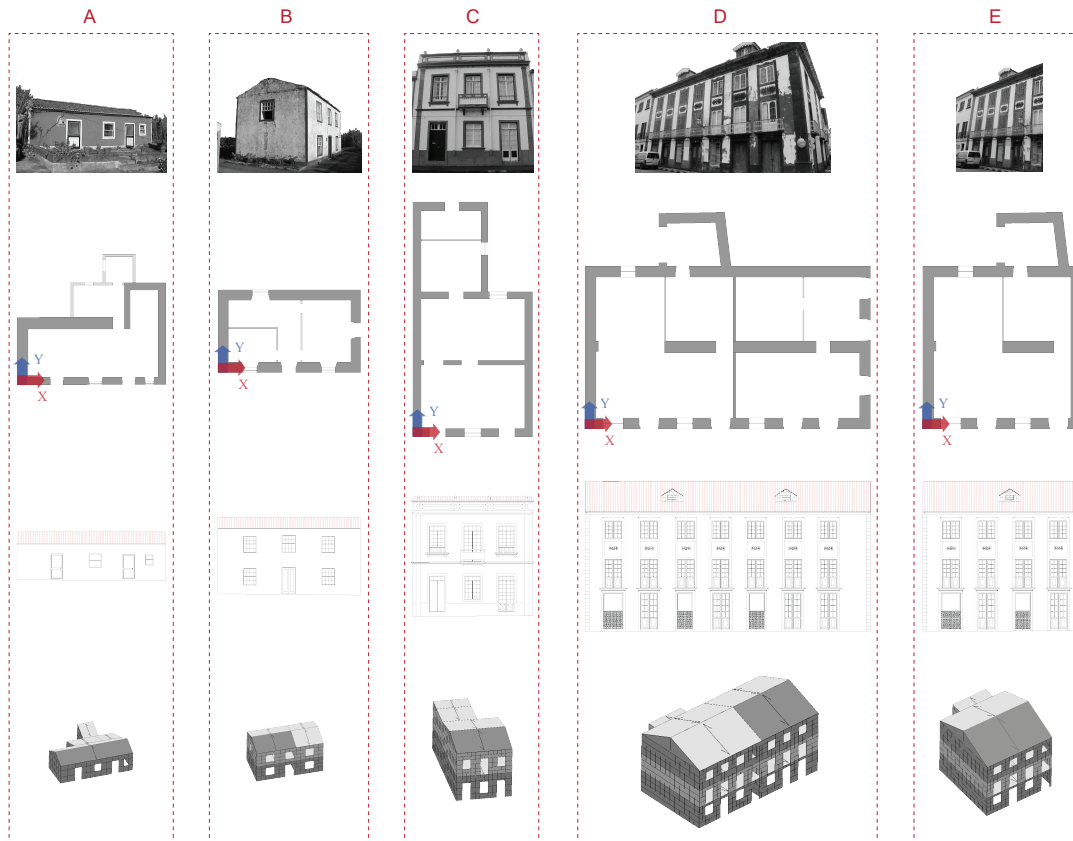
Figure 5.14: Overview of the geometry and building typology of each case study (from A to E): ground floor plans and the respective main façade elevations. Please note that traditional stone masonry elements are coloured in grey, while masonry brick blocks are coloured in light grey. Moreover, the reference axes (X and Y) considered throughout this section for each model are identified in the respective ground floor plans.

In a first phase, the vulnerability index, I^*_v, was determined, following the same assumptions and considerations described in Section 5.4. The bar chart presented in Figure 5.15 (left) compares the I^*_v value estimated to each case study, with that corresponding to the average of the generated sample of 112 prototypes (equal to 184.2). According to these results, it is possible to conclude that the I^*_v of case studies C, D and E, are quite close to the average value of the generated sample of 112 prototypes. Conversely, the I^*_v value of case studies A and B is far off from that obtained for the average of the 112 prototypes. This shows that, in terms of I^*_v, case studies A and B are less representative of the vulnerability index associated with the average prototype's building typology.

Subsequently, the expected value of each output variable was determined from the ana-

lytical expressions derived from the linear curve fitting process discussed in Section 5.7.3 for a soil type C, the respective number of storeys, and for the original weights of the vulnerability index method [7].
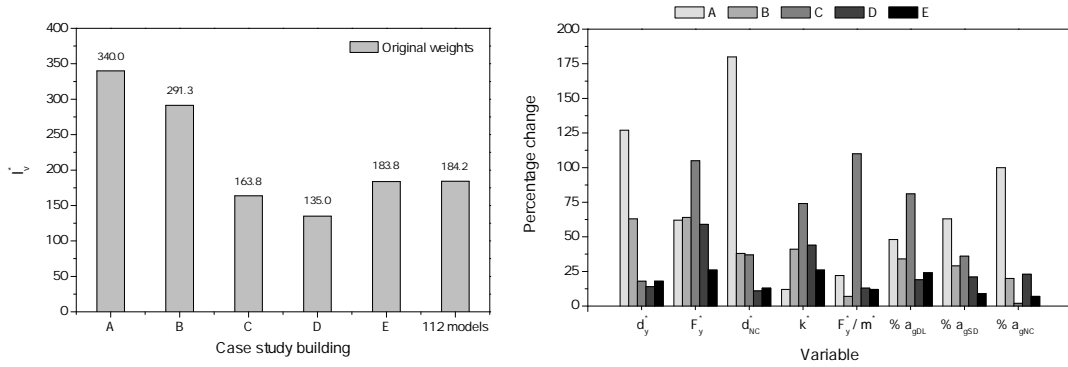
Figure 5.15: Vulnerability index values, I^*_v, estimated for each case study building (upper row) and the percentage change between the numerical and the expected values for each variable considered (bottom row), by using the original weights proposed in [7] and assuming a soil type C.

The case studies were then modelled according to their geometry and by following the same considerations and procedure as in Section 5.5. Nonlinear static analyses were performed, and the iterative procedure of the N2 Method was applied to determine the numerical values of each output variable. Both expected and numerical values of variables F^*_y/m^* and $\%a_{gNC}$, are compiled in the following Table 5.6, together with the respective parameters b (y-intercept) and m (slope), from the linear analytical expression in a slope-intercept form. The numerical values are, in fact, median values, as they result from the set of pushover analyses carried out for the positive and negative directions of the main planar directions X and Y, considering a uniform load pattern distribution and both positive and negative accidental eccentricity (in a total of 12 analyses for each model).

Table 5.6: Expected and numerical values for variables F^*_y/m^* and $\%a_{gNC}$, estimated for each case study building. These values were derived from the respective linear regression models considering a soil type C, the respective number of storeys, and for the original weights of the vulnerability index method [7].

Variable	Parameter	Case study building				
		A	B	C	D	E
I^*_v	–	340.0	291.3	163.8	135.0	183.8
F^*_y/m^*	y-intercept, b	5.520	5.660	5.660	4.076	4.076
	Slope, m	-0.002	-0.009	-0.009	-0.006	-0.006
	Expected value	**4.9**	**3.1**	**4.2**	**3.2**	**2.9**
	Numerical value	**4.0**	**2.9**	**2.0**	**2.8**	**2.6**
$\% a_{gNC}$	y-intercept, b	174.1	140.8	140.8	145.7	145.7
	Slope, m	-0.057	-0.167	-0.167	-0.180	-0.180
	Expected value	**154.5**	**92.0**	**113.4**	**121.4**	**112.7**
	Numerical value	**77.3**	**76.9**	**115.9**	**99.0**	**121.2**

According to the values presented in Table 5.6, the highest deviations between the expected and numerical values were observed for case studies A and C, in the case of F^*_y/m^*. In the case of $\%a_{gNC}$, the highest deviations were found for case studies A, B and D.

The comparative analysis of the deviations found between expected and numerical values was extended to the set of the 8 variables in the following Figure 5.15 (right), by evaluating the percentage change. Again, these results were computed by assuming the original weights of the vulnerability index formulation proposed by Vicente [7] and a soil type C. From this figure, it is possible to observe that, in overall terms, and to the exception of stiffness and strength variables (k^*, F^*_y, F^*_y/m^*), the highest percentage change values were observed to case study A. In the case of stiffness and strength variables, the highest percentage change values were observed to case study C. On the one hand, if considering the average of all case studies, the highest percentage changes are associated to variables d^*_y, F^*_y and d^*_{NC}. On the other hand, the lowest percentage changes are associated, in general, to variables F^*_y/m^*, $\%a_{gSD}$ and $\%a_{gNC}$.

5.9 Final remarks

In this chapter, a new hybrid approach for the seismic risk assessment of UCH assets within historic centres was investigated. This approach attempted to revert the original use of the vulnerability index method developed by Vicente [7], in which the analytical expression proposed in [82] is generally used to correlate hazard with the mean damage grade. In a first phase, the main particularities of the vulnerability index method were discussed, as well as the drawbacks commonly associated with the current use of this macroseismic approach. In a second phase, the strategy adopted to establish the dependencies between the parameters of the vulnerability index method and the numerical models, was explained. The discussion of the results was carried out by first analysing the scatter plots for each parameter of the capacity curve and seismic performance-based assessment, versus the vulnerability index values, and secondly, the goodness-of-fit of different curve fitting models, through the comparison of the respective adjusted-R^2 values.

This exercise has validated the original use of the vulnerability index method, that of ranking the seismic vulnerability of existing UCH assets within the same building typology. However, when reverting the use of the vulnerability index method by replacing the Macroseismic Intensity by a response spectrum, the results were not as interesting as initially expected, since the correlations between the vulnerability index and the main properties of the capacity curves derived from numerical models, presented, generally, a poor fitting. For this reason, these results must be understood with due care and diligence.

There are several possible causes for such poor fitting. Firstly, one should acknowledge that the formulation behind the vulnerability index method might need to be revised or upgraded, in order to overcome some limitations already identified in this chapter, such as the eventual inaccuracy on the definition of the vulnerability class of parameter P11, for example. Secondly, the mismatch between these results might be related to the software code herein used to compute the capacity curves. As demonstrated in Table 5.4, the worst correlations were observed, in general, for the variables associated with the displacement capacity. Numerical instability issues or the development of local mechanisms that might have occurred in some cases, which in turn, might have anticipated the achievement of the stopping criteria recommended in current seismic codes for the computation of nonlinear

static analyses, and therefore, compromised the global response of a given building. For this reason, this exercise should be cross-validated in future by using a different software code or numerical model of similar simplicity. In addition to the previous causes, the use of the analytical expression proposed by Bernardini et al. [82] might also be responsible for such poor fitting. Furthermore, and as initially suspected, the consideration of a constant value for the ductility factor, Q, is also very arguable. This is indeed, an aspect of great interest that shall be also addressed in future developments. Lastly, one should keep in mind the possibility of "no correlation" between the vulnerability index method and the results derived from nonlinear static procedures.

As a final comment, this study demonstrated the potential of such type of approach, hoping that, in the near future, a new methodology for the seismic risk assessment of UCH assets within historic centres can be developed and validated by extending the current sample, cross-checking these results with those obtained with different numerical models, and eventually using more sophisticated tools for the identification of data clusters.

Chapter 6

Conclusions and future developments

Abstract *This final chapter summarises the key conclusions that have been pointed out in the previous chapters of the thesis and outlines the grounds of future developments and research paths.*

Chapter outline

6.1 Summary of the main conclusions

The main conclusions of each chapter of this thesis are going to be now summarised in the following subsections.

6.1.1 Literature review

Having in mind the literature review on earthquake risk mitigation of UCH assets, presented in Chapter 2, it is worth highlighting the following conclusions:

- From a policy-driven and decision-making viewpoint, the protection of UCH assets should be based on a comprehensive knowledge of earthquake risk in order to define more proficient mitigation strategies and outline strengthening interventions that can possibly contribute to the reduction of their specific vulnerability and, consequently, for the increase of the overall urban resilience of historic centres;

- The need for a common approach and adequate recommendations for the structural assessment of UCH assets should be further considered a must-need priority;

- From the risk modelling viewpoint, if on the one hand it is fundamental to address uncertainties and inconsistencies often concealed in estimations, avoiding this way the

dissemination of erroneous conclusions and biased results, on the other hand, it is not less important that risk intensity measures and indicators can be easily understood and interpreted not only by governing and civil protection authorities, but also by stakeholders and citizens.

6.1.2 Seismic response assessment

In what concerns to the seismic response assessment of UCH assets, addressed in Chapter 3, it is important to highlight the following conclusions:

- As explained in Section 3.1, in the context of historic centres, survey operations are particularly difficult to handle due to several inherent uncertainties. Therefore, the need for a specific survey and investigation plan is of great importance for the effectiveness of conservation interventions in terms of structural and seismic safety. By doing so, one is not only contributing for a more reliable and accurate assessment of the seismic response of UCH assets located in historic centres, but also supporting the documentation and recording of UCH assets, whose building techniques and materials, that are an inexorably part of our tangible and intangible cultural heritage, are being lost at a pace as never seen before;

- The comparison of different macroelement approaches in Section 3.2 has confirmed that the selection of a numerical tool for the seismic response assessment of unreinforced masonry structures is indeed a very complex and often non-consensual task that should be supported by weighing several aspects, namely the compatibility between the analysis tool and the study object, the type and the amount of input data, as well as the financial resources available and eventual time constraints. Associated with these aspects, a deep knowledge of the main features and drawbacks of each model, as well as the end-user ability to critically analyse the quality of both input and output data, is also highly recommendable to guarantee the efficiency of the analysis and the reliability of the results;

- Good-judgement capacity and utmost care on interpreting the results provided by analytical methods should be key skills for the new generation of structural engineers. This is of paramount importance given the new arrangement applicable to the renovation of existing buildings and building units [58], namely after the approval of the Ordinance no. 302/2019 [59], that, as mentioned before, defines not only the terms in which the seismic vulnerability of existing buildings must be or not evaluated and reported, but also the terms where seismic retrofitting or strengthening is required. Therefore, critically analysing and double-checking outputs by considering different modelling assumptions or even different analytical methods, and not just simply accept them blindly or as an absolute truth, is now more important than never;

- In addition to the results provided by these simplified models, and from the seismic safety viewpoint, it is essential to extend the assessment with complementary approaches at the local level, particularly when dealing with UCH assets with flexible diaphragms and of complex geometry. In this sense, understanding the potential and limitations of different models and software codes currently available for the seismic vulnerability assessment of UCH assets is fundamental to promote a more informed decision not only on the type of software that could possibly serve the best interest

of end-users and stakeholders, but also represent in a more accurate way, the actual response and the particularities of each case study in hands;

- It is important to stress out that the use of models based on macroelements, despite the limitations and assumptions herein identified and discussed, still offers a very interesting compromise between computational effort and accuracy on the estimation of the nonlinear response of existing masonry buildings, being recommendable, with due diligence, also in the case of UCH assets.

6.1.3 Cost-benefit analyses

The most important conclusions regarding the cost-benefit analyses carried out in Chapter 4, are highlighted below:

- The preconceived idea that investing in strengthening strategies to reduce the seismic vulnerability of UCH assets is extremely costly, was demystified in Section 4.1. In fact, the results obtained proved not only that this investment is easily dissolved in the total renovation costs, but also the implementation of such strategies have a major impact on the reduction of damage and losses in the event of an earthquake;

- The repair costs associated with interventions strategies implemented by preserving traditional construction techniques and materials, resulted, in the majority of the scenarios considered, quite attractive from the economic viewpoint. According to these results, it is more likely that the costs associated with seismic strengthening may become even more dissolved when operating in UCH assets;

- It is believed that the functions herein proposed can be used to derive rough estimates of repair costs for similar building typologies and different scenarios in Azores. However, it is important to stress these results require further validation with current intervention costs practiced in different regions of Portugal. Moreover, the repair cost functions derived from the Faial database might be extremely useful for academic purposes and studies to come, as well as to raise the awareness of all stakeholders involved in the renovation process of our building stock (from property owners to policy makers) to the importance of integrating seismic strengthening design into the structural project, and the consequences of not doing so;

- Despite the definition and valuation of built heritage is always arguable since it is ultimately shaped by both individual perception and social interaction, which is constantly evolving over time, it is up to conservators and heritage professionals to raise their voices for the protection of traditional construction techniques and materials in UCH assets, as part of the cultural identity of our historic centres. It is therefore necessary not only to conduct nation-wide operations on documenting and cataloguing these techniques and materials, but also to raise the society's awareness and consciousness for the value of cultural heritage and to the consequences of its loss;

- The cost-benefit analyses carried out in Section 4.2, demonstrated that, in general, the use of the traditional seismic retrofitting strategies, allowed, indeed, to the improvement of the seismic performance of this specific building typologies;

- It was demonstrated that the cost of application of traditional retrofitting strategies does not embody a significant weight over the total replacement cost, that could possibly turn the use of these strategies economically unviable;

- Another interesting conclusion has to do with the large dispersion of the results, as a consequence of considering in the analyses, aspects such as the type of lateral load pattern distribution (uniform and pseudo-triangular), accidental eccentricity, or loading direction, for example;

- For the great majority of the cases analysed, the use of traditional seismic retrofitting strategies show a quite satisfactory benefit-cost ratio, being for this reason recommendable for both rural and urban building stock of Faial Island. In particular, the consolidation of the horizontal structure has proved to be the most attractive strategy for all the case studies if exclusively focusing on the benefit-to-cost ratio value. However, and unexpectedly, this attractiveness was not echoed in terms of seismic performance upgrading. This fact broaches the subject of how the formulation of horizontal diaphragms in this type of software codes should be revised or adapted in order to enhance the compatibility between numerical models and the values recommended by the NZSEE guidelines for flexible diaphragms;

- Replacement costs associated with the use of traditional materials and building techniques were, in general, lower than those associated with current construction. For this reason, higher benefit-cost ratios were obtained in the first case. This finding constitutes, therefore, a great incentive for promoting the proper renovation of UCH assets particularly for the building stock of Faial Island.

6.1.4 Casting a new light on the seismic risk assessment of historic centres

Finally, in what regards the investigation of a new hybrid approach for the seismic risk assessment of stone masonry buildings within historic centres, carried out in Chapter 5, it is worth highlighting the following conclusions:

- This exercise has validated the original use of the vulnerability index method, that of ranking the seismic vulnerability of existing UCH assets within the same building typology. However, when reverting the use of the vulnerability index method by replacing the Macroseismic Intensity by a response spectrum, the results were not as interesting as envisaged, since the correlations between the vulnerability index and the main properties of the capacity curves derived from numerical models, presented, generally, a poor fitting;

- There are several possible causes for this generalised poor fitting. Firstly, one should acknowledge that the formulation behind the vulnerability index method might need to be revised or upgraded, in order to overcome some limitations already identified in this chapter, such as the eventual inaccuracy on the definition of the vulnerability class of parameter P11, for example. Secondly, the mismatch between these results might be related to the software code herein used to compute the capacity curves. Numerical instability issues or the development of local mechanisms might anticipate the achievement of the stopping criteria recommended in current seismic codes for the computation of nonlinear static analyses, and compromise the global response

of a given building. Lastly, it should be also considered that the "no correlation" possibility, could be also a valid outcome, suggesting the unlikelihood of the considered vulnerability index method being correlated with the results derived from nonlinear static procedures.

6.2 Future developments

It is known that in most of research projects, the number of ideas and alternative paths increases proportionally in time. Moreover, time constraints often dictate to what extent the investigation of alternative paths might be included in the initial research path. As a result, several ideas, variants, and further validation processes, end up not being addressed or investigated as they should. Instead, these are usually highlighted as future developments. Hence, the most relevant suggestions for future developments are identified in the following paragraphs.

With respect to Section 3.1, further research and guidelines on how to address the "aggregate" effect in the seismic assessment of UCH assets are necessary. Moreover, the list of current investigation techniques presented should be updated and upgraded in order to include more information and more reliable data, namely in what concerns average costs (also for different countries). As for Section 3.2 the results obtained by using these macroelement models, should be compared in future works to different numerical models, either of higher or lower complexity. Ideally, this exercise should be carried out not only by comparing different approaches for the nonlinear response assessment of masonry structures, but also by using a case study from which reliable experimental data is available, so that the subsequent numerical models can be properly calibrated.

In what regards the study carried out in Section 4.1, the consideration of the uncertainties associated with the quantification of strengthening costs is one of the issues to be addressed in future developments. Additionally, it would be interesting to bring the costs associated to the patrimonial value of UCH assets into discussion, which alone would practically require an independent investigation. This issue, often disregarded or lightly addressed in literature, is indeed of great relevance for a more accurate evaluation of economic losses caused by both natural or man-made disasters.

In Section 4.2, it is suggested that the improvement of the connections between horizontal diaphragms and load-bearing walls could be numerically investigated more in detail, so that the seismic performance upgrading in the numerical models can result more approximated to the expected contribution of such retrofitting strategy. Additionally, the current formulation of horizontal diaphragms used by the software codes herein analysed, which are based on the macroelement approach, should be revised or adapted, in order to improve the compatibility between numerical models and the values recommended by the NZSEE guidelines for flexible diaphragms.

Finally, with respect to Chapter 5, extending the sample size considered, cross-checking the results by using different numerical models or even using more sophisticated tools for the identification of data clusters, are some of the possible future developments. Moreover, in future developments, the strategy adopted in this first attempt of drafting a new hybrid method for the seismic risk assessment of UCH assets within historic centres, should be revised and improved.

Bibliography

[1] Azzaro R., Tertulliani A., Bernardini F., Camassi R., Del Mese S., Ercolani E., Graziani L., Locati M., Maramai A., Pessina V., Rossi A., Rovida A., Albini P., Arcoraci L., Berardi M., Bignami C., Brizuela B., Castellano C., Castelli V., D'Amico S., D'Amico V., Fodarella A., Leschiutta I., Piscini A., and Sbarra M. The 24 august 2016 amatrice earthquake: Macroseismic survey in the damage area and EMS intensity assessment. *Annals of Geophysics*, 59(Fast Track 5):1–8, 2016. URL `http://hdl.handle.net/2122/11439`.

[2] Guidetti M. and S. Perini. Civil war and cultural heritage in Syria, 2011 - 2015. *Syrian Studies Association Bulletin*, 20(1):42, 2015. URL `https://ojcs.siue.edu/ojs/index.php/ssa/article/view/3115`.

[3] Silva V. *Development of open models and tools for seismic risk assessment: Application to Portugal*. Ph.D. thesis, Department of Civil Engineering of the University of Aveiro, 2013. URL `http://ria.ua.pt/handle/10773/11948`.

[4] Mota de Sá F. *Seismic risk - New instruments for analysis and communication*. Ph.D. thesis, School on Engineering (IST) of the University of Lisbon, 2016.

[5] Giovinazzi S. *The vulnerability assessment and the damage scenario in seismic risk analysis*. Ph.D. thesis, Technical University Carolo–Wilhelmina in Braunschweig and University of Florence, 2005.

[6] Abbas N., Calderini C., Cattari S., Lagomarsino S., Rossi M., Corradini R. Ginanni, Marghella G., and Piovanello V. Deliverable D4. Classification of the cultural heritage assets , description of the target performances and identification of damage measures. Technical report, PERPETUATE PERformance-based aPproach to Earthquake proTection of cUlturAl heriTage in European and mediterranean countries, FP7 - Theme ENV.2009.3.2.1.1 - Environment. Grant agreement no. 244229, 2010.

[7] Vicente R. *"Estratégias e metodologias para intervenções de reabilitação urbana - Avaliação da vulnerabilidade e do risco sísmico do edificado da baixa de Coimbra"*. Ph.D. thesis, Department of Civil Engineering of the University of Aveiro, 2008. URL `http://hdl.handle.net/10773/2410`. (in Portuguese).

[8] Maio R., Ferreira T.M., Vicente R., and Estêvão J.M.C. Seismic vulnerability assessment of historical urban centres: case study of the old city centre in Faro, Portugal. *Journal of Risk Research*, 19(5): 551–580, 2016. URL `http://www.tandfonline.com/doi/abs/10.1080/13669877.2014.988285#.VMka58ZgjKM`.

[9] Ferreira T.M., Maio R., and Vicente R. Seismic vulnerability assessment of the old city centre of Horta, Azores: Calibration and application of a seismic vulnerability index method. *Bulletin of Earthquake Engineering*, 15(7):2879–2899, 2017. URL `https://link.springer.com/article/10.1007/s10518-016-0071-9`.

[10] Vicente R., Ferreira T.M., Maio R., Costa A., Costa A.A., Oliveira C.S., Varum H., and Estêvão J.M.C. *"URBSIS - Avaliação da vulnerabilidade e gestão do risco sísmico à escala urbana"*. Tipografia Lusitânia, Aveiro, Portugal, 2016. ISBN 978-989-20-6667-7. (in Portuguese).

[11] Ortega J. *Seismic vulnerability of vernacular architecture*. Ph.D. thesis, Department of Civil Engineering of the University of Minho, 2018.

[12] S.T.A. DATA. *3Muri program: Seismic analysis program for 3D masonry buildings*. Release 12.0.0.0, Turin, Italy, 2019. URL `http://www.stadata.com`. User Manual.

[13] Gruppo Sismica Srl. *3D-Macro, "Il software per le murature"*. Release 4.3.7, Catania, Italy, 2017. URL `http://www.stadata.com`. User Manual (in Italian).

[14] Vicente R., S. Parodi, Lagomarsino S., Varum H., and Mendes da Silva J.A.R. Seismic vulnerability and risk assessment: Case study of the historic city centre of Coimbra, Portugal. *Bulletin of Earthquake Engineering*, 9(4):1067–1096, 2011. URL `https://link.springer.com/article/10.1007/s10518-010-9233-3`.

[15] Fajfar P. Capacity spectrum method based on inelastic demand spectra. *Earthquake Engineering and Structural Dynamics*, 28(9):979–993, 1999. URL `https://doi.org/10.1002/(SICI)1096-9845(199909)28:9<979::AID-EQE850>3.0.CO;2-1`.

[16] Maio R., Ferreira T.M., and Vicente R. The use of macro-element approach for the seismic vulnerability assessment of stone masonry buildings. In *Proceedings of the 3rd International Conference on Protection of Historical Constructions*, 12–15 July, Lisbon, Portugal, 2017.

[17] World Bank. Cultural heritage and development - A framework for action in the Middle East and North Africa. Technical report, The World Bank, Orientations in Development Series, Middle East and North Africa region, Washington DC, United States of America, 2001.

[18] Dalmas L., Geronimi V., Noël J.F., and Tsang King Sang J. Economic evaluation of urban heritage: An inclusive approach under a sustainability perspective. *Journal of Cultural Heritage*, 16(5):681–687, 2015. URL `https://doi.org/10.1016/j.culher.2015.01.009`.

[19] UNESCO. New life for historic cities: The historic urban landscape approach explained. Technical report, United Nations Educational, Scientific and Cultural Organization, Paris, France, 2013.

[20] Agapiou A., Alexakis D.D., Lysandrou V., Sarris A., Cuca B., Themistocleous K., and Hadjimitsis D.G. Impact of urban sprawl to cultural heritage monuments: The case study of Paphos area in Cyprus. *Journal of Cultural Heritage*, 16(5):671–680, 2015. URL `https://doi.org/10.1016/j.culher.2014.12.006`.

[21] United Nations. World urbanization prospects: The 2014 revision. Technical report, United Nations, United Nations Department of Economic and Social Affairs/Population Division, New York, United States of America, 2014.

[22] Blanco I., Bonet J., and Walliser A. Urban governance and regeneration policies in historic city centres: Madrid and Barcelona. *Urban Research and Practice*, 4(3):326–343, 2011. URL `https://doi.org/10.1080/17535069.2011.616749`.

[23] Maio R., Ferreira T.M., and Vicente R. The morphology of old urban centres: Architectural and constructive survey of Bairro Ribeirinho of Faro, Portugal. *Conservar Património*, 21(5–24):1–20, 2015. URL `http://revista.arp.org.pt/pdf/2015002.pdf`.

[24] Laprise M., Lufkin S., and Rey E. An indicator system for the assessment of sustainability integrated into the project dynamics of regeneration of disused urban areas. *Building and Environment*, 86:29–38, 2015. URL `http://dx.doi.org/10.1016/j.buildenv.2014.12.002`.

[25] Radoslav R., Branea A.M., and Găman M.S. Rehabilitation through a holistic revitalization strategy of historical city centres - Timisoara, Romania. *Journal of Cultural Heritage*, 14(3):1–6, 2013. URL `http://dx.doi.org/10.1016/j.culher.2012.11.031`.

[26] Jigyasu R. and Arora V. Disaster risk management of cultural heritage in urban areas - A training guide. Technical report, Research Center for Disaster Mitigation of Urban Cultural Heritage, Ritsumeikan University (RitsDMUCH), Kyoto, Japan, 2014.

[27] UNESCO. Managing disaster risks for world heritage. Technical report, United Nations Educational, Scientific and Cultural Organization, Paris, France, 2010.

[28] Wang J.J. Flood risk maps to cultural heritage: Measures and process. *Journal of Cultural Heritage*, 16(2):210–220, 2015. URL http://dx.doi.org/10.1016/j.culher.2014.03.002.

[29] Oliveira C.S., Costa A., and Nunes J.C. *"Sismo 1998 - Açores. Uma década depois"*. Sersilito empresa gráfica, Lda, 2008. ISBN 978-989-20-1223-0. (in Portuguese).

[30] Chester D.K. The effects of the 1755 Lisbon earthquake and tsunami on the Algarve region, southern Portugal. *Geography*, 93(2):78–90, 2008. URL https://livrepository.liverpool.ac.uk/742/5/742.pdf.

[31] Formisano A. Theoretical and numerical seismic analysis of masonry building aggregates: Case studies in san pio delle camere (L'Aquila, italy). *Journal of Earthquake Engineering*, 21:227–245, 2017. URL http://dx.doi.org/10.1080/13632469.2016.1172376.

[32] Parisi F. and Augenti N. Earthquake damages to cultural heritage constructions and simplified assessment of artworks. *Engineering Failure Analysis*, 34:735–760, 2013. URL http://dx.doi.org/10.1016/j.engfailanal.2013.01.005.

[33] Romão X., Costa A.A., Paupério E., Rodrigues H., Vicente R., Varum H., and Costa A. Field observations and interpretation of the structural performance of constructions after the 11 May 2011 Lorca earthquake. *Engineering Failure Analysis*, 34:670–692, 2013. URL http://dx.doi.org/10.1016/j.engfailanal.2013.01.040.

[34] Daniell J.E., Khazai B., Wenzel F., and Vervaeck A. The CATDAT damaging earthquakes database. *Natural Hazards and Earth System Science*, 11(8):2235–2251, 2011. URL http://dx.doi.org/10.5194/nhess-11-2235-2011.

[35] Tierney K.J., Lindell M.K., and Perry R.W. *Facing the unexpected*. Disaster preparedness and response in the United States, Washington DC, United States of America, 2001. ISBN 978-0-309-51518-4.

[36] Oliveira C.S., Ferreira M., and Oliveira M. Planning in seismic risk areas: The case of Faro, Algarve - A first approach. In *Proceedings of the 11th Italian National Association of Earthquake Engineering (ANIDIS)*, 25–29 May, Genoa, Italy., 2017.

[37] ISDR. *Living with risk: A global review of disaster reduction initiative*. International Strategy for Disaster Reduction, Geneva, Switzerland, 2004. ISBN 92-1-101064-0. URL http://www.unisdr.org/files/657_lwr1.pdf.

[38] Mouroux P and Le Brun B. Presentation of RISK-UE project. *Bulletin of Earthquake Engineering*, 4 (4):323–339, 2006. URL http://dx.doi.org/10.1007/s10518-006-9020-3.

[39] Elgin K. Istanbul seismic risk mitigation and emergency preparedness project (ISMEP). In *Proceedings of the ATC/SEI Conference on Improving the Seismic Performance of Existing Buildings and Other Structures*, San Francisco, California, United States of America, 2009. doi: 10.1061/41084(364)103.

[40] Ranghieri F. and Ishiwatari M. Learning from megadisasters: Lessons from the Great East Japan Earthquake. Technical report, The World Bank, International Bank for Reconstruction and Development, Washington DC, United States of America, 2014. URL http://dx.doi.org/10.1596/978-1-4648-0153-2.

[41] UNISDR. Hyogo framework for action 2005-2015: ISDR international strategy for disaster reduction. Technical report, United Nations Office for Disaster Risk Reduction, Building Resilience Nations Communities to Disasters. Extract from the final report of the World Conference on Disaster Reduction (A/CONF.206/6), Kobe, Hyogo, Japan, 2017.

[42] Maio R., Ferreira T.M., and Vicente R. Mitigation and management strategies for earthquake risk at the national scale. In Lourenço L. and Santos Â., editors, *Risks and Catastrophes Series*, chapter 37. Coimbra, Portugal. Imprensa da Universidade de Coimbra, 2017. (in Portuguese).

[43] Calderini C., Cattari S., Lagomarsino S., and Brunenghi M.M. Deliverable D42 – Final Report to the EU Project Office. Technical report, PERPETUATE PERformance-based aPproach to Earthquake proTection of cUlturAl heriTage in European and mediterranean countries, 2012.

[44] Žarnić R., Rajčić V., and Vodopivec B. Heritage protection, from documentation to interventions. In *Proceedings of the EU-CHIC International Conference on Cultural Heritage Preservation*, 29 May–1 June, Split, Croatia, 2012. ISBN 978-953-6272-51-8.

[45] Maierhofer C., Köpp C., Binda L., Zanzi L., Rodríguez Santiago J., Knupfer B., Johansson B., Modena C., Porto F. da, Marchisio M., Gravina F., Falci M., Galvez Ruiz J.C., Tomǎzevič M., Bosiljkov V., Hennen C., Lorente Toledo D.E., Zajc A., Delli Paoli S., Drdácky M., and Válek J. Onsiteformasonry project. On-site investigation techniques for the structural evaluation of historic masonry buildings. Technical report, EUR 21696 EN, Luxembourg: Office for Official Publications of the European Commission, European Commission, 2006. URL http://www.ndt.net/article/ndtce03/index.htm.

[46] Mazzolani F.M. Protection of historical buildings. In *Proceedings of the 1st International Conference PROHITECH 09*, 21–24 June, Rome, Italy, 2009. ISBN 978-0415558037.

[47] Modena C., Porto F. da, Valluzzi M.R., and Munari M. Criteria and technologies for the structural repair and strengthening of architectural heritage. In *Proceedings of International Conference on Rehabilitation and Restoration of Structures*, 13–16 February, Chennai, India, 2013.

[48] Lagomarsino S. and Cattari S. Perpetuate – guidelines for seismic performance-based assessment of cultural heritage masonry structures. *Bulletin of Earthquake Engineering*, 13(1):13–47, 2014. URL http://doi.org/10.1007/s10518-014-9674-1.

[49] Lagomarsino S., Modaressi H., Pitilakis K., Bosiljkov V., Calderini C., D'Ayala D., Benouar D., and Cattari S. Perpetuate project: The proposal of a performance-based approach to earthquake protection of cultural heritage. *Advanced Materials Research*, 133–134:1119–1124, 2010. URL https://doi.org/10.4028/www.scientific.net/AMR.133-134.1119.

[50] Covello V.T. Strategies for overcoming challenges to effective risk communication. In *Handbook of risk and crisis communication*, chapter 7. Routledge, 2008. URL https://www.routledgehandbooks.com/doi/10.4324/9780203891629.ch7.

[51] Vicente R., Ferreira T.M., Maio R., and Koch H. Awareness, perception and communication of earthquake risk in Portugal: Public survey. *Procedia Economics and Finance*, 18(4th International Conference on Building Resilience):271–278, 2014. URL https://doi.org/10.1016/S2212-5671(14)00940-X.

[52] Modena C., Casarin F., da Porto F., and Munari M. L'Aquila 6th april 2009 earthquake: Emergency and post-emergency activities on cultural heritage buildings. In M. Garevski and A. Ansal, editors, *Earthquake Engineering in Europe*, pages 495–521. Springer, Dordrecht, 2010. URL https://doi.org/10.1007/978-90-481-9544-2_20.

[53] Grimaz S. Management of urban shoring during a seismic emergency: advances from the 2009 L'Aquila (Italy) earthquake experience. *Bollettino di Geofisica Teorica ed Applicata*, 52(2):341–355, 2011.

[54] Teves-Costa P., Batlló J., Matias L., Catita C., Jiménez M.J., and García-Fernández M. Maximum intensity maps (mim) for portugal mainland. *Journal of Seismology*, 23(3):417–440, 2019. URL https://doi.org/10.1007/s10950-019-09814-5.

[55] Lei n. 32/2012. "Procede à primeira alteração ao Decreto-Lei n.º 307/2009, de 23 de outubro, que estabelece o regime jurídico da reabilitação urbana, e à 54.ª alteração ao Código Civil, aprovando medidas destinadas a agilizar e a dinamizar a reabilitação urbana", "Assembleia da República. Diário da República n. 157/2012, Série I de 2012-08-14", Lisbon, Portugal, 2012. URL http://data.dre.pt/eli/lei/32/2012/08/14/p/dre/pt/html. (in Portuguese).

[56] Lei n. 307/2009. "No uso da autorização concedida pela Lei n.º 95-A/2009, de 2 de Setembro, aprova o regime jurídico da reabilitação urbana", "Assembleia da República. Diário da República n.º 206/2009, Série I de 2009-10-23", Lisbon, Portugal, 2009. URL https://data.dre.pt/eli/dec-lei/307/2009/10/23/p/dre/pt/html. (in Portuguese).

[57] RERU. "decreto-lei n. 53/2014 - Regime Excecional para a Reabilitação Urbana", "Ministério do Ambiente, Ordenamento do Território e Energia. Diário da República n. 69/2014, Série I de 2014-04-08", Lisbon, Portugal, 2014. URL https://dre.pt/pesquisa/-/search/25344757/details/maximized. (in Portuguese).

[58] Decreto-Lei n. 95/2019. Decreto-lei n. 95/2019 de 18 de Julho de 2019 - "Estabelece o regime aplicável à reabilitação de edifícios ou frações autónomas", Presidência do Conselho de Ministros, Infraestruturas e Habitação, Lisbon, Portugal, 2019. URL `https://dre.pt/application/conteudo/123279819`. (in Portuguese).

[59] Portaria n. 302/2019. Portaria n. 302/2019 de 12 de Setembro de 2019 - "Define os termos em que obras de ampliação, alteração ou reconstrução estão sujeitas à elaboração de relatório de avaliação de vulnerabilidade sísmica, bem como as situações em que é exigível a elaboração de projeto de reforço sísmico", Presidência do Conselho de Ministros, Infraestruturas e Habitação, Lisbon, Portugal, 2019. URL `https://dre.pt/application/conteudo/124642991`. In Portuguese.

[60] Cox-Jr. L.A.T. What's wrong with hazard-ranking systems? An expository note. *Risk Analysis*, 29(7): 940–948, 2009. URL `https://doi.org/10.1111/j.1539-6924.2009.01209.x`.

[61] Scharlig A. "Décider sur plusieurs critères. panorama de l'aide à la décision multicritère". Technical report, Presses Polytechniques et Universitaires Romandes, Collection Diriger l'Entreprise, 1999. (in French).

[62] Hunter P.R. and Fewtrell L. Acceptable risk. In Fewtrell L. and Bartam J., editors, *Water Quality: Guidelines, Standards and Health*, chapter 10, pages 207–227. World Health Organization, London, United Kingdom, 2001. URL `http://www.who.int/water_sanitation_health/dwq/iwachap10.pdf`.

[63] Caicedo C., Barbat A.H., Canas J.A., and Aguiar R. "Vulnerabilidad sísmica de edificios. Monografías de ingeniería sísmica". In *Proceedings of the CIMNE-IS-6*, Barcelona, Spain, 1994. (in Spanish).

[64] Corsanego A. and Petrini V. Seismic vulnerability of buildings - Work in progress. In *Workshop II on Seismic Risk Vulnerability and Risk Assessment*, pages 577–598, Trieste, Italy, 1990.

[65] Calvi G.M., Pinho R., Magenes G., Boomer J.J., Restrep-Vélez L.F., and Crowley H. Development of seismic vulnerability assessment methodologies over the past 30 years. *ISET Journal of Earthquake Technology*, 43(3):75–104, 2006. URL `http://home.iitk.ac.in/~vinaykg/Iset472.pdf`.

[66] Whitman R.V., Reed J.W., and Tien H.S. Earthquake damage probability matrices. In *Proceedings of the 5th World Conference on Earthquake Engineering (WCEE)*, 25–29 June 1973, Rome, Italy, 1974.

[67] Benedetti D. and Petrini V. "Sulla vulnerabilità sismica di edifici in muratura: Un metodo di valutazione". *L'industria delle costruzioni*, 149:66–74, 1984.

[68] Chever L. Use of seismic assessment methods for planning vulnerability reduction of existing building stock. In *Proceedings of the 15th World Conference on Earthquake Engineering (WCEE)*, 24–28 September, Lisbon, Portugal, 2012.

[69] Silva V., Crowley H., Varum H., and Pinho R. Seismic risk assessment for mainland Portugal. *Bulletin of Earthquake Engineering*, 13(2):429–457, 2015. URL `https://link.springer.com/article/10.1007/s10518-014-9630-0`.

[70] D'Ayala D.F. and Speranza E. An integrated procedure for the assessment of seismic vulnerability of historic buildings. In *Proceedings of the 12th World Conference on Earthquake Engineering (WCEE)*, 30 January - 4 February 2000, London, United Kingdom, 2002.

[71] Marques R. and Lourenço P.B. Unreinforced and confined masonry buildings in seismic regions: Validation of macro-element models and cost analysis. *Engineering Structures*, 64(3):52–67, 2014. URL `https://doi.org/10.1016/j.engstruct.2014.01.014`.

[72] Maio R, Estêvão JMC, Ferreira TM, and Vicente R. The seismic performance of stone masonry buildings in Faial island and the relevance of implementing effective seismic strengthening policies. *Engineering Structures*, 141:41–58, 2017. URL `https://doi.org/10.1016/j.engstruct.2017.03.009`.

[73] Boschi S. *Seismic risk analysis of masonry buildings in aggregate*. Ph.D. thesis, Department of Civil and Environmental Engineering of the University of Florence, 2016.

[74] Maio R. *Seismic vulnerability assessment of old building aggregates*. M.Sc. thesis, Department of Civil Engineering of the University of Aveiro, 2013. URL `http://hdl.handle.net/10773/12839`.

[75] Foerster E., Krien Y., Dandoulaki M., Priest S., Tapsell S., Delmonaco G., Margottini C., and Bonadonna C. WP 1: State-of-the art on vulnerability types. Methodologies to assess vulnerability of structural systems. Technical report, ENSURE project, 2009. URL `http://www.ensureproject.eu/ENSURE_Del1.1.1.pdf`.

[76] Florio G. *Vulnerability of historical masonry buildings under exceptional actions*. Ph.D. thesis, Faculty of Engineering of the University of Naples Federico II, 2010.

[77] D'Ayala D. and Novelli V. D8 - Review and validation of existing vulnerability displacement-based models. Technical report, PERPETUATE PERformance-based aPproach to Earthquake proTection of cUlturAl heriTage in European and mediterranean countries, 2010.

[78] Restrepo-Vélez L.F. and Magenes G. Simplified procedure for the seismic risk assessment of unreinforced masonry buildings. In *Proceedings of the 13th World Conference on Earthquake Engineering (WCEE)*, 1–6 August, Vancouver, Canada, 2004.

[79] S.T.A. DATA. *3Muri program: Seismic analysis program for 3D masonry buildings*. Release 10.0.1, Turin, Italy, 2011. URL `http://www.stadata.com`. User Manual.

[80] DIANA. *Displacement method ANAlyser - release 9.4 TNO*. Finite element analysis, Netherlands, 2009. User Manual.

[81] Di Pasquale G.D., Orsini G., and Romeo R.W. New developments in seismic risk assessment in Italy. *Bulletin of Earthquake Engineering*, 13(1):101–128, 2005. URL `https://doi.org/10.1007/s10518-005-0202-1`.

[82] Bernardini A., Giovinazzi S., Lagomarsino S., and Parodi S. "Vulnerabilità e previsione di danno a scala territoriale secondo una metodologia macrosismica coerente con la scala ems-98". In *Proceedings of the 12th Conference of the Italian National Association of Earthquake Engineering (ANIDIS)*, 10–14 June, Pisa, Italy, 2007. URL `http://ir.canterbury.ac.nz/handle/10092/4060`. (in Italian).

[83] Bernardini A., Gori R., and Modena C. "Valutazioni di resistenza di nuclei di edifici in muratura per analisi di vulnerabilità sismica". Technical report, Internal Report 2/1988, Department of Civil, Environmental and Architectural Engineering (DICEA) of the University of Padua, 1988. (in Italian).

[84] Ferreira T.M., Vicente R., and Varum H. Seismic vulnerability assessment of masonry façade walls: Development, application and validation of a new scoring method. *Structural Engineering and Mechanics*, 50(4):541–561, 2014. URL `https://doi.org/10.12989/sem.2014.50.4.000`.

[85] Lagomarsino S. and Giovinazzi S. Macrosseismic and mechanical models for the vulnerability and damage assessment of current buildings. *Bulletin of Earthquake Engineering*, 4(4):415–443, 2006. URL `https://doi.org/10.1007/s10518-006-9024-z`.

[86] Grünthal G. European macroseismic scale 1998. Technical report, European Seismological Commission - Subcommission on Engineering Seismology - Working Group Macroseismic Scales (Vol. 15). Cahiers du Centre Européen de Géodynamique et de Séismologie, 1988.

[87] Jaiswal K.S., Wald D.J., and D'Ayala D.F. Developing empirical collapse fragility functions for global building types. *Earthquake Spectra*, 27(3):775–795, 2001. URL `https://doi.org/0.1193/1.3606398`.

[88] Kappos A.J., Stylianidis K.C., and Pitilakis K. Development of seismic risk scenarios based on a hybrid method of vulnerability assessment. *Natural Hazards*, 17(2):177–192, 1998. URL `https://doi.org/10.1023/A:1008083021022`.

[89] Dolce M. and Moroni C. "La valutazione della vulnerabilità e del rischio sismico degli edifici pubblici mediante le procedure VC e VM". Technical report, Gruppo Nazionale per la Difesa dei Terremoti - INGV/GNDT, 2005. (in Italian).

[90] Kappos A.J. An overview of the development of the hybrid method for seismic vulnerability assessment of buildings. *Structure and Infrastructure Engineering*, 12(12):1573–1584, 2016. URL `https://doi.org/10.1080/15732479.2016.1151448`.

[91] Asteris P.G. and Giannopoulos I.P. Vulnerability and restoration assessment of masonry structural systems. *Electronic Journal of Structural Engineering*, 12(1):82–94, 2012.

[92] Spyrakos C.C. Seismic risk of historic structures and monuments: A need for a unified policy. In *Proceedings of the 5th Thematic Conference on Computational Methods in Structural Dynamics and Earthquake Engineering (COMPDYN)*, 25–27 May, Crete Island, Greece, 2015.

[93] CEN. Eurocode 8: Design of structures for earthquake resistance - Part 3: Assessment and retrofitting of buildings (EC8-3), European Committee for Standardization, Brussels, Belgium, 2005.

[94] Bosiljkov V., Bokan-Bosiljkov V., Strah B., Velkavr J., and Cotič P. Deliverable D6. Review of innovative techniques for the knowledge of cultural assets. Guide for the structural rehabilitation of heritage buildings. Technical report, PERPETUATE PERformance-based aPproach to Earthquake proTection of cUlturAl heriTage in European and mediterranean countries, Ljubljana, Slovenia, 2010.

[95] CEN. Eurocode 8: Design of structures for earthquake resistance - Part 1: General rules, seismic actions and rules for buildings (EC8-1), European Committee for Standardization, Brussels, Belgium, 2004.

[96] NTC. Decreto ministeriale 14 gennaio 2008 - Nuove norme tecniche per le costruzioni, Ministero delle Infrastrutture. Gazzetta Ufficiale 4 febbraio 2008 n.29 - S.O. n. 30, Rome, Italy, 2008. (in Italian).

[97] OPCM. "Direttiva del presidente del consiglio dei ministri n. 3961 del 9/2/2011", "Valutazione e riduzione del rischio sismico del patrimonio culturale con riferimento alle Norme tecniche per le costruzioni di cui al decreto del Ministero delle infrastrutture e dei Trasporti del 14 gennaio 2008. (11A02374). Gazzetta Ufficiale S.G. n. 47 del 26-02-2011 - S.O. n. 54", 2011. (in Italian).

[98] Cattari S. and Lagomarsino S. Criteria for the seismic assessment of masonry existing buildings. Technical report, DPC RELUIS 2010-2013. Final report of UNIGE research unit. Rete dei Laboratori Universitari di Ingegneria Sismica (RELUIS), 2013.

[99] Franchin P., Pinto P.E., and Pathmanathan R. Confidence factor? *Journal of Earthquake Engineering*, 14(7):989–1007, 2017. URL `https://doi.org/10.1080/13632460903527948`.

[100] Tondelli M., Rota M., Penna A., and Magenes G. Evaluation of uncertainties in the seismic assessment of existing masonry buildings. *Journal of Earthquake Engineering*, 16(S1):36–64, 2012. URL `https://doi.org/10.1080/13632469.2012.670578`.

[101] Cattari S., Lagomarsino S., Bosiljkov V., and D'Ayala D.F. Sensitivity analysis for setting up the investigation protocol and defining proper confidence factors for masonry buildings. *Bulletin of Earthquake Engineering*, 13(1):129–151, 2015. doi: https://doi.org/10.1007/s10518-014-9648-3.

[102] Haddad J., Cattari S., and Lagomarsino S. The use of sensitivity analysis for the probabilistic-based seismic assessment of existing buildings. In *Proceedings of the 16th World Conference on Earthquake Engineering (WCEE)*, 9–13 January 2017, Santiago Chile, Chile, 2017.

[103] Haddad J., Cattari S., and Lagomarsino S. Preliminary and sensitivity analysis to set the investigation plan for the seismic assessment of existing buildings. In *Proceedings of the 3rd International Conference on Protection of Historical Constructions (PROHITECH'17)*, 12–15 July 2017, Lisbon, Portugal, 2017.

[104] Ferreira T.M., Vicente R., and Mendes da Silva J.A.R. Estratégias e processos de inspeção para avaliação e diagnóstico do património edificado. *Conservar Património*, 18(2013):21–33, 2013. URL `http://doi.org/10.14568/cp2013007`.

[105] NIKER. Deliverable 3.3. Critical review of methodologies and tools for assessment of failure mechanisms and interventions. Technical report, New integrated knowledge based approaches to the protection of cultural heritage from earthquake-induced risk (NIKER). Padua, Italy, European Commission, 2010. URL `http://www.niker.eu`.

[106] Carocci C.F. Small centres damaged by 2009 L'Aquila earthquake: On site analyses of historical masonry aggregates. *Bulletin of Earthquake Engineering*, 10(1):45–71, 2012. URL `http://doi.org/10.1007/s10518-011-9284-0`.

[107] Vicente R., Ferreira T.M., and Mendes da Silva J.A.R. Supporting urban regeneration and building refurbishment. Strategies for building appraisal and inspection of old building stock in city centres. *Journal of Cultural Heritage*, 16(2015):1–14, 2015. URL `http://doi.org/10.1016/j.culher.2014.03.004`.

[108] Watt D. *Surveying historical buildings*. Taylor & Francis, London, United Kingdom, 2nd edition, 2015. ISBN 978-1-873394-67-0.

[109] Binda L., Roberti G.M., and Abbaneo S. The diagnosis research project. *Earthquake Spectra*, 10(1): 151–170, 1994. URL `https://doi.org/10.1193/1.1585766`.

[110] Silva V.C. and Lourenço P.B. Survey and assessment of portuguese heritage using non-destructive methods, in view of its seismic rehabilitation. In *Proceedings of Monument 98 - Workshop on Seismic Performance of Monuments*, pages 157–166, Lisbon, Portugal, 1998.

[111] Cóias V. *Inspecções e ensaios na reabilitação de edifícios*. Lisbon, IST Press, Lisbon, Portugal, 2nd edition, 2009. ISBN 978-972-8469-53-5. (in Portuguese).

[112] Formisano A., Florio G., Landolfo R., and Mazzolani F.M. Numerical calibration of an easy method for seismic behaviour assessment on large scale of masonry building aggregates. *Advances in Engineering Software*, 80(7):116–138, 2015. URL `https://doi.org/10.1016/j.advengsoft.2014.09.013`.

[113] Ferreira T.M., Vicente R., Mendes da Silva J.A.R., Varum H., Costa A., and Maio R. Urban fire risk: Evaluation and emergency planning. *Journal of Cultural Heritage*, 20:739–745, 2016. URL `https://doi.org/10.1016/j.culher.2016.01.011`.

[114] Ferreira T.M., Vicente R., and Varum H. Vulnerability assessment of building aggregates: A macroseimic approach. In *Proceedings of the 15th World Conference on Earthquake Engineering (WCEE)*, Lisbon, Portugal, 2012.

[115] Formisano A., Mazzolani F.M., Florio G., and Landolfo R. A quick methodology for seismic vulnerability assessment of historical masonry aggregates. In *Proceedings of the COST C26 Final Conference "Urban Habitat Constructions under Catastrophic Events"*, Naples, Italy, 2010. URL `https://doi.org/10.13140/2.1.1706.3686`.

[116] Ferreira T.M., Santos C., Vicente R., and Mendes da Silva J.A.R. Caracterização arquitectónica e construtiva do património edificado do núcleo urbano antigo do seixal. *Conservar Património*, 17: 21–37, 2013. URL `http://doi.org/10.14568/cp2012008`.

[117] Garagnani S. and Manferdini A.M. Parametric accuracy: Building information modelling process applied to the cultural heritage preservation. In *Proceedings of the International Archives of the Photogrammetry, Remote Sensing and Spatial Information Sciences. Volume XL-5/W1, 2013 3D-ARCH 2013 - 3D Virtual Reconstruction and Visualization of Complex Architectures*, 25–26 February 2013, Trento, Italy, 2013.

[118] Logothetis S., Delinasiou A., and Stylianidis E. Building information modelling for cultural heritage: A review. *ISPRS Ann. Photogramm. Remote Sens. Spatial Inf. Sci.*, II-5(W3):177–183, 2015. URL `https://doi.org/10.5194/isprsannals-II-5-W3-177-2015`.

[119] Senaldi I.E. *Numerical investigations on the seismic response of masonry building aggregates*. M.Sc. thesis, European School for Advanced Studies in Reduction of Seismic Risk (Rose School), 2009.

[120] Ferrari F. *"Seismic response evaluation of aggregate buildings: A case study in Castenuovo (AQ)"*. M.Sc. thesis, School of Engineering of the University of Florence, 2012. (in Italian).

[121] Maio R., Vicente R., Formisano A., and Varum H. Seismic vulnerability of building aggregates through hybrid and indirect assessment techniques. *Bulletin of Earthquake Engineering*, 13(10):2995–3014, 2015. URL `https://doi.org/10.1007/s10518-015-9747-9`.

[122] Fagundes C., Bento R., and Cattari S. On the seismic response of buildings in aggregate: Analysis of a typical masonry building from azores. *Structures*, 10:184–196, 2017. URL http://dx.doi.org/10.1016/j.istruc.2016.09.010.

[123] Ferreira T.M., Costa A.A., and Costa A. Analysis of the out-of-plane seismic behaviour of unreinforced masonry: A literature review. *International Journal of Architectural Heritage*, 9:949–972, 2015. URL https://doi.org/10.1080/15583058.2014.885996.

[124] RELUIS. "Linee guida per il rilievo, l'analisi ed il progetto di interventi di riparazione e rafforzamento di edifici in aggregato". Technical report, "Rete dei Laboratori Universitari di Ingegneria Sismica", 2010. (in Italian).

[125] Warnotte V. Mitigation of pounding between adjacent buildings in earthquake situations. In *Proceedings of LESSLOSS Final Workshop - Risk mitigation for earthquakes and landslides integrated project. Sub-project 7 - Vulnerability reduction in structures*, 19–20 July 2007, Belgirate, Italy, 2007.

[126] Maio R., Ferreira T.M., and Vicente R. A critical discussion on the earthquake risk mitigation of urban cultural heritage assets. *International Journal of Disaster Risk Reduction*, 27(2018):239–247, 2018. URL https://doi.org/10.1016/j.ijdrr.2017.10.010.

[127] Ferreira T.M., Maio R., and Vicente R. Seismic vulnerability assessment of the old city centre of horta, azores: Calibration and application of a seismic vulnerability index method. *Bulletin of Earthquake Engineering*, 15(7):2879–2899, 2017. URL https://doi.org/10.1007/s10518-016-0071-9.

[128] Lang K. *Seismic vulnerability of existing buildings*. Ph.D. thesis, Institute of Structural Engineering of the Swiss Federal Institute of Technology, Switzerland, 2002.

[129] Penna A. Tools and strategies for the performance-based seismic assessment of masonry buildings. In *Dolšek M. (eds) Protection of built environment against earthquakes*, pages 147–167. Springer, Dordrecht, 2011. ISBN 978-94-007-1448-9. URL https://doi.org/10.1007/978-94-007-1448-9_8.

[130] Penna A. Seismic assessment of existing and strengthened stone-masonry buildings: Critical issues and possible strategies. *Bulletin of Earthquake Engineering*, 13(4):1051–1071, 2015. URL https://doi.org/10.1007/s10518-014-9659-0.

[131] D'Ayala D. Assessing the seismic vulnerability of masonry buildings. In *Tesfamariam, S. and Goda, K. (eds) Handbook of Seismic Risk Analysis and Management of Civil Infrastructure Systems*, Woodhead Publishing Series in Civil and Structural Engineering, pages 334–365. Woodhead Publishing, 2013. ISBN 978-0-85709-268-7. URL http://www.sciencedirect.com/science/article/pii/B978085709268750013X.

[132] Asteris P.G., Chronopoulos M.P., Chrysostomou C.Z., Varum H., Plevris V., Kyriakides N., and Silva V. Seismic vulnerability assessment of historical masonry structural systems. *Engineering Structures*, 62–63:118–134, 2014. URL https://doi.org/10.1016/j.engstruct.2014.01.031.

[133] Marques R. and Lourenço P.B. Benchmarking of commercial software for the seismic assessment of masonry buildings. In *Proceedings of the International Seminar on Seismic Risk and Rehabilitation of Stone Masonry Housing*, Horta, Faial Island, Azores, Portugal, 2008.

[134] Pantò B., Raka E., Cannizzaro F., Camata G., Caddemi S., Spacone E., and Caliò I. *Numerical macro-modelling of unreinforced masonry structures: A critical appraisal*. In *Proceedings of the 15th International Conference on Civil, Structural and Environmental Engineering Computing (eds B. H. V. Topping and P. Iványi)*, Stirlingshire: Civil-Comp Press, 2015.

[135] Magenes G., Bolognini D., and Braggio C. "Metodi semplificati per l'analisi sismica non lineare di edifici in muratura". Technical report, CNR, Gruppo Nazionale per la Difesa dai Terremoti - GNDT, Rome, Italy, 2000.

[136] Casapulla C., Argiento L.U., and Maione A. Seismic safety assessment of a masonry building according to Italian guidelines on cultural heritage: Simplified mechanical-based approach and pushover analysis. *Bulletin of Earthquake Engineering*, 16(7):2809–2837, 2015. URL `https://link.springer.com/article/10.1007/s10518-017-0281-9`.

[137] Caddemi S., Caliò I., Cannizzaro F., and Pantò B. New frontiers on seismic modelling of masonry structures. *Frontiers in Built Environment*, 3:1–16, 2017. URL `https://doi.org/10.3389/fbuil.2017.00039`.

[138] Marques R. and Lourenço P.B. Possibilities and comparison of structural component models for the seismic assessment of modern unreinforced masonry buildings. *Computers and Structures*, 89(21–22): 2079–2091, 2011. URL `https://doi.org/10.1016/j.compstruc.2011.05.021`.

[139] Magenes G. and Della Fontana A. Simplified non-linear seismic analysis of masonry buildings. In *Proceedings of the 5th International Masonry Conference*, October 12-14. London, London, United Kingdom, 1998.

[140] Brencich A., Gambarotta L., and Lagomarsino S. A macroelement approach to the three-dimensional seismic analysis of masonry buildings. In *Proceedings of the 11th European Conference on Earthquake Engineering (ECEE)*, 6–11 September, Paris, France, 1998.

[141] OPCM. "Ordinanza del presidente del consiglio dei ministri n. 3274 del 20/3/2003. G.U. n. 105 dell'8/5/2003", "Primi elementi in material di criteri generali per la classificazione sismica del territorio nazionale e di normative tecniche per le costruzioni in zona sismica", 2003. (in Italian).

[142] OPCM. "Ordinanza del presidente del consiglio dei ministri n. 3431 del 3/5/2005. G.U. n. 107 del 10/5/2005", "Ulteriori modifiche ed integrazioni all'ordinanza del Presidente del Consiglio dei Ministri n. 3274 del 20 marzo 2003", 2005. (in Italian).

[143] Vanin A. and Foraboschi P. Modelling of masonry panels by truss analogy - Part 1. *International Masonry Society*, 22(1):1–10, 2009.

[144] Caliò I., Marletta M., and Pantò B. A simplified model for the evaluation of the seismic behaviour of masonry buildings. In *Proceedings of the 10th International Conference on Civil, Structural and Environmental Engineering Computing*, 30 August - 2 September, Rome, Italy, 2005.

[145] Caliò I., Marletta M., and Pantò B. A new discrete element model for the evaluation of the seismic behaviour of unreinforced masonry buildings. *Engineering Structures*, 40:327–338, 2012. URL `https://doi.org/10.1016/j.engstruct.2012.02.039`.

[146] Pantò B., Cannizzaro F., Caliò I., and Lourenço P.B. Numerical and experimental validation of a 3D macro-model for the in-plane and out-of-plane behaviour of unreinforced masonry walls. *International Journal of Architectural Heritage*, 11(7):946–964, 2017. URL `http://doi.org/10.1080/15583058.2017.1325539`.

[147] Lagomarsino S., Penna A., Galasco A., and Cattari S. TREMURI program: An equivalent frame model for the nonlinear seismic analysis of masonry buildings. *Engineering Structures*, 56:1787–1799, 2013. URL `https://doi.org/10.1016/j.engstruct.2013.08.002`.

[148] Penna A., Lagomarsino S., and A. Galasco. A nonlinear macroelement model for the seismic analysis of masonry buildings. *Earthquake Engineering and Structural Dynamics*, 43:159–179, 2014. URL `https://doi.org/10.1002/eqe.2335`.

[149] S. Lagomarsino and S. Cattari. *Seismic performance of historical masonry structures through pushover and nonlinear dynamic analyses*, volume 39. Springer-Verlag Berlin Heidelberg, 2015.

[150] Turnšek V. and Sheppard P. The shear and flexural resistance of masonry walls. In *Proceedings of the International Research Conference on Earthquake Engineering*, Skopje, Japan, 1980.

[151] Simões A., Milošević J., Meireles H., Bento R., Cattari S., and Lagomarsino S. Fragility curves for old masonry building types in Lisbon. *Bulletin of Earthquake Engineering*, 13(10):3083–3105, 2015. URL `https://doi.org/10.1007/s10518-015-9750-1`.

[152] Siano R., Roca P., Camata G., Pelà L., Sepe V., Spacone E., and Petracca M. Numerical investigation of non-linear equivalent-frame models for regular masonry walls. *Engineering Structures*, 173(2018): 512–529, 2018. URL https://doi.org/10.1016/j.engstruct.2018.07.006.

[153] Quagliarini E., Maracchini G., and Clementi F. Uses and limits of the equivalent frame model on existing unreinforced masonry building for assessing their seismic risk: A review. *Journal of Building Engineering*, 10:166–182, 2017. URL https://doi.org/10.1016/j.jobe.2017.03.004.

[154] Marino S., Cattari S., Lagomarsino S., Dizhur D., and Ingham J.M. Post-earthquake damage simulation of two colonial unreinforced clay brick masonry buildings using the equivalent frame approach. *Structures*, 19:212–226, 2019. URL https://doi.org/10.1016/j.istruc.2019.01.010.

[155] Caliò I., Marletta M., and Pantò B. A discrete element approach for the evaluation of the seismic response of masonry buildings. In *Proceedings of the 14th World Conference of Earthquake Engineering*, October 12-17. Beijing, China, 2008.

[156] Raka E., Spacone E., Sepe V., and Camata G. Advanced frame element for seismic analysis of masonry structures: Model formulation and validation. *Earthquake Engineering and Structural Dynamics*, 44 (14):2489–2506, 2015. URL https://doi.org/10.1002/eqe.2594.

[157] Pantò B., Giresini L., Sassu M., and Caliò I. Nonlinear modelling of masonry churches through a discrete macro-element approach. *Earthquakes and Structures*, 12(2):223–236, 2017. URL https://doi.org/10.12989/eas.2017.12.2.223.

[158] Caddemi S., Caliò I., Cannizzaro F., Pantò B., and Rapicavoli D. Discrete macroelement modeling. In Ghiassi Bahman and Milani Gabriele, editors, *Numerical modeling of masonry and historical structures, Chapter 14*, Woodhead Publishing Series in Civil and Structural Engineering, pages 503–533. Woodhead Publishing, 2019. ISBN 978-0-08-102439-3. doi: https://doi.org/10.1016/B978-0-08-102439-3.00014-2.

[159] Maio R. and Tsionis G. Seismic fragility curves for the european building stock: Review and evaluation of analytical fragility curves (EUR 27635 EN). Technical report, JRC, Joint Research Centre, Ispra, Italy, 2016.

[160] Betti M., Galano L., and Vignoli A. Comparative analysis on the seismic behaviour of unreinforced masonry buildings with flexible diaphragms. *Engineering Structures*, 61:195–208, 2014. URL https://doi.org/10.1016/j.engstruct.2013.12.038.

[161] Nakamura Y., Derakhshan H., Griffith M.C., Magenes G., and Sheikh A.H. Applicability of nonlinear static procedures for low-rise unreinforced masonry buildings with flexible diaphragms. *Engineering Structures*, 137(15):1–18, 2017. URL https://doi.org/10.1016/j.engstruct.2017.01.049.

[162] Lu S., Beyer K., Bosiljkov V., Butenweg C., D'Ayala D.F., Degee H., Gams M., Klouda J., Lagomarsino S., Penna A., Mojsilovic N., Da Porto F., Sorrentino L., and Vintzileou E. *Brick and block masonry - Trends, innovations and challenges. Next generation of Eurocode 8, Masonry chapter*. London, UK. Taylor & Francis Group, 2016.

[163] Cannizzaro F., Pantò B., Lepidi M., Caddemi S., and Caliò I. Multi-directional seismic assessment of historical masonry buildings by means of macro-element modelling: Application to a building damaged during the L'Aquila earthquake (Italy). *Buildings*, 7(4), 2017. URL https://doi.org/10.3390/buildings7040106.

[164] Fajfar P. and Gašperšič P. The N2 method for the seismic damage analysis of RC buildings. *Earthquake Engineering and Structural Dynamics*, 25(1):31–46, 1996.

[165] NP EN 1998-1. "Eurocódigo 8: Projecto de estruturas para resistência aos sismos - Parte 1: Regras gerais, acções sísmicas e regras para edifícios", "Comité Europeu de Normalização", Brussels, Belgium, 2010. (in Portuguese).

[166] NP EN 1998-3. "Eurocódigo 8: Projecto de estruturas para resistência aos sismos - Parte 3: Avaliação e reforço de edifícios (NP EN 1998-3)", "Comité Europeu de Normalização", Brussels, Belgium, 2017. (in Portuguese).

[167] Costa A. and Arêde A. Strengthening of structures damaged by the Azores earthquake of 1998. *Construction and Building Materials*, 20(4):252–268, 2006. URL https://doi.org/10.1016/j.conbuildmat.2005.08.029.

[168] Diz S., Costa A., and Costa A.A. Efficiency of strengthening techniques assessed for existing masonry buildings. *Engineering Structures*, 101:205–215, 2015. URL https://doi.org/10.1016/j.engstruct.2015.07.017.

[169] Costa A. Determination of mechanical properties of traditional masonry walls in dwellings of Faial Island, Azores. *Earthquake Engineering and Structural Dynamics*, 31(February 2000):1361–1382, 2002. URL https://doi.org/10.1002/eqe.167.

[170] Silva B., Guedes J. M., Arêde A., and Costa A. Calibration and application of a continuum damage model on the simulation of stone masonry structures: Gondar church as a case study. *Bulletin of Earthquake Engineering*, 10(1):211–234, 2012. URL https://doi.org/10.1007/s10518-010-9216-4.

[171] Ramos L.F. and Lourenço P.B. Modelling and vulnerability of historical city centers in seismic areas: A case study in Lisbon. *Engineering Structures*, 26(9):1295–1310, 2004.

[172] Simões A., Bento R., Cattari S., Lagomarsino S., Cattari S., and Lagomarsino S. Seismic performance-based assessment of "Gaioleiro" buildings. *Engineering Structures*, 80:486–500, 2014. URL https://doi.org/10.1016/j.engstruct.2014.09.025.

[173] NZSEE. Assessment and improvement of the structural performance of buildings in earthquake, Recommendations of a NZSEE study group. New Zealand Society for Earthquake Engineering, Wellington, New Zealand, 2015.

[174] ASCE. Seismic evaluation and retrofitting of existing buildings. Technical report, Federal Emergency Management Agency, ASCE 41–13. American Society of Civil Engineers, Reston, Virginia, United States of America, 2014.

[175] Bernardini C., Maio R., Boschi S., Ferreira T. M., Vicente R., and Vignoli A. The seismic performance-based assessment of a masonry building enclosed in aggregate in Faro (Portugal) by means of a new target structural unit approach. *Engineering Structures*, 191(April):386–400, 2019. URL https://doi.org/10.1016/j.engstruct.2019.04.040.

[176] Greco A., Lombardo G., Pantò B., and Famà A. Seismic vulnerability of historical masonry aggregate buildings in oriental Sicily. *International Journal of Architectural Heritage*, 2018. doi: https://doi.org/10.1080/15583058.2018.1553075.

[177] Bessi N., D'Amore M., and Focosi M. *"Interventi di miglioramento sismico nel museo di Casa Vasari"*. M.Sc. thesis, School of Engineering of the University of Florence, 2016. (in Italian).

[178] Roders A. *Re-Architecture: Lifespan rehabilitation of built heritage*. Technische Universiteit Eindhoven, Eindhoven, 2007. ISBN 9789038617862. doi: 10.6100/IR751759.

[179] De la Torre M. Assessing the values of cultural heritage. Volume 2: Supporting documentation. Technical report, The Getty Conservation Institute, The Getty Conservation Institute, Los Angeles, California, United States of America, 2002.

[180] Rizzo I. and Throsby D. Cultural heritage: Economic analysis and public policy. In Ginsburgh V.A. and Throsby D., editors, *Handbook of the economics of art and culture*, chapter 28, pages 983–1016. Elsevier B.V., 2006. ISBN 1574-0676. doi: 10.1016/S1574-0676(06)01028-3.

[181] Mrak I. Evaluation methods in the protection of built heritage. *Journal of the Croatian Association of Civil Engineers*, 66:127–138, 2014. ISSN 03502465. doi: 10.14256/JCE.940.2013.

[182] Borges J.F., Bezzeghoud M., Buforn E., Pro C., and Fitas A. The 1980, 1997 and 1998 Azores earthquakes and some seismo-tectonic implications. *Tectonophysics*, 435(1-4):37–54, 2007. ISSN 00401951. URL https://doi.org/10.1016/j.tecto.2007.01.008.

[183] Matias L.M., Dias N.A., Morais I., Vales D., Carrilho F., Madeira J., Gaspar J.L., Senos L., and Silveira A.B. The 9th of July 1998 Faial Island (Azores, North Atlantic) seismic sequence. *Journal of Seismology*, 11(3):275–298, 2007. ISSN 13834649. URL https://doi.org/10.1007/s10950-007-9052-4.

[184] Marques F.O., Catalão J., Hildenbrand A., Costa A., and Dias N.A. The 1998 Faial earthquake, Azores: Evidence for a transform fault associated with the Nubia-Eurasia plate boundary? *Tectonophysics*, 633:115–125, 2014. ISSN 00401951. URL https://doi.org/10.1016/j.tecto.2014.06.024.

[185] Neves F., Costa A., Vicente R., Oliveira C.S., and Varum H. Seismic vulnerability assessment and characterisation of the buildings on Faial Island, Azores. *Bulletin of Earthquake Engineering*, 10(1):27–44, 2012. URL http://doi.org/10.1007/s10518-011-9276-0.

[186] Ferreira T.M., Costa A.A., Arêde A., Varum H., and Costa A. In situ out-of-plane cyclic testing of original and strengthened traditional stone masonry walls using airbags. *Journal of Earthquake Engineering*, 20(5):749–772, 2016. URL http://www.tandfonline.com/doi/full/10.1080/13632469.2015.1107662. (in English).

[187] Ferreira T.M., Maio R., and Vicente R. Analysis of the impact of large scale seismic retrofitting strategies through the application of a vulnerability-based approach on traditional masonry buildings. *Earthquake Engineering and Engineering Vibration*, 16(2):329–348, 2017. URL https://link.springer.com/article/10.1007/s11803-017-0385-x.

[188] Neves N., Arêde A., and Costa A. Seismic analysis of a building block. *Bulletin of Earthquake Engineering*, 10(1):1–33, 2012. ISSN 1570-761X. URL https://doi.org/10.1007/s10518-011-9310-2.

[189] Oliveira C.S., Costa A., and Neves F. The reconstruction process that followed the July 9, 1998 earthquake. An analysis of a few topics. In *"Sismo 1998 - Açores. Uma década depois"*, chapter 42, pages 522–530. Sersilito empresa gráfica, Lda, 2008. ISBN 978-989-20-1223-0.

[190] Filippi M. Remarks on the green retrofitting of historic buildings in Italy. *Energy and Buildings*, 95:15–22, 2015. URL https://doi.org/10.1016/j.enbuild.2014.11.001. Special Issue: Historic, historical and existing buildings: designing the retrofit. An overview from energy performances to indoor air quality.

[191] Mazzarella L. Energy retrofit of historic and existing buildings. The legislative and regulatory point of view. *Energy and Buildings*, 95:25–31, 2015. URL https://doi.org/10.1016/j.enbuild.2014.10.073. Special Issue: Historic, historical and existing buildings: designing the retrofit. An overview from energy performances to indoor air quality.

[192] Webb A.L. Energy retrofits in historic and traditional buildings: A review of problems and methods. *Renewable and Sustainable Energy Reviews*, 77:748–759, 2017. ISSN 1364-0321. URL https://doi.org/10.1016/j.rser.2017.01.145.

[193] Neves F., Costa A., and Oliveira C.S. Seismic vulnerability of the building stock in Faial and Pico Islands. In *Sismo 1998 - Açores. Uma década depois*, chapter 39, pages 481–512. Sersilito empresa gráfica, Lda, 2008. ISBN 978-989-20-1223-0.

[194] Olsen A.H. Demand Surge Following Earthquakes. In *Proceedings of the 15th World Conference on Earthquake Engineering (15WCEE)*, Lisbon, Portugal, 2012.

[195] ATC. Earthquake damage evaluation data for California - ATC-13. Technical report, Applied Technology Council, Redwood City (CA), USA, 1985.

[196] Bramerini F., Pasquale G. di, Orisini A., Pugliese A., Romeo R., and Sabetta F. "Rischio sismico del territorio Italiano: proposta per una metodologia e risultati preliminary, technical report SN/RT/95/01". Technical report, Servizio Sismico Nazionale, Rome, Italy, 1995.

[197] FEMA-NIBS. Earthquake loss estimation methodology. Technical report HAZUS99. Technical report, Federal Emergency Management Agency under a contract with the National Institute of Building Sciences, Washington DC, USA, 1999.

[198] Dolce M., Marino M., Masi A., and Vona M. Seismic vulnerability analysis and damage scenarios of Potenza. In *Proceedings of the International Workshop on Seismic Risk and Earthquake Damage Scenarios of Potenza*, Potenza, Italy, 2000.

[199] Portaria no. 379/2017. "Portaria que fixa o valor médio de construção por metro quadrado, para efeitos do artigo 39. do Código do Imposto Municipal sobre Imóveis, a vigorar no ano de 2018", "Finanças. Diário da República n.º 242/2017, Série I de 2017-12-19", 2017. URL https://data.dre.pt/eli/port/379/2017/12/19/p/dre/pt/html. (in Portuguese).

[200] Costa A., Guedes J.M., and Varum H. *Structural rehabilitation of old buildings*. Springer-Verlag Berlin Heidelberg, 2014. ISBN 978-3-642-39685-4. doi: https://doi.org/10.1007/978-3-642-39686-1.

[201] Maio R., Ferreira T.M., Vicente R., and Costa A. Is the use of traditional seismic strengthening strategies economically attractive in the renovation of urban cultural heritage assets in Portugal? *Bulletin of Earthquake Engineering*, 10, 2018. URL https://doi.org/10.1007/s10518-018-00527-7.

[202] FEMA-255. Seismic rehabilitation of federal buildings: A benefit/cost model - Volume 1: A user's manual. Technical report, Federal Emergency Management Agency, Washington DC, United States of America, 1994.

[203] FEMA-256. FEMA-256. Seismic rehabilitation of federal buildings: A benefit/cost model - Volume 2: Support documentation. Technical report, Federal Emergency Management Agency, Washington DC, United States of America, 1994.

[204] Kappos A.J., Pitilakis K., Stylianidis K., Morfidis K., and Asimakopoulos N. Cost-benefit analysis for the seismic rehabilitation of buildings in thessaloniki, based on a hybrid method of vulnerability assessment. In *Proceedings of the 5th International Conference on Seismic Zonation*, Nice, France, October 17–19, 1995.

[205] Kappos A.J. and Dimitrakopoulos E.G. Feasibility of pre-earthquake strengthening of buildings based on cost-benefit and life-cycle cost analysis, with the aid of fragility curves. *Natural Hazards*, 45:33–54, 1995. URL https://doi.org/10.1007/s11069-007-9155-9.

[206] Liel A.B. and Deierlein G.G. Cost-benefit evaluation of seismic risk mitigation alternatives for older concrete frame buildings. *Earthquake Spectra*, 29(4):1391–1411, 2013. URL https://doi.org/10.1193/030911EQS040M.

[207] Marques R., Lamego P., Lourenço P.B., and Sousa M.L. Efficiency and cost-benefit analysis of seismic strengthening techniques for old residential buildings in Lisbon. *Journal of Earthquake Engineering*, 2017. URL https://doi.org/10.1080/13632469.2017.1286616.

[208] Chrysostomou C.Z., Kyriakides N., Papanikolaou V.K., Kappos A.J., Dimitrakopoulos E.G., and Giouvanidis A.I. Vulnerability assessment and feasibility analysis of seismic strengthening of school buildings. *Bulletin of Earthquake Engineering*, 13(12):3809–3840, 2015. URL https://doi.org/10.1007/s10518-015-9791-5.

[209] Jaimes M.A. and Niño M. Cost-benefit analysis to assess seismic mitigation options in Mexican public school buildings. *Bulletin of Earthquake Engineering*, 15(9):3919–3942, 2017. URL https://doi.org/10.1007/s10518-017-0119-5.

[210] Bento R., Lopes M., and R. Cardoso. Seismic evaluation of old masonry buildings. Part II: Analysis of strengthening solutions for a case study. *Engineering Structures*, 27(14):2014–2023, 2005. URL https://doi.org/10.1016/j.engstruct.2005.06.011.

[211] Branco M. and Guerreiro L.M. Seismic rehabilitation of historical masonry buildings. *Engineering Structures*, 33(5):1626–1634, 2011. URL https://doi.org/10.1016/j.engstruct.2011.01.033.

[212] Scotta R., Trutalli D., Marchi L., and Pozza L. Seismic response of masonry buildings with alternative techniques for in-plane strengthening of timber floors. *"Revista Portuguesa de Engenharia de Estruturas"*, 3(4):47–58, 2017. ISSN 2183–8488.

[213] Moreira S. *Seismic retrofit of masonry-to-timber connections in historical constructions*. Ph.D. thesis, School of Engineering, University of Minho, 2015.

[214] Braga A.M.G.S. and Estêvão J.M.C. Feasibility of confined masonry design in Azores. In *Proceedings of the Azores 1998 - International Seminar on Seismic Risk and Rehabilitation of Stone Masonry Housing*, pages 1–10, Azores, Portugal, 2008.

[215] Barbat A.H., Pujades L.G., and Lantada N. Seismic damage evaluation in urban areas using the capacity spectrum method: Application to Barcelona. *Soil Dynamics and Earthquake Engineering*, 28(10-11): 851–865, 2008. ISSN 02677261. URL https://doi.org/10.1016/j.soildyn.2007.10.006.

[216] FEMA & NIBS. Multi-hazard loss estimation methodology: earthquake model, HAZUS-MH MR4. Technical report, Federal Emergency Management, Mitigation Division, Washington DC, United States of America, 2003.

[217] Lamego P. *Seismic strengthening of residential buildings. Risk analysis and mitigation*. Ph.D. thesis, School of Engineering, University of Minho, 2014. (in Portuguese).

[218] Ferreira T.M., Mendes N., and Silva R. Multiscale seismic vulnerability assessment and retrofit of existing masonry buildings. *Buildings*, 9(4):1–22, 2019. URL https://doi.org/10.3390/buildings9040091.

[219] Barbat A.H., Carreño M.L., Pujades L.G., Lantada N., Cardona O.D., and Marulanda M.C. Seismic vulnerability and risk evaluation methods for urban areas. A review with application to a pilot area. *Structure and Infrastructure Engineering*, 6(1–2):17–38, 2010. URL https://doi.org/10.1080/15732470802663763.

[220] Basaglia A., Aprile A., Spacone E., and Pilla F. Performance-based Seismic Risk Assessment of Urban Systems. *International Journal of Architectural Heritage*, 12(7–8):1131–1149, 2018. URL https://doi.org/10.1080/15583058.2018.1503371.

[221] Ródenas J.L., García-Ayllón S., and Tomás A. Estimation of the Buildings Seismic Vulnerability: A Methodological Proposal for Planning Ante-Earthquake Scenarios in Urban Areas. *Applied Sciences*, 8 (7), 2018. URL https://doi.org/10.3390/app8071208.

[222] Chieffo N., Clementi F., Formisano A., and Lenci S. Comparative fragility methods for seismic assessment of masonry building located in Muccia (Italy). *Journal of Building Engineering*, 25(2019), 2019. URL https://doi.org/10.1016/j.jobe.2019.100813.

[223] Liu Y., Li Z., Wei B., Li X., and Fu B. Seismic vulnerability assessment at urban scale using data mining and GIScience technology: application to Urumqi (China). *Geomatics, Natural Hazards and Risk*, 10(1):958–985, 2019. URL https://doi.org/10.1080/19475705.2018.1524400.

[224] Kassem M.M., Nazri F.M., and Farsangi E.N. Development of seismic vulnerability index methodology for reinforced concrete buildings based on nonlinear parametric analyses. *MethodsX*, 6(2019):199–211, 2019. URL https://doi.org/10.1016/j.mex.2019.01.006.

[225] Ortega J., Vasconcelos G., Rodrigues H., and Correia M. A vulnerability index formulation for the seismic vulnerability assessment of vernacular architecture. *Engineering Structures*, 197, 2019. URL https://doi.org/10.1016/j.engstruct.2019.109381.

[226] GNDT-SSN. "scheda di esposizione e vulnerabilità e di rilevamento danni di primo livello e secondo livello (muratura e cemento armato)". Rome, Italy. Technical report, Gruppo Nazionale per la Difesa dai Terremoti - GNDT, 1994.

[227] Ferreira T.M., Maio R., and Vicente R. Seismic vulnerability assessment of historical urban centres: case study of the old city centre in seixal, portugal. *Bulletin of Earthquake Engineering*, 15(5):1753–1773, 2013. URL https://doi.org/10.1007/s10518-013-9447-2.

[228] Sandi H. and Floricel I. Analysis of seismic risk affecting the existing building stock. In *Proceedings of the 10th European Conference on Earthquake Engineering*, pages 1105–1110, Vienna, Austria, 1995.

[229] NTC. Decreto ministeriale 17 gennaio 2018 - Aggiornamento delle "norme tecniche per le costruzioni", Ministero delle Infrastrutture e dei Trasporti. Gazzetta Ufficiale 20 febbraio 2018 n.42 - S.O. n.8, Rome, Italy, 2018. (in Italian).

[230] Estêvão João M. C. An Integrated Computational Approach for Seismic Risk Assessment of Individual Buildings. *Applied Sciences*, 9(23):5088, nov 2019. URL `https://doi.org/10.3390/app9235088`.

Appendix A

Cost-benefit analyses

This appendix is complementary to the cost-benefit analyses carried out in Section 4.2, and summarises the results obtained for all the case studies considered, namely in terms of pushover and capacity curves, $\%a_g$ values, and fragility curves. Additionally, the probabilities of exceeding each damage state considered and the benefit-cost ratios associated with the 16th and 84th PCTLs, are also summarised.
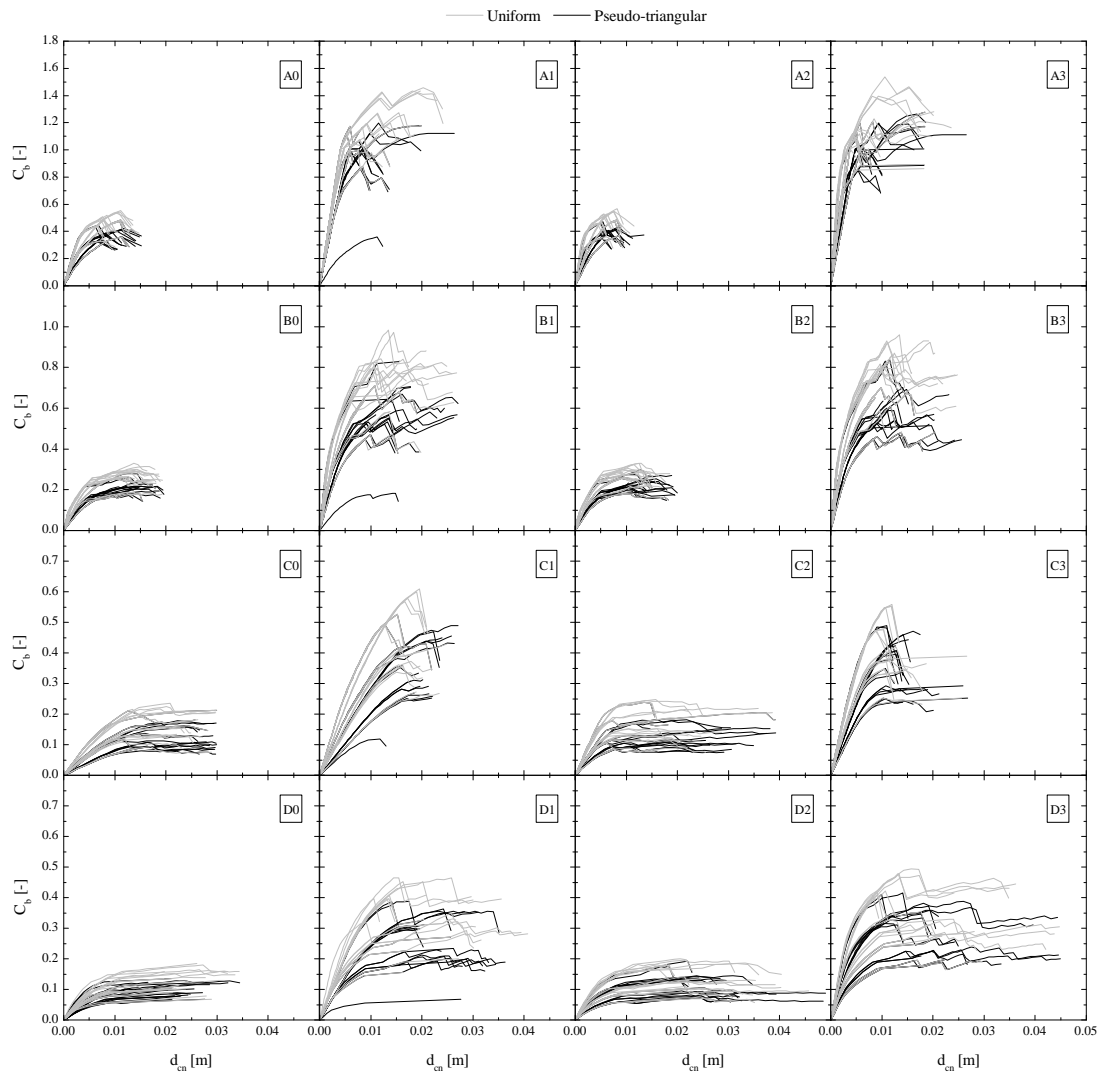
Figure A.1: Pushover curves obtained for each model (from A to D) and retrofitting condition (from 0 to 3) and grouped by horizontal load pattern distribution (uniform and pseudo-triangular).

Figure A.2: Capacity curves obtained for each model (from A to D) and retrofitting condition (from 0 to 3) and grouped by horizontal load pattern distribution (uniform and pseudo-triangular).
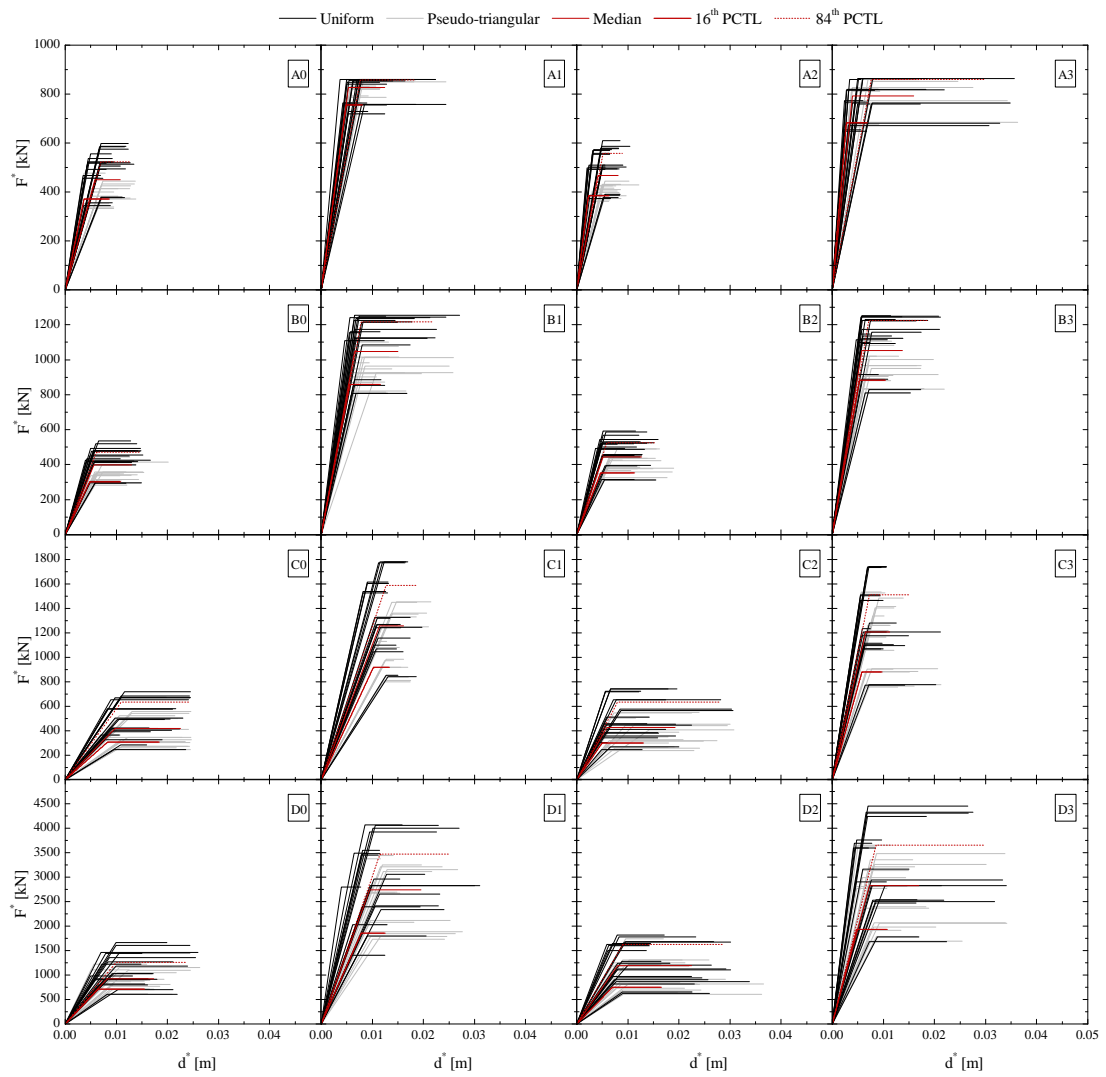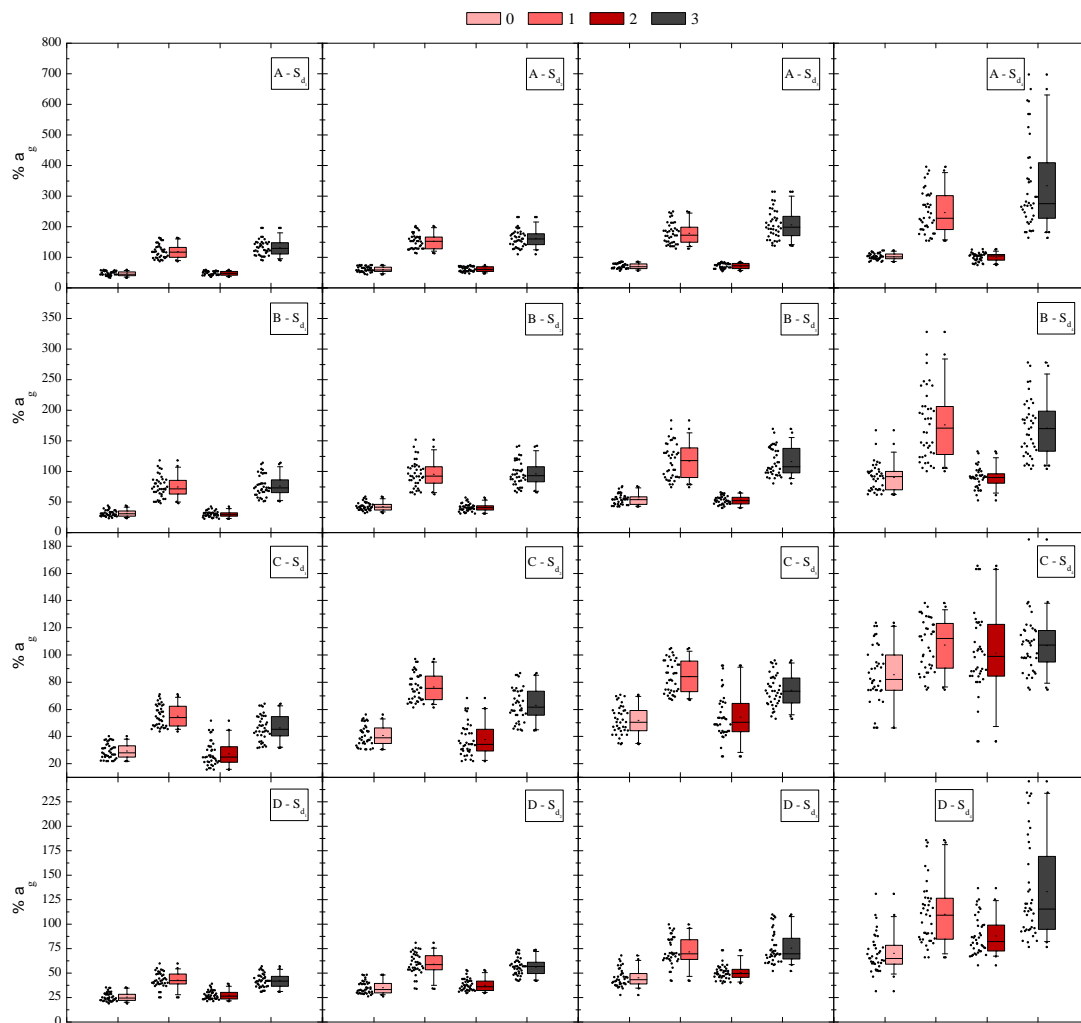
Figure A.3: Box-plot diagrams in terms of %a_g for the set of 40 pushover analyses performed for each model (from A to D) and retrofitting condition (from 0 to 3) and grouped by limit state (from S_{d_1} to S_{d_4}).

Figure A.4: Fragility curves associated with the median values of the capacity curves for each model (from A to D) and retrofitting co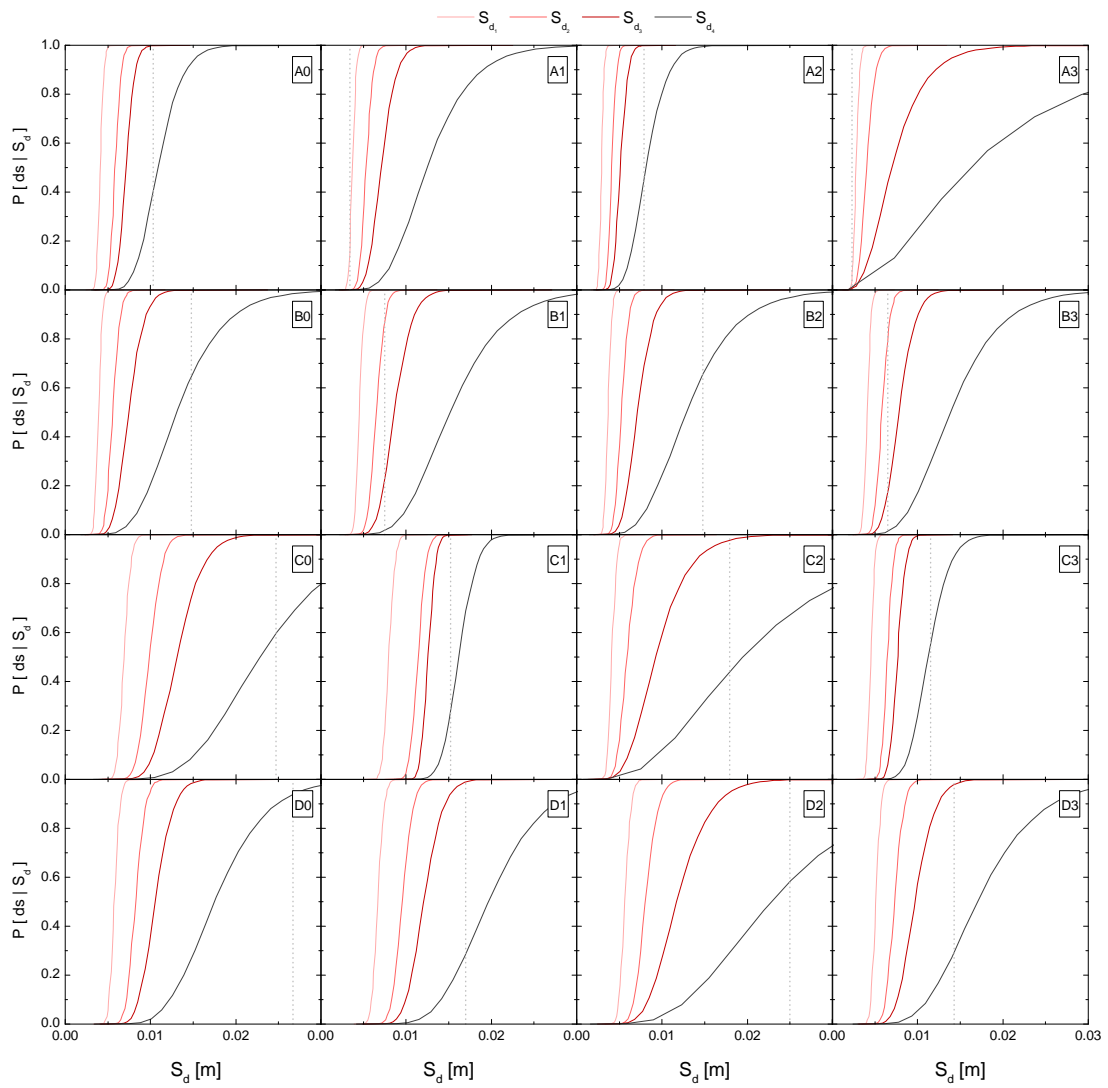ndition (from 0 to 3). Please note that the performance point of the equivalent bilinear SDoF system, d^*_t, is represented for each case by the vertical dashed line in light grey.

Table A.1: Probabilities of exceeding each damage state (from ds_0 to ds_4), for each model (from A to D), retrofitting condition, and central tendency measure (median, 16th and 84th PCTLs).

Building	Central tendency measure	Retrofitting condition	ds_0 No damage	ds_1 Slight damage	ds_2 Moderate damage	ds_3 Severe damage	ds_4 Collapse
A	Median	0	0%	0%	0%	60%	40%
		1	80%	20%	0%	0%	0%
		2	0%	0%	0%	54%	46%
		3	93%	7%	0%	0%	0%
	16th PCTL	0	0%	0%	1%	59%	41%
		1	99%	1%	0%	0%	0%
		2	0%	0%	2%	59%	39%
		3	99%	1%	0%	0%	0%
	84th PCTL	0	0%	0%	1%	44%	56%
		1	100%	0%	0%	0%	0%
		2	0%	0%	0%	17%	83%
		3	100%	0%	0%	0%	0%
B	Median	0	0%	0%	0%	35%	65%
		1	0%	12%	65%	22%	2%
		2	0%	0%	0%	34%	66%
		3	0%	20%	63%	16%	1%
	16th PCTL	0	0%	0%	0%	27%	73%
		1	0%	87%	12%	1%	0%
		2	0%	0%	0%	33%	67%
		3	4%	93%	2%	0%	0%
	84th PCTL	0	0%	0%	0%	35%	65%
		1	0%	8%	66%	23%	3%
		2	0%	0%	0%	43%	57%
		3	0%	5%	64%	28%	3%
C	Median	0	0%	0%	0%	41%	59%
		1	0%	0%	0%	72%	28%
		2	0%	0%	2%	54%	44%
		3	0%	0%	0%	44%	56%
	16th PCTL	0	0%	0%	0%	32%	68%
		1	0%	0%	0%	70%	30%
		2	0%	0%	0%	32%	68%
		3	0%	0%	1%	77%	22%
	84th PCTL	0	0%	0%	0%	20%	80%
		1	0%	0%	0%	53%	47%
		2	0%	0%	6%	58%	35%
		3	0%	0%	0%	58%	42%
D	Median	0	0%	0%	0%	6%	94%
		1	0%	0%	1%	70%	29%
		2	0%	0%	0%	42%	58%
		3	0%	0%	2%	68%	30%
	16th PCTL	0	0%	0%	0%	14%	86%
		1	0%	0%	0%	22%	78%
		2	0%	0%	0%	26%	74%
		3	0%	0%	0%	50%	49%
	84th PCTL	0	0%	0%	0%	19%	81%
		1	0%	0%	5%	75%	20%
		2	0%	0%	0%	42%	57%
		3	0%	0%	21%	59%	20%

Table A.2: Global results of the cost-benefit analysis for each model (from A to D), retrofitting condition (from 0 to 3), and central tendency measure (median, 16th and 84th PCTLs), considering the traditional construction replacement cost, $C_{R,CT}$.

Building	Central tendency measure	Retrofitting condition	C_{RD}	C_{BC}	C_{HL}	Total losses	Benefit	BCR_{CT}
			€	€	€	€	€	[–]
A	Median	0	53010	15894	1029	69932	–	–
		1	338	169	0	507	69425	8.11
		2	28861	17034	1187	47082	22850	14.20
		3	277	156	8	442	69491	6.83
	16th PCTL	0	53010	16043	1055	70108	–	–
		1	16	8	0	24	70083	8.19
		2	24875	15672	1015	41563	28545	17.74
		3	12	6	0	19	70089	6.89
	84th PCTL	0	53010	18841	1437	73287	–	–
		1	3	2	0	5	73282	8.56
		2	46630	23566	2092	72289	998	0.62
		3	34	15	0	48	73239	7.20
B	Median	0	69392	20286	6549	96227	–	–
		1	4094	3487	360	7941	88286	5.84
		2	50832	20473	6653	77958	18269	6.42
		3	3872	2862	299	7032	89195	4.96
	16th PCTL	0	69392	21700	7333	98425	–	–
		1	2394	986	36	3417	95008	6.28
		2	51616	20696	6777	79090	19335	6.80
		3	2104	812	8	2923	95501	5.31
	84th PCTL	0	69392	20314	6565	96270	–	–
		1	5076	3924	500	9500	86770	5.73
		2	45017	18876	5773	69666	26605	9.35
		3	4959	4311	508	9778	86492	4.81
C	Median	0	127119	19358	4526	151002	–	–
		1	18378	13846	2233	34457	116546	3.70
		2	27599	16502	3405	47507	103496	17.49
		3	33868	18704	4253	56825	94177	2.52
	16th PCTL	0	127119	20890	5163	153171	–	–
		1	19890	14287	2415	36592	116580	3.70
		2	39899	20872	5156	65927	87244	14.74
		3	14633	12742	1792	29167	124004	3.32
	84th PCTL	0	127119	23009	6045	156173	–	–
		1	29408	17215	3633	50256	105916	3.37
		2	22661	14705	2780	40147	116026	19.61
		3	26592	16305	3260	46157	110016	2.94
D	Median	0	246394	25443	9411	281248	–	–
		1	24826	13949	3074	41849	51069	3.38
		2	46099	19163	5933	71196	51837	18.22
		3	25633	14062	3177	42871	238377	3.27
	16th PCTL	0	246394	23981	8599	278975	–	–
		1	58191	22657	7865	88712	70289	4.65
		2	55614	21868	7427	84909	42357	14.89
		3	40124	17614	5072	62810	216164	2.97
	84th PCTL	0	246394	23125	8124	277643	–	–
		1	17660	12135	2215	32011	3698	0.24
		2	45364	18956	5828	70148	40612	14.27
		3	0	10951	2224	13175	264468	3.63

Appendix B

Casting a new light on the seismic risk assessment of historic centres

This appendix is complementary to the study carried out in Chapter 5, and presents the full extent of outputs generated for each considered variable, assuming the variability in terms of soil type, number of storeys and curve fitting model. It is worth noting that the vulnerability index value, I^*_v, plotted in the following figures, was obtained by assuming the original weights of the parameters, as suggested by Vicente [7].
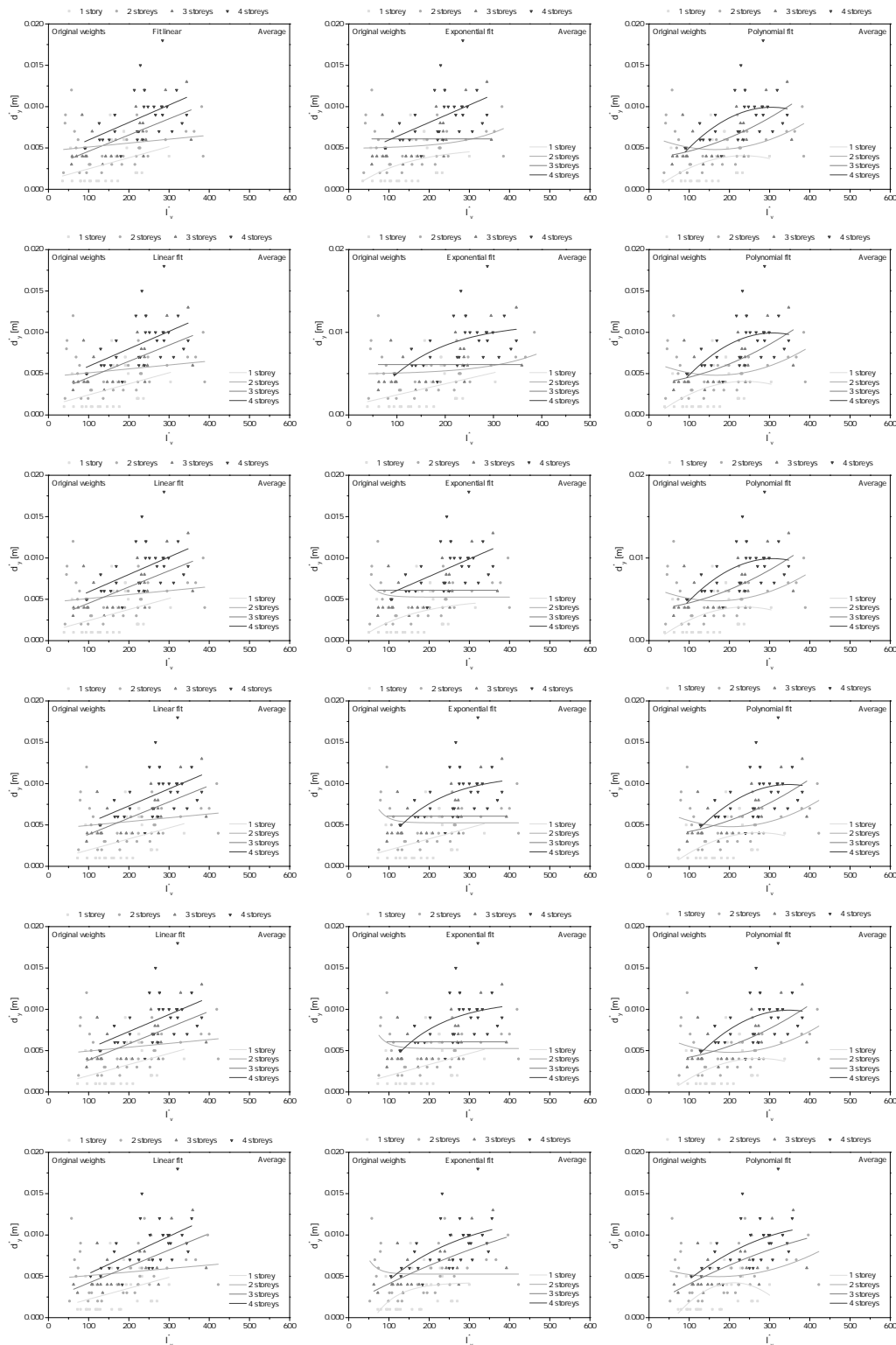
Figure B.1: Scatter plot of the d*ᵧ average values, considering the original weights of the the vulnerability index method [7]: soil type A to E (first to fifth row) and a random soil type distribution (bottom row).
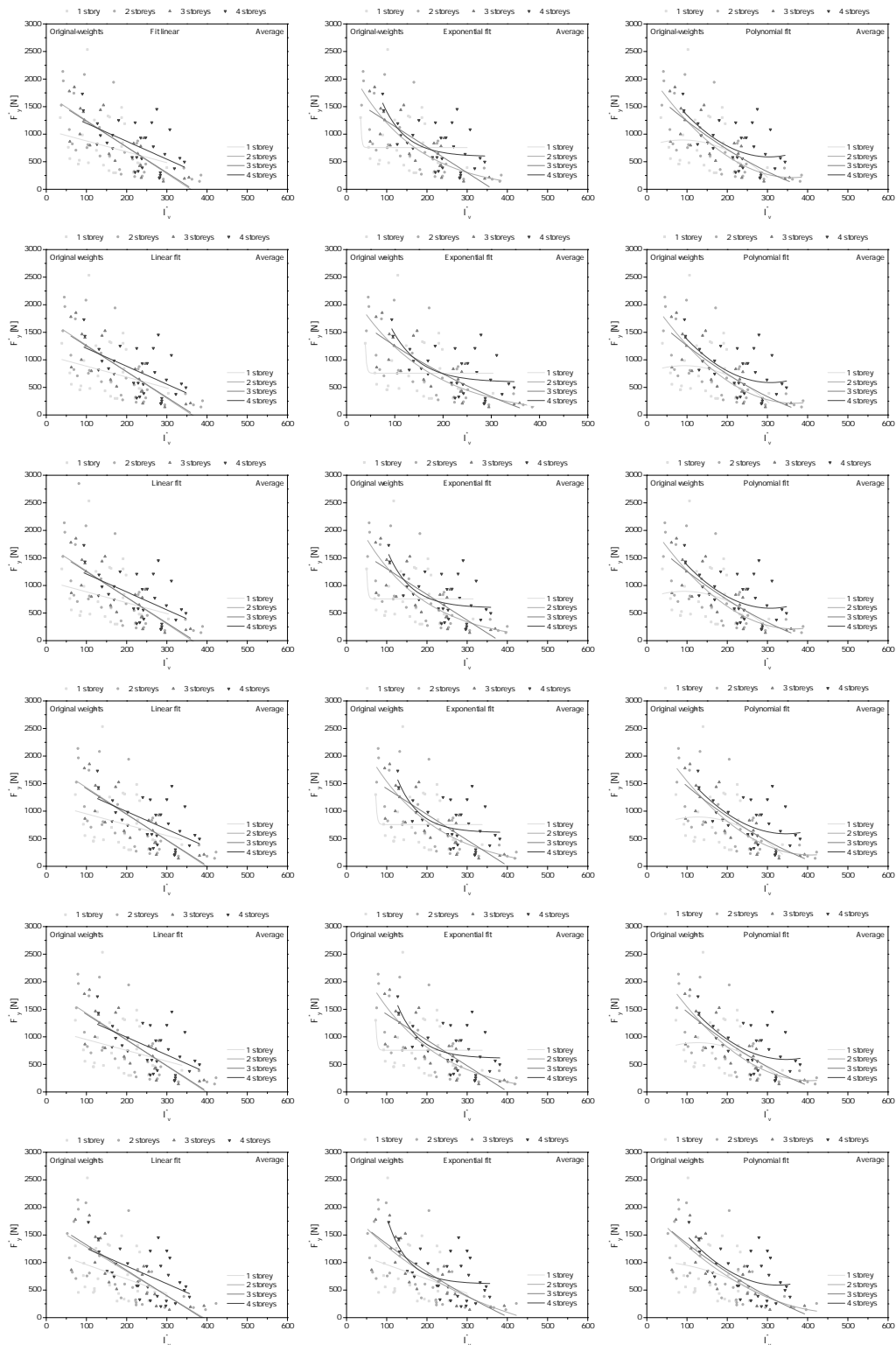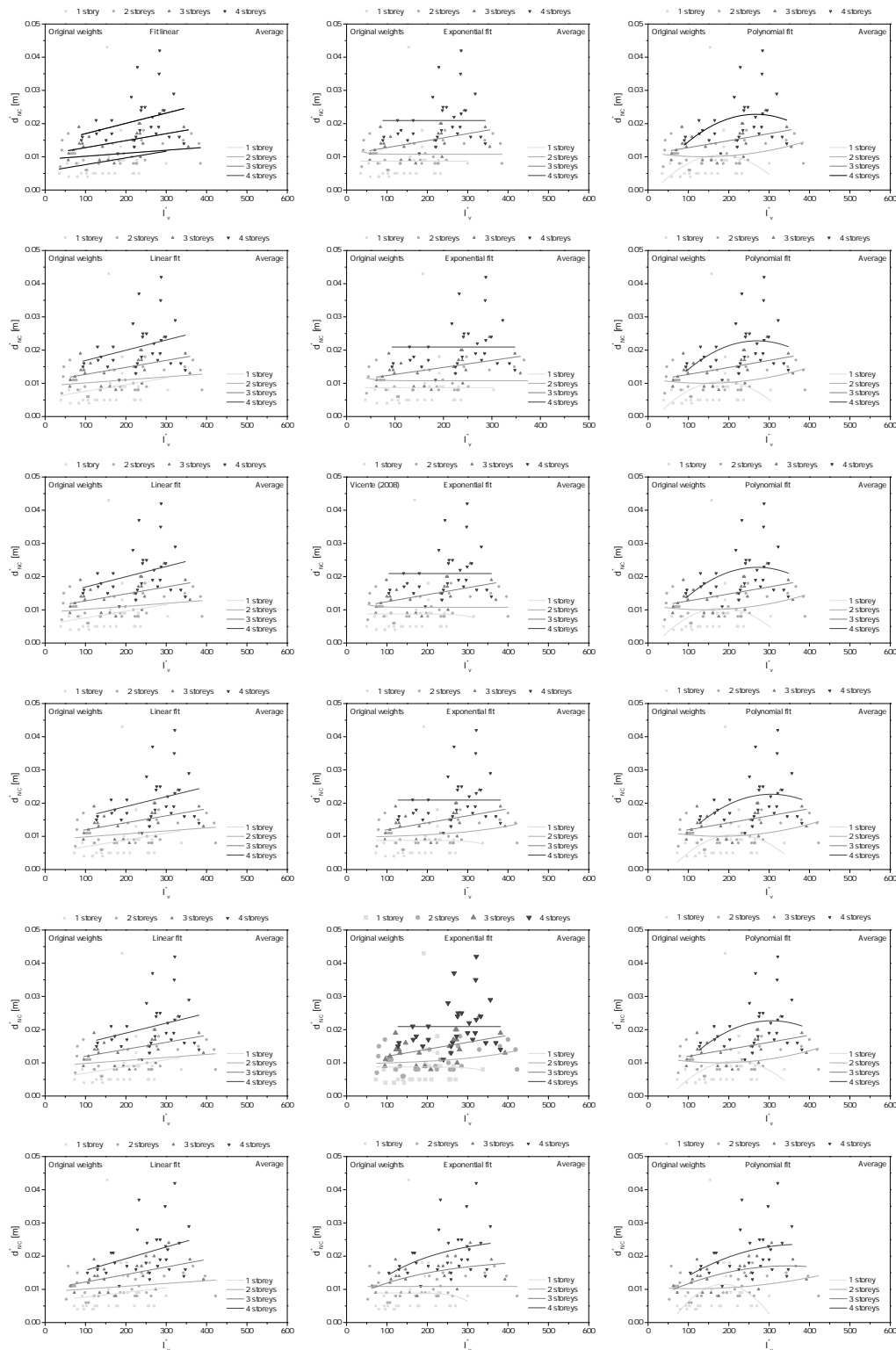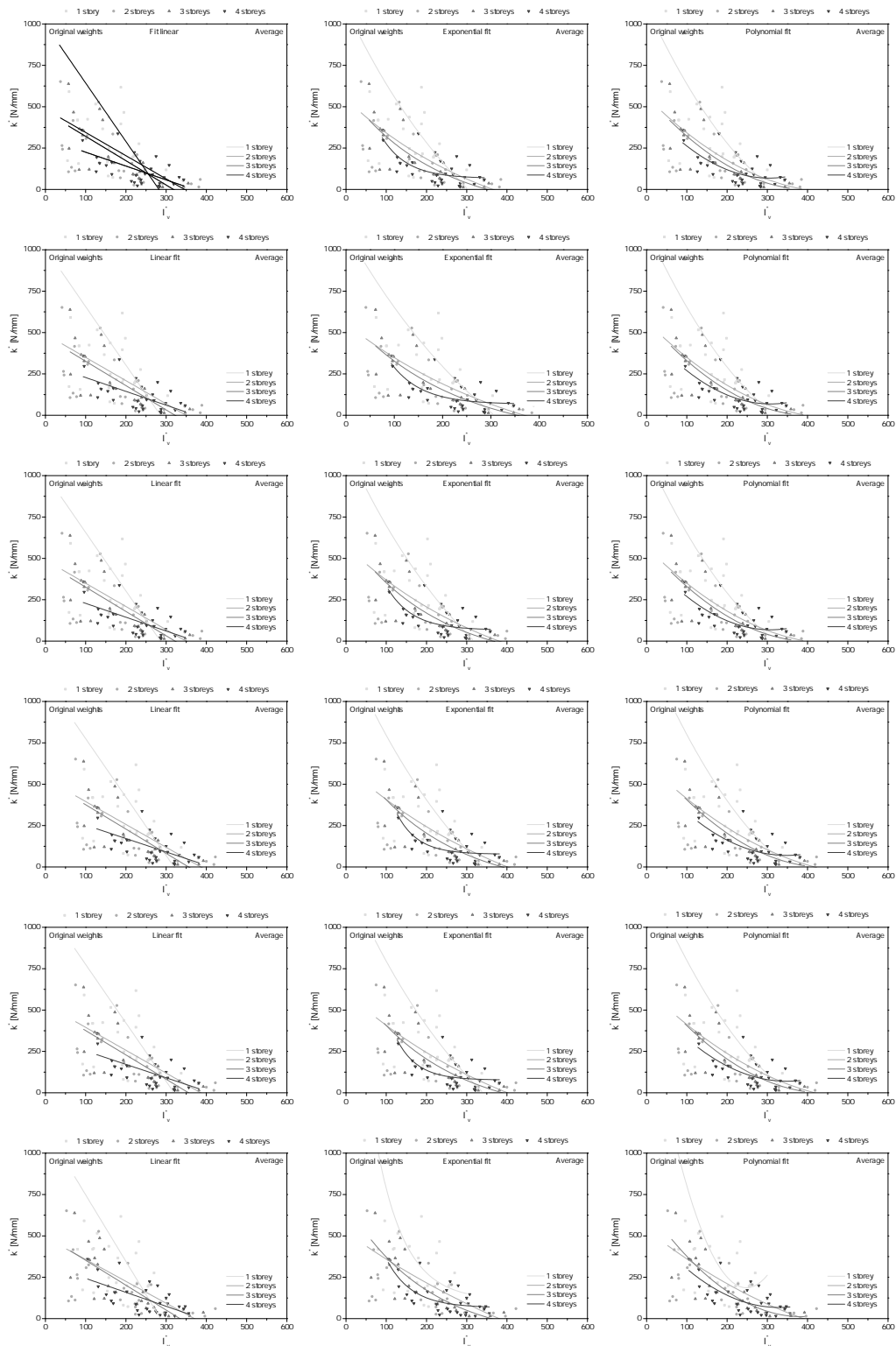
Figure B.2: Scatter plot of the F^*_y average values, considering the original weights of the the vulnerability index method [7]: soil type A to E (first to fifth row) and a random soil type distribution (bottom row).
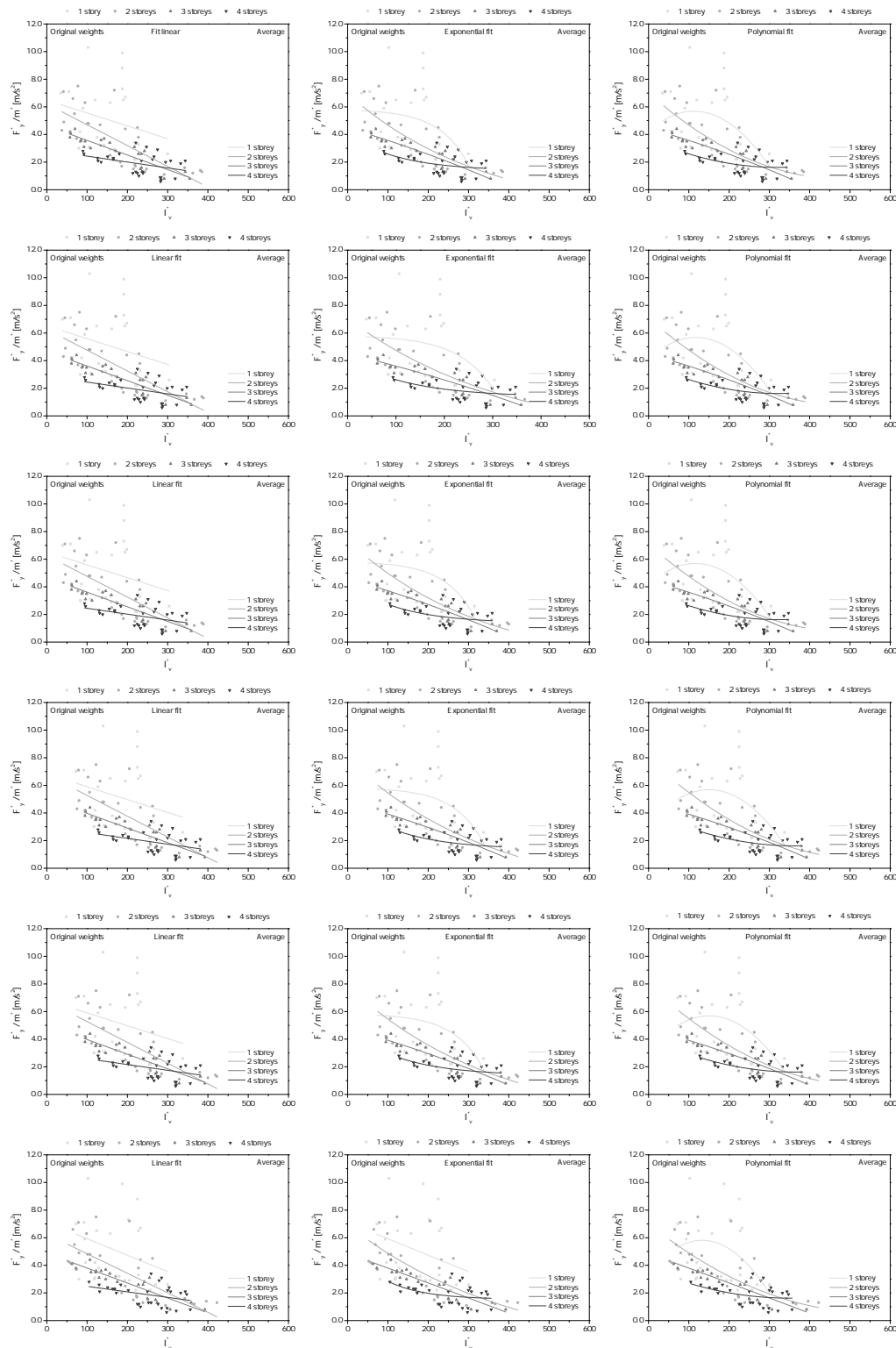
Figure B.3: Scatter plot of the d*$_{NC}$ average values, considering the original weights of the the vulnerability index method [7]: soil type A to E (first to fifth row) and a random soil type distribution (bottom row).

Figure B.4: Scatter plot of the k* average values, considering the original weights of the the vulnerability index method [7]: soil type A to E (first to fifth row) and a random soil type distribution (bottom row).
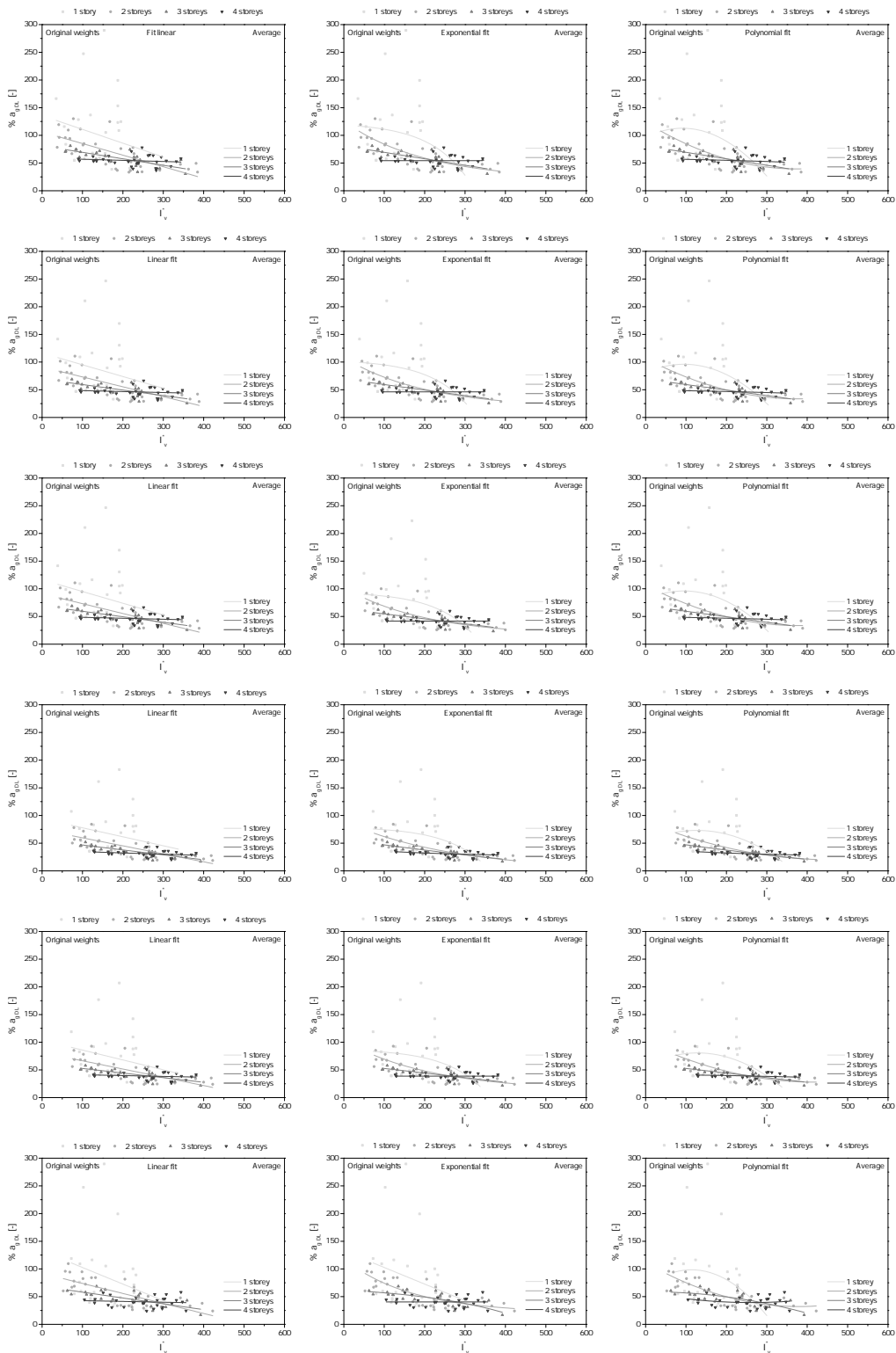
Figure B.5: Scatter plot of the F_y^*/m^* average values, considering the original weights of the the vulnerability index method [7]: soil type A to E (first to fifth row) and a random soil type distribution (bottom row).

Figure B.6: Scatter plot of the %$a_{g\,DL}$ average values, considering the original weights of the the vulnerability index method [7]: soil type A to E (first to fifth row) and a random soil type distribution (bottom row).
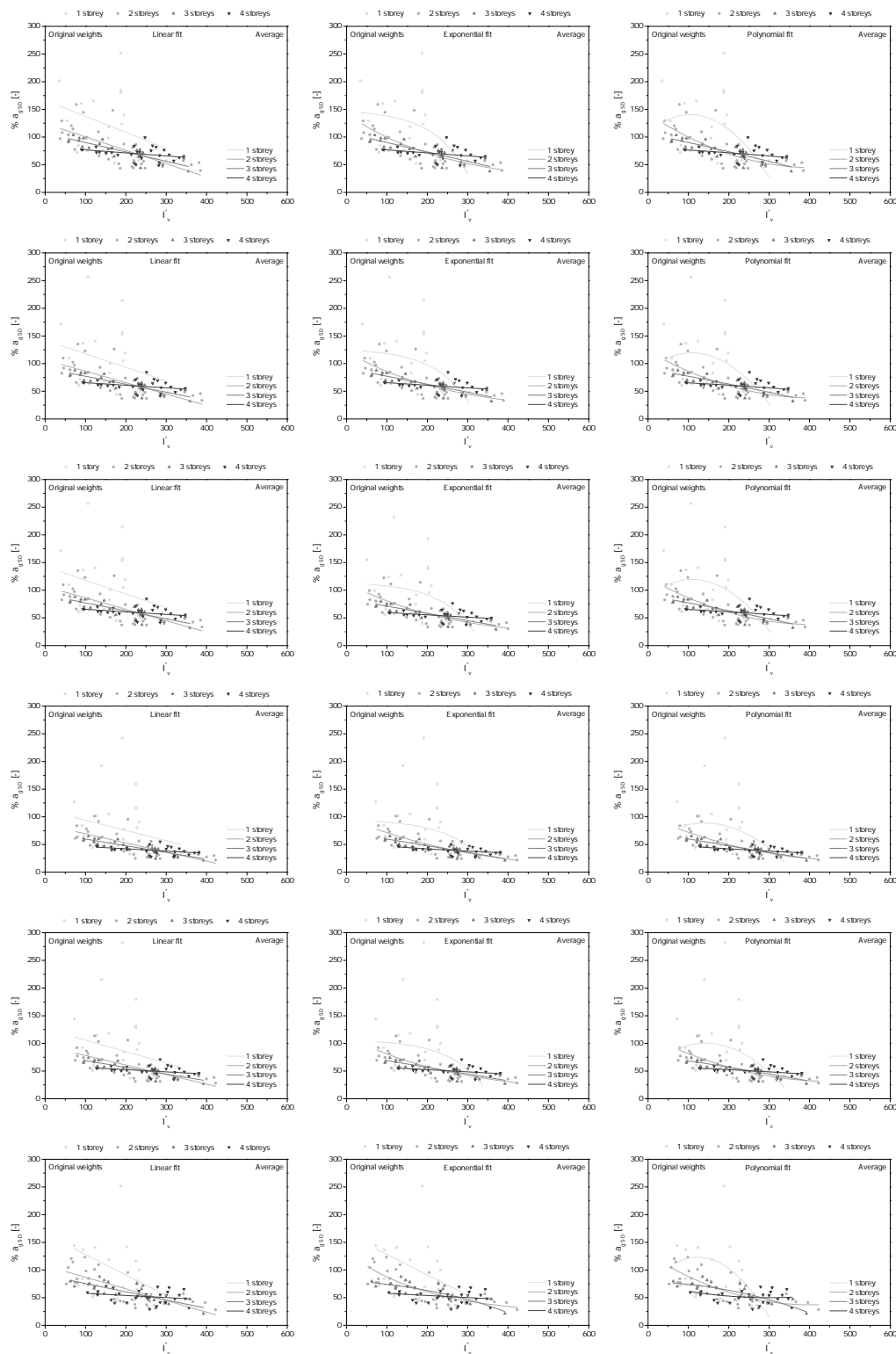
Figure B.7: Scatter plot of the %$a_{g\,SD}$ average values, considering the original weights of the the vulnerability index method [7]: soil type A to E (first to fifth row) and a random soil type distribution (bottom row).
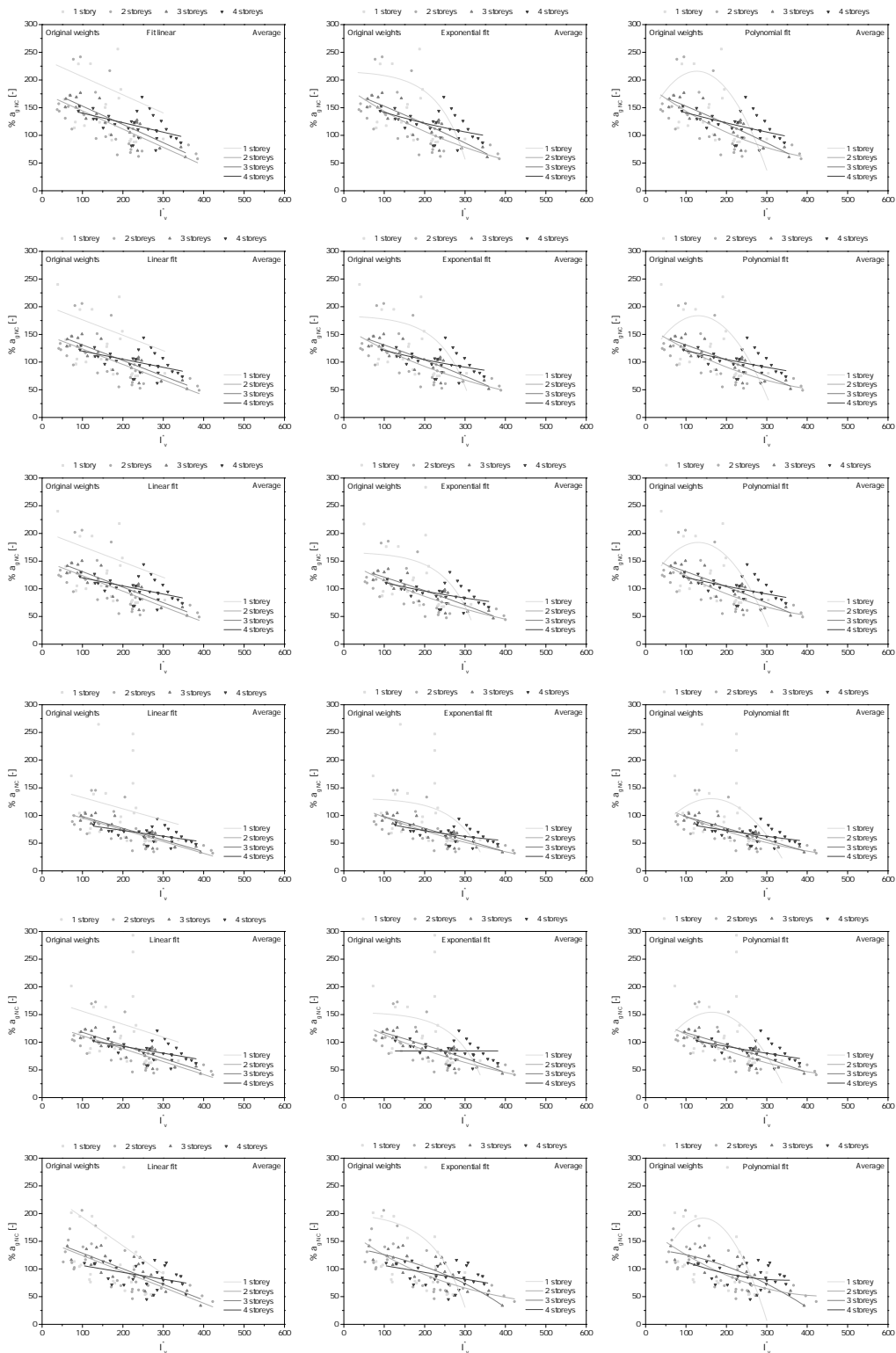
Figure B.8: Scatter plot of the %$a_{g\,NC}$ average values, considering the original weights of the the vulnerability index method [7]: soil type A to E (first to fifth row) and a random soil type distribution (bottom row).